LNTDL

Laboratoire des Nouvelles technologies et le développement local

People's Democratic Republic Of Algeria Ministry Of Higher Education And Scientific Research

University Of Echahid Hamma Lakhdar - El Oued

Faculty of Technology

Option: Electrical Network

Thesis prepared at the Laboratory of New Technologies and Local Development (LNTDL)

Doctoral Thesis

Submitted by: **Fettah Khaled**

Entitled

Improvement of Electrical Grid Stability with the Integration of Renewable Energy

Defended on 19/12/ 2024, before the jury composed of:

Mr. Laid Zellouma	Professor	University of El Oued	President
Mr. Talal Guia	MCA	University of El Oued	Supervisor
Mr. Salhi Ahmed	MCA	University of Biskra	Co-Supervisor
Mr. Naimi Djemai	Professor	University of El Oued	Examiner
Mr. Abdelhafid Rouina	MCA	University of Biskra	Examiner
Mr. Ali Khechekhouche	MCA	University of El Oued	Examiner

University Year: 2024/2025

LNTDL

Laboratoire des Nouvelles technologies et le développement local

Republique Algerienne Democratique Et Populaire

Miniistere De L'enseignement Superieur Et De La Recherche Scientifique Universite Echahid Hamma Lakhdar - El Oued

Faculté de Technologie

Option: Electrical Network

Mémoire préparé au sein du Laboratoire des Nouvelles technologies et le developpement local (LNTDL)

Thèse de Doctorat

Présentée par: **Fettah Khaled**

Intitulé

Amélioration de la stabilité du réseau éléctrique avec la pénétration des énergies renouvelables

Soutenue le 19/ 12/ 2024, devant le jury composé:

Mr. Laid Zellouma	Professeur	Université El Oued	President
Mr. Talal Guia	MCA	Université El Oued	Superviseur
Mr. Salhi Ahmed	MCA	Université Biskra	Co-Superviseur
Mr.Naimi Djemai	Professeur	Université Biskra	Examinateur
Mr. Abdelhafid Rouina	MCA	Université Biskra	Examinateur
Mr. Ali Khechekhouche	MCA	Université El Oued	Examinateur

Année universitaire: 2024/2025

Abstract

This work is part of a study on the optimal integration of Distributed Generation (DG) based on renewable photovoltaic energy sources and capacitor banks in radial distribution networks, specifically IEEE 33-JB, IEEE 69-JB, and ALG-AB-Hassi Sida 157, which are widely used in the literature for distribution system planning and operation. To optimize the use of both photovoltaic sources and capacitor banks, recent meta-heuristic optimization methods have been proposed to determine their optimal location and size. These methods include the Grey Wolf Optimizer (GWO), Particle Swarm Optimization (PSO), Whale Optimization Algorithm (WOA), and the EM-BT algorithm. However, the backwards-forward method was used for power flow calculations. For optimal and proper integration, three studies were proposed: the first aims to minimize only the energy losses in distribution networks through the integration of multiple distributed generation sources. The second study focuses on minimizing daily energy losses and voltage profile deviations, adapting to dynamic 24-hour load conditions. This objective is captured in a unified objective function (Obj1), which expands to minimize costs associated with energy losses and power supplied by Photovoltaic and Reactive Energy Source Capacitor Banks (PVRES-CBs), forming a comprehensive objective model (Obj2). The effectiveness of the proposed MOMVO algorithm is rigorously evaluated through a comparative analysis with three other optimization algorithms: Multi-Objective Jellyfish Search (MOJS), Multi-Objective Flower Pollination Algorithm (MOFPA), and Multi-Objective Lichtenberg Algorithm (MOLA). The comparison results in a Pareto front, which is essential for decision-makers or power system operators facing ambiguous or fuzzy objectives for each function. The fuzzy logic theory is employed to assist in selecting the optimal operating point from the array of Pareto-optimal solutions, identifying the best non-dominated solution by maximizing the normalized sum of membership function values across all objectives. Furthermore, the study explores the variations in the best compromise solutions derived from the mentioned algorithms, offering valuable insights into their performance and suitability under varying network conditions. Another study was conducted using the Energy Valley Optimizer, which proved its effectiveness in comparison to other optimization algorithms such as the Liver Cancer Algorithm, Walrus Optimization Algorithm, and Zebra Optimization Algorithm. This algorithm optimizes the objective function for the total cost of energy over 24 years by integrating photovoltaic sources and capacitor banks, accounting for the intermittent nature of these sources and load variations over 24 hours. The results demonstrate high-quality solutions compared to other methods reported in the literature. Simulation results also show that the proposed algorithms are reliable and applicable for the optimal integration of distributed generation sources in various distribution networks of different sizes and complexities.

Keywords:

Distributed Generation (DG), Photovoltaic Energy Sources (PVRES), Capacitor Banks (CB), Radial Distribution Networks, Meta-heuristic Optimization, Grey Wolf Optimizer (GWO), Particle Swarm Optimization (PSO) Whale Optimization Algorithm (WOA), EM-BT Algorithm, Multi-Objective Optimization (MOO), Energy Loss Minimization, Voltage Profile Stability, Energy Valley Optimizer (EVO), Fuzzy Logic Theory.

Résume

Ce travail fait partie d'une étude sur l'intégration optimale de la production décentralisée (DG) basée sur des sources d'énergie photovoltaïque renouvelable et des batteries de condensateurs dans les réseaux de distribution radiaux, notamment les réseaux IEEE 33-JB, IEEE 69-JB et ALG-AB-Hassi Sida 157, largement utilisés dans la littérature pour la planification et l'exploitation des systèmes de distribution. Pour optimiser l'utilisation des sources photovoltaïques et des batteries de condensateurs, des méthodes d'optimisation méta-heuristiques récentes ont été proposées pour déterminer leur emplacement et leur taille optimaux. Ces méthodes incluent le Grey Wolf Optimizer (GWO), l'Optimisation par Essaim Particulaire (PSO), l'Algorithme d'Optimisation des Baleines (WOA) et l'algorithme EM-BT. Cependant, la méthode "backward-forward" a été utilisée pour les calculs de flux de puissance.

Pour une intégration optimale, trois études ont été proposées : la première vise uniquement à minimiser les pertes d'énergie dans les réseaux de distribution par l'intégration de plusieurs sources de production décentralisée. La deuxième étude se concentre sur la minimisation des pertes d'énergie quotidiennes et des écarts de profil de tension, en s'adaptant aux conditions de charge dynamiques sur 24 heures. Cet objectif est capturé dans une fonction objective unifiée (Obj1), qui s'étend à la minimisation des coûts liés aux pertes d'énergie et à l'énergie fournie par les sources photovoltaïques et les batteries de condensateurs de source d'énergie réactive (PVRES-CBs), formant ainsi un modèle objectif global (Obj2).

L'efficacité de l'algorithme MOMVO proposé est rigoureusement évaluée à travers une analyse comparative avec trois autres algorithmes d'optimisation : la Recherche Multi-Objectifs de Méduse (MOJS), l'Algorithme de Pollinisation Florale Multi-Objectifs (MOFPA) et l'Algorithme Multi-Objectifs de Lichtenberg (MOLA). La comparaison produit un front de Pareto, essentiel pour les décideurs ou les opérateurs de systèmes électriques confrontés à des objectifs ambigus ou flous pour chaque fonction. La théorie de la logique floue est utilisée pour aider à sélectionner le point de fonctionnement optimal à partir de l'ensemble des solutions Pareto optimales, en identifiant la meilleure solution non dominée en maximisant la somme normalisée des valeurs de la fonction d'appartenance sur tous les objectifs.

De plus, l'étude explore les variations dans les meilleures solutions de compromis issues des algorithmes mentionnés, offrant des informations précieuses sur leurs performances et leur adéquation dans différentes conditions de réseau. Une autre étude a été menée en utilisant l'Optimiseur de la Vallée d'Énergie, qui a démontré son efficacité par rapport à d'autres algorithmes d'optimisation, tels que l'Algorithme du Cancer du Foie, l'Algorithme d'Optimisation des Morse et l'Algorithme d'Optimisation des Zèbres. Cet algorithme optimise la fonction objective du coût total de l'énergie sur 24 ans en intégrant des sources photovoltaïques et des batteries de condensateurs, en tenant compte de la nature intermittente de ces sources et des variations de charge sur 24 heures. Les résultats montrent des solutions de haute qualité comparées à d'autres méthodes rapportées dans la littérature. Les résultats des simulations montrent également que les algorithmes proposés sont fiables et applicables pour l'intégration optimale des sources de production décentralisée dans divers réseaux de distribution de tailles et de complexités différentes.

Mots clés:

Production Décentralisée (DG), Sources d'Énergie Photovoltaïque (PVRES), Batteries de Condensateurs (CB), Réseaux de Distribution Radiaux, Optimisation Méta-heuristique, Optimiseur de Loups Gris (GWO), Optimisation par Essaim Particulaire (PSO), Algorithme d'Optimisation des Baleines (WOA), Algorithme EM-BT, Optimisation Multi-Objectifs (MOO), Minimisation des Pertes d'Énergie, Stabilité du Profil de Tension, Optimiseur de la Vallée d'Énergie (EVO), Théorie de la Logique Floue.

الملخص

يعد هذا العمل جزءًا من دراسة حول التكامل الأمثل للتوليد الموزع (DG) القائم على مصادر الطاقة الكهروضوئية المتجددة وبنوك المكثفات في شبكات التوزيع الشعاعية، وهي شبكات IEEE 33-JB وIEEE 69-JB و ALG-AB-Hassi Sida 157، المستخدمة على نطاق واسع في الأدبيات لتخطيط وتشغيل أنظمة التوزيع. ولتحسين استخدام المصادر الكهروضوئية وبنوك المكثفات على النحو الأمثل، تم اقتراح طرق تحسينية حديثة لتحديد موقعها وحجمها الأمثل. وتشمل هذه الأساليب مُحسِّن الذئب الرمادي (GWO)، وخوارزمية تحسين سرب الجسيمات (PSO)، وخوارزمية تحسين الحوت (WOA)، وخوارزمية EM-BT. و مع ذلك، تم استخدام الطريقة العكسية إلى الأمام لحسابات تدفق الطاقة.
بالنسبة للتكامل الأمثل، تم اقتراح ثلاث دراسات: الأولى تركز فقط على تقليل خسائر الطاقة في شبكات التوزيع من خلال دمج العديد من مصادر التوليد الموزعة. أما الدراسة الثانية فتركز على تقليل خسائر الطاقة اليومية وانحرافات ملف الجهد، والتكيف مع ظروف الحمل الديناميكية على مدار 24 ساعة. يتم تسجيل هذا الهدف في دالة هدف موحدة (Obj1)، والتي تمتد إلى تقليل التكاليف المرتبطة بخسائر الطاقة والطاقة التي توفرها المصادر الكهروضوئية وبنوك مكثفات مصادر الطاقة التفاعلية (PVRES-CBs)، وبالتالي تشكيل نموذج هدف شامل .(Obj2)
يتم تقييم فعالية خوارزمية MOMVO المقترحة بدقة من خلال تحليل مقارن مع ثلاث خوارزميات تحسين أخرى: خوارزمية البحث متعدد الأهداف (MOJS)، وخوارزمية التلقيح متعدد الأهداف (MOFPA) وخوارزمية ليشتنبرغ متعددة الأهداف .(MOLA) تنتج المقارنة جبهة باريتو، وهو أمر ضروري لصانعي القرار أو مشغلي أنظمة الطاقة الذين يواجهون أهدافًا غامضة أو ضبابية لكل وظيفة. يتم استخدام نظرية المنطق الضبابي للمساعدة في تحديد نقطة التشغيل المثلى من مجموعة حلول باريتو المثلى، وتحديد أفضل حل غير مهيمن من خلال تعظيم المجموع الطبيعي لقيم دالة العضوية على جميع الأهداف.
وبالإضافة إلى ذلك، تستكشف الدراسة الاختلافات في أفضل الحلول التوفيقية المستمدة من الخوارزميات المذكورة، مما يوفر معلومات قيمة حول أدائها ومدى ملاءمتها في ظل ظروف الشبكة المختلفة. أُجريت دراسة أخرى باستخدام مُحسِّن وادي الطاقة، الذي أظهر فعاليته مقارنةً بخوارزميات التحسين الأخرى، مثل خوارزمية سرطان الكبد وخوارزمية تحسين الفأر وخوارزمية تحسين الحمار الوحشي. تعمل هذه الخوارزمية على تحسين دالة الهدف المتمثلة في التكلفة الإجمالية للطاقة على مدار 24 عامًا من خلال دمج المصادر الكهروضوئية وبنوك المكثفات، مع مراعاة الطبيعة المتقطعة لهذه المصادر والتغيرات في الأحمال على مدار 24 ساعة. تُظهر النتائج حلولاً عالية الجودة مقارنةً بالطرق الأخرى المذكورة في الأدبيات. تُظهر نتائج المحاكاة أيضًا أن الخوارزميات المقترحة موثوقة وقابلة للتطبيق من أجل الدمج الأمثل لمصادر التوليد الموزعة في شبكات توزيع مختلفة الأحجام والتعقيد.

الكلمات المفتاحية : التوليد اللامركزي (DG) ، مصادر الطاقة الكهروضوئية (PVRES)، بنوك المكثفات (CB) ، شبكات التوزيع الشعاعية، التحسين الفوقي، محسن الذئب الرمادي (GWO)، تحسين سرب الجسيمات (PSO) ، خوارزمية تحسين الحوت (WOA)، خوارزمية (EM-BT)، التحسين متعدد الأهداف (MOO) , تقليل فقدان الطاقة، استقرار ملف الجهد، محسن وادي الطاقة (EVO)، نظرية المنطق الضبابي.

Dedication

I dedicate this thesis to...

My dear mother

My dear father

My dear grandmother and my dear aunts

My dear sister Riham

My dear brothers Mohamed and Louai

The whole family

My dear friends

All my teachers

Everyone I value and hold dear.

Acknowledgements

First and foremost, I thank Allah, the Almighty, who has given me the strength, patience, and will to complete this modest work.

I would also like to thank my thesis director, Mr. Guia Talal, a doctor at the University of Hamma Lakhder El Oued. With his experience in research and teaching, along with his advice and availability, I was able to explore the world of scientific research in the field of Optimization and Analysis of Electrical Networks. I am also grateful for his encouragement and kindness throughout the preparation of my thesis. It has truly been a pleasure working under his supervision.

Likewise, I warmly thank Dr. Ahmed Salhi, a distinguished research professor at Mohamed Khider University of Biskra. Dr. Salhi has been an indispensable part of my thesis journey, providing expert guidance and crucial support throughout the entire research process. His deep knowledge and experience in areas such as applying meta-heuristic methods in power system optimization, integrating renewable energy in power systems, FACTS controllers, and power system stability and security have greatly enriched my work. His invaluable insights in these fields have significantly guided my research direction and methodology, and his support has been crucial in advancing my thesis.

Dr. Salhi’s willingness to share his expertise, his constructive feedback, and his timely advice have been instrumental in overcoming various challenges and advancing my thesis. His dedication to my academic growth and his commitment to excellence have significantly impacted my research, and I am deeply appreciative of his unwavering assistance and encouragement. Working with Dr. Salhi has been a privilege, and his support has been a cornerstone of my academic achievements.

I would like to sincerely thank the members of the jury:

- Mr. Laid Zellouma , Doctor at University Hamma Lakhder el oued, for accepting to chair this thesis and for his valuable support.
- Mr. Naimi Djemai , Professor at the University of Mohamed Khaider biskra, for his interest in our work and his participation in the jury as an examiner.
- Mr. Abdelhafid Rouina , Doctor at University Mohamed Khaider biskra, for his presence and for the time he generously dedicated to evaluating this work.

Finally, I must not forget to thank the members of the Electrical Engineering Laboratory of Biskra (LMSE) and (LGEB) for all their help and encouragement in completing this work.

List of Figures

CHAPTER I

Overview of Distribution Networks

CHAPTER II

Power Flow in Distribution Networks

CHAPTER III

Metaheuristic Techniques for Distribution Networks

CHAPTER IV

Results and Discussions: Single-Objective and Multi-Objective Planning of Distributed Generation

CHAPTER V

Results and Discussions: A Comparison of Recently Developed Metaheuristic Optimization Techniques on the Real Distribution Networks of ALG-AB-Hassi Sida, Algeria

List of Tables

CHAPTER I

Overview of Distribution Networks

CHAPTER II

Power Flow in Distribution Networks

CHAPTER III

Metaheuristic Techniques for Distribution Networks

CHAPTER IV

Results and Discussions: Single-Objective and Multi-Objective Planning of Distributed Generation

CHAPTER V

Results and Discussions: A Comparison of Recently Developed Metaheuristic Optimization Techniques on the Real Distribution Networks of ALG-AB-Hassi Sida, Algeria

List of Contents

GENERAL INTRODUCTION

CHAPTER I

Overview of Distribution Networks

CHAPTER II

Power Flow in Distribution Networks

CHAPTER III

Metaheuristic Techniques for Distribution Networks

CHAPTER IV

Results and Discussions: Single-Objective and Multi-Objective Planning of Distributed Generation

CHAPTER V

Results and Discussions: A Comparison of Recently Developed Metaheuristic Optimization Techniques on the Real Distribution Networks of ALG-AB-Hassi Sida, Algeria

General Conclusion and Perspectives

LIST OF REFERENCES

ANNEXES

Publications

List of abbreviations

AC	Alternating Current
HV	High Voltage
MV	Medium Voltage
LV	Low Voltage
DG	Distributed Generation
PV	Photovoltaic (related to renewable energy and generation units)
SCADA	Supervisory Control and Data Acquisition
GRTE	Gestionnaire du Réseau de Transport d'Électricité (Transmission Network Operator)
GRDE	Gestionnaire du Réseau de Distribution d'Électricité (Distribution Network Operator)
FACTS	Flexible AC Transmission Systems
RTU	Remote Terminal Unit
RES	Renewable Energy Sources
BFS	Backward Forward Sweep
SLACK	Slack Bus (Reference Bus)
PV	Power-Voltage Bus (Control Bus)
PQ	Load Bus (Power-Load Bus)
IEEE	Institute of Electrical and Electronics Engineers
VSI	Voltage Stability Index
NR	Newton-Raphson (Method)
GS	Gauss-Seidel (Method)
RD	Radial Distribution Network
OLTC	On Load Tap Changer
THD	Total Harmonic Distortion
PU	Per Unit System
MVA	Mega Volt-Ampere
KVL	Kirchhoff's Voltage Law
KCL	Kirchhoff's Current Law
GA	Genetic Algorithm
PSO	Particle Swarm Optimization
GWO	Grey Wolf Optimization
WOA	Whale Optimization Algorithm
EM-BT	Electromagnetism-Like BitTorrent Algorithm
NFL	No Free Lunch (theorem)
EA	Evolutionary Algorithm
SI	Swarm Intelligence
CEC	Congress on Evolutionary Computation
LP	Linear Programming
NLP	Non-Linear Programming
GMP	Geometric Programming
QPP	Quadratic Programming Problem
SA	Simulated Annealing
TS	Tabu Search

GRASP	Greedy Randomized Adaptive Search Procedure
VNS	Variable Neighborhood Search
ILS	Iterated Local Search
BH	Black Hole Algorithm
GSA	Gravitational Search Algorithm
BB-BC	Big Bang-Big Crunch Algorithm
OIO	Optics-Inspired Optimization
CBO	Collision-Based Optimization
LCA	League Championship Algorithm
TLBO	Teaching-Learning-Based Optimization
MBO	Mine Blast Algorithm
SKF	Simulated Kalman Filter
SCA	Sine Cosine Algorithm
PVRES	Photovoltaic Renewable Energy Sources
CB	Capacitor Banks
EM-BT	Efficient Metaheuristic BitTorrent
GWO	Grey Wolf Optimizer
PSO	Particle Swarm Optimization
WOA	Whale Optimization Algorithm
MOMVO	Multi-Objective Multi-Verse Optimization
MOJS	Multi-Objective Jellyfish Search
MOFPA	Multi-Objective Flower Pollination Algorithm
MOLA	Multi-Objective Lichtenberg Algorithm
IEEE	Institute of Electrical and Electronics Engineers
kVAr	Kilovolt-Amperes Reactive
pu	Per Unit (used for voltage levels)
MPP	Maximum Power Point
Isc	Short-Circuit Current
Voc	Open-Circuit Voltage
FF	Filling Factor
VDD	Voltage Deviation per Day
ELD	Energy Loss per Day
TOC	Total Operating Cost
KP	Coefficient for PV Penetration
Closs	Cost of Energy Losses
Tj	Junction Temperature
Rti	Temperature-Dependent Resistance
AC	Alternating Current
QCB	Reactive Power from Capacitor Banks
PD	Power Demand
CB	Capacitor Bank
EVO	Energy Valley Optimizer
LCA	Liver Cancer Algorithm
ZOA	Zebra Optimization Algorithm
WaOA	Walrus Optimization Algorithm
PSO	Particle Swarm Optimization
GA	Genetic Algorithm
BFOA	Bacterial Foraging Optimization Algorithm

List of abbreviations

PV	Photovoltaic
HRES	Hybrid Renewable Energy Systems
kVAr	Kilovolt-Amperes Reactive
kW	Kilowatt
pu	Per Unit (used for voltage levels)
VMPP	Voltage at Maximum Power Point
IMPP	Current at Maximum Power Point
Voc	Open-Circuit Voltage
Isc	Short-Circuit Current
Tcy	Cell Temperature
Tj	Junction Temperature
CCE	Cenergy Cost of Energy
Qcb	Reactive Power of Capacitor Bank
PDG	Active Power of Distributed Generation
NPV	Net Present Value
ROI	Return on Investment
PDF	Probability Density Function

GENERAL INTRODUCTION

General Introduction

The rapid advancement of technology, global environmental concerns, and the deregulation of the electricity market have sparked increasing interest in Distributed Generation (DG). As a result, implementing DG within distribution systems has emerged as a key solution for delivering energy to consumers. Among the various DG technologies, the use of renewable energy resources, such as solar power and capacitor banks, has gained significant attention due to their environmental benefits.

The optimal planning of renewable energy-based DG in distribution systems offers numerous technical and economic benefits, aiming to enhance the overall system performance. However, the optimal integration of DG, particularly photovoltaic (PV) and capacitor banks (CB), remains a challenging task due to the stochastic behaviour of renewable resources.

The installation of Distributed Generation (DG) offers numerous potential benefits, including improved system reliability, reduced power losses in transmission lines, enhanced voltage quality, and minimized operational and maintenance costs, as well as the cost of power losses. Additionally, reducing costs associated with power losses and lowering greenhouse gas emissions demonstrate that DG is environmentally friendly.

To fully benefit from these advantages, it is essential to optimally select the size and location of DG units to maximize these benefits and avoid undesirable issues. Otherwise, their installation could negatively impact energy quality and system operation. Improper sizing and placement may lead to increased power losses and poor energy quality. To ensure optimal DG integration, several factors must be considered, including the best technology to use, the number of DG units, the size and location of each unit, and the type of connection.

The integration of DG into distribution systems requires comprehensive analysis and planning tools. This process typically involves technical, economic, regulatory, and potentially environmental challenges. Recently, various algorithms have been widely implemented and proposed to address the optimization challenges associated with DG integration in different systems. Optimization techniques are constantly evolving and have become a focal point of many new research studies. The main differences among these solutions lie in the problem formulation, methodology, constraints, and assumptions made. DG planning can be viewed as a discrete, nonlinear, and constrained optimization problem, often formulated as an optimal power flow problem with either a single-objective or multi-objective optimization function. The objectives must be properly optimized while ensuring the system's operational constraints are met.

This thesis presents significant advancements in the optimization of distribution networks with Distributed Generation (DG) through the introduction of several novel algorithms and methodologies. The first contribution is the application of the Energy Metaheuristic BitTorrent (EM-BT) algorithm, which aims to minimize daily energy losses and voltage profile deviations while incorporating temperature effects on Photovoltaic Renewable Energy Sources (PVRES) and capacitor banks (CB). This approach not only optimizes the allocation of these resources but also outperforms traditional algorithms such as Particle Swarm Optimization (PSO), Grey Wolf Optimizer (GWO), and Whale Optimization Algorithm (WOA) in reducing energy losses and voltage deviations. The second key contribution introduces the Multi-Objective Multi-Verse Optimization (MOMVO) algorithm, which enhances the optimization process by including temperature variations and irradiance levels, providing superior performance compared to other multi-objective optimization techniques like Jellyfish Search (MOJS) and Flower Pollination Algorithm (MOFPA). Finally, the Energy Valley Optimizer (EVO) is proposed as a dynamic solution that adapts to the variability of load patterns over 24 hours and minimizes energy costs over a 24-year lifespan. This method demonstrates notable improvements in CB and DG placement, addressing both technical and economic aspects effectively. Together, these contributions provide a comprehensive and innovative approach to optimizing DG integration in distribution networks, considering both operational efficiency and cost-effectiveness.

Two types of renewable DG sources will be studied: photovoltaic sources and capacitor banks (CB). This study will consider the number of DG units, the size of each unit, and whether each DG provides only active power or also reactive power. To ensure their optimal integration, various new metaheuristic algorithms will be employed. The objective is to improve the distribution network's performance by minimizing daily energy losses, voltage profile deviations, and energy costs over a 24-year lifespan while meeting constraints within a specified tolerance for distribution systems of varying sizes and complexities. Additionally, the study will account for uncertainty in load demand and DG power over 24 hours, allowing for the assessment of their impact on network parameters throughout the day.

Each chapter explores a key component of this transformation, from understanding the foundations of conventional electrical systems to adopting innovative solutions through advanced technologies. The chapters are structured as follows:

- **In Chapter 1,** Algeria's electrical network, which forms the backbone of the country's energy distribution, operates through a standardized three-phase alternating current (AC) system at 50 Hz. Historically, these networks were designed for centralized power generation, delivering electricity from large power plants to consumers. However, with increasing energy demands and rising environmental concerns, there is a critical need to modernize these systems. This chapter highlights the transition toward smarter and more sustainable energy solutions, emphasizing the integration of renewable energy sources such as solar and wind. This transformation involves updating infrastructure, including distribution networks, to support decentralized energy production and the implementation of smart grid technologies. These smart grids leverage advanced communication and control systems to enhance network management, improve reliability, and reduce energy losses, thereby positioning Algeria to sustainably meet its growing energy needs.
- **In Chapter 2,** the efficient operation of electrical distribution networks relies heavily on accurate power flow calculations, which are crucial for effective planning and management of electricity distribution. This chapter focuses on the Backward/Forward

Sweep (BFS) method, a prominent technique for addressing power flow problems in radial distribution networks, commonly found in Algeria. Radial networks are characterized by a central power source feeding multiple branches, resulting in unidirectional power flow. The BFS method is particularly suited for these networks, as it calculates branch currents through a backward sweep and bus voltages through a forward sweep. The chapter applies the BFS method to various network configurations, illustrating its effectiveness in minimizing energy losses and maintaining stable voltage profiles, even in complex or unbalanced scenarios. Through optimization of power flow, this chapter demonstrates how the BFS method can enhance the efficiency and reliability of Algeria's distribution network.

- **Chapter 3,** explores the foundational principles of metaheuristic algorithms, focusing on their application in optimizing distribution networks, especially in contexts like renewable energy integration. The chapter covers various metaheuristic techniques, highlighting their ability to handle complex optimization problems. These techniques are classified and examined based on factors such as solution space exploration, search history, and algorithmic inspiration. Furthermore, the chapter discusses the extension of metaheuristics to multi-objective, multi-population, parallel, and hybrid models. Real-world applications, including energy distribution optimization, are presented, demonstrating the robustness and versatility of these methods in solving electrical network problems efficiently.
- **In Chapter 4,** the need for optimized management of distributed generation (DG) resources, such as photovoltaic renewable energy sources (PVRES), becomes increasingly critical as Algeria aims to integrate more renewables into its grid. This chapter introduces the Efficient Metaheuristic BitTorrent (EM-BT) algorithm, designed specifically to optimize the allocation and sizing of DGs and capacitor banks (CBs) within distribution networks. The EM-BT algorithm accounts for the 24-hour variability in load patterns, solar irradiance, and temperature, ensuring efficient network operation throughout the day. By applying the algorithm to test networks like the IEEE 33-bus and 69-bus systems, the chapter demonstrates that EM-BT surpasses other optimization methods in reducing energy losses and enhancing voltage profiles. Additionally, the chapter presents the Multi-Objective Multi-Verse Optimization (MOMVO) algorithm, which further boosts network efficiency by optimizing multiple objectives simultaneously, such as minimizing both energy losses and voltage deviations.
- **In Chapter 5,** several newly developed metaheuristic algorithms are applied to real-world distribution networks in Algeria. The chapter compares the Energy Valley Optimizer (EVO), Liver Cancer Algorithm (LCA), Zebra Optimization Algorithm (ZOA), and Walrus Optimization Algorithm (WaOA) in optimizing the placement and sizing of distributed generation (DG) and capacitor banks (CB) within the Algerian 157-bus radial distribution network. These algorithms are evaluated under dynamic conditions, accounting for hourly load variations and the long-term objective of minimizing energy costs over 24 years. Through a detailed performance comparison, the chapter highlights the strengths and weaknesses of each algorithm in addressing both technical and economic challenges. By presenting case studies, it demonstrates

how these advanced optimization techniques can enhance grid efficiency, reduce energy losses, and maintain voltage stability, contributing to Algeria’s sustainable energy future.

CHAPTER I

Overview of Distribution Networks

I.1. Introduction

Electrical networks are fundamental to modern infrastructure, ensuring the reliable delivery of electricity from generation plants to end users. These systems operate on a standardized three-phase alternating current (AC) at 50 Hz and consist of key components such as generators, transformers, transmission lines, and protection systems. However, electrical networks worldwide are undergoing significant transformations driven by market liberalization, environmental concerns, and the rise of advanced technologies that enable decentralized power generation.

In Algeria, the electrical network serves as the backbone of the country's energy infrastructure. Originally designed for a unidirectional flow of electricity, the network now faces new challenges with the increasing integration of renewable energy sources like solar and wind. This shift introduces complexities in grid stability, voltage control, and overall management, prompting efforts to modernize the distribution network. Central to these efforts is the development of Distribution Smart Grids, which utilize advanced communication technologies and intelligent management systems to enhance efficiency and reliability.

This chapter explores the evolution of Algeria’s electrical networks, focusing on both conventional and smart distribution networks, their characteristics, and the integration of decentralized power generation. It begins with a comprehensive overview of conventional networks, examining their structure, function, and the challenges posed by the growing penetration of renewable energy sources. The discussion then shifts to smart distribution networks, highlighting advanced features such as real-time monitoring, bidirectional power flows, and intelligent management systems. The chapter also delves into the role of decentralized power generation—including solar, wind, and other renewable sources—in reshaping Algeria’s grid. It analyzes the impact of these distributed energy resources on grid stability, voltage control, and protection schemes, and explores how smart grids facilitate their integration.

The chapter emphasizes the technical, operational, and economic implications of these changes and outlines the strategies employed, such as network reinforcement, optimization of decentralized production, and the adoption of advanced technologies. By providing a detailed analysis of both conventional and smart grid architectures, this chapter aims to establish a solid foundation for understanding the complexities and potential of modern electrical networks. It highlights the ongoing transition towards a resilient, sustainable, and adaptable energy infrastructure that supports the country’s energy transition goals.

I.2. Electrical Network Structure

The term "Electrical Network" encompasses the entire electricity supply chain, a complex system that ensures the flow of electricity from its point of generation to the point of consumption. This chain can be broken down into three crucial stages:

- **Power Generation:** This stage lies at the heart of the system, where electricity is produced using various sources. Traditionally, large-scale and controllable sources dominate this area. Fossil fuel power plants, nuclear power plants, and hydroelectric dams are prime examples. These sources offer the flexibility to adjust energy production based on safety and economic considerations, ensuring the grid has enough power to meet demand [1].

- **Transmission Networks:** Once generated, electricity needs to travel long distances efficiently. This is where high voltage (*HV*) transmission lines, typically exceeding 50 *kV* in voltage, come into play. These interconnected lines form the backbone of the network, often arranged in a mesh structure. This design offers several advantages. It ensures reliable and readily available energy throughout the system, even during faults on individual lines. The interconnected nature allows for efficient routing of electricity, minimizing transmission losses [2].
- **Distribution Systems:** Finally, electricity reaches its destination – homes, businesses, and industries – through medium voltage (*MV*) and low voltage (*LV*) distribution networks. MV networks typically operate between 1 kV and 50 kV, while LV networks operate below *1 kV*. These networks deliver electricity directly to consumers. Unlike transmission lines, they primarily operate in a radial structure, resembling branches stemming from a central trunk line. This simpler design facilitates the implementation of robust protection schemes that quickly isolate faults and minimize disruptions [3]. This radial structure, however, limits the flow of electricity to a single direction – from generation to consumption.

The transmission and distribution network structure is organized into subdivisions based on voltage levels, as depicted in Figure I.1.

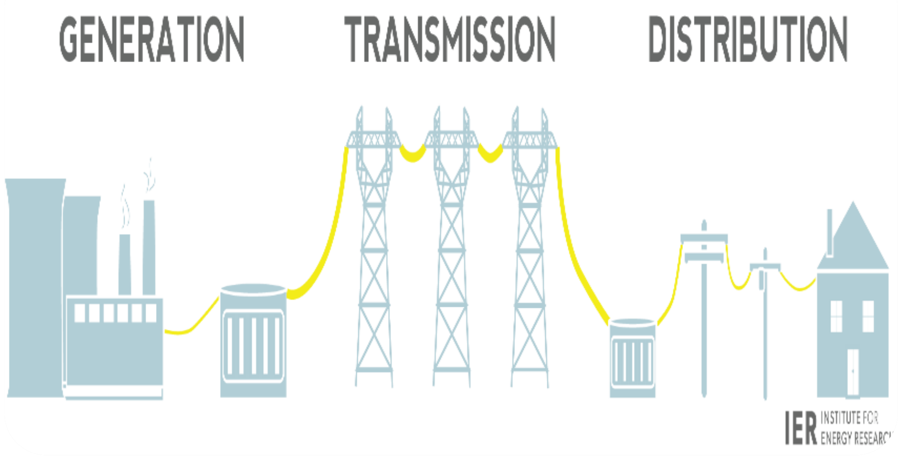

Figure I.1. Diagram depicting the organizational structure of electrical networks categorized by their voltage levels [4].

The entire electricity supply chain operates under a crucial principle: the constant balance between generated and consumed electrical power. To achieve this, the network relies on real-time control of power generation. A central authority, often the electricity transmission network operator, constantly monitors and adjusts generation output based on fluctuations in demand. This vertically integrated structure offers several benefits:

- **Reduced Operating Costs:** By centrally managing generation and coordinating power plants, the system avoids inefficiencies and optimizes resource allocation.
- **Shared Generator Reserve Margins:** Power plants can maintain lower individual reserves knowing there's a collective backup plan in case of unexpected demand surges.
- **Enhanced Efficiency of Large Generators:** Large-scale power plants operate most efficiently within a specific output range. The system ensures these generators function within their optimal range for maximum efficiency.
- **Minimized Failure Risks:** The centralized control system can anticipate potential problems and take preventive measures to minimize the risk of widespread outages [3].

I.3. Operation of Electrical Networks

Physically, the electrical network is segmented into different voltage levels: the transmission network and the distribution network. The transmission network connects large centralized production groups and handles the high-voltage transport of electricity across long distances. In contrast, the distribution network caters to the majority of consumers, distributing electricity at lower voltage levels for residential, commercial, and industrial use [5], Figure I.2 illustrates the general architecture of electrical networks in Algeria, showcasing the hierarchical structure and the relationship between the transmission and distribution networks.

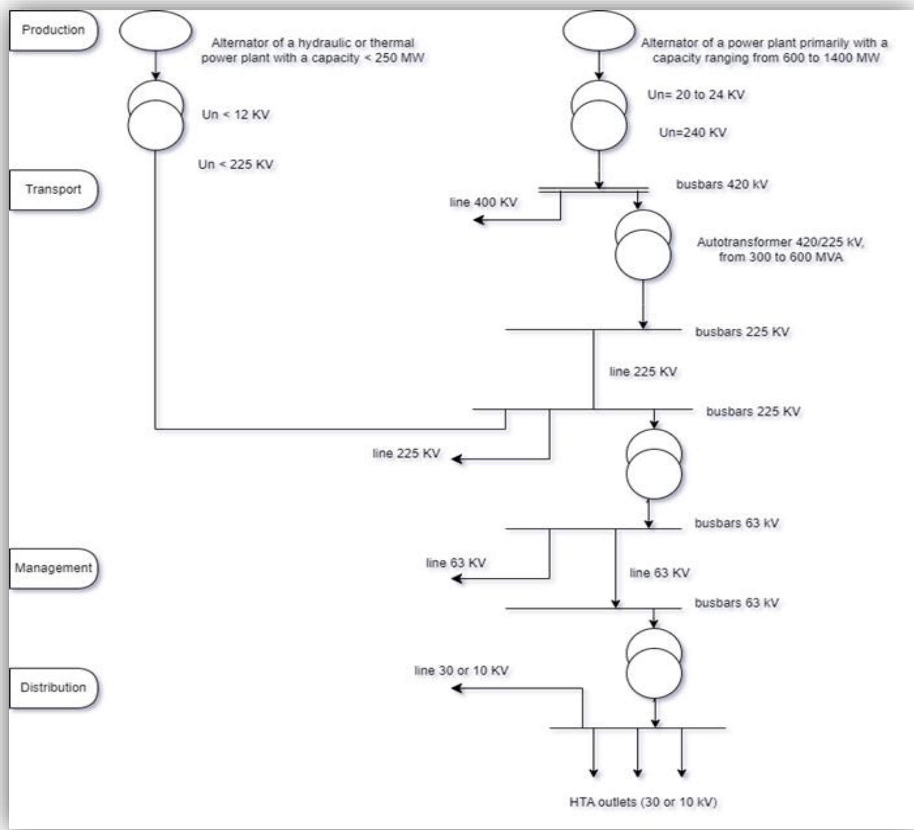

Figure I.2. General Architecture of the Electrical Network in Algeria.

I.3.1. Production

The backbone of large-scale electricity production is primarily composed of substantial synchronous alternators driven by steam, gas, or hydraulic turbines. These production units are connected to the transmission network via step-up transformers. The active power outputs of these units range from about 100 MW in smaller thermal power plants to up to 1650 MW in the most powerful nuclear power plant units.

The categorization of production units is based on the primary energy source utilized for electricity generation, which includes fossil fuels (coal, natural gas, and oil), nuclear energy, and renewable resources such as hydroelectric power, wind, and solar energy. Each type of production unit has its own set of advantages, operational characteristics, and impacts on the electrical grid, contributing to the overall stability and efficiency of the power supply system.

Fossil fuel plants are reliable and can produce large amounts of electricity, but they emit significant amounts of greenhouse gases. Nuclear plants produce vast amounts of electricity with low greenhouse gas emissions, but they pose challenges related to radioactive waste and safety concerns. Renewable energy sources, while environmentally friendly and sustainable, can be intermittent and require advanced technologies and infrastructure for integration into the grid. Each production type thus plays a vital role in maintaining a balanced and resilient power system [6].

I.3.2. Transmission

Transmission networks serve the critical function of transporting electrical energy over long distances. Operating at very high voltages, from 63 kV to 400 kV, these networks are designed to reduce joule losses and improve efficiency. Structurally, these networks are either meshed or interconnected to efficiently collect and transport large quantities of electricity generated by major power plants to consumption areas, serving both transport and interconnection functions. Predominantly, these networks are composed of overhead lines. Given their integral role in the system, they are equipped with robust protection systems to ensure stability and security.

The management of these networks is complex due to substantial and fluctuating power transfers between production and consumption areas. This necessitates meticulous monitoring to manage voltage, frequency, power flow distribution, production costs, and other critical parameters. The techno-economic optimization of transmission networks is particularly challenging compared to distribution networks. This complexity arises from the need to balance efficiency and cost-effectiveness while maintaining the reliability and stability of the entire electrical grid [6].

I.3.3. Distribution

Distribution networks serve as the crucial infrastructure for local electrical energy distribution, operating at voltages lower than or equal to 50 kV. The distribution system comprises two types of networks: the medium voltage (MV) network and the low voltage (LV) network. The MV

network typically operates at voltage levels of 10 *kV* and 30 *kV* and is connected to the transmission network. The *LV* network operates at 0.4 kV and forms the final segment of the electrical system, with segments linked to the *MV* network through *MV/LV* transformation substations.

The chosen voltage levels represent a balance between technical efficiency and economic viability, aiming to reduce voltage drops, limit the necessity for additional substations, and alleviate the constraints associated with higher voltages. This strategic selection of voltage levels helps to optimize the performance of the distribution network, ensuring reliable and cost-effective delivery of electricity to end consumers, including residential, commercial, and industrial users [6].

I.3.4. Consumption

In electrical networks, consumption primarily involves the generation of thermal, light, and mechanical energy, serving both residential and industrial needs. Consumers, or loads, are defined by their active and reactive power consumption. Assessing these consumptions over specific timeframes provides insights into peak and average power demands. Load curves, which illustrate how loads vary over time, are derived by measuring currents at transformation stations between transmission and distribution networks. These curves are instrumental for network operators to anticipate consumption patterns and develop accurate production forecasts.

Understanding load curves is essential for maintaining the balance between supply and demand, ensuring the stability of the electrical grid. By analyzing these curves, network operators can optimize the scheduling of power generation, manage the distribution of electricity more efficiently, and plan for future infrastructure needs. This data-driven approach helps in minimizing energy waste, reducing operational costs, and improving the overall reliability and efficiency of the electrical network [6].

I.3.5. Supervision

The efficient transmission and distribution of electrical energy are managed by two types of network operators: the electricity transmission network operators (GRTE) and the electricity distribution network operators (GRDE). Supervision is conducted from dispatching centers operating in a hierarchical manner across the country. This hierarchy spans from a national dispatching center overseeing the electrical system at a national level down to regional and local units responsible for transmission and distribution networks.

Supervision is vital for ensuring a balance between production and demand, maintaining frequency regulation, and the overall stability of the electrical system. Dispatching centers play a crucial role in voltage regulation by adjusting the tap settings of transformers and modulating the production or absorption of reactive power through devices like synchronous or static compensators. This ensures optimal network performance and helps to maintain the reliability and efficiency of the electrical grid. Additionally, these centers monitor and control various parameters of the network to prevent outages, manage emergency situations, and facilitate the integration of renewable energy sources [6].

I.4. Distribution Networks

I.4.1. Classification

Distribution networks are categorized into two types based on voltage levels, distinguishing between medium voltage (*MV*) networks, connected to the transmission network, and low voltage (*LV*) networks [7].

Table I.1. Table presenting the characteristics of architectures.

Medium Voltage Distribution Networks	Low Voltage Distribution Networks
- Medium voltage lines facilitate local-scale electricity transportation to small industries. Common voltage levels for medium voltage include 30 kV and 10 kV. The neutral point is grounded through a resistor. Current is limited to 300 A for overhead networks. Current is limited to 1000 A for underground networks. Underground networks are typically designed in an open-loop configuration.	- Low voltage lines, the smallest in the network, power everyday household appliances. - The typical voltage level for low voltage is 230/400 V. - The neutral point is directly grounded. - Low voltage networks can be of three types : radial, meshed, and looped configurations

I.4.2. Characteristics of different types of architectures.

Table I.2. Table presenting the characteristics of architectures.

Architecture		Utilization	Advantage	Disadvantage
Radial	Single antenna	Service continuity-low-demand process	Simplest structure, easy to protect, minimal cost	Low power availability, long fault interruption time – a single fault leads to antenna power cut-off.
	Double antenna	Continuous process in steelmaking, petrochemicals	Good power continuity, possible maintenance of the main switchboard	Costly solution - partial operation of the bus bar during maintenance
	Double derivation	Urban networks with limited extensions	Good power continuity, simplicity of protection	Need for automation functions
	Double bus bar	High-service continuity processes, processes with high load variation	Good power continuity, flexibility of use: seamless transfer, easy maintenance	Costly solution - need for automation functions
	Open loop	Extensive networks with significant future expansions, bearing	Less expensive than closed-loop systems, simplicity of protection.	Power cut-off of a section during a fault during loop reconfiguration - need for automation functions

Loop		concentrated loads in different zones of a site		
	Closed loop	Networks with high service continuity, extensively covering various zones of a site	Good power continuity, no need for automation functions	Costly solution - complexity of the protection system
Internal energy production	Local production	Industrial sites with self-power generation processes	Good power continuity	costly solution
	Replacement	Industrial and tertiary sites	Good continuity of power supply for priority loads	Need for automation functions

I.4.3. Structure of distribution networks:

I.4.3.1. General structure of a private distribution network

In the general case with a high voltage supply, a private distribution network consists of several key components. These include a high voltage delivery point supplied by one or more sources, which comprises one or more bus bars and protective circuit breakers. It also features an internal production source and one or more high voltage to medium voltage transformers. A main medium voltage panel, consisting of one or more bus bars, connects to an internal medium voltage distribution network that supplies secondary panels or *HV/LV* substations. The network includes medium voltage receivers, *HV/LV* transformers, low voltage panels, and low voltage networks. These components work together to supply low voltage receivers [8].

Figure I.3. Illustrates the general structure of a private distribution network, highlighting the interconnected components and their roles within the system.

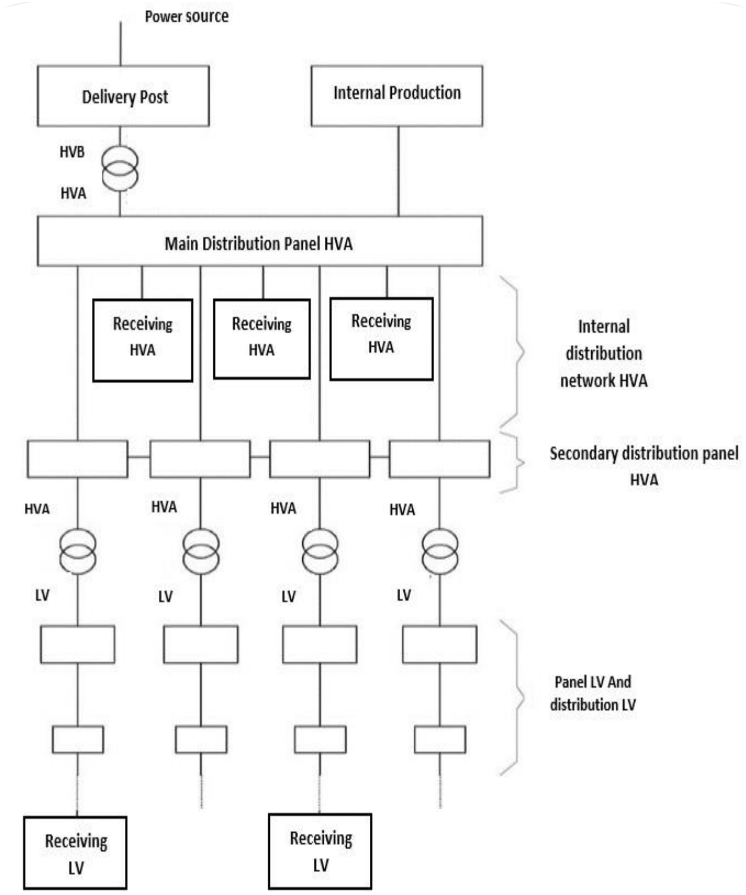

Figure I.3. General structure of a private distribution network.

I.4.4. Operating Schemes of the Distribution Network

I.4.4.1. HVB/HVA Primary Substations

Distribution networks receive their supply from *HVB/HVA* (High Voltage B/High Voltage A) primary substations, which are pivotal components in the infrastructure. These substations typically comprise a setup where a second transformer is incorporated, forming an assembly known as half-frame transformers on the *HVA* side. Additionally, another set of bus bars is dedicated to supplying the various branches of the distribution network. While these transformers generally operate in a radial configuration, they can adapt to different scenarios. In specific instances, *HVA* branches are organized into half-frames, a categorization that depends on factors such as whether they are overhead or underground and the similarity in their load curves. The load curve classification is primarily determined by the type of customers connected to each branch, ensuring an efficient and tailored distribution of power across the network [9].

Figure I.4. illustrates the schematic diagram of *HVB/HVA* primary substations across three phases: initial, second, and final phases.

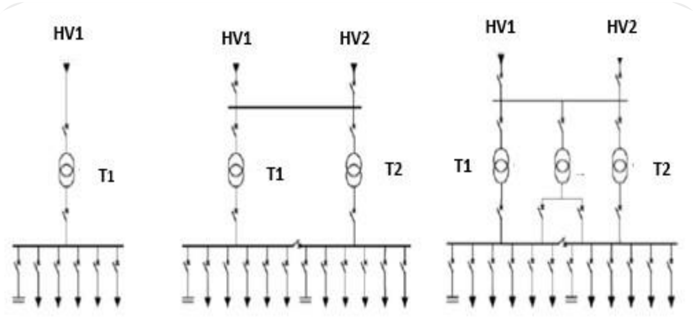

a/ Initial phase b/ Second phase c/ Final phase

Figure I.4. Schematic diagram of HVB/HVA primary substations.

I.4.4.2. HVA Lines or Departures

The *HVA* network predominantly exhibits a radial tree structure, often reinforced by additional half-loops or substations to enhance operational safety and reliability. Characteristically, it comprises a primary artery or backbone from which branches extend to distribute power to various areas. Depending on the load density and geographical factors, the distribution network may be implemented as either overhead lines or underground cables, each suited to specific environmental and operational requirements.

Overhead lines are typically used in rural or less densely populated areas due to their cost-effectiveness and ease of maintenance. However, they are more susceptible to weather-related disruptions. In contrast, underground cables are preferred in urban or densely populated areas where space is limited, and aesthetic or safety concerns are paramount. Although more expensive to install and maintain, underground cables offer greater protection against environmental factors and lower the risk of outages.

The design of the *HVA* network aims to optimize efficiency and reliability while meeting the specific demands of the connected loads. This involves careful planning to ensure that the network can handle peak loads and provide redundancy to maintain service during maintenance or unexpected failures. The network's flexibility allows for adjustments and expansions to accommodate future growth and technological advancements [10].

I.4.4.3. Overhead HVA Networks

Overhead *HVA* networks consist of conductors, insulators, pylons, and guard cables for high-voltage lines, primarily tasked with transporting electrical energy from generation sites to consumption areas. They are favored for their lower installation and repair costs compared to underground lines, speedy repair post-accidents or faults, and ease of condition monitoring. Furthermore, they maintain voltage constancy along the line and accommodate higher current intensities without significant risk, contributing to their overall efficiency.

However, overhead *HVA* networks have several disadvantages. They can produce radio frequency interference affecting radio and TV reception, face opposition from affected landowners, and pose aesthetic and environmental concerns. Additionally, they are susceptible to atmospheric overvoltage's and can induce harmful electromotive forces in telecommunication circuits. The potential health impacts of electric and magnetic fields, along with the danger posed by conductor breakage, are also noteworthy disadvantages.

Despite these drawbacks, overhead *HVA* networks remain a practical choice due to their cost-effectiveness and operational efficiency. They are essential for the reliable transmission of electricity over long distances, ensuring that power generated at plants reaches the end consumers efficiently. Careful planning and design, along with technological advancements, continue to mitigate some of the negative impacts associated with overhead *HVA* networks. Figure I.5 Overhead lines.

Figure I.5. Overhead lines.

I.4.4.4. Underground HVA Networks

Underground cables, characterized by the absence of an electric field outside their metallic sheath, offer several advantages over overhead lines. They provide protection from atmospheric overvoltage's and are the preferred choice in densely populated areas or for crossing large water bodies where distances exceed 3 km. Additionally, underground cables do not cause interference with radio and television reception nor do they affect telecommunication circuits.

However, these networks come with notable disadvantages. They are significantly more expensive than overhead lines and require careful protection of their armor and sheaths against corrosion, particularly in regions prone to ground movements such as mining areas. Repairs are costly and challenging due to the difficulty in locating faults underground. Moreover, insulation can deteriorate from conductor temperature increases during overloads, adding to maintenance complexities.

The sizing of underground cables is subject to operational and external constraints influenced by climate conditions. Despite these challenges, underground cables remain indispensable in urban environments and for critical infrastructure projects requiring reliable, uninterrupted electricity supply. Their implementation and maintenance necessitate meticulous planning and investment to mitigate risks and ensure long-term operational efficiency. Figure I.6 Underground lines.

Figure I.6. Underground lines.

I.5. Smart Distribution Networks

I.5.1. Definition

Smart grids, a concept that emerged in the electrical sector several years ago, are now expanding across all energy networks, encompassing gas, heat, and water as well. They are sophisticated systems designed to integrate and coordinate the actions of various users – both consumers and producers – to ensure an efficient, sustainable, cost-effective, and secure supply of electricity. Smart grids are defined as a combination of infrastructure and embedded intelligence, leveraging software, automation, information transmission, and processing deployed at multiple levels of the energy chain. This integration enhances the functionality of production, transmission, distribution, and consumption, optimizing overall energy management and grid operations [11].

I.5.2. Objectives of Smart Grids

The increasing global demand for electricity necessitates the evolution of electric grids into smarter systems. Smart grids aim to address several fundamental shortcomings by enhancing network security at all levels, efficiently integrating and managing intermittent renewable energy sources, and promoting energy conservation through intelligent battery management. They also prioritize demand management by enabling grid users to adjust their consumption patterns in response to tariff signals, thereby optimizing the balance between production and consumption [12]. Smart grids thus represent a crucial advancement towards more resilient, efficient, and sustainable energy infrastructure worldwide.

I.5.3. Characteristics of Smart Grids

Smart grids are designed to address multiple challenges in modern energy systems, including aging infrastructure, persistent demand growth, rising integration of renewable sources and electric vehicles, and the imperative to enhance network security while reducing emissions. They are characterized by several key features: flexibility to manage the balance between production and consumption more effectively, enhanced reliability and efficiency of operations, improved accessibility to facilitate the integration of renewable energy sources, and economic benefits through advanced system management and energy savings [13]. Smart grids thus represent a pivotal advancement in energy infrastructure, offering solutions to improve resilience, sustainability, and overall performance in electricity distribution and management.

I.5.4. Architecture of Smart Grids

Typically, electricity grids follow a traditional architecture where electricity is generated at large plants, transmitted to substations, and then distributed to end-users. Smart grids revolutionize this concept with a bidirectional power flow that impacts both production and consumption, offering increased flexibility and transforming our relationship with electricity. They encompass a sophisticated system of interconnected devices that span energy transport, distribution, metering, and domestic usage. These devices, sourced from a diverse industrial ecosystem, interact and exchange continuous information flows crucial for energy applications.

The architecture of smart grids is structured into three main levels: infrastructure equipment for managing electricity routing, communication architectures for collecting data, and applications and services for real-time monitoring and automation [13]. As the demands and characteristics of current electrical grids evolve, smart grids represent a critical advancement in adapting to these changes [14, 15, 16]. They facilitate improved efficiency, resilience, and integration of renewable energy sources, marking a significant step towards a more sustainable and responsive energy infrastructure.

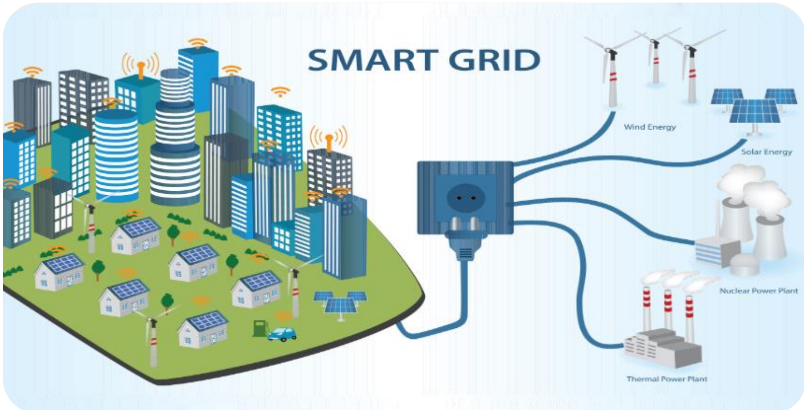

Figure I.7. Example of a Smart Grid Architecture.

Table I.3 below represents the main characteristics that distinguish conventional electrical grids from smart grids.

Table I.3. Comparison between Traditional and Smart Electrical Grids [14].

Characteristics of Traditional Electrical Grids	Characteristics of Smart Electrical Grids
Analog	Digital
Unidirectional	Bidirectional
Centralized production	Decentralized production
Communication limited to a part of the network	Communication throughout the entire network
Single economic actor	Choice of supplier

Electricity system balance managed through supply (production)	Electricity system balance managed through demand (consumption)
Consumers	Prosumer (Consum'acteur - Consumer and Producer)
Limited instrumentation	Fully instrumented
Hierarchical	Meshed

I.5.5. Advanced Functionalities of Smart Grids

Traditional electrical grids face significant challenges including aging infrastructure, inadequate communication systems, increasing energy demand, and cybersecurity issues. In response, the concept of smart grids has emerged, revolutionizing the energy sector. Smart grids integrate advanced information and communication technologies to enable bidirectional communication between utilities and consumers. They represent a next-generation network that seamlessly incorporates advanced communication systems, distributed generation, and advanced metering infrastructure.

The overarching objective of smart grids is to transform the traditional grid into an electrical network that is not only cost-effective but also energy-efficient. By doing so, smart grids align with contemporary energy demands and sustainability goals, promoting optimal utilization of resources and enhancing grid reliability and resilience [13]. Smart grids are pivotal in addressing the evolving needs of modern society while paving the way towards a more sustainable and adaptable energy infrastructure.

I.5.5.1. Demand Management

At the core of smart grid energy management lies demand management, a crucial set of programs that empower consumers to actively monitor and adjust their electricity usage. Demand management enables users to optimize energy consumption by strategically managing their electricity demands, particularly during peak periods, and shifting usage to off-peak hours where possible. This approach helps to smooth out the demand curve, leading to enhanced system reliability, fewer instances of power outages, and improved voltage profile adjustments.

Demand management plays a pivotal role in mitigating power system emergencies and improving the overall efficiency and reliability of the electrical network. By enabling consumers to participate in managing their energy consumption patterns, smart grids promote a more responsive and sustainable energy infrastructure that meets contemporary energy demands effectively.

1.5.5.2. Electric Energy Storage Systems

The electricity production landscape is experiencing a profound transformation, driven significantly by the increasing adoption of renewable energies such as solar and wind power. While these sources offer sustainability benefits, their variable and intermittent nature poses challenges for grid stability and reliability. To address these challenges, especially at the local level, the development of energy storage systems plays a crucial role.

Energy storage systems offer several advantages. They can store surplus energy production during periods of high generation, thereby enhancing supply security with quick start-up capabilities when demand exceeds supply. Additionally, these systems help alleviate grid stress during consumption peaks by providing stored energy when needed most. Moreover, energy storage contributes to maintaining power quality by regulating voltage and frequency, ensuring stable and reliable electricity supply [17].

As renewable energy integration continues to expand, energy storage systems are becoming indispensable in optimizing grid operations, improving energy efficiency, and supporting the transition towards a more sustainable and resilient electricity infrastructure.

I.5.5.3. Electric Vehicles

The anticipated surge in electric vehicle (*EV*) adoption is poised to significantly impact the future electrical grid. While EVs are not a new concept, recent technological advancements and societal shifts have propelled their widespread adoption. EVs can be charged through regular charging or fast charging, each drawing varying power levels. The increased adoption of EVs introduces substantial additional loads that the distribution grid must manage. Without intelligent charging management, this could exacerbate consumption peaks, especially during evening hours when most vehicles are typically charged.

Addressing these challenges requires innovative strategies such as spreading out charging times and leveraging EVs as a flexibility tool through Vehicle-to-Grid (*V2G*) technology. V2G enables EV batteries to store or supply energy based on grid demands, thereby enhancing grid stability and efficiency [18].

In essence, smart grids with their advanced functionalities offer a promising solution to the diverse challenges faced by traditional grids. They envision a future where the electrical network is not only more responsive and efficient but also plays a crucial role in fostering a sustainable energy landscape. Through ongoing innovation and strategic implementation, smart grids are poised to transform how electricity is produced, distributed, and consumed, paving the way towards a more resilient and sustainable energy future.

I.5.5.4. Microgrids

Microgrids represent a revolutionary concept within the broader electrical grid, functioning as small-scale, intelligent networks that serve localized consumer bases. These advanced systems are designed to deliver reliable electricity supply to specific areas such as neighbourhoods, cities, industrial zones, or individual buildings. Central to their design is the integration of various components, including renewable distributed generation facilities, energy storage systems, and consumption sites, which collectively contribute to a more sustainable and efficient energy system.

One of the most notable features of micro grids is their transformation of end-users into "prosumers" - individuals who actively participate in both the generation and management of electricity they consume. This active involvement is facilitated by sophisticated demand supervision and management tools, empowering users to enhance the overall stability and efficiency of the network.

Microgrids exhibit versatility in operation. While they typically remain connected to the larger distribution grid, they also have the capability to operate independently, known as "islanding mode," especially during grid faults. This capability significantly boosts the reliability of electricity supply. Furthermore, micro grids can collaborate with neighbouring micro grids or draw upon the larger distribution grid to ensure continuous supply and maintain a balance between production and consumption, showcasing their flexibility and resilience.

Overall, micro grids exemplify innovation in energy infrastructure, offering localized solutions that enhance reliability, sustainability, and consumer engagement in electricity management. Their ability to integrate renewable energy sources and operate autonomously during disruptions underscores their pivotal role in shaping a more resilient and adaptive energy future.

I.5.5.5. Decentralized Production

Decentralized production is increasingly crucial in modern electrical networks, involving smaller-scale electricity generation units directly connected to distribution grids, contrasting with large centralized plants linked to transmission grids. This shift is reshaping electricity generation and distribution, offering advantages to both providers and consumers. For providers, decentralized production means installing power generation closer to consumers, reducing transportation and distribution costs, minimizing electrical losses, and enhancing grid stability. These units also install more quickly and access diverse locations, often employing cleaner technologies like renewables and cogeneration for higher energy efficiency. Microgrids and decentralized production embody smart grid principles of sustainability, efficiency, reliability, and consumer engagement, playing pivotal roles in shaping a sustainable energy future. They offer benefits such as proximity to consumers, access to diverse locations, rapid installation, cleaner operation, and cogeneration efficiency. Advanced technologies like SCADA, RTUs, and µ-PMUs are employed to manage decentralized generation effectively, ensuring real-time monitoring and precise control. This shift towards decentralized production signifies a move towards a more distributed, efficient, and sustainable energy system, necessitating ongoing innovation and investment in management systems and infrastructure to support its growth and development.

I.6. Decentralized Production and Its Influence on the Distribution Grid

I.6.1. Understanding Decentralized Production

Since the early 1990s, the structure and organization of the electrical system have faced challenges driven by economic, ecological, and political shifts. A noticeable slowdown in electricity demand growth has led to reduced investments in large-scale power plants. Public sentiment reflects a desire for affordable electricity but resistance to having large power plants nearby. Concurrently, heightened environmental awareness is pushing producers towards decentralized electricity production, contrasting with centralized production linked to the transmission grid. Decentralized production utilizes renewable energy sources and cogeneration to improve production facility energy efficiency, promoting cleaner energy generation and fostering a new category of producers known as Distributed Generation (DG).

The definition of decentralized production varies globally. Some countries categorize it based on the voltage level of connection, others by direct load supply, and some define DG based on characteristics like reliance on renewables, cogeneration, or non-dispatch ability. Decentralized production units differ from centralized units primarily by their connection to the distribution grid and smaller size. These units are categorized by their power capacity: micro DGs range from 1 W to 5 kW, small DGs from 5 kW to 5 MW, medium DGs from 5 MW to 50 MW (strictly connected to the distribution grid), and centralized production units range from 50 MW to 300 MW [19, 20].

This shift towards decentralized production is not just a technical adjustment; it signifies a fundamental change in electricity generation, distribution, and consumption. It reflects broader societal shifts towards sustainability, efficiency, and local energy production. As this trend continues, understanding its implications for the distribution grid becomes increasingly crucial.

I.6.2. Categorization of Decentralized Production

Decentralized production is divided into two principal categories: renewable and non-renewable energy sources. This classification distinguishes between energy generation methods that rely on sustainable, renewable resources such as solar, wind, biomass, and hydroelectric power, and those that utilize non-renewable resources like fossil fuels (coal, natural gas, oil) and nuclear energy. Each category has distinct implications for energy sustainability, environmental impact, and the resilience of the electrical grid.

I.6.2.1. Based on Energy Source

Decentralized production is divided into two principal categories: renewable and non-renewable energy.

- **Renewable Energy Sources :**

  - **Hydraulic:** Hydraulic power plants harness the potential energy of water to generate electricity. Micro-hydropower plants, typically with capacities around 5 MW, are favored for decentralized production due to their consistent energy production using freely available water resources. However, they require significant upfront investments and may have environmental impacts, particularly on aquatic ecosystems.
  - **Wind:** Wind turbines capture the kinetic energy from wind and convert it into electricity. Advancements in technology have made wind energy increasingly viable, with offshore wind farms gaining popularity despite high initial costs. Wind power is considered environmentally beneficial due to its renewable nature and minimal greenhouse gas emissions during operation.
  - **Geothermal:** Geothermal power plants utilize heat from underground water reservoirs to generate steam that drives turbines. This energy source provides a

reliable supply of electricity, particularly in regions with favorable geothermal conditions. Geothermal energy is known for its sustainability and low environmental impact compared to fossil fuels.

- **Solar:** Solar energy can be harnessed in two primary ways: photovoltaic (PV) installations convert sunlight directly into electricity using solar cells, while solar thermal systems use sunlight to heat water or other fluids, which can then be used to generate electricity through steam turbines. Solar power is clean and renewable, offering long-term benefits despite initial installation costs.
- **Biomass:** Biomass power plants convert organic materials such as agricultural waste, biogas, or forestry residues into heat and electricity. This method is particularly suitable for decentralized production in rural areas where biomass resources are abundant. Biomass energy helps reduce waste disposal issues and contributes to local energy security.

- **Non-renewable energy Sources :**

  - **Fossil Fuels (gas, coal, oil):** These technologies operate similarly to large-scale thermal power plants by burning fossil fuels to produce heat and electricity. They include flame thermal plants, gas turbines, and reciprocating engines. These systems are noted for their high efficiency in converting fuel into electricity. However, they also contribute to greenhouse gas emissions and are subject to environmental regulations. Despite these drawbacks, they remain a significant source of decentralized electricity generation due to their reliability and established infrastructure.
  - **Hydrogen:** Fuel cells generate electricity through a chemical reaction between hydrogen and oxygen, producing water and heat as byproducts. This technology holds promise for decentralized production as it offers high efficiency and emits no greenhouse gases when hydrogen is produced from renewable sources. However, hydrogen production currently requires energy input, often from fossil fuels, which diminishes its environmental benefits. Proton Exchange Membrane Fuel Cells (*PEMFC*) and Solid Oxide Fuel Cells (*SOFC*) are two prominent types of fuel cells used in decentralized applications. Although still costly and less widespread than conventional technologies, ongoing research and development aims to enhance efficiency and reduce costs, potentially expanding their role in future energy systems.

I.6.2.2. Based on Ability to Supply Power

Decentralized production units are categorized based on their capacity to provide active and reactive power, highlighting their diverse functionalities within electrical grids:

- Type 1 units exclusively supply active power and include technologies like photovoltaics and micro-turbines equipped with converters or inverters for seamless grid integration.

- Type 2 units deliver both active and reactive power, typically using synchronous machines such as cogeneration systems and gas turbines.
- Type 3 units focus solely on supplying reactive power, such as synchronous compensators that adjust power factors to optimize grid stability.
- Type 4 units generate active power while absorbing reactive power, a characteristic often found in induction generators used in wind farms.

This classification system underscores the multifaceted nature of decentralized production, offering insights into its operational capabilities and integration requirements within modern electrical grids. By comprehensively understanding these types and their respective roles, stakeholders can effectively plan, deploy, and manage decentralized production assets, thereby enhancing grid sustainability, efficiency, and resilience.

I.6.3. Implications of Decentralized Production on Distribution Networks

Research indicates that escalating decentralized production rates are likely to have foreseeable consequences on the operational dynamics of distribution networks [21, 22]. Notably, the integration of Distributed Generators (*DGs*) can drastically modify the network's voltage profile, potentially causing voltages to exceed safe levels at specific bus bars while staying within acceptable limits near the source substation [23, 24]. Additionally, an increased presence of DGs poses risks to the protection scheme due to increased short-circuit currents downstream of protection devices, potential reversal of active power flow, and a decrease in the time available to isolate faults [21].

Distributed Generators are instrumental in delivering energy nearer to the point of consumption, effectively reducing the transit of active power and, consequently, the line losses in the distribution network. However, the variable nature of primary energy sources like wind and solar used by some DGs introduces unpredictability in their production capabilities in the short term [22]. This variability impedes their ability to consistently provide a stable output and fulfil the total power demand of the market [25].

Connecting a Distributed Generator (*DG*) to a distribution network has profound implications on the system's performance, influencing aspects such as power flow, voltage stability, and overall system reliability. These impacts must be carefully considered and managed to ensure efficient and reliable network operation. The integration of DGs requires a thorough analysis of their effects on voltage profiles and protection schemes. For instance, voltage levels can rise unexpectedly at various points in the network, particularly during periods of low demand when the output from DGs may exceed local consumption, leading to over-voltages that exceed the network’s safe operating limits. Consequently, advanced voltage regulation techniques, such as the use of on-load tap changers and reactive power compensation, are essential to maintain voltage stability. Moreover, DGs can complicate the coordination of protection devices due to the increased short-circuit currents they introduce. Traditional protection schemes may need to be revaluated and upgraded to ensure they can handle the altered current levels and potential changes in fault direction. Adaptive protection schemes that can adjust settings in real-time based on current network conditions are becoming increasingly important in managing these challenges. The unpredictable nature of renewable energy sources like wind and solar also necessitates the integration of energy storage systems. These systems can buffer the variability in DG output, storing excess energy during periods of high generation and releasing it during low generation periods. This helps to stabilize the power supply and ensures that DGs can contribute effectively to meeting the market's power demand. Furthermore, the strategic placement and sizing of DGs are critical to optimizing their benefits while mitigating potential drawbacks. Placing DGs near load centres can reduce transmission losses and improve the overall efficiency of the network. However, improper placement or sizing can lead to inefficiencies and increased operational challenges. While DGs offer significant advantages in terms of reducing transmission losses and promoting renewable energy use, their integration into distribution networks requires careful planning and management. By addressing the impacts on voltage profiles, protection schemes, and power stability, and by utilizing advanced technologies and strategic planning, the benefits of DGs can be maximized, contributing to a more efficient and reliable energy system.

I.6.3.1. Impact on Power Flow

Integrating a Distributed Generator (*DG*) significantly alters the conventional operation of distribution networks, which are typically configured for unidirectional flow. The addition of a DG introduces an alternative energy source to the system. If the output from the DG surpasses the downstream demand, the surplus energy is redirected upstream, effectively inverting the direction of power flow. This leads to scenarios where the net power flow between the DG and the source substation reaches a null point due to the opposing flows. As depicted in Figure 1.8, the introduction of a DG changes the dynamics between the maximum and minimum power flow within the network [26].

In the absence of a generator, the peak power flow aligns with maximum consumption, while the lowest flow corresponds with minimal consumption. Conversely, the installation of a DG shifts these dynamics, with the peak flow occurring at minimum consumption and the lowest at maximum consumption. These shifts have critical implications for managing voltage drops across the distribution network. The reversal and fluctuation in power flow necessitate advanced strategies for voltage management and stability. Traditional distribution networks are designed to handle a single direction of power flow, where the voltage gradually decreases along the length of the feeder from the substation to the load. With the introduction of DGs, the voltage profile can become more complex, exhibiting local peaks where DGs inject power into the network. This can lead to over-voltage conditions during periods of low demand and under-voltage conditions when DG output is insufficient. Effective voltage regulation becomes essential to address these challenges. Techniques such as the use of on-load tap changers, voltage regulators, and reactive power compensation are necessary to maintain voltage levels within acceptable limits throughout the network. Additionally, the implementation of real-time monitoring systems can help operators dynamically adjust the network configuration in response to changing power flows, ensuring stability and reliability. The integration of DGs also impacts the protection schemes within the network. Traditional protection devices, designed for unidirectional flow, may not function correctly under bidirectional flow conditions. Adaptive protection schemes and advanced fault detection technologies are required to ensure the protection system remains effective. These systems need to account for the potential reversal of power flow and increased short-circuit currents introduced by DGs. While the integration of DGs into distribution networks offers benefits such as reduced transmission losses and increased use of renewable energy, it also presents significant challenges. Managing these challenges requires a comprehensive approach that includes advanced voltage regulation techniques, real-time monitoring, and adaptive protection schemes. By addressing these issues, the integration of DGs can enhance the efficiency and reliability of the power distribution network, contributing to a more sustainable energy system.

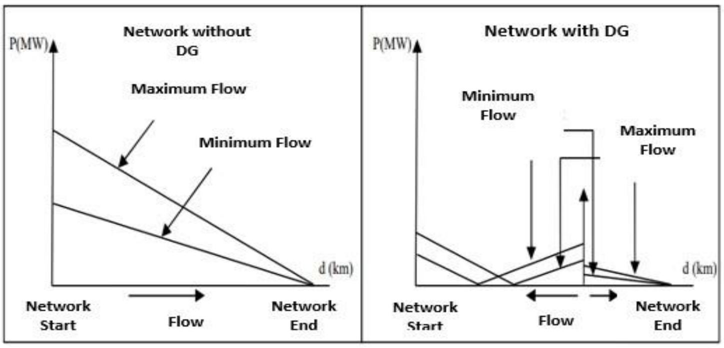

Figure I.8. Impact of DG on Power Flow.

In Figure I.8, the network is delineated into two principal sections to illustrate the flow of energy within the system. The first section, labeled 'ag', extends from the network's origin towards the generator. This section represents the flow pathway that traverses the zero point, where the energy originating from the network's beginning and that produced by the generator converge. Essentially, at this zero point, the incoming energy from both sources balances out. The second section, labeled 'gc', runs through the generator towards the network's end. In this section, the energy flow can be perceived as the cumulative sum of the energy emanating from both the network and the generator. This demarcation in Figure I.9 helps in understanding the dynamic interaction between distributed generation and the traditional power flow within the network, illustrating how distributed generation can influence and potentially reverse the usual flow of energy in a distribution network [26].

The 'ag' section highlights the segment of the network where the generator's output begins to impact the overall energy flow. At the zero point, where the power contributions from the generator and the upstream network equalize, the flow direction can change based on real-time demand and generation levels. This balancing point is critical for managing voltage stability and ensuring that neither over-voltage nor under-voltage conditions arise. The 'gc' section underscores the downstream effects of distributed generation. As energy flows from the generator to the end of the network, it combines with the energy from the upstream portion of the network. This cumulative flow must be carefully managed to prevent overloading the system and to maintain a stable voltage profile. The interaction between the generator's output and the network's existing power flow can lead to complex dynamics, including potential reverse power flows and fluctuating voltage levels. Understanding these two sections and their interactions is essential for optimizing the integration of DGs. Operators must consider the impact on both sections when planning the placement and operation of DGs. Advanced monitoring and control systems are necessary to dynamically adjust to the changing power flows and ensure the network operates within safe and efficient parameters. The demarcation in Figure I.9 thus provides a clear framework for analyzing the effects of distributed generation on traditional power flow. It illustrates how DGs can shift the balance of power within the network, requiring new strategies for voltage regulation, protection coordination, and overall system management. By comprehensively understanding these interactions, network managers can better plan for the integration of DGs, enhancing the reliability and efficiency of the power distribution system.

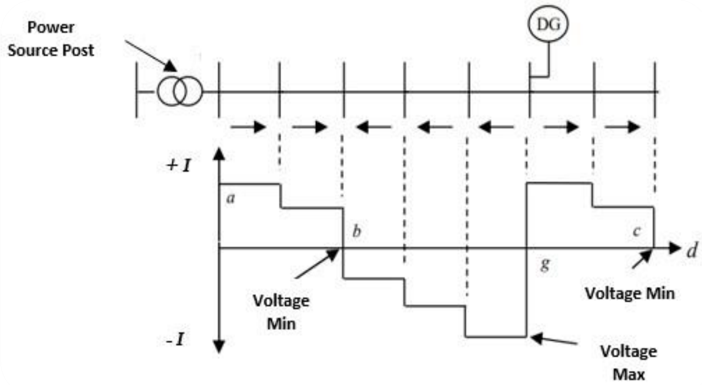

Figure I.9. Example of Power Flow for an Operating Condition.

I.6.3.2. Impact on Voltage Profile and Stability

Distributed Generators (*DGs*) significantly influence the voltage profile and stability of distribution networks. In a typical feeder without DG, the voltage tends to decrease progressively as the distance from the substation increases, a phenomenon depicted in Figure I.10 However, the introduction of one or more DGs into the network can be locally because voltage rises at various points along the feeder. These voltage increases can potentially lead to over-voltages, particularly during periods of low load, which can exceed the network's acceptable voltage limits [27].

Managing the effects of Distributed Generators (*DGs*) on voltage stability is crucial, focusing on maintaining network voltage within permissible limits through their careful and optimal integration. Properly located and sized DGs can help support voltage levels and reduce losses by providing power close to where it is consumed. Advanced control mechanisms, such as on-load tap changers, voltage regulators, and reactive power compensation, are essential for managing the voltage impacts of DGs. The variability and intermittency of renewable energy sources like solar and wind, which are often used in DGs, add complexity to voltage management, necessitating dynamic voltage control strategies and energy storage systems to buffer fluctuations. Real-time monitoring and control systems provide operators with the data to make informed decisions about DG operations, dynamically adjusting DG output, switching capacitors, and managing load tap changers to maintain voltage within safe limits. While DGs offer significant benefits in terms of efficiency and reliability, their integration must be carefully managed to avoid voltage stability issues. Through optimal placement, advanced control strategies, and real-time monitoring, DGs can contribute positively to the modernization and improvement of electrical distribution networks, enhancing both reliability and efficiency.

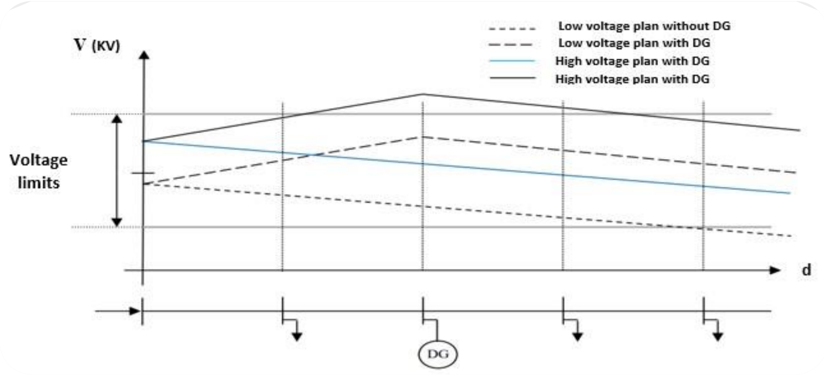

Figure I.10. Variations of network voltage without and with DGs.

I.6.3.3. Impact on Power Losses

The incorporation of Distributed Generators (DGs) into distribution networks, which were originally engineered for unidirectional flow from the source substation, markedly modifies power flow and affects power losses. For operators, minimizing these losses is critical to reducing energy distribution costs, augmenting transit margins on power lines, and enhancing voltage profiles [27, 25]. Research has demonstrated that the impact of dispersed generation on power losses is significant, with changes in the system's characteristics, especially the location and size of DGs, playing a crucial role in the technical parameters of the network [28, 29].

DGs can either reduce or increase power losses depending on their placement within the network. When strategically located near load centres, DGs can significantly decrease power losses by supplying power close to where it is consumed, thus reducing the distance electricity needs to travel through the network and minimizing resistive losses in the conductors. Conversely, if DGs are poorly sited or improperly sized, they can exacerbate power losses and even cause reverse power flows, leading to inefficiencies and potential instability in the network. Additionally, the integration of DGs impacts the voltage profile across the distribution network. While DGs can help support voltage levels during peak demand periods, they can also cause over-voltage issues during low demand periods, especially if their output exceeds local consumption. Therefore, maintaining voltage levels within permissible limits requires careful planning and control strategies. Techniques such as voltage regulation, reactive power compensation, and advanced inverter functionalities are often employed to mitigate these challenges. Effective management and optimization of DG integration can enhance the overall reliability and efficiency of power distribution systems. This involves leveraging advanced grid management technologies, including real-time monitoring, automated control systems, and predictive analytics, to dynamically adjust the operation of DGs in response to changing load conditions and generation patterns. By doing so, DGs can provide substantial benefits, including improved energy efficiency, enhanced grid stability, and reduced environmental impact, aligning with the broader objectives of modernizing and improving electrical networks [28, 29].

I.6.3.4. Impact on Network Stability

Network stability is susceptible to the types of generators employed in decentralized production. For example, synchronous generators can change the critical fault elimination time, thus affecting the dynamic stability limit and overall network stability [30]. This underscores the importance of careful consideration in the choice and integration of generators within the distribution network.

Synchronous generators, commonly used in conventional power plants, have inherent properties that provide grid support by contributing to the system's inertia. This inertia helps maintain frequency stability and improves the system's response to disturbances. However, their integration into distribution networks must be managed carefully to avoid issues such as oscillations and reduced fault tolerance. If a fault occurs, synchronous generators can affect the timing and effectiveness of protective relays, potentially leading to delayed fault clearance and further destabilizing the network. On the other hand, asynchronous generators, such as those found in many wind turbines and some solar photovoltaic systems, do not contribute to system inertia in the same way. This lack of inertia can lead to faster frequency deviations in the event of a disturbance, posing additional challenges for network stability. However, modern power electronic interfaces used with these generators can provide some level of synthetic inertia and reactive power support, helping to mitigate these challenges. The integration of different types of DGs requires a comprehensive understanding of their dynamic behaviours and interactions with the existing network infrastructure. Advanced modelling and simulation tools are essential for predicting the impacts of various generator types on network stability and for designing appropriate control strategies. Furthermore, regulatory frameworks and grid codes must evolve to ensure that all types of DGs contribute to grid stability and reliability effectively, the choice and integration of generators in a decentralized production setup significantly influence network stability. By carefully selecting and managing these generators, and employing advanced control and monitoring technologies, distribution networks can maintain stability and reliability, supporting the broader goals of efficient and resilient energy systems.

I.6.3.5. Impact on Protection Plan

The integration of new generators alters the short-circuit currents and subsequently the protection thresholds. Such changes can lead to improper selectivity, false tripping, or even a complete impairment of the protection system, presenting substantial challenges in upholding network integrity and safety [30].

When Distributed Generators (*DGs*) are added to a distribution network, they can significantly change the fault current levels at various points in the system. The increased short-circuit current contributions from DGs may exceed the ratings of existing protective devices, such as circuit breakers and fuses, leading to potential equipment damage or failure. Additionally, the direction of fault currents can also reverse, complicating the coordination of protective relays designed for unidirectional current flow. Improper selectivity arises when protective devices cannot discriminate between fault conditions and normal operating conditions, leading to false tripping of circuit breakers. This not only disrupts power supply but also stresses the electrical infrastructure, causing wear and reducing the lifespan of equipment. In severe cases, the protection system may fail to operate altogether, leaving sections of the network vulnerable to sustained faults, which can escalate into larger, more damaging outages [31].

To address these challenges, it is crucial to re-evaluate and update protection schemes whenever new DGs are integrated into the network. Adaptive protection systems, which can adjust their settings in real-time based on changing network conditions, are increasingly being developed and deployed. These systems utilize advanced communication protocols and intelligent algorithms to ensure proper coordination and selectivity under varying fault conditions. Moreover, the implementation of directional relays, differential protection schemes, and other advanced protection technologies can help manage the complexities introduced by DGs. These technologies are capable of distinguishing between normal and fault conditions with higher accuracy, ensuring reliable protection performance. While the integration of new generators into distribution networks brings numerous benefits, it also poses significant challenges to the protection systems. By adopting advanced protection technologies and adaptive schemes, it is possible to maintain network integrity and safety, ensuring a resilient and reliable power distribution system [32].

I.6.3.6. Impact on System Observability and Controllability

The intermittency of primary energy sources in Distributed Generators (DGs), particularly those reliant on renewable energy, introduces unpredictability in power output estimation. This unpredictability complicates the network's observability and controllability, presenting significant challenges for operators in maintaining a stable and efficient system [30].

Renewable energy sources such as wind and solar are inherently variable due to their dependence on weather conditions. This variability can cause sudden fluctuations in power generation, making it difficult for operators to predict and manage the overall power supply. These rapid changes in power output can lead to voltage instability, frequency deviations, and increased wear on grid components as the system continuously adjusts to balance supply and demand [33]. The unpredictability of renewable DGs complicates network observability, which is the ability to monitor the state of the network in real-time. Accurate and timely data is crucial for effective decision-making and control. However, the variable nature of renewables means that traditional monitoring and forecasting methods may not be sufficient. Advanced sensors, real-time data analytics, and machine learning algorithms are increasingly being used to improve the accuracy of power output predictions and enhance the observability of the network. Controllability, or the ability to influence the network's behaviour to maintain stability, is also affected by the intermittency of DGs. Operators need to implement sophisticated control strategies to manage the variable output from renewable sources. This includes using energy storage systems to buffer the fluctuations, demand response programs to adjust consumption patterns, and flexible grid resources that can quickly respond to changes in generation. Moreover, integrating DGs into the existing grid infrastructure requires robust communication systems and advanced grid management technologies. These systems enable real-time coordination between different parts of the network, ensuring that power flows smoothly and efficiently even as generation levels vary. The intermittency of renewable energy sources in DGs introduces significant challenges in terms of network observability and controllability. By leveraging advanced technologies and implementing adaptive control strategies, operators can mitigate these challenges and maintain a stable, efficient, and reliable power distribution system [34].

I.6.3.7. Impact on Service Continuity

The intermittent nature of Distributed Generators (*DGs*) can lead to their unavailability precisely when the system requires them the most. This can result in power outages and disruptions due to insufficient power supply, thus impacting service continuity and reliability [30].

Renewable energy sources like wind and solar, commonly used in Distributed Generators (*DGs*), are subject to fluctuations based on environmental conditions. Solar power generation heavily depends on sunlight, which varies with weather conditions and time of day, while wind power generation depends on wind speed, which can be highly variable and unpredictable. These fluctuations mean that renewable DGs may not always be able to supply power when demand is high or during critical periods, such as peak consumption times or sudden increases in demand due to unforeseen circumstances. This unavailability poses a significant challenge to maintaining a stable and reliable power supply. When renewable DGs are unable to generate sufficient power, the grid must rely on backup generation sources, often conventional power plants that can be ramped up quickly to meet the shortfall. However, this transition is not always seamless and can lead to temporary power outages or disruptions. The impact on service continuity and reliability is a major concern for both utility companies and consumers. Power outages can cause significant inconvenience, economic losses, and, in some cases, safety hazards. Therefore, ensuring that the power supply is reliable and continuous is a top priority for grid operators [35].

To mitigate the risks associated with the intermittency of DGs, several strategies can be employed [36]:

- **Energy Storage Systems:** Implementing energy storage solutions such as batteries can help store excess energy generated during periods of high renewable output. This stored energy can then be used to supply power during periods when renewable generation is low, thereby smoothing out the fluctuations and ensuring a more reliable power supply.
- **Demand Response Programs:** Encouraging consumers to reduce or shift their electricity usage during peak times through demand response programs can help balance supply and demand, reducing the strain on the grid when renewable DGs are not generating sufficient power.
- **Grid Flexibility and Resilience:** Enhancing the flexibility and resilience of the grid through advanced grid management technologies, real-time monitoring, and automated control systems can improve the ability to quickly respond to changes in power generation and demand.

- **Hybrid Systems:** Combining renewable DGs with other forms of generation, such as natural gas or hydroelectric power, can provide a more stable and reliable power supply. Hybrid systems can take advantage of the strengths of different generation sources to compensate for the weaknesses of any single source.

While the intermittent nature of DGs presents challenges to power supply reliability and service continuity, implementing advanced technologies and strategic measures can help mitigate these challenges and ensure a stable and reliable power distribution system [37].

I.6.3.8. Impact on Service Quality

Asynchronous Distributed Generators (*DGs*) consume reactive power for their operation, which can lead to significant current draw when connected to the network. This, in turn, contributes to voltage dips and potentially severe voltage sags. Additionally, the use of power electronics interfaces in DGs can increase harmonic levels, further deteriorating the quality of the service provided. These issues underscore the need for robust strategies and technologies to mitigate the adverse effects of DGs on service quality [30].

Asynchronous Distributed Generators (*DGs*), such as those used in many wind turbines and small-scale generators, inherently require reactive power to maintain their magnetic fields. This consumption of reactive power can strain the network, especially if the supply of reactive power is not adequately managed. Voltage dips occur when the demand for reactive power exceeds the supply, causing voltage levels to drop below acceptable limits. Severe voltage sags can lead to the malfunctioning of sensitive equipment, disruptions in industrial processes, and general discomfort for consumers [38].

The integration of power electronics interfaces in DGs, while essential for converting and controlling power flows, introduces harmonics into the electrical system. Harmonics are distortions in the voltage and current waveforms that can cause overheating of equipment, interference with communication lines, and reduced efficiency of electrical devices. High harmonic levels can lead to a deterioration in power quality, affecting both the reliability and efficiency of the power supply.

To address these issues, several strategies and technologies can be employed [39]:

- **Reactive Power Compensation:** Using devices such as capacitors, synchronous condensers, or static var compensators (*SVCs*) can help manage the reactive power requirements of asynchronous DGs. These devices can supply the necessary reactive power locally, reducing the strain on the network and helping to maintain stable voltage levels.
- **Advanced Power Electronics:** Employing advanced power electronics with built-in harmonic filters can mitigate the harmonic distortions introduced by DGs. These filters can smooth out waveforms and improve overall power quality.
- **Network Upgrades:** Upgrading the network infrastructure to handle the additional reactive power and harmonics can also be beneficial. This includes reinforcing

transmission lines, upgrading transformers, and installing advanced monitoring and control systems.

- **Energy Storage Systems:** Energy storage systems can help buffer fluctuations in voltage and power quality. By storing excess energy during periods of low demand and releasing it during high demand, these systems can help maintain a more stable and reliable power supply.
- **Real-Time Monitoring and Control:** Implementing real-time monitoring and control systems allows operators to quickly identify and respond to issues related to reactive power consumption and harmonics. These systems can dynamically adjust settings to optimize performance and mitigate adverse effects.

While decentralized production introduces numerous benefits and the potential for more sustainable and efficient energy systems, it also brings complex challenges that affect every aspect of the distribution network. From altering power flows and stability to impacting protection plans and service quality, the effects are far-reaching. Addressing these challenges requires a multifaceted approach, including technological advancements, network upgrades, and innovative management strategies to ensure a reliable, efficient, and high-quality power supply.

I.6.4. Solutions to Limit the Impacts of Decentralized Production

I.6.4.1. Network Reinforcement

To mitigate the impacts of Decentralized Generation (DG) on distribution networks, reinforcement methods are often employed. This involves upgrading existing conductors to those with a larger cross-section to handle increased load and generation capacity. During studies for DG connections, network conductors identified as constrained are specifically targeted for strengthening [40]. Additionally, other solutions like the installation of auto-transformers, load tap changers, series and parallel capacitors for line compensation, and D-FACTS (Distribution Flexible AC Transmission System) power electronics devices are considered. However, these modifications often require significant investment and time, making them less than instantaneous [40].

Reinforcement methods are essential for ensuring that distribution networks can handle the additional power flow and maintain stability with the integration of Distributed Generators (*DGs*). Upgrading conductors to larger cross-sections supports higher current levels, reduces overload risks, and enhances system reliability, while targeted strengthening of constrained conductors optimizes resource use and improves performance. Installing auto-transformers and load tap changers helps regulate voltage levels, providing real-time adjustments to maintain stability despite varying conditions. Series and parallel capacitors manage reactive power and maintain voltage levels, with series capacitors increasing line transfer capacity and parallel capacitors providing local support. Advanced approaches like D-FACTS (Distribution Flexible AC Transmission System) devices dynamically control power flow, offering flexibility and responsiveness beyond traditional methods. Despite requiring substantial financial investment and extended implementation periods, these reinforcement methods are critical for accommodating decentralized generation growth. Careful planning, significant capital expenditure, and coordinated efforts are necessary to minimize network disruption. In summary, conductor upgrades, voltage regulation equipment, line compensation techniques, and advanced power electronics are vital for mitigating DG impacts, ensuring the reliability, stability, and efficiency of modern power distribution systems [41].

I.6.4.2. Optimization of Decentralized Production Planning

Optimizing the planning of decentralized production is crucial for maximizing its benefits while ensuring the reliability and security of the distribution network. Network managers strive to leverage the majority of energy supplied by DGs while minimizing their adverse impacts. Achieving this goal necessitates a comprehensive understanding of DGs' behaviour and their effective planning within the network. It involves strategic placement, sizing, and operational coordination of DGs to optimize network performance and maintain stability. This approach not only enhances the efficiency of the distribution network but also contributes to the overall sustainability of the energy system [42].

Strategic placement of Distributed Generators (*DGs*) is essential to maximize their positive impacts and minimize potential issues such as voltage fluctuations, power losses, and protection challenges. By positioning DGs close to load centres, the distance electricity needs to travel is reduced, decreasing resistive losses and improving voltage profiles. This strategic placement also helps balance the load more effectively across the network, reducing strain on any single part of the distribution system. Sizing of DGs is another critical factor. Properly sized DGs ensure that the generation capacity matches the local demand, preventing situations where excess power needs to be exported back to the grid, which can cause reverse power flows and associated challenges. Accurate sizing also helps maintain voltage levels within acceptable limits and avoids over-voltage conditions during periods of low demand. Operational coordination involves integrating advanced control systems and communication technologies to manage the real-time operation of DGs. This includes techniques such as demand response, where consumption patterns are adjusted based on the availability of DGs, and the use of energy storage systems to buffer the variability in DG output. Advanced grid management systems can dynamically adjust the operation of DGs in response to changing conditions, ensuring that the network remains stable and efficient. Additionally, predictive analytics and simulation tools are used to model the behaviour of DGs under various scenarios, allowing network managers to anticipate potential issues and plan accordingly [43]. These tools help identify optimal locations for new DG installations, determine the best sizes for DGs, and devise strategies for integrating them into the existing network infrastructure. By focusing on strategic placement, proper sizing, and effective operational coordination, network managers can optimize the performance of the distribution network and ensure its reliability and security. This not only improves the efficiency of energy distribution but also enhances the overall sustainability of the energy system. The integration of DGs in a well-planned manner supports the transition to a more decentralized and renewable-based energy system, aligning with global efforts to reduce carbon emissions and combat climate change. Optimizing the planning of decentralized production involves a comprehensive approach that includes strategic placement, accurate sizing, and coordinated operation of DGs. This approach enhances the efficiency, reliability, and sustainability of the distribution network, contributing to a more resilient and environmentally friendly energy system [44].

I.7. Conclusion

In conclusion, this chapter provided a comprehensive overview of electrical distribution networks, with a specific focus on the growing integration of decentralized production and renewable energy sources. We examined the evolution from traditional networks to smart grid systems, emphasizing the challenges and opportunities posed by this transition. Key aspects such as network stability, voltage regulation, and the implications of distributed generation on the network's overall efficiency were discussed. This chapter has established the foundational understanding required to analyse modern electrical grids and their components, particularly in the context of Algeria's energy infrastructure.

In the next chapter, we will explore the methodologies for power flow analysis in distribution networks, focusing on advanced techniques like the backward/forward sweep method. This approach will be critical for optimizing energy distribution, reducing losses, and ensuring voltage stability in various network configurations.

CHAPTER II

Power Flow in Distribution Networks

II.1. Introduction

Power flow calculation is a pivotal element for the effective planning and operation of distribution networks. In our study, this primarily relies on the calculation of power flow within the distribution network. Several methods have been utilized to address the power flow problem in radial distribution networks, but the most widely used is the backward/forward sweep method, known as the "Backward Forward Sweep" (*BFS*). This technique is essential for achieving efficient network management, minimizing Energy losses, maintaining a good voltage profile, and ensuring a significant margin of voltage stability at the network's bus bars.

Power flow is a key component in enhancing the planning and functioning of distribution networks. A considerable focus has been placed on analyzing power flow in distribution networks to minimize power losses, maintain an optimal voltage profile, and ensure a substantial margin of voltage stability at the bus bars. Various power flow methods reported in the literature can be categorized into two groups: Newtonian methods and backward/forward sweep methods. While Newtonian methods are generally employed for power flow problems in transmission networks, their application in large distribution networks often results in failure due to divergences, as these networks have different typical characteristics compared to transmission networks.

The backward/forward sweep methods are based on a backward sweep for branch current calculation and a forward sweep for bus bar voltage calculation. This method has garnered more attention and is utilized for power flow calculations in unbalanced and harmonically polluted distribution networks. In this chapter, our focus is on power flow calculation in radial distribution networks using the backward/forward sweep technique. This approach relies on understanding the network topology by reading its data (bus bars and branches). The identification process begins with determining the type of each bus bar (terminal, common, and intermediate bus bars) and then identifying the type of each line (main, lateral, sub-lateral, and minor lines). This topology is subsequently used in the power flow calculation employing the double sweep line technique.

The performance of this technique will be tested on IEEE 33 bus, IEEE 69 bus, and the ALG-AB-Hassi Sida 157-bus distribution network. These tests aim to demonstrate the effectiveness of the backward/forward sweep method in accurately calculating power flow across different types of distribution networks, highlighting its adaptability and efficiency in managing complex distribution systems.

II.2. Importance of Radial Distribution Network Analysis

The analysis of radial distribution networks is essential due to their unique characteristics and the specific challenges they pose. Commonly used in urban and suburban electrical distribution systems, radial networks are characterized by a single path for power flow from the source to any point in the network. This simplicity offers high reliability and ease in fault isolation and service restoration, alongside cost-effectiveness in construction and maintenance. However, these networks often face significant voltage drops over long distances and can incur substantial power losses due to longer distances and higher line resistances.

Analyzing radial networks is crucial for several reasons. Firstly, it ensures voltage stability and helps maintain power supply within acceptable voltage ranges, vital for customer satisfaction. Secondly, it aids in minimizing Energy losses, enhancing overall network efficiency. This analysis is also critical for the optimal sizing and placement of equipment like transformers and capacitors, essential for effective load management, especially given the variable nature of residential and commercial loads. Moreover, it plays a pivotal role in fault analysis and system protection, designing schemes to quickly isolate faults and minimize customer impact.

With the growing integration of renewable energy sources, the analysis of radial networks has gained even more importance. It is crucial for managing the variability of distributed generation and mitigating its impact on network stability and power quality. Furthermore, such analysis is integral to planning and expansion efforts, particularly in urban areas, to accommodate future growth and technological integration.

Analyzing radial distribution networks is indispensable for maintaining system stability, ensuring reliable and quality power supply, optimizing operational costs, and preparing the network for future demands and technological advancements.

II.3. Network Configuration and Bus Classification

Understanding network configuration and bus classification is crucial in power flow analysis, forming the backbone of how power systems are analyzed and comprehended. Power networks typically consist of generation units, transmission and distribution lines, transformers, and load centers. Their configuration can vary from radial designs, commonly seen in distribution networks, to looped or interconnected layouts typical in transmission networks. The configuration significantly influences how power flows from generators to loads, affecting the system's stability and reliability [45].

In terms of bus classification within power systems, buses are categorized based on their role and characteristics. The main types include the SLACK Bus (Reference Bus), which typically serves as the source bus balancing the system's active and reactive power, the PQ Bus (Load Bus) with specified active and reactive power demands but unknown voltage magnitude and angle, and the PV Bus (Generator Bus) which has a specified active power generation and voltage magnitude. Special bus types like Isolated and Inter-Tie Buses also play specific roles, connecting different areas or utilities and managing power with no generation or load.

The bus types are critical in power flow analysis as they provide the starting point for calculations, defining known and unknown parameters. This classification is essential for voltage stability analysis and impacts network design, influencing decisions on equipment placement and ratings. Understanding these bus types aids in formulating operational strategies, including load management and contingency planning, and guides the planning for system expansion, upgrades, and the integration of renewable energy sources [45].

The network configuration and bus classification are integral in power flow analysis, determining the system's modeling and analysis. These aspects impact everything from operational decisions to long-term planning and system design, underscoring their importance in the efficient and reliable operation of power systems.

II.3.1. Definitions and Types of Buses in Power Flow Analysis

In power flow analysis, buses are critical nodes where power is either generated, distributed, or consumed. Understanding the types of buses and their roles is essential for analyzing and managing power systems. Here are the primary types of buses.

II.3.1.1. Reference Bus (SLACK BUS)

The Reference Bus, also known as the Slack Bus, serves as a reference point for all other buses in the system. It is typically assigned a fixed voltage magnitude and angle (usually 1.0 per unit and 0°, respectively). This bus balances the active and reactive power in the system, compensating for losses and maintaining system stability. It is generally chosen as the bus closest to the main generation source. In terms of its role in power flow, the Reference Bus acts as the balancing point for power discrepancies in the network, adjusting its generation output to ensure that total generation equals total demand plus losses [46].

II.3.1.2. Control Bus (CONTROL BUS)

Control Buses, often known as PV (Power-Voltage) Buses, are typically associated with generator units. They have a specified active power (P) generation and voltage magnitude, while the reactive power (Q) and voltage phase angle are variables to be computed. These buses are common in systems with multiple-generation sources. In terms of their role in power flow, Control Buses help maintain voltage levels within desired limits and contribute to system stability by controlling the voltage and power generated [46].

II.3.1.3. Load Bus (LOAD BUS)

Load Buses, or PQ Buses, are where power is consumed. The active (P) and reactive (Q) power demands at these buses are known, while voltage magnitude and phase angle are unknowns to be determined. They represent the majority of buses in a typical power system. In terms of their role in power flow, Load Buses are the points of power consumption in the network, and maintaining voltage levels at these buses is crucial for ensuring efficient operation and customer satisfaction. Each bus type plays a distinct role in the power system and is represented with specific parameters in power flow studies. Understanding these types aids in designing and operating the network efficiently, ensuring stability, and meeting demand reliably [46].

Table II.1. Known and Unknown Quantities for Each Type of Bus [47].

Type of Bus	Known Quantities	Unknown Quantities
Slack Bus	$\|V\|,\delta$	P,Q
Control (PV) Bus	P, $\|V\|$	Q,δ
Load (PQ) Bus	P, Q	$\|V\|$, δ

II.4. Identification Methods for Bus Types in Power Flow Analysis

The identification of bus types in a power system is crucial for accurate power flow analysis. Two common methods used for this purpose are the Comparative Method and the Matrix Method [48].

II.4.1. Comparative Method

This method involves a comparative analysis of the network's characteristics to classify buses into their respective types: SLACK, CONTROL, and LOAD. It typically involves comparing specified parameters like power generation, load demand, and voltage levels against predefined criteria. Buses are analyzed based on their operational data, such as generation capacity, load demand, and voltage requirements. For example, a bus with a specified voltage level and power generation but unknown reactive power would be classified as a CONTROL bus. This method is used in systems where bus data is readily available and needs to be categorized for analysis. It is particularly useful in dynamically changing networks where bus roles may shift due to operational changes [49].

II.4.2. Matrix Method

The Matrix Method uses mathematical matrices to represent the power system and determine bus types based on the system's network configuration and electrical properties. This method involves the formulation of matrices like the bus admittance matrix or impedance matrix. Each bus in the system is represented as a node in the matrix. The type of bus is inferred from the matrix's properties, such as connectivity and the type of elements (generators, loads) connected to each node. For instance, a node with high connectivity and generator presence might be identified as a CONTROL bus. This method is suitable for complex and large-scale power systems where automated and computational methods are preferred. It is often used in computer-based power flow analysis tools for systematic and efficient bus type identification. Both methods have their distinct applications and are chosen based on the complexity of the network, the availability of data, and the specific requirements of the power flow study. The Comparative Method is more straightforward and intuitive, while the Matrix Method is more systematic and suited for automated analysis [50].

II.5. Power Flow Solution Techniques

II.5.1. Traditional Methods

Power flow solution techniques are essential for analyzing electrical power systems. Here's a detailed look at traditional and advanced methods

II.5.1.1. Gauss-Seidel Method

This method uses successive displacement in solving the non-linear equation, such that the latest value of the bus voltage is immediately substituted in the equation of subsequent rows. The solution for the bus voltage and power flow equations is obtained when the difference between the voltage values of the successive iteration is less than a specified tolerance value ε [51].

Gauss-Seidel power flow equations:

$$(V_i)^{k+1} = \frac{\frac{p_i^{sch} - \sum_i^{sch}}{v_i^{(k)}} + \sum\ y_{ij} V_j^{(k)}}{\sum\ y_{ij}}\ j \neq i \tag{II.1}$$

$$\Delta V_i^{k+1} = (V_i)^{k+1} - (V_i)^k \tag{II.2}$$

$$\Delta V_{i,acc}^{k+1} = (V_i)^k + \alpha\Delta(V_i)^{k+1} \tag{II.3}$$

$$P_i^{(k+1)} = \Re\left\{V_i^{*(k)}\left[V_i^{*(k)}\sum_{j=0}^{n}\ y_{ij} - \sum_{j=1}^{n}\ y_{ij} j_j^{(k)}\right]\right\} \tag{II.4}$$

$$Q_i^{(k+1)} = -\Im\left\{V_i^{*(k)}\left[V_i^{*(k)}\sum_{j=0}^{n}\ y_{ij} - \sum_{j=1}^{n}\ y_{ij} V_j^{(k)}\right]\right\} \tag{II.5}$$

$$\Delta V_i^{k+1} \leq \varepsilon \tag{II.6}$$

II.5.1.2. Newton-Raphson Method

This method is an iterative method which approximates a set of non-linear simultaneous equations to a set of linear simultaneous equations. The solution for the bus voltage and power flow equations is obtained when the maximum power mismatch in ΔP and ΔQ values of the successive iteration is less than a specified tolerance value ε.

NR's method is mathematically superior to the GS method because of its quadratic convergence property when near the solution, this method is found to be more efficient and practically used for large power systems as the number of iterations is independent of the power network size [52].

Newton Raphson power flow equation:

$$P_i^{[k]}, Q_i^{[k]} \tag{II.7}$$

$$\Delta P_i^{[k]} = P_{isch} - P_i^{[k]} \tag{II.8}$$

$$\Delta Q_i^{[k]} = Q_{isch} - Q_i^{[k]} \tag{II.9}$$

Solve the equation for the correction vector:

$$\begin{bmatrix} \Delta\delta \\ \Delta|V| \end{bmatrix} = \begin{bmatrix} \frac{\partial P}{\partial \delta} & \frac{\partial P}{\partial V} \\ \frac{\partial Q}{\partial \delta} & \frac{\partial Q}{\partial V} \end{bmatrix}^{-1} \begin{bmatrix} \Delta P \\ \Delta Q \end{bmatrix} \tag{II.10}$$

Update new Voltage and Angle:

$$\delta_i^{[k+1]} = \delta_i^{[k]} + \Delta\delta_i^{[k]} \tag{II.11}$$

$$\left|V_i^{[k+1]}\right| = \left|V_i^{[k]}\right| + \Delta \left|V_i^{[k]}\right| \quad \text{(II.12)}$$

Check for convergence:

$$\left|\Delta P_i^{[k]}\right|, \left|\Delta Q_i^{[k]}\right| \leq \varepsilon \quad \text{(II.13)}$$

II.5.2. Advanced Sweep Methods

- **Backward/Forward Sweep Method**

Kirchhoff's Current Law (*KCL*) and Kirchhoff's Voltage Law (*KVL*) are used during the backward sweep to calculate bus voltages from the last node to the first node of each line or transformer branch. The linear proportional principle is then applied to find the ratios of the real and imaginary parts of the specified voltage to the calculated voltages at the bus of the substation. During the forward sweep, the bus voltages from the first node to the last node are updated by multiplying the calculated bus voltages with the corresponding ratios. The process stops when the mismatch between the calculated and specified voltages at the substation is within the tolerance limit and the convergence rate is below the specified tolerance.

The backward/forward sweep method has been widely used to solve power flow problems in distribution networks because it converges very quickly and consumes less computational memory [53].

II.5.2.1. Backward Sweep

Starting from the end node/bus and moving towards the slack bus, the power flow in each branch can be calculated using:

$$S_n = S_i \sum_{mgM} S_m + loss_n \quad \text{(II.14)}$$

S_n : The power flowing in the branch (n);
(i) : The end node of the branch (n);
S_i : The load power connected at bus/node (i);
S_m : The power in the branch (m);
$loss_n$: The losses in the branch (m);
M : The number of branches connected to branch (n) from node (i).

II.5.2.2. Forward Sweep

Starting from the branches connected to the slack bus and moving towards the end branches, the current in the sending bus "j" of branch (n) and the voltage in the receiving bus "i" are calculated using the following equations:

$$I_n = \left(\frac{S_n}{V_j}\right)^* \tag{II.15}$$

$$V_i = V_j - Z_n \times I_n \tag{II.16}$$

Branch power losses can be calculated using :

$$lossn = (Vj - Vi) \times I \tag{II.17}$$

II.5.2.3. Convergence Criteria

The calculated voltages from previous and current iterations are compared. If the maximum deviation between the voltages in successive iterations is less than the specified tolerance, i.e., 0.0001, the solution is considered convergent. The voltage deviation can be calculated using the following equation [53].

$$\Delta V_i^{(K)} = |V_i^{(K)}| - |V_i^{(K+1)}| \tag{II.18}$$

K : The number of iterations.

II.5.2.4. Properties of the Method

- It follows a bottom-up approach, meaning that the reasoning deduction moves from the bottom to the top;
- It is also known as a data-driven approach since it relies on existing data to reach the target state;
- It is conclusion-oriented, aiming to conclude the initial state.

II.5.2.5. Steps of the Backward/Forward Sweep Method

1. Insert Line Types: Identify the type of lines (main, lateral, sub-lateral, and minor) by determining the bus vectors constituting each line type;
2. Initialize Voltage Profile: Set the voltage profile for all buses (JB) to 1.0 pu;
3. Calculate Currents and Power in Backward Sweep: Compute load currents, branch currents in minor, sub-lateral, lateral, and main lines, as well as the power flowing in the branches using the backward sweep;
4. Calculate Voltages in Forward Sweep: Determine the voltages in the forward sweep. This iterative process repeats with the new voltages obtained at each bus, using the maximum difference in voltage magnitudes between two successive iterations as the convergence criterion;
5. Calculate Total Power Losses: Calculate total power losses based on the resistance and reactance characteristics of each branch, the power flowing through each branch, and the voltages at each bus. Figure II.1 shows the flowchart for the BFSM calculation method.

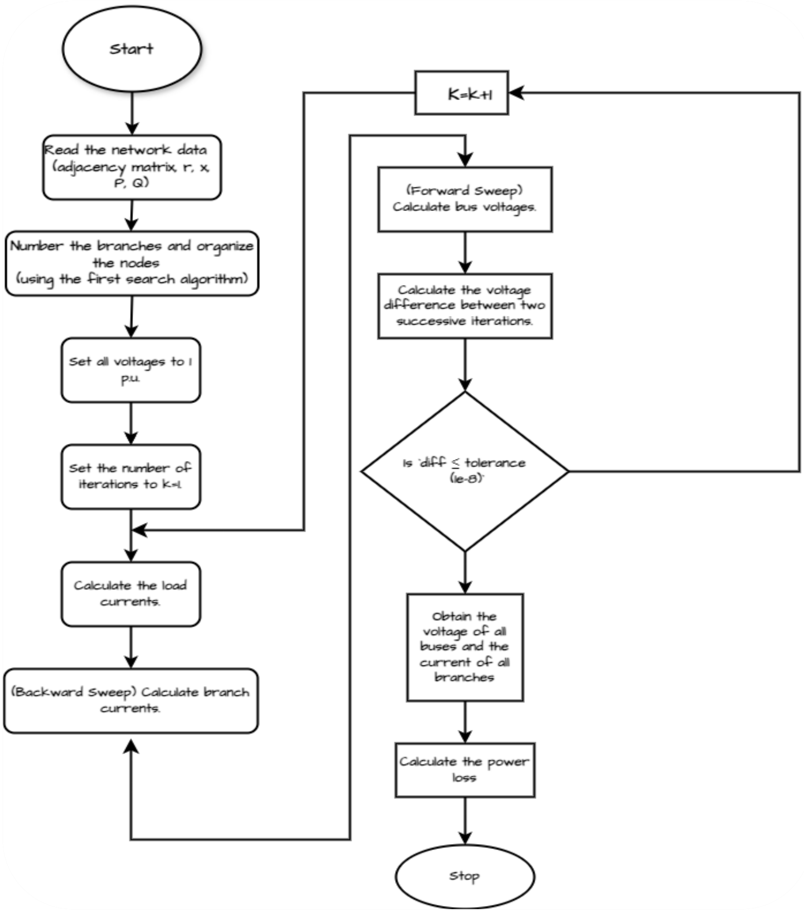

Figure II.1. Flowchart of the BFA Method.

II.5.3. Comparison

- **Complexity :**
  - Gauss-Seidel is simpler but slower, ideal for smaller systems.
  - Newton-Raphson is more complex but faster and more accurate, suitable for larger and more complex systems.
  - BFS is specialized for radial networks, simpler than Newton-Raphson but more suited to distribution than transmission systems.
- **Convergence :**
  - Gauss-Seidel has slower convergence, particularly in heavily loaded or ill-conditioned systems.
  - Newton-Raphson offers rapid convergence but requires a good initial guess.
  - BFS provides good convergence in distribution networks, especially when load changes are not drastic.
- **Application :**
  - Gauss-Seidel is used for basic studies or smaller networks.
  - Newton-Raphson is preferred in industry-standard power flow studies for its accuracy and speed.
  - BFS is tailored for distribution network analysis, particularly in systems with radial topology.

Each method has its unique advantages and is chosen based on the specific characteristics and requirements of the power system under study.

II.6. Radial distribution network power flow

Medium voltage distribution networks typically exhibit a radial configuration, characterized by their tree-like structure where power flows in a single direction from the substation to the end users. This design is generally simpler and less expensive to implement compared to meshed or looped networks. However, the radial structure also contributes to lower reliability since a single fault can interrupt the supply to all downstream customers.

These networks operate within a voltage range of 10 kV to 30 kV, which is suitable for regional distribution while minimizing power losses over longer distances compared to low-voltage networks. The radial design also simplifies fault isolation and service restoration processes, albeit with the trade-off of potentially longer outage times [54].

Each branch within these networks is composed of a series of elements, specifically a resistance (R) and an inductance (L). The resistance represents the real power losses due to the heating of conductors, while the inductance accounts for the reactive power losses due to the magnetic fields around the conductors. These parameters are critical for accurate power flow calculations and for the design of protective devices.

Furthermore, medium voltage distribution networks typically include various protection and control equipment such as circuit breakers, reclosers, and voltage regulators to maintain service continuity and quality. Automation technologies are increasingly being integrated to enhance these networks' monitoring, control, and resilience [54].

Overall, the design and operation of medium voltage distribution networks involve a careful balance between cost, reliability, and efficiency, making them a crucial component in the electrical power supply chain.

II.6.1 Power and Current in Branches

Distribution networks have a radial configuration and consist of a set of branches. Each branch in this network is modelled as a series resistance with a pure inductance [55], as shown in Figure.II.2:

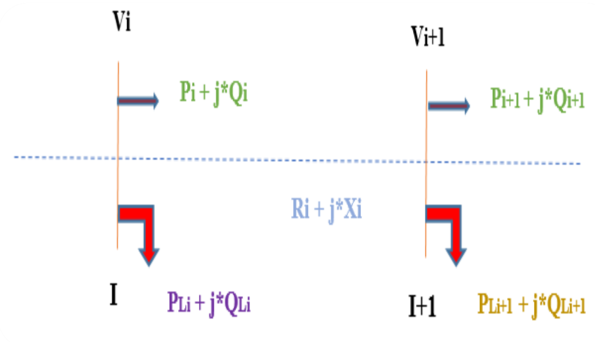

Figure II.2. Representation of Two Buses in the Radial Distribution Network.

- **Power in the Branches**

The calculation of power is a prerequisite for determining the node voltages. These powers include the power at the end of the branches, the power losses within them, and the power at the beginning of the branches [55]. The active and reactive power transferred from bus "*i*" to bus "*i+1*" can be calculated as follows:

$$\Delta V_i^{(K)} = |V_i^{(K)}| - |V_i^{(K+1)}| \tag{II.19}$$

$$P_i = \mathrm{P}'^2_{i+1} + R_i \frac{\mathrm{P}^2_{i+1} + \mathrm{Q}^2_{i+1}}{\mathrm{V}^2_{i+1}} \tag{II.20}$$

$$\mathrm{Q}_i = \mathrm{Q}'^2_{i+1} + \mathrm{X}_i \frac{\mathrm{P}^2_{i+1} + \mathrm{Q}^2_{i+1}}{\mathrm{V}^2_{i+1}} \tag{II.21}$$

Or:

$$P'_{i+1} = P_{i+1} + P_{Li+1} \tag{II.22}$$

$$Q'_{i+1} = Q_{i+1} + Q_{Li+1} \tag{II.23}$$

P_{Li+1} and Q_{Li+1} : The active and reactive power of the load at bus "i+1".

P_i and Q_i : The active and reactive power flowing out of bus "i".

- **Currents in the branches**

The current through branch "i" is expressed as follows:

$$I_i = \frac{(V_\mathrm{i}\angle\delta_\mathrm{i} - \mathrm{V}_{\mathrm{i}+1}\angle\delta_{\mathrm{i}+1})}{\mathrm{R_i} + \mathrm{j} * X_\mathrm{i}} \tag{II.24}$$

II.6.2. Amplitude and Angle of Voltage at Each Bus

The current in the branch (i, i+1) can be expressed in two ways [56]:

$$\begin{cases} I_i = \dfrac{(P_i - \mathrm{j} * Q_i)}{V_i\angle(-\delta_i)} \\ I_i = \dfrac{(V_i\angle\delta_i) - (V_{i+1}\angle\delta_{i+1})}{R_i + \mathrm{j} * X_i} \end{cases} \tag{II.25}$$

By analyzing the equations (II.24), we obtain:

$$\frac{(V_i\angle\delta_i - V_{i+1}\angle\delta_{i+1})}{R_i + \mathrm{j} * X_i} = \frac{(P_i - \mathrm{j} * Q_i)}{V_i\angle(-\delta_i)} \tag{II.26}$$

By equating the real and imaginary parts on both sides of Equation (II.25), we have:

$$(\mathrm{V_i^2} - \mathrm{V_i} * \mathrm{V_{i+1}})\angle(\delta_{\mathrm{i}+1} - \delta_\mathrm{i}) = (\mathrm{P_i} - \mathrm{j} * \mathrm{Q_i}) * (\mathrm{R_i} + \mathrm{j} * \mathrm{X_i}) \tag{II.27}$$

$$\begin{cases} (V_i * V_{i+1})\cos(\delta_{i+1} - \delta_i) = [V_i^2 - (P_i * R_i + Q_i * X_i)] \\ (V_i * V_{i+1})\sin(\delta_{i+1} - \delta_i)^2 = (\mathrm{Q}_i * R_i - \mathrm{P}_i * X_i) \end{cases} \tag{II.28}$$

By squaring both sides of equations (II.27), we obtain:

$$\begin{cases}(V_i * V_{i+1})^2 \cos(\delta_{i+1} - \delta_i)^2 = [V_i^2 - (P_i * R_i + Q_i * X_i)]^2 \\ (V_i * V_{i+1})^2 \sin(\delta_{i+1} - \delta_i)^2 = (\mathrm{Q}_i * R_i - \mathrm{P}_i * X_i)^2\end{cases} \quad \text{(II.29)}$$

By combining equations (II.28) side by side, a new equation is obtained:

$$(V_i * V_{i+1})^2 = [V_i^2 - (P_i * R_i + Q_i * X_i)]^2 + (\mathrm{Q}_i * R_i - \mathrm{P}_i * X_i)^2 \quad \text{(II.30)}$$

$$V_{i+1}^2 = V_i^2 - 2 * (P_i * R_i + Q_i * X_i) + (P_i * R_i + Q_i * X_i)^2 + (P_i * R_i + Q_i * X_i)^2 \quad \text{(II.31)}$$

$$V_{i+1}^2 = V_i^2 - 2 * (P_i * R_i + Q_i * X_i) + (P_i * R_i)^2 + (\mathrm{Q_i} * \mathrm{X_i})^2 + (\mathrm{Q_i} * \mathrm{R_i})^2 + (\mathrm{P_i} * \mathrm{X_i})^2 \quad \text{(II.32)}$$

Finally, the voltage amplitude equation at each bus in the radial distribution network is obtained as follows:

$$V_{i+1}^2 = \left[V_i^2 - 2 * (P_i * R_i + Q_i * X_i) + (R_i^2 + X_i^2) * \left(\frac{P_i^2 + Q_i^2}{V_i^2}\right)\right]^{1/2} \quad \text{(II.33)}$$

Continuing from equations (II.27), the voltage angle can be expressed as:

$$\tan(\delta_{i+1} - \delta_i) = \frac{(Q_i * R_i - P_i * X_i)}{V_i^2 - (P_i * R_i + Q_i * X_i)} \quad \text{(II.34)}$$

$$\delta_{i+1} = \delta_i + \tan^{-1}\frac{(Q_i * R_i - P_i * X_i)}{V_i^2 - (P_i * R_i + Q_i * X_i)} \quad \text{(II.35)}$$

II.6.3. Active and Reactive Power Losses

If R_i and X_i are the resistance and reactance of branch "i" respectively, the active and reactive power losses, regardless of the branch type [57] , are given by:

$$P_{Loss,i} = R_i \frac{\mathrm{P}_i^2 + \mathrm{Q}_i^2}{|V_i|^2} \quad \text{(II.36)}$$

The total active power losses in the network can be determined by summing the losses from all branches as given in Equation (II.36):

$$P_{T,\,\mathrm{Loss}} = \sum_{i=1}^{N} P_{\mathrm{Loss,i}} \quad \text{(II.37)}$$

The reactive power losses at a branch "i" are given by:

$$Q_{\mathrm{Loss}\,,i} = \mathrm{X}_i \frac{\mathrm{P}_i^2 + \mathrm{Q}_i^2}{|V_i|^2} \quad \text{(II.38)}$$

The total reactive power losses in the network can be determined by summing the losses from all branches according to equation (II.38):

$$Q_{T,Loss} = \sum_{i=1}^{N} Q_{\mathrm{Loss},i} \tag{II.39}$$

II.6.4. Voltage Deviation

Voltage deviation can be defined as the difference between the voltage at the reference bus and the voltage at bus (i). The smaller the voltage deviation, the better the voltage quality of the network [58]. Voltage deviation (*VD*) is defined as follows:

$$VD = \sum_{i=1}^{N} (Vi - Vref)^2 \tag{II.40}$$

Where VD is the total voltage deviation, (*Vi*) is the voltage magnitude at bus (*i*), and (*Vref*) is the nominal voltage (1.0 p.u).

II.6.5. Energy Losses

Energy losses in a power distribution network can be described as the amount of energy dissipated due to the inherent inefficiencies within the system. These losses arise from various factors such as the resistance of the transmission lines and the reactive components in the network. Energy losses are quantified by calculating the difference between the total energy input and the energy that is actually delivered to the end-users. These losses can be classified into active power losses and reactive power losses, where active power losses are due to the resistive heating of conductors, and reactive power losses are associated with the inductive and capacitive elements of the network [59]. The total energy losses (*EL*) in the system are given by:

$$EL = \sum_{n=1}^{N} Ploss,n \tag{II.41}$$

Where *EL* represents the total energy losses, and *Ploss,n* denotes the active power loss in branch *n*. Minimizing these losses is crucial for improving the overall efficiency and reliability of the power distribution network.

II.7. Power Flow Solution

Initially, the type of each bus is established through a comparative method. Each line type—whether main, lateral, sub-lateral, or minor—is identified by analyzing the vectors associated with the buses forming these lines. All buses are assigned an initial voltage profile of 1.0 per unit. The calculation process involves determining load currents and the currents flowing through the branches of minor, sub-lateral, lateral, and main lines in the backward sweep phase. Voltage calculations are performed during the forward sweep phase. This iterative process continues with updated voltages for each bus, and convergence is assessed by the maximum difference in voltage magnitudes between successive iterations. Following this, the Energy losses, and voltage deviations, are computed to evaluate the system's performance.

To test the effectiveness of the technique for identifying network topology by determining the types of buses and lines for power flow solutions, we programmed it in MATLAB and applied it to three test networks: IEEE 33-bus, IEEE 69-bus, and ALG-AB-Hassi Sida 157-bus networks. These networks are presented in Figures II.3, II.5, and II.7, respectively.

II.7.1. Application to the IEEE 33-bus test network

The characteristics of the IEEE 33-bus distribution network shown in Figure II.3 are as follows:

- Number of buses = 33
- Number of branches = 32
- Reference bus No. = 1
- Base voltage = 12.66 kV
- Base power = 100 MVA

The data for this network are presented in Appendix 1.

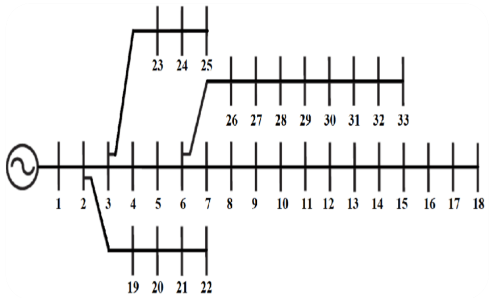

Figure II.3. Simplified representation of the IEEE 33-bus distribution network.

Table II.2 represents the type of each bus and each line constituting the IEEE 33-bus distribution network.

Table II.2. Results of Topology Identification for the IEEE 33-Bus Distribution Network.

Reference Bus	1
Terminal Buses	18, 22, 25,33
Intermediate Buses	4,5,7,8,9,10,11,12,13,14,15,16,17,19,20,21,23,24,26,27,28,29,30,31,32
Common Buses	2, 3, 6
Main Line	1,2,3,4,5,6,7,8,9,10,11,12,13,14,15,16,17,18
Side Lines	2, 19, 20, 21,22
	3, 23, 24,25
	6, 26, 27, 28, 29, 30, 31, 32,33

Figure II. (4), (7) and (10) reveals that the peak demand for the load profile occurs around 12:00 p.m. and extends for 4 hours, during which the entire load is utilized, satisfying 100% of the demand for both the IEEE 33 and IEEE 69 systems. In contrast, Figure II.10 shows that the peak demand for the ALG-AB-Hassi Sida 157 system emerges around 6:00 p.m. and lasts for 3 hours, with the system utilizing 100% of the load.

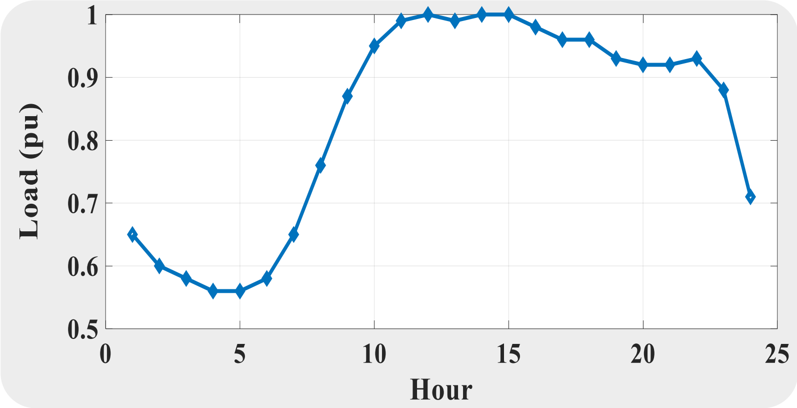

Figure II.4. Annual daily average variations for the IEEE 33-bus distribution network.

In the IEEE 33-bus distribution network, as depicted in Table II.3, the daily energy loss in the base case is approximately 3567.7 kWh. The voltage profile, illustrated in Figure II.5, shows significant variations over 24 hours, with the maximum bus voltage reaching 1 per unit (pu) and the minimum bus voltage dropping to 0.9038 pu at the 15th hour. This indicates notable fluctuations in voltage levels throughout the day.

Table II.3. Daily energy loss for the IEEE 33-bus distribution network with the minimum and the maximum bus voltage.

Base case	IEEE 33
Energy Loss (kWh)	3.5677e+03
Maximum bus voltage (pu)	1
Minimum bus voltage (pu) /15h	0.9038

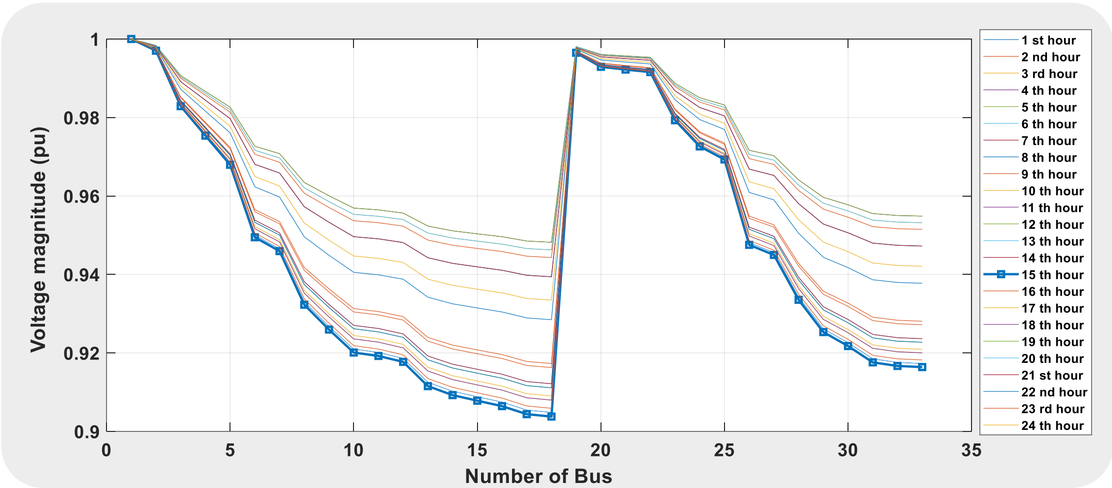

Figure II.5. Voltage profile variation over 24 hours for the IEEE 33-bus distribution network.

II.7.2. Application to the IEEE 69-bus test network

The characteristics of the IEEE 69-bus distribution network shown in Figure II.6 are as follows:

- Number of buses = 69
- Number of branches = 68
- Reference bus No. = 1
- Base power = 100 MVA
- Base voltage = 12.66 kV

The data for this network are presented in Appendix 2.

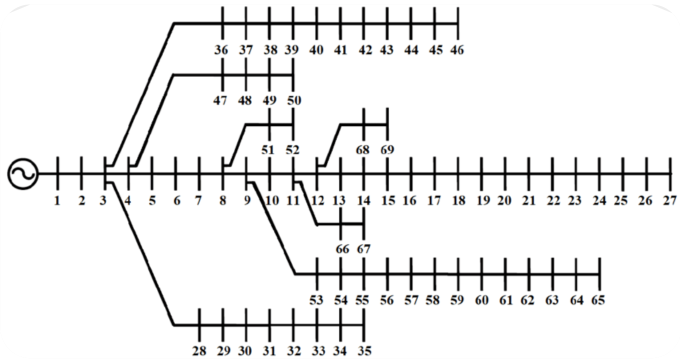

Figure II.6. Simplified representation of the IEEE 69-bus distribution network.

Table II.4 represents the type of each bus and each line constituting the IEEE 69-bus distribution network.

Table II.4. Results of Topology Identification for the IEEE 69-bus Distribution Network.

Reference Bus	1
Terminal Buses	27, 35, 46, 50, 52, 65, 67,69
Intermediate Buses	2, 5, 6, 7, 10, 13, 14, 15, 16, 17, 18, 19, 20, 21, 22, 23, 24, 25, 26, 28, 29, 30, 31, 32, 33, 34, 36, 37, 38, 39, 40, 41, 42, 43, 44, 45, 47, 48, 49, 51, 53,54, 55, 56, 57, 58, 59, 60, 61, 62, 63, 64, 66, 68.
Common Buses	3, 4, 8, 9,11, 12
Main Line	1, 2, 3, 4, 5, 6, 7, 8, 9, 10, 11, 12, 13, 14, 15, 16, 17,18, 19, 20, 21, 22, 23, 24, 25, 26, 27
Side Lines	3, 28, 29, 30, 31, 32, 33, 34, 35
	3, 36, 37, 38, 39, 40, 41, 42, 43, 44, 45, 46
	4, 47, 48, 49, 50
	8, 51, 52
	9, 53, 54, 55, 56, 57, 58, 59, 60, 61, 62, 63, 64, 65
	11, 66, 67
	12, 68, 69

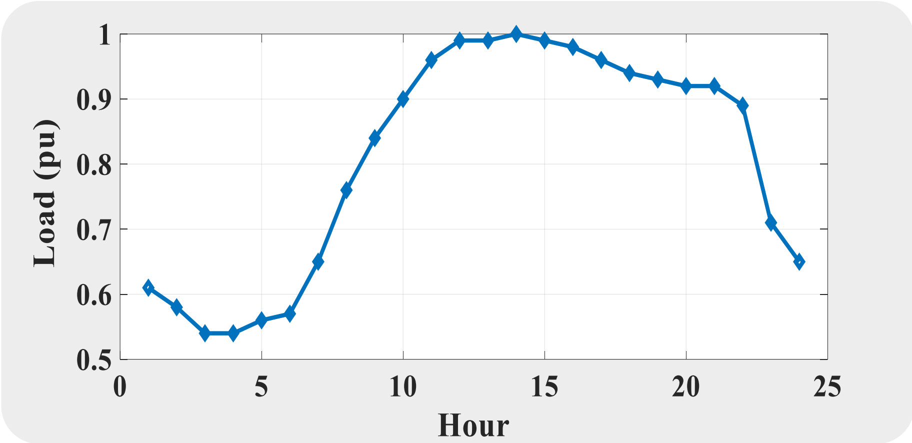

Figure II.7. Annual daily average variations for the IEEE 69-bus distribution network.

In the IEEE 69-bus distribution network, as detailed in Table II.5, the daily energy loss in the base case scenario amounts to approximately 3797.0 kWh. The voltage profile, illustrated in Figure II.8, demonstrates significant variations over 24 hours, with the maximum bus voltage reaching 1 per unit (*pu*) and the minimum bus voltage dropping to 0.9092 pu at the 15th hour. This indicates notable fluctuations in voltage levels throughout the day.

Table II.5. Daily energy loss for the IEEE 69-bus distribution network with the minimum and the maximum bus voltage.

Base case	IEEE 69
Energy Loss (kWh)	3.7970e+03
Maximum bus voltage (pu)	1
Minimum bus voltage (pu) /15h	0.9092

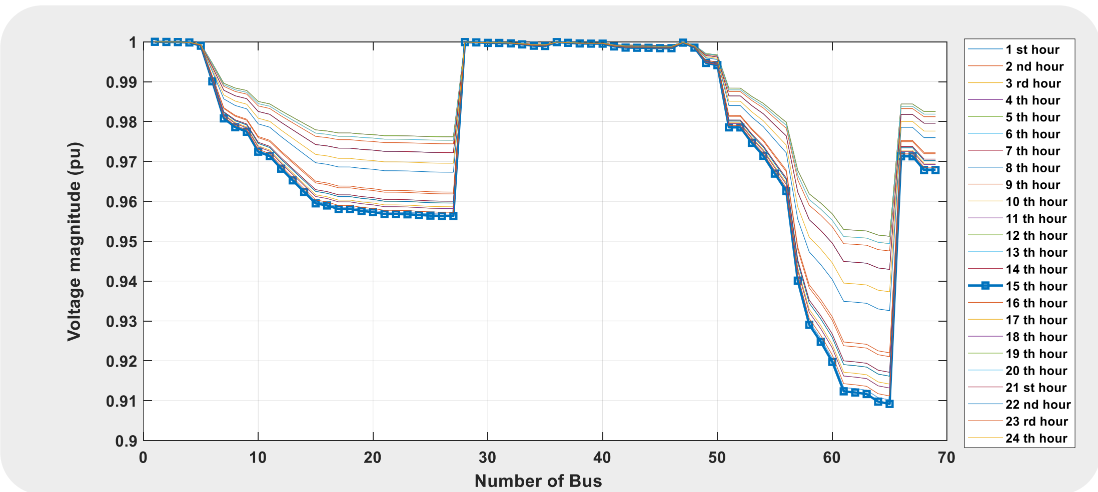

Figure II.8. Voltage profile variation over 24 hours for the IEEE 69-bus distribution network.

II.7.3. Application to the ALG-AB-Hassi Sida 157-bus network

The characteristics of the ALG-AB-Hassi Sida 157-bus distribution network shown in Figure II.9 are as follows:

- Number of buses = 157
- Number of branches = 156
- Reference bus No. = 1
- Base power = 100 MVA
- Base voltage = 12.66 kV

The data for this network are presented in Appendix 3.

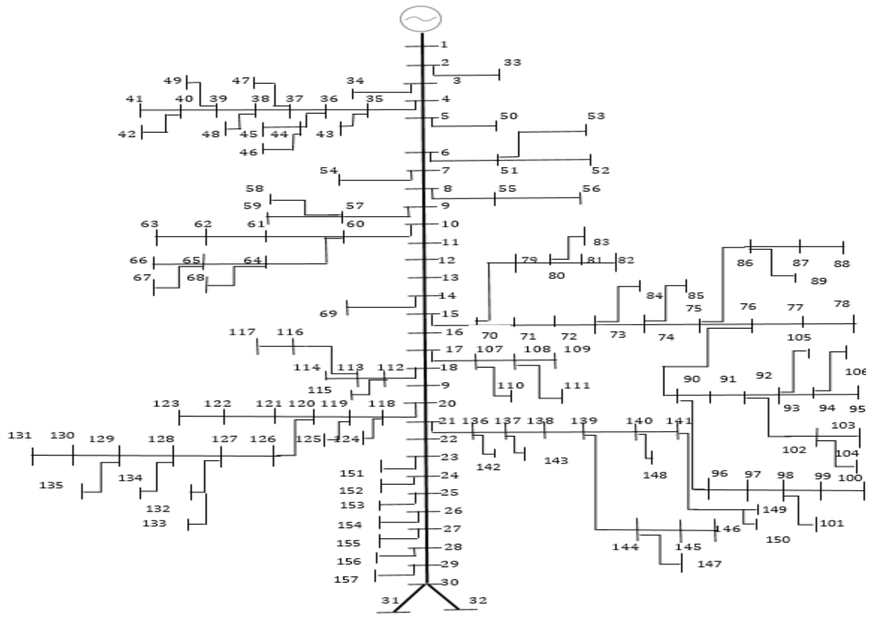

Figure II.9. Simplified representation of the ALG-AB-Hassi Sida 157-bus distribution network.

Table II.6 represents the type of each bus and each line constituting the ALG-AB-Hassi Sida 157-bus distribution network.

Table II.6. Results of Topology Identification for the ALG-AB-Hassi Sida 157-bus Distribution Network.

Reference Bus	1
Terminal Buses	31, 32,33,41,42 ,50,52,54,56,59,63,69,78,109,114,131,150
Intermediate Buses	11,12,13,16,9,22,30
Common Buses	2,3, 4, 5, 6, 7, 8, 9, 10, 14, 15, 17, 18, 20, 21, 23, 24, 25, 26, 27, 28, 29, 30
Main Line	1,2,3,4,5,6,7,8,9,10,11,12,13,14,15,16,17,18,19,20,21,22,23,24,25,26,27,28, 29,30
Side Lines	2,33

	3, 34
	4 ,35, 36, 37, 38, 39, 40, 41
	5,50
	6,51, 52
	7, 54
	8 ,55, 56
	9, 57, 59
	10,60, 61,62, 63
	14 ,69
	15,70, 71, 72, 73, 74, 75, 76, 77, 78
	17, 107, 108, 109
	18, 112, 113, 114
	20, 118, 119, 120, 121, 122, 123
	21, 136, 137, 138, 139, 140, 141, 149
	23, 151
	24 ,152
	25 ,153
	26 ,154
	27 ,155
	28 ,156
	29 ,157
	30 ,31, 32

Table II.7. Daily energy loss for the ALG-AB-Hassi Sida 157-bus distribution network with the minimum and the maximum bus voltage.

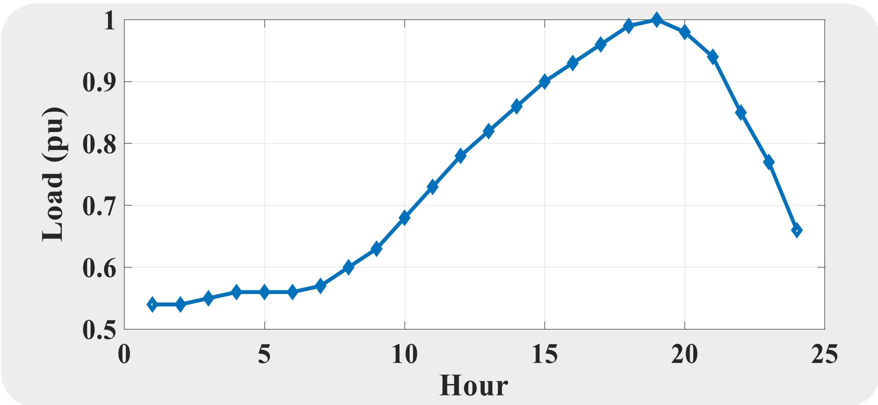

Figure II.10. Annual daily average variations for the ALG-AB-Hassi Sida 157-bus distribution network.

In the ALG-AB-Hassi Sida 157-bus distribution network, as shown in Table II.7, the daily energy loss in the base case scenario is approximately 17995.0 kWh. The voltage profile, depicted in Figure II.11, illustrates significant variations over a 24-hour period, with the maximum bus voltage reaching 1 per unit (*pu*) and the minimum bus voltage dropping to 0.8906 pu at the 15th hour. This indicates considerable fluctuations in voltage levels throughout the day.

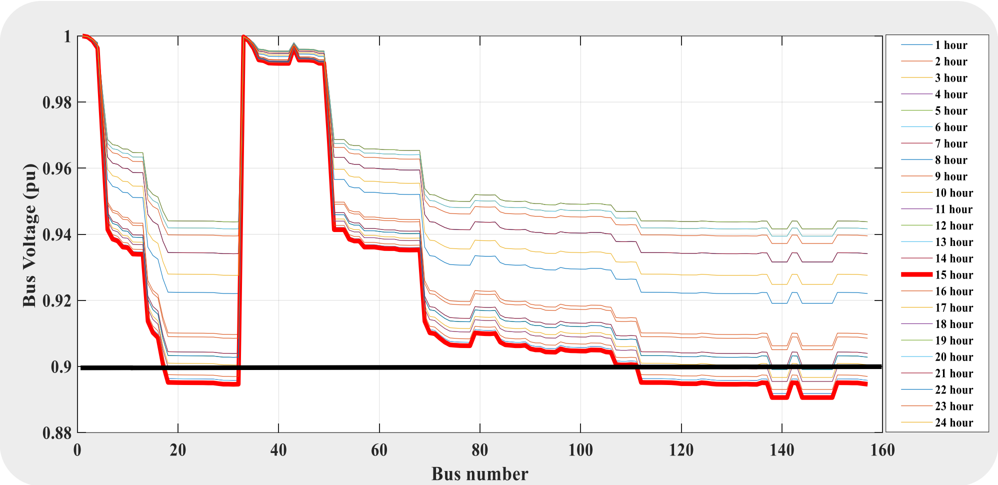

Figure II.11. Voltage profile variation over 24 hours for ALG-AB-Hassi Sida 157-bus distribution network.

Base case	ALG-AB-Hassi Sida157
Energy Loss (kWh)	1.7995e+04
Maximum bus voltage (pu)	1
Minimum bus voltage (pu) /15h	0.8906

II.8. Conclusion

In this chapter, we explored the critical role of power flow analysis in distribution networks, focusing on radial configurations. The backward/forward sweep method was highlighted as an effective solution for power flow problems, particularly due to its fast convergence and adaptability in unbalanced and harmonically polluted systems. Through tests on networks like the IEEE 33-bus and 69-bus systems, the method demonstrated its capability in reducing power losses and maintaining voltage stability. The chapter emphasized the importance of network topology and bus classification in ensuring efficient and reliable network operation.

In the next chapter, we will introduce metaheuristic techniques, which are probabilistic optimization methods used to tackle complex problems where traditional methods fall short. These algorithms are highly adaptable and are applied in fields like energy systems and logistics to solve optimization challenges efficiently. The chapter will explore their principles, applications, and potential benefits.

CHAPTER III

Metaheuristic Techniques for Distribution Networks

III.1. Introduction

Metaheuristics are approximate optimization methods developed to solve challenging problems that are difficult to address with exact methods or would require excessive computational time. These techniques employ probabilistic mechanisms to explore the search space, aiming to identify or approximate a global optimum. Unlike traditional optimization approaches that often rely on gradient information or deterministic rules, metaheuristics incorporate randomness, which enables them to avoid being trapped in local optima and explore the global search space more effectively.

Metaheuristics have gained significant traction in a wide range of domains, including power distribution networks, renewable energy integration, electronics, mechanics, cryptography, logistics, finance, and bioinformatics. Their flexibility and robustness make them particularly suitable for tackling complex real-world problems characterized by non-linearity, high dimensionality, and the presence of multiple local optima.

This chapter specifically explores the application of metaheuristic techniques in optimizing power distribution networks. It reviews the foundational principles of various metaheuristic algorithms, their practical implementation, and the specific types of problems they address within the context of distribution networks. By understanding the advantages and limitations of different metaheuristic approaches, researchers and practitioners can make more informed decisions when selecting and customizing these methods for complex optimization challenges in distribution networks.

III.2. Optimization

Many problems in operations research, applied mathematics, analysis, statistics, and control theory can be considered optimization problems. Generally, an optimization problem involves determining a solution x that belongs to a search space X. This solution minimizes or maximizes an objective function f. Additionally, an optimization problem may include equality and/or inequality constraints on the candidate solutions, which typically serve as additional conditions that limit the search space [60].

Mathematical Formulation:

The optimization problem can be mathematically expressed as follows:

Find x ∈ X and $\boldsymbol{x} = \begin{bmatrix} \boldsymbol{x_1} \\ \boldsymbol{x_2} \\ \vdots \\ \boldsymbol{x_n} \end{bmatrix}$ that minimizes (or maximizes) f (x).

Under the contraints:

$$g\,j(x)\; j = 1 \cdots m \qquad \text{(III.1)}$$

Where the variables $\boldsymbol{x} = \begin{bmatrix} x_1 \\ x_2 \\ \vdots \\ x_n \end{bmatrix}$ are called 'optimization variables' or decision variables, the function f is the objective function (also called the cost function or fitness function), it is defined according to the problem posed, and m is the number of constraints.

Solving an optimization problem then amounts to finding the points of local (or global) minimum (or maximum) of the function, f. Figure III.1 provides an example of local and global minima and maxima.

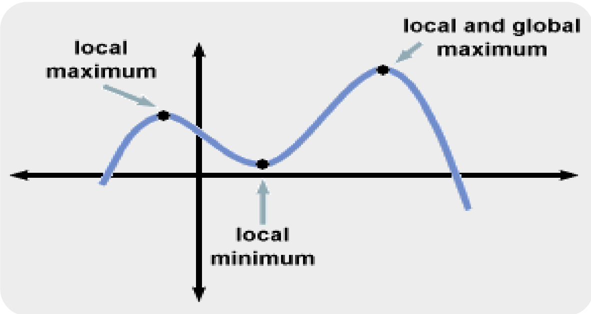

Figure III.1. The local and global minima and maxima of a function.

III.2.1. Classification of Optimization Problems

There are several criteria for classifying optimization problems [61, 62]:

Classification according to the existence of constraints: the optimization problem can be without or with constraints.

- **Classification according to the nature of the variables:** according to the nature of the variables, optimization problems can be classified into two categories:
    1. In the first category, the problem involves finding the optimal value of a parameter, for example:

Find x ∈ X and $\boldsymbol{x} = \begin{bmatrix} x_1 \\ x_2 \\ \vdots \\ x_n \end{bmatrix}$ that minimizes (or maximizes) f (x).

2. In the second category, the problem involves finding a set of values for a parameter that depends on another parameter, for example:

Find x ∈ X and $\boldsymbol{x}(\boldsymbol{t}) = \begin{bmatrix} x_1(t) \\ x_2(t) \\ \vdots \\ x_n(t) \end{bmatrix}$ that minimizes (or maximizes) f {x(t)}.

This type of problem, where each variable is a function of one or more parameters, is known as a dynamic or trajectory optimization problem.

- **Classification based on the nature of the equations involved:** This classification groups optimization problems into four categories: linear, non-linear, geometric, and quadratic.
    1. Linear: If the objective function and all the constraints are linear functions, the problem is called a linear programming (*LP*) problem ;
    2. Non-linear: If any of the objective functions or constraints are non-linear, the problem is called a non-linear programming (*NLP*) problem ;
    3. Geometric: In a geometric programming (*GMP*) problem, the objective function and the constraints are expressed as polynomials in (*X*) ;
    4. Quadratic: If the objective function is quadratic and the constraints are linear, the problem is called a quadratic problem.

Usually, it is formulated as follows:

$$f(x) = c + \sum_{i=1}^{n} q_i x_i + \sum_{i=1}^{n} \sum_{j=1}^{n} Q_{i,j} x_i x_j \tag{III.2}$$

Under the constraints:

$$\sum_{i=1}^{n} a_{i,j} x_i = b_j \tag{III.3}$$

Where c, q_i, Q_{ij}, b_j and, a_{ij} are constants.

- **Classification based on the type of variables:** The variables of the optimization problem take continuous or discrete values, and consequently, there are continuous optimization problems and discrete optimization problems.
- **Classification according to the deterministic nature of variables:** if some or all variables in an optimization problem are probabilistic (non-deterministic or stochastic), the problem is a stochastic programming problem; otherwise, the problem is a deterministic programming problem.
- **Classification according to the number of objective functions:** depending on the number of objective functions to minimize (or maximize), the optimization problem can be single-objective or multi-objective.

III.2.2. Optimization Techniques

Optimization techniques encompass a wide range of methods, and they can be broadly classified into two categories based on their incorporation of randomness: deterministic (exact) techniques and non-deterministic (approximate) techniques [63, 64, 65, 66] (see Figure III.2).

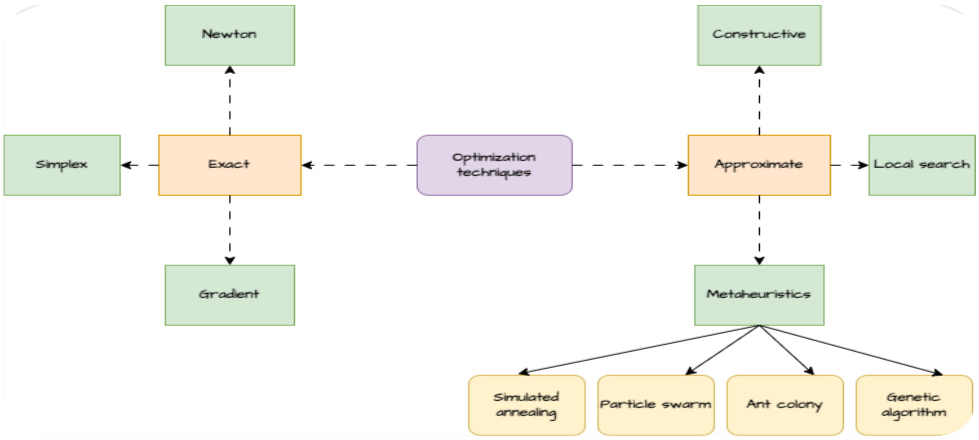

Figure III.2. Classification of Optimization Techniques.

III.2.2.1 Exact Techniques

Exact techniques, also known as deterministic methods, were introduced to solve optimization problems with absolute certainty, guaranteeing the identification of the global optimal solution for specific types of optimization problems. Examples of these methods include Newton's method, the simplex method, and the gradient method. These methods often achieve successful results. However, several limitations restrict their applicability:

- **Convexity, Continuity, and Differentiability:** Exact methods require the objective function to be convex, continuous, and differentiable.
- **Limited Applicability to Large Problems:** Their effectiveness is limited to problems with a small number of variables.
- **Inability to Escape Local Optima:** Objective functions may exhibit multiple local minima. Exact methods may fail to detect and avoid these local minima, converging to the first encountered optimum, which could have a significantly inferior fitness value compared to the global optimum.
- **High Computational Cost:** Exact methods often demand excessive computational time.

While exact techniques guarantee optimal solutions for certain problem types, their limitations in terms of function properties, problem size, and computational cost make them unsuitable for a wide range of optimization problems.

III.2.2.2. Approximative Techniques

In cases where exact methods fail to solve an optimization problem or require an exceedingly high computation time, it is often necessary to resort to approximative techniques. Approximative techniques, or heuristics, provide an approximate solution without guaranteeing optimality, benefiting from reduced computation time. Among these methods are constructive methods, local searches, and metaheuristics.

Metaheuristics are more advanced heuristics. The term metaheuristic was coined by Fred Glover in 1986. It comprises two words: 'heuristic,' which means 'to find,' and the prefix 'meta,' which means 'beyond' or 'at a higher level.' The main advantage of these methods is their adaptability to a wide range of optimization problems. Generally, these methods start by randomly generating a number of candidate solutions. These solutions iteratively change their positions until they converge to an optimal solution (see Figure III.3).

III.3. Metaheuristics

Metaheuristics are stochastic optimization algorithms designed to solve difficult optimization problems. They have been successfully applied in various fields due to their simplicity and robustness.

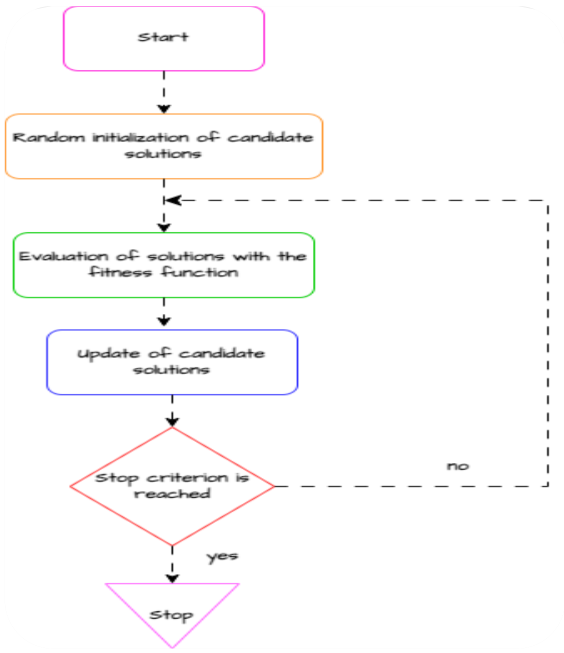

Figure III.3. The General Framework of Metaheuristic Techniques.

According to studies conducted by Kashif et al. in 2018 [67], there are almost 1222 publications on metaheuristics, classified into different types. Table III.1 and the graph presented in Figure III.4 show the number of published works on metaheuristics across various journals. Generally, all metaheuristic techniques share common characteristics [63,64,65]:

- They begin with a random selection of a number of candidate solutions. Then, random search processes are used to manipulate these solutions, improving them from low-quality solutions to the optimal solution.
- Metaheuristics are iterative algorithms, where the same search pattern is repeated multiple times during the optimization process.

Type of Publication

Table III.1. Types of Publications on Metaheuristics.

Journal	New Methods	Modified Methods	Hybrid Methods	Studies	Comparison and Analysis	Applications	Total Number
Elsevier	54	77	26	55	54	43	309
Springer	28	61	24	85	37	38	273
Hindawi	14	96	29	11	14	49	213
IEEE Xplore	16	51	18	7	21	65	178
ACM	5	47	9	27	23	8	119
Other	10	11	0	24	8	16	69
Wiley	3	7	3	31	5	12	61

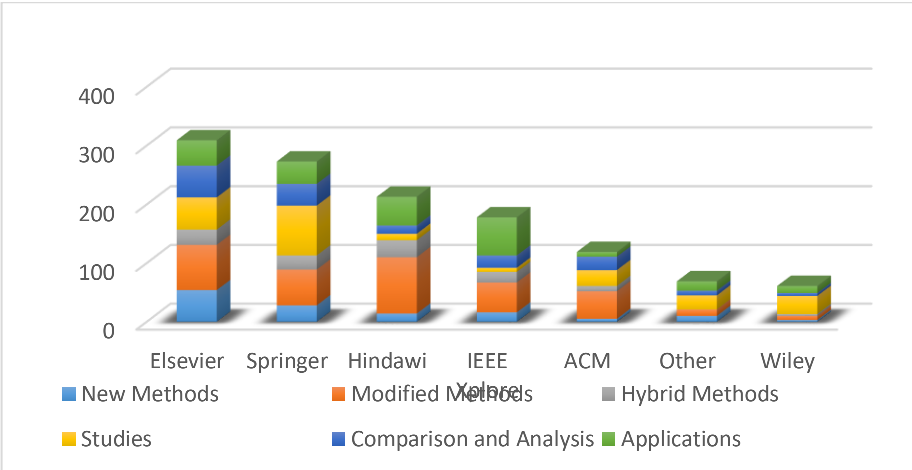

Figure III.4. Graph on Metaheuristics Publications.

- They do not use gradient information of the objective function.
- They are capable of solving difficult optimization problems with minimal information.
- They can find a high-quality solution in a reasonable amount of time without guaranteeing optimality.
- The stochastic nature of metaheuristics helps avoid local optima.
- They are adaptable to a wide range of optimization problems.
- Often, they are inspired by natural phenomena (see Figure III.5).

(a) Genetic Algorithm

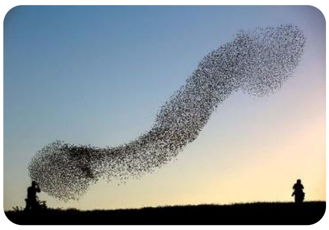

(b) Particle Swarm Optimization

(c) Grey Wolf Optimization

Figure III.5. Some Sources of Inspiration for Metaheuristic Techniques.

Satisfactory resolution of an optimization problem using a metaheuristic technique depends on its ability to strike a good balance between exploration (diversification) and exploitation (intensification) [68].

- **Exploration** refers to the algorithm's ability to visit different regions in the search space to avoid local optima and premature convergence.
- **Exploitation** refers to the algorithm's ability to focus the search in promising regions of the search space (see Figure III.6).

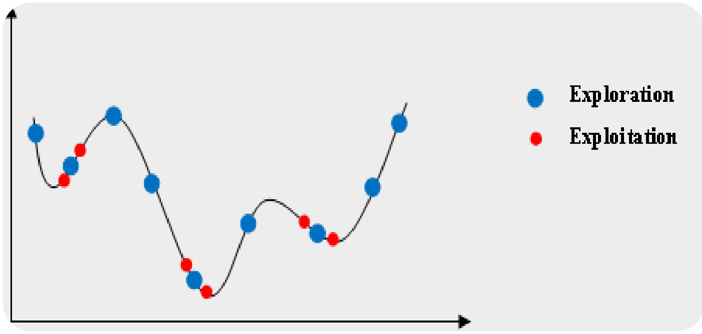

Figure III.6. Exploration and Exploitation in Metaheuristics.

III.3.1. Classification of Metaheuristics

The list of metaheuristic techniques is quite extensive; they can be classified in several ways based on the number of solutions, search history, or inspiration (see Figure III.7).

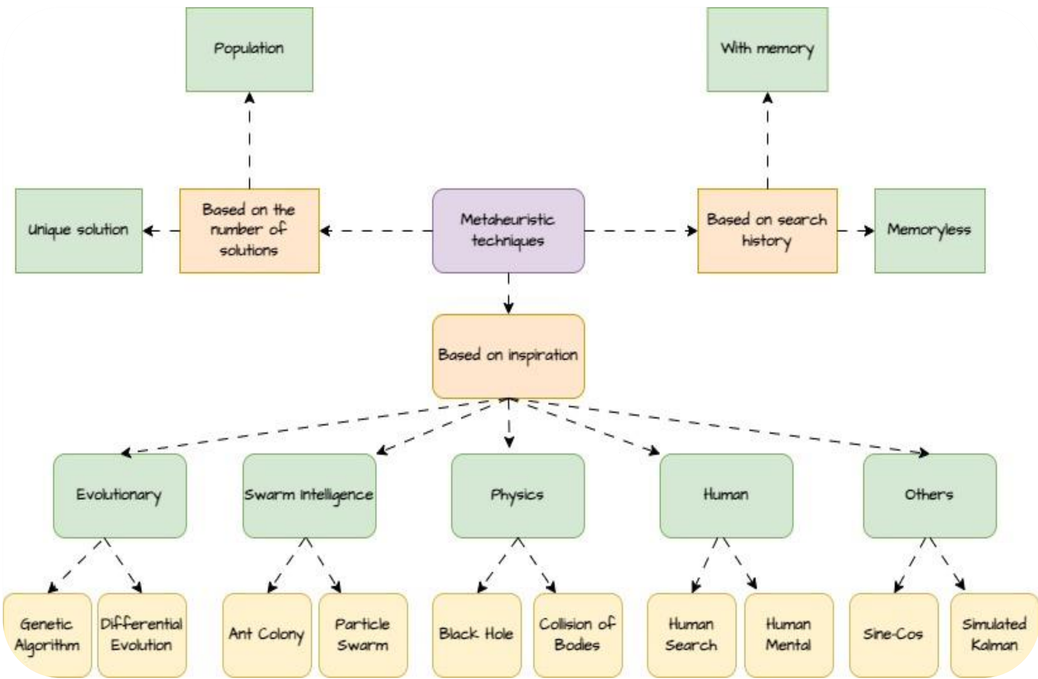

Figure III.7. Classification of Metaheuristics.

According to the number of candidate solutions, we have:

- Single-solution-based methods, also known as trajectory methods. They start with a single initial solution and gradually move away from it by constructing a trajectory in the search space. Among these methods are simulated annealing [1069], descent methods [70], tabu search [71], GRASP [72], variable neighbourhood search [73], and iterated local search [74].
- Population-based methods involve manipulating a set of solutions simultaneously. Among these methods are stochastic fractal search, particle swarm optimization, the sine-cos algorithm, etc. [75, 76, 77, 78].

Generally, single-solution-based metaheuristics are more oriented towards exploitation, whereas population-based metaheuristics are oriented towards exploration [66].

Regarding the use of search history, many metaheuristic techniques utilize their search history to guide optimization in subsequent iterations, whether in the short term (recently visited solutions) or long term (memorization of a set of synthetic parameters describing the search). For instance, the tabu search method memorizes recently visited solutions and prohibits returning to them. The particle swarm optimization method saves the best global solution and the best solution reached by each particle. However, the space required to store the set of solutions can be significant in terms of memory space [79].

According to inspiration, there are:

- Evolutionary Algorithms (EA) are inspired by biological evolution of species, such as genetic algorithms [80], evolutionary strategies [81], evolutionary programming [82], genetic programming [83], and differential evolution [84]. Most EAs typically involve three main processes: selection, crossover, and mutation, which balance exploration and exploitation [85].
- Swarm Intelligence (SI) algorithms are inspired by social intelligence and collective behavior observed in groups of animals. They are based on mathematical and computational modeling of biological phenomena encountered in ethology [86]. This category includes Particle Swarm Optimization (PSO) [87], Bacterial Foraging Optimization Algorithm [88], Dolphin Partner Optimization [89], Ant Colony Optimization [90], and Grey Wolf Optimizer [91]. Ant Colony Optimization uses pheromone and heuristic information to balance between global and local search [86].
- Algorithms inspired by physical phenomena include Black Hole Algorithm [92], Gravitational Search Algorithm [93], Big Bang-Big Crunch Algorithm [94], Galaxy-based Search Algorithm [95], Optics-inspired Optimization [96], and Collision-based Optimization [97].
- Human-based techniques draw inspiration from human behavior and model various human characteristics, such as Champions League Algorithm [98], Teaching-Learning-Based Optimization [99], Mine Blast Algorithm [100].
- Other inspirations include techniques inspired by sources like Simulated Kalman Filter [101] and Sine-Cosine Algorithm [78].

The "No Free Lunch" theorem (NFL) [102] has demonstrated that if we consider the set of all possible optimization problems, then no algorithm is better than another on average. Indeed, comparing metaheuristic algorithms can only be meaningful once the specific problem being addressed is well-defined. According to [103], optimization is not only a mathematical theory but also relies on user experience to guide the choice of the algorithm to implement.

According to recent results from the applications of metaheuristics in various fields, it has been demonstrated that the use of evolutionary algorithms offers numerous advantages and leads to better outcomes compared to other metaheuristics, especially for highly complex problems. This superiority arises from the fact that distinct solutions from the population are randomly selected and then combined to generate new solutions. The weighted combination of these good partial solutions can lead to excellent overall results. However, a drawback of these methods is that the use of multiple update processes can increase the number of evaluations of the fitness function.

III.3.2. Extensions of Metaheuristics

A very interesting characteristic of metaheuristic techniques is their natural ability to be extended to adapt to a wide range of optimization problems [104, 105]. Among these extensions, we can mention:

- **Multi-objective:** These methods aim not for a single optimal solution but for a set of optimal solutions, known as Pareto optimal solutions. A solution is Pareto optimal if any improvement in one objective function inevitably leads to a deterioration relative to another objective function.
- **Multi-population:** Algorithms with multiple populations (or swarms) use several sub-populations to perform different tasks, with the possibility of overlap (or fusion) between sub-populations.
- **Parallel:** This implementation is used to speed up execution by distributing computing tasks across multiple processors.
- **Hybrid:** This approach involves combining metaheuristic techniques with other optimization methods, whether exact or metaheuristic, to leverage their respective advantages.

III.3.3. Design of New Metaheuristic Methods

The "No Free Lunch" theorem (NFL) has opened the door for researchers to develop new metaheuristic techniques [106,107, 108] or improve existing ones [109, 110, 111]. Designing a new effective and efficient metaheuristic technique is not an easy task; several essential characteristics must be considered. The new metaheuristic technique should be capable of:

- Providing a good balance between exploration (to avoid local optima) and exploitation (to converge quickly towards the minimum of a given valley from a starting point).

- Finding a robust optimum, meaning obtaining a solution that is less sensitive to uncertainties.
- Handling a wide range of optimization problems, including single-objective and multi-objective problems.
- Implementing the method should be simple and efficient, with reduced computational complexity and few parameters to adjust.

III.3.4. Applications of Metaheuristics

III.3.4.1 Test Functions

Each new metaheuristic technique must be validated using test functions where the global optimum is known a priori and the number of iterations is fixed to compare results with other techniques. For population-based metaheuristics, the population size is consistently set to 100 candidate solutions across all 23 functions. These test functions are categorized into three groups:

- **Unimodal High-Dimensional Functions (F01 - F07):** These functions have only one global optimal solution and are designed to test the exploitation capability of metaheuristics (see Figure III.8).
- **Multimodal High-Dimensional Functions (F08 - F13):** These are the most challenging optimization functions because they contain multiple local optima. Overcoming these requires a high level of exploration to avoid premature convergence (see Figure III.9).
- **Multimodal Low-Dimensional Functions (F14 - F23):** Similar to the previous category but with lower dimensions, hence fewer local optima (see Figure III.10).

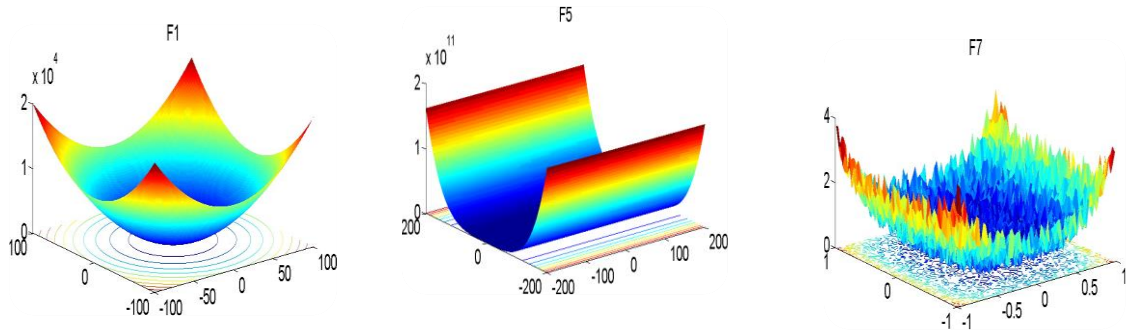

Figure III.8. Examples of High-Dimensional Unimodal Functions F1, F3, and F7.

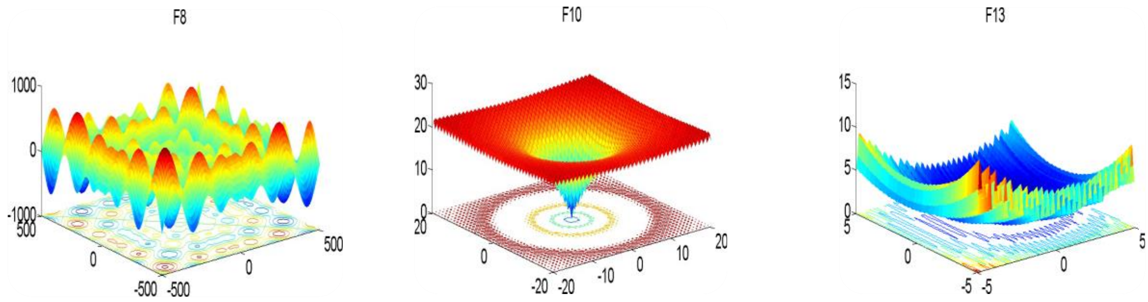

Figure III.9. Examples of High-Dimensional Multimodal Functions F8, F10, and F13.

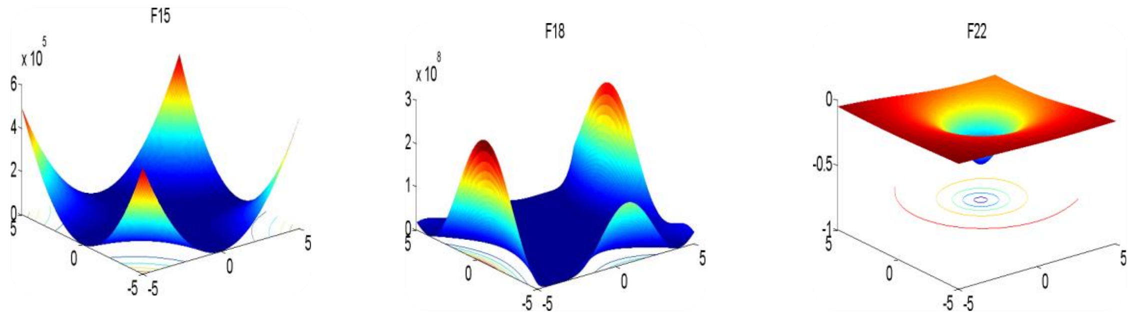

Figure III.10. Examples of Low-Dimensional Multimodal Functions F15, F18, and F22.

III.3.4.2 Real-World Applications

In terms of application, metaheuristic techniques have been successfully applied in several research domains such as: telecommunications networks, production cell formation, medical applications, electrical systems, renewable energy integration in distribution networks, traveling salesman problem, project scheduling, communication systems security, knapsack problem, multimedia applications, automated storage and retrieval systems, quadratic assignment problems, resource allocation problems, vehicle routing, reconfigurable production systems, allocation in logistics chains, assembly sequence planning, Open Shop scheduling, and routing in optical networks.

Several metaheuristic optimization algorithms have been applied across various fields of electrical network optimization. These include the most well-known applications such as economic dispatch and environmental dispatch, energy storage, optimal power flow, reconfiguration of the electric power distribution system, generation, transmission, and distribution, load frequency control, electrical conversion and management, as well as the optimal placement of FACTS (Flexible AC Transmission Systems) devices. These algorithms play a crucial role in enhancing the efficiency, reliability, and stability of electrical networks, addressing complex challenges by providing robust and near-optimal solutions in a reasonable computational time. They are particularly valuable in dealing with the non-linear, multi-objective, and dynamic nature of power systems, ensuring effective management and operation under varying conditions.

Metaheuristic optimization techniques are highly regarded for their ability to effectively address complex optimization problems, making them particularly valuable in maximizing the advantages offered by distributed generators. These techniques are applied to various optimization problems across different fields, providing a wide range of options. Numerous studies have focused on minimizing system losses, reducing costs, improving reliability, and enhancing the overall efficiency of the power grid by optimizing the capacity and placement of distributed generators, and employing diverse methodologies and techniques.

In the context of distributed generation, metaheuristic algorithms are utilized to intelligently explore and exploit the search space, aiming to avoid local optima and quickly converge towards the best global solution. The flexibility and robustness of metaheuristics make them superior to classical optimization techniques, particularly in handling the multifaceted nature of power systems optimization.

III.3.5. Some Metaheuristic Techniques

Metaheuristic techniques are advanced optimization algorithms designed to find optimal or near-optimal solutions for complex problems. These techniques, often inspired by natural phenomena such as evolution, social behavior, or physical processes, are widely used to solve various optimization problems. In our study and investigation, we first applied these algorithms in a mono-objective framework to minimize system losses. In the second part, we employed a multi-objective approach to simultaneously reduce costs, improve reliability, and enhance the overall efficiency of the power grid by optimizing the capacity and placement of distributed generators.

- **Mono-objective:**

III.3.5.1 Particle Swarm Optimization

1. Définition

Particle Swarm Optimization (*PSO*) is an optimization algorithm inspired by the social behavior of bird flocking or fish schooling, first proposed by Kennedy and Eberhart in 1995. PSO simulates a simplified social system where a population of candidate solutions, called particles, move within the search space to find an optimal solution. Each particle adjusts its position based on both its own experience and the experiences of neighboring particles. The velocity and position of each particle are updated iteratively, allowing the swarm to converge toward the global best solution. Originally designed to simulate the graceful yet unpredictable choreography of a bird flock, PSO leverages the collective awareness of the swarm to explore a larger search space, which helps in finding the global minima of a fitness function. This meta-heuristic algorithm efficiently mimics swarm behavior observed in nature to solve complex optimization problems [112].

2. Mathematical model

- Each particle in particle swarm optimization has an associated position, velocity, fitness value.
- Each particle keeps track of the particle_best Fitness_value particle_best Fitness_position.
- A record of global_best Fitness_position and global_best Fitness_value is maintained.

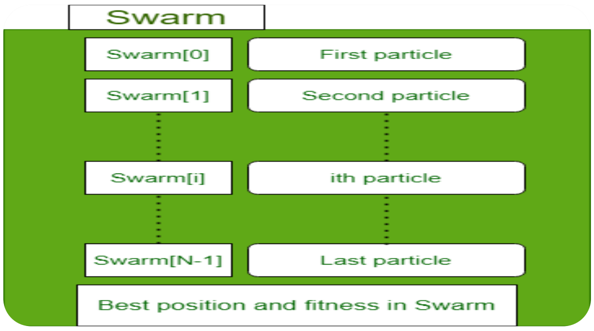

Figure III.11. Data structure to store Swarm population.

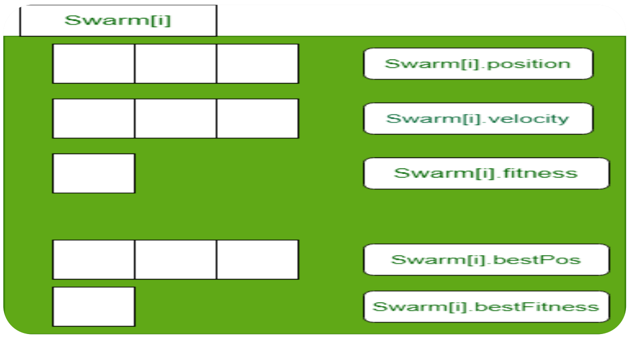

Figure III.12. Data structure to store ith particle of Swarm.

Parameters of problem:

- Number of dimensions (*d*)
- Lower bound (*minx*)
- Upper bound (*maxx*)

Hyperparameters of the algorithm:

- Number of particles (*N*)
- Maximum number of iterations (max_iter)
- Inertia (*w*)
- Cognition of particle (*C1*)
- Social influence of swarm (*C2*)

3. Algorithm

Step1: Randomly initialize Swarm population of N particles Xi (i=1, 2, …, n)

Step2: Select hyperparameter values

w, c1 and c2

Step 3: For Iter in range(max_iter): # loop max_iter times

For i in range(N): # for each particle:

a. Compute new velocity of ith particle

swarm[i].velocity =

w*swarm[i].velocity +

r1*c1*(swarm[i].bestPos - swarm[i].position) +

r2*c2*(best_pos_swarm - swarm[i].position)

b. Compute new position of ith particle using its new velocity

swarm[i].position += swarm[i].velocity

c. If position is not in range [minx, maxx] then clip it

if swarm[i].position < minx:

swarm[i].position = minx

elif swarm[i].position > maxx:

swarm[i].position = maxx

d. Update new best of this particle and new best of Swarm

if swaInsensitive to scaling of design variables.rm[i].fitness < swarm[i].bestFitness:

swarm[i].bestFitness = swarm[i].fitness

swarm[i].bestPos = swarm[i].position

if swarm[i].fitness < best_fitness_swarm

best_fitness_swarm = swarm[i].fitness

best_pos_swarm = swarm[i].position

End -for

Step 4: Return best particle of Swarm

4. Advantages of PSO

1. Insensitive to scaling of design variables.
2. Derivative free.
3. Very few algorithm parameters.

4. Very efficient global search algorithm.
5. Easily parallelized for concurrent processing.

III.3.5.2 Grey Wolf Optimization

1. Définition

Grey Wolf Optimization (*GWO*) is a nature-inspired, population-based meta-heuristic algorithm introduced by Seyedali Mirjalili et al. in 2014. It is based on the leadership hierarchy and hunting mechanism of grey wolves in nature, where the wolves are considered apex predators at the top of the food chain. Grey wolves typically live in packs of 5 to 12 individuals, each following a strict social dominance structure, consisting of alpha, beta, delta, and omega wolves. In GWO, the alpha wolves lead the hunt (representing the search for the optimal solution), while beta and delta wolves assist, and the omega wolves follow. The wolves' positions are updated based on their relative distance to the prey (optimal solution), ensuring a balance between exploration and exploitation in the search space, mimicking the wolves' collective intelligence in finding the optimal solution [113].

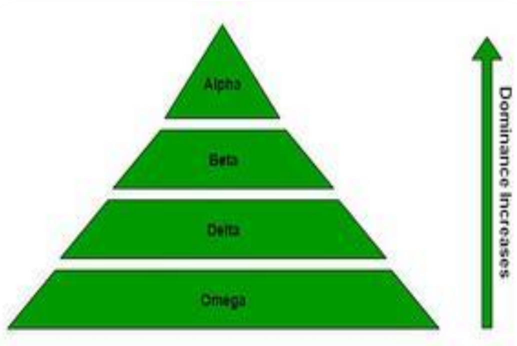

Figure III.13. Social hierarchy of Grey wolves.

1. Alpha α wolf is considered the dominant wolf in the pack and his/her orders should be followed by the pack members.
2. Beta β are subordinate wolves, which help the alpha in decision-making and are considered the best candidate to be the alpha.
3. Delta δ wolves have to submit to the alpha and beta, but they dominate the omega. There are different categories of delta-like Scouts, Sentinels, Elders, Hunters, Caretakers etc.
4. Omega ω wolves are considered as the scapegoats in the pack, are the least important individuals in the pack and are only allowed to eat at last.

2. Main phases of grey wolf hunting:

1. Tracking, chasing and approaching the prey.
2. Pursuing, encircling, and harassing the prey until it stops moving.
3. Attack towards the prey.

The social hierarchy and hunting behaviour of grey wolves are mathematically modelled to design GWO.

3. Mathematical model and algorithm

- **Social hierarchy:**
  - The Fittest solution as an Alpha wolf (*α)*
  - Second best solution as a Beta wolf (*β)*
  - Third best solution as a Delta wolf (*δ)*
  - Rest of the candidate solutions as Omega wolves (*ω*)
- **Encircling the Prey:**

$$\vec{D} = \left|\vec{C} \cdot \vec{X}_p(t) - \vec{X}_p(t)\right| \quad \text{(III.4)}$$

$$\vec{X}(t+1) = \vec{X}_p(t) - \vec{A} \cdot \vec{D} \quad \text{(III.5)}$$

Where t indicates the current iteration, $\vec{A}$ and $\vec{C}$ are coefficient vectors, $\overrightarrow{X_p}$ is the position vector of the prey, and $\vec{X}$ indicates the position vector of a grey wolf. $\vec{X}_1(t+1) = X(t) - \overrightarrow{A_1} \cdot \vec{D}$

$$\vec{A} = 2\vec{a}\vec{r}_1 - \vec{a} \ \text{ and } \ \vec{C} = 2\overrightarrow{r_2} \quad \text{(III.6)}$$

Components of $\vec{a}$ are linearly decreased from 2 to 0 over the course of iterations and $\overrightarrow{r_1}, \overrightarrow{r_2}$ are random vectors in[0,1].

- **Hunting:**

In each iteration, omega wolves update their positions by the positions α, β, and δ alpha, beta, and delta because α, β, and δ have better knowledge about the potential location of prey.

$$D = \left|\vec{C}_1 \cdot \overrightarrow{X(t)} \overrightarrow{-\vec{X}(t)}\right|, D = \left|\vec{C}_2 \cdot \overrightarrow{X(t)} \overrightarrow{-\vec{X}(t)}\right|, D = \left|\overrightarrow{C_3} \cdot \vec{X}(t) - \vec{X}(t)\right| \quad \text{(III.7)}$$

$$\vec{X}_1(t+1) = X(t) - \overrightarrow{A_1} \cdot \vec{D}\,,\ \overrightarrow{X_2}(t+1) = X(t) - \overrightarrow{A_2} \cdot \vec{D}\,,\ \overrightarrow{X_3}(t+1) = X(t) - \overrightarrow{A_3} \cdot \vec{D} \quad \text{(III.8)}$$

$$\vec{X}(t+1) = \left(\vec{X}_1 + \vec{X}_2 + \vec{X}_3\right)/3 \quad \text{(III.9)}$$

- **Attacking prey (exploitation):**

When the prey stops moving the grey wolf finishes the hunting by attacking the prey and mathematically models that we decrease the value of $\vec{a}$. $\vec{A}$ is a random value in the interval [-2a, 2a], where a is decreased from 2 to 0 throughout iterations.

|A|<1 forces the wolves to attack the prey (exploitation).

- **Searching for prey (exploration)**

|A|>1 forces the grey wolves to diverge from the prey to hopefully find a fitter prey (exploitation)

Another component of GWO that favours exploration is $\vec{C}$. It contains random values between [0, 2]. C>1 emphasize the attack while C<1 deemphasize the attack.

4. Pseudocode of the GWO algorithm:

- **Step1:** Randomly initialize the population of grey wolves X_i (i=1,2,…,n)
  - **Step2:** Initialize the value of a=2, A and C (using eq. III.6)
- **Step3:** Calculate the fitness of each member of the population
  - X_α=member with the best fitness value
  - X_β=second best member (in terms of fitness value)
  - X_δ=third best member (in terms of fitness value)
- **Step4:** FOR t = 1 to Max_number_of_iterations:
  - Update the position of all the omega wolves by eq. III.7, III.8 and III.9
  - Update a, A, C (using eq. III.6)
  - a = 2(1-t/T)
  - Calculate Fitness of all search agents
  - Update Xα, Xβ, Xδ.
  - END FOR
- **Step5:** return X_α

III.3.5.3 Whale Optimization

1. Définition

The Whale Optimization Algorithm (*WOA*) is inspired by the bubble-net hunting strategy of humpback whales. Proposed by Mirjalili and Lewis in 2016, WOA mimics the foraging behavior of whales, where they create bubble nets to encircle prey. In an optimization context, candidate solutions are treated as whales, and they encircle the best solution found so far. The algorithm updates the positions of the whales based on the best-known position, incorporating mechanisms to simulate both exploration (searching for prey) and exploitation (encircling prey) [114].

Humpback whales' foraging behaviour, known as the bubble-net feeding method, involves hunting schools of krill or small fish near the surface. This behaviour is characterized by whales creating distinctive bubbles along a circular or "9"-shaped path as shown in Figure. III.14. Two primary manoeuvres associated with bubble-net feeding are the 'upward-spirals' and 'double-loops' techniques:

In the 'upward-spirals' manoeuvre, humpback whales dive about 12 meters deep, then create bubbles in a spiral shape around the prey as they swim upwards toward the surface.

The 'double-loops' manoeuvre includes three distinct stages: the coral loop, the lobtail, and the capture loop.

Figure III.14. Bubble-net feeding behaviour of humpback whales.

2. Mathematical Model

Bubble-net feeding is a unique behaviour that can only be observed in humpback whales. In the whale optimization algorithm (*WOA*) the spiral bubble-net feeding manoeuvre is mathematically modelled to perform optimization.

- WOA simulated hunting behaviour with random or the best search agent to chase the prey.
- WOA uses a spiral to simulate the bubble-net attacking mechanism of humpback whales.

Encircling Prey Current best candidate solution is assumed to be close to target prey and other solutions update their position towards the best agent.

$$\vec{D} = \left|\vec{C} \cdot \vec{X}_{\text{best}}(t) - \vec{X}(t)\right| \tag{III.10}$$

$$\vec{X}(t+1) = \vec{X}_{\text{best}}(t) - \vec{A} \cdot \vec{D} \tag{III.11}$$

Where t indicates the current iteration, $\vec{A}$ and $\vec{C}$ are coefficient vectors, $\vec{X}_{\text{best}}$ is the position vector of the best solution, and $\vec{X}$ indicates the position vector of a grey wolf.

$$\vec{A} = 2\vec{a}\vec{r}_1 - \vec{a} \tag{III.12}$$

$$\vec{C} = 2\overrightarrow{r_2} \tag{III.13}$$

Where $\overrightarrow{r_1}, \overrightarrow{r_2}$ are random vectors in [0,1].

Shrinking encircling mechanism

- This behaviour is achieved by decreasing the value of $\vec{a}$. a is decreased from 2 to 0 throughout iterations.

Spiral updating position

$$\vec{D}^t = \left|\vec{X}_{\text{best}}(t) - \vec{X}(t)\right| \tag{III.14}$$

$$\vec{X}(t+1) = \vec{D}^t \cdot e^{bl} \cdot \cos(2\pi l) + \vec{X}_{\text{best}}(t) \tag{III.15}$$

Search for prey

Humpback whales search randomly according to the position of each other.

$$\vec{D} = \left|\vec{C} \cdot \vec{X}_{\text{rand}}(t) - \vec{X}(t)\right| \tag{III.16}$$

$$\vec{X}(t+1) = \vec{X}_{\text{rand}}(t) - \vec{A} \cdot \vec{D} \tag{III.17}$$

3. Algorithm

Step1: Initialize the whales population

$X_i=(i=1,2,\ldots..,n)$

Step2: Calculate fitness of each search agent

X_{best} = the best search agent

Step3: while (t < maximum number of iterations)

for each search agent:

a, A, C, l and p

Update

if(p<0.5):

if(|A|<1):

Update current agent by eq. (III.10)

else:

Select a random agent

Xrand

update current agent by eq (III.16)

else:

update search agent by eq (III.14)

end-for

Check if any search agent goes beyond the search space and amend it

Calculate fitness of each search agent

Update

X_{best}

if there is a better solution

t = t+1

end-while

Step4: return

X_{best}

III.3.5.4. EM-BT algorithm

1. Définition

In 2022, the Efficient Metaheuristic BitTorrent (*EM-BT*) algorithm was introduced as a novel optimization method, drawing inspiration from the BitTorrent protocol, commonly used for peer-to-peer file sharing. This protocol allows users to share file segments directly with each other, reducing the load on central servers. The EM-BT algorithm adapts this principle by promoting interaction and information exchange between candidate solutions, thereby enhancing their collective performance [115]. What sets EM-BT apart is its ability to deliver innovative solutions across various fields, even in areas where many other metaheuristic techniques have been applied. This highlights the algorithm's flexibility and effectiveness in solving problems that may not be as effectively addressed by traditional optimization approaches.

2. Mathematical model of the EM-BT algorithm

Like other metaheuristic methods, the EM-BT approach starts by randomly generating a population of candidate solutions.

$$x = B_{Low} + (B_{Up} - B_{Low}) \times rand \quad \text{(III.18)}$$

Where, B_{Low} and B_{Up} represent the minimum and maximum boundaries of the search space, and $rand$ signifies a random number uniformly distributed within the range [0, 1].

The matrix comprising all candidate solutions can be represented in the following manner:

$$X = \begin{bmatrix} x_{1,1} & x_{1,2} & \cdots & x_{1,D} \\ x_{2,1} & x_{2,2} & \cdots & x_{2,D} \\ \vdots & \vdots & \ddots & \vdots \\ x_{N,1} & x_{N,2} & \cdots & x_{N,D} \end{bmatrix} \quad \text{(III.19)}$$

N and D indicate the population size and the problem’s dimension respectively.

This population is then evaluated using a fitness function, to measure the abilities of each solution, comparing them at each iteration, and selecting the best one.

$$F = [f(x_1) \quad f(x_2) \quad \dots \quad f(x_i) \quad \dots \quad f(x_N)] \tag{III.20}$$

F is a vector that stores the fitness values acquired from the considered fitness function, denoted as f.

In the BitTorrent protocol, users are regrouped into three levels: seed, peers, and new peers. Users within the same level download certain file pieces from those in the higher level while exchanging the remaining pieces.

Using the same concept of the BitTorrent protocol, and based on the fitness values, the EM-BT algorithm divides the population into three groups: seed, peers, and new peers. The seed represents the best solution discovered thus far, while the peers comprise the first, second, third, and fourth best solutions. The remaining individuals in the population form the new peer group.

The candidate solutions are updated at each iteration as follows:

a) The seed x_s, representing the optimal global solution, is updated in each iteration utilizing the following equation:

$$x_s^{iter+1} = \underset{i=1:N}{argmin}(f(x_i)) \tag{III.21}$$

b) The peers, which denote the solutions in the second level, download file pieces by communicating with the seed x_s and among themselves (peer-to-peer communication). Thus, the peer solutions are updated in two phases using the following equations:

- Communication with the seed

$$\begin{cases} x_{i,j}^{iter+1} = x_{s,j}^{iter} - \alpha \times r \times (x_{s,j}^{iter} - x_{i,j}^{iter}) & if\ rand \leq 0.5 \\ x_{i,j}^{iter+1} = x_{i,j}^{iter} & Otherwise \end{cases} \tag{III.22}$$

Each peer solution $x_{i,j}^{iter+1}$ is updated using (III.22)

The EM-BT flowchart is illustrated in Figure III.15.

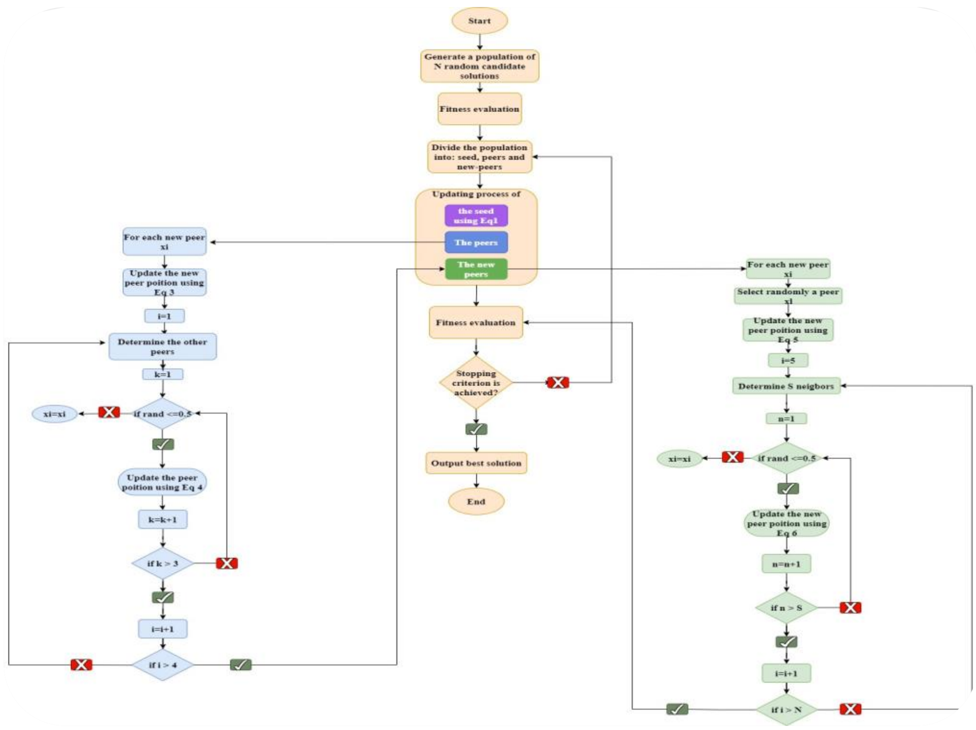

Figure. III.15. Flowchart of EM-BT.

Where, the subscripts i and j denote the solution and dimension indices, respectively. $i = 1, 2, 3, 4$ and $j = 1,2, \dots, D$.

r and $rand$ are two random numbers taken uniformly from [0,1]

The parameter α decreases from 2 to 0, enabling the algorithm to transition from exploration to exploitation.

This progression is controlled using the following equation:

$$\alpha = 2 - \frac{iter}{MaxIter} \times 2 \tag{III.23}$$

To introduce a random aspect into the EM-BT approach, the candidate solutions are updated, if a random number, $rand$, is less than or equal to 0.5; otherwise, it remains unchanged.

- Communication peer-to-peer

$$\begin{cases} x_{i,j}^{iter+1} = x_{k,j}^{iter} - \alpha \times r \times (x_{k,j}^{iter} - x_{i,j}^{iter}) & if\ rand \leq 0.5 \\ x_{i,j}^{iter+1} = x_{i,j}^{iter} & Otherwise \end{cases} \tag{III.24}$$

For each peer solution $x_{i,j}^{iter}$, another peer $x_{k,j}^{iter}$ is selected, then it is updated using (III.20).

$$k = 1, 2, 3, 4, with\ k \neq i$$

c) **N**ew-peers communicate with the peers and with other New peers to share information, they update their positions, in two phases, using the following equations:

- Communication with the peers

$$\begin{cases} x_{i,j}^{iter+1} = x_{l,j}^{iter} - \alpha \times r \times (x_{l,j}^{iter} - x_{i,j}^{iter}) & if\ rand \le 0.5 \\ x_{i,j}^{iter+1} = x_{i,j}^{iter} & Otherwise \end{cases} \tag{III.25}$$

For each new peer $x_{i,j}^{iter}$, a peer solution $x_{l,j}^{iter}$ is selected, where $i = 5,6,7, \dots, N$, and l assumes values within the range [1 - 4].

- Communication with other new peers

$$\begin{cases} x_{i,j}^{iter+1} = x_{n,j}^{iter} - \alpha \times r \times (x_{n,j}^{iter} - x_{i,j}^{iter}) & if\ rand \le 0.5 \\ x_{i,j}^{iter+1} = x_{i,j}^{iter} & Otherwise \end{cases} \tag{III.26}$$

For each new peer solution $x_{i,j}^{iter}$, another new peer $x_{n,j}^{iter}$ is selected from its neighbors, then it is updated using (III.25), where. $n = 5,6,7, \dots, N,\ with\ n \neq i$

In the EM-BT algorithm, new solutions replace older ones if their fitness values show improvement. This updating process continues through multiple iterations until a specified stopping condition is met. Each optimization algorithm operates with unique parameters that impact its overall performance. For example, EM-BT incorporates a parameter 'a' that controls the electromagnetism force and is tied to temperature. In Particle Swarm Optimization (PSO), parameters such as cognitive and social coefficients, along with inertia weight, guide the algorithm's behaviour. Similarly, the Grey Wolf Optimizer (GWO) relies on parameters that define the positions of alpha, beta, and delta search agents, while the Whale Optimization Algorithm (WOA) uses parameters that balance exploration and exploitation rates.

❖ Multi-objective:

III.3.5.5 Multi-Objective Jellyfish Search (MOJS)

1. Definition

The **Multi-Objective Jellyfish Search (*MOJS*)** algorithm is a nature-inspired optimization technique that mimics the behaviour of jellyfish in the ocean. Jellyfish exhibit two main types of movement: passive movement driven by ocean currents and active swimming to search for food. MOJS leverages these behaviours to solve multi-objective optimization problems, aiming to find a set of Pareto-optimal solutions that balance multiple objectives [116].

2. Main Features

- **Passive Movement:** This is akin to jellyfish drifting with ocean currents. In MOJS, this phase allows for exploration by encouraging a broad search of the solution space.
- **Active Movement:** Mimics jellyfish swimming towards food. This is the exploitation phase, where solutions refine and move toward more promising areas of the search space.
- **Population-based:** MOJS evolves a population of solutions over several generations.

- **Pareto dominance** is used to compare solutions concerning multiple objectives, helping to find trade-offs between competing objectives.

3. Flow Chart

1. **Initialize** the population of jellyfish (randomly).
2. **Evaluate** the population using objective functions.
3. **Apply passive movement**: Explore new areas by drifting.
4. **Apply active movement**: Exploit current good solutions by searching in local neighborhoods.
5. **Pareto dominance sorting**: Select non-dominated solutions.
6. **Check termination criteria** (e.g., number of generations).
7. **Output the Pareto front** of solutions.

III.3.5.6 Multi-Objective Flower Pollination Algorithm (MOFPA)

1. Definition

The **Multi-Objective Flower Pollination Algorithm (*MOFPA*)** is an evolutionary algorithm inspired by the pollination process of flowering plants. The core idea is based on the pollination mechanism where pollinators (such as bees) transfer pollen, leading to fertilization. The algorithm simulates both global and local pollination modes [117].

- **Global Pollination**: Represents cross-pollination using Lévy flights, which helps in exploring the search space widely.
- **Local Pollination**: Represents self-pollination, focusing on exploitation by refining solutions in the local vicinity.

MOFPA is particularly useful in balancing exploration (global search) and exploitation (local search), aiming to find a diverse set of Pareto-optimal solutions for multi-objective problems.

2. Main Features

- **Global Pollination** (Exploration): Uses Lévy flight-based random walks to search the global solution space.
- **Local Pollination** (Exploitation): Nearby flowers are pollinated through local random walks, refining the search.
- **Switch Probability**: Determines whether a global or local pollination process is used at each iteration.

3. Flow Chart

1. **Initialize** the population (flowers).
2. **Evaluate** the fitness of each flower using multi-objective functions.

3. **Global pollination** using Lévy flights (explore new regions).
4. **Local pollination** in neighbourhoods of flowers (refine solutions).
5. **Update solutions** based on dominance and fitness.
6. **Check termination criteria** (e.g., max iterations or convergence).
7. **Output Pareto front of solutions**

III.3.5.7. Multi-Objective Lichtenberg Algorithm (MOLA)

1. Definition

The **Multi-Objective Lichtenberg Algorithm (*MOLA*)** is inspired by the physical phenomenon of **Lichtenberg figures**, which are branching, tree-like electrical discharges that form in insulating materials. This branching behavior mimics the search for optimal solutions in a multi-objective context. The algorithm explores the solution space by simulating the formation of these fractal-like discharges, which allows for both exploration and exploitation [118].

2. Main Features

- **Fractal Search** : The algorithm leverages the branching nature of Lichtenberg figures to explore the solution space efficiently.
- **Exploration vs. Exploitation**: By simulating the electric discharges, MOLA achieves a balance between searching broadly (exploration) and fine-tuning solutions (exploitation).
- **Multi-objective focus**: Like other multi-objective algorithms, MOLA uses Pareto dominance to identify the trade-offs between conflicting objectives.

3. Flow Chart

1. **Initialize** the population of discharges.
2. **Evaluate** discharges concerning multi-objective functions.
3. **Fractal branching**: Simulate Lichtenberg discharges to explore new areas of the search space.
4. **Local refinement**: Adjust the solution based on nearby best-performing discharges.
5. **Pareto sorting**: Identify non-dominated solutions.
6. **Check termination criteria**.
7. **Output Pareto-optimal solutions**.

III.3.5.8 Multi-Objective Multi-Verse Optimization

1. Definition

Multi-Objective Multi-Verse Optimization (MOMVO) is a metaheuristic optimization algorithm designed to address problems with multiple conflicting objectives. It builds upon the concept of Multi-Verse Optimization (MVO) by incorporating multiple solution spaces or "universes" to simultaneously explore and optimize various objectives. MOMVO uses the concept of diverse universes to effectively search for a set of Pareto-optimal solutions, representing the best trade-offs between competing objectives. This approach allows MOMVO to efficiently handle complex optimization problems where balancing multiple criteria is essential [119].

2. Mathematical Model of MOMVO

The realm of multi-objective optimization is significantly enriched by the advent of the Multi-Objective Multi-Verse Optimization (MOMVO) algorithm, which provides a nuanced approach to navigating the complexities inherent in optimizing multiple conflicting objectives simultaneously. This advanced algorithm stands out for its capability to efficiently identify a spectrum of Pareto-optimal solutions. These solutions embody the principle of Pareto efficiency, where any attempt to improve one objective leads to the compromise of at least one other, emphasizing the necessity of balance in multi-objective optimization scenarios.
MOMVO innovates by envisioning each potential solution as a unique universe within an expansive multiverse, with the 'fittest' universes showcasing higher inflation rates, a metaphor for their optimization fitness. The algorithm employs cosmological concepts such as white holes, black holes, and wormholes to facilitate the flow of elements across these universes. This process not only encourages diversity within the solution space but also ensures a thorough exploration and exploitation of potential solutions, guiding the algorithm towards the Pareto front. This front represents an optimal trade-off curve where no solution can be considered superior to another based on all objectives, highlighting the relative efficiency of each solution within the defined multi-objective context.
The MOMVO algorithm's operation is akin to navigating a cosmos of possibilities, where each iteration brings it closer to the ideal set of solutions that best reconcile the competing objectives. This approach is particularly effective in complex decision-making environments that demand a delicate balance between different, often conflicting, criteria. The MOMVO algorithm's introduction into the field of optimization heralds a significant advancement, leveraging the metaphorical richness of cosmic phenomena to provide a fresh perspective on solving multi-objective problems. By expanding the metaheuristic optimization toolbox, MOMVO offers researchers and practitioners a sophisticated mechanism for making well-informed, balanced decisions across a broad spectrum of multi-objective optimization scenarios. This innovative approach not only enhances the theoretical framework of multi-objective optimization but also has practical implications for a wide range of applications, from engineering design to resource management and beyond, where complex trade-offs between multiple criteria are a common challenge.

The MVO algorithm relies on some principles during optimization:

- Each candidate solution represents a universe, and each variable is an object in that universe. Each solution is given an inflation rate corresponding to the fitness function value;
- With a higher inflation rate, the probability of having white holes’ increases, while the probability of having block holes’ decreases;

- While solutions with higher inflation rates often send objects through white holes, those with reduced inflation rates tend to receive more objects via black holes;
- Through wormholes, the objects make random movements in the direction of the best universe.

The mathematical model of the MVO can be described as follows:

a) **Initialization:** MVO is a population-based method, start the search with a number n of candidate solutions, initialized randomly in the search space. These solutions are evaluated through a fitness function, and sorted from the best to the worst. Black and white holes are then used for exploring the search space and wormholes for exploitation.

b) Exploration phase

The MVO relies on the roulette wheel strategy to determine the universe that has the white hole, and uses Eq.1 to move black and white holes between different universes:

$$x_i^j = \begin{cases} x_w^j, & r < NF_i \\ x_i^j, & r \geq NF_i \end{cases} \tag{III.27}$$

Where x_i^j represents the j^{th} variable of the candidate solution i. w denotes the white hole Index selected randomly by the roulette wheel mechanism. r is a random number uniformly distributed in the range [0, 1]. NF_i indicates the normalized value of the fitness function of i^{th} solution.

c) Exploitation phase:

Utilizing the wormholes, the MVO makes local adjustments for each universe to perform an effective exploitation of the search space. The following formula describes how this process works:

$$x_i^j \begin{cases} \begin{cases} X_j + TDR \times \left((UB_j - LB_j) \times r1 + LB_j\right), r2 < 0.5 \\ X_j - TDR \times \left((UB_j - LB_j) \times r1 + LB_j\right), r2 \geq 0.5 \end{cases} & , r3 < WEP \\ x_i^j & , r3 \geq WEP \end{cases} \tag{III.28}$$

X_j is the best solution found as far, UB_j and LB_j represent the upper and lower bounds of the search space. Three random numbers between [0,1] are chosen as $r1$, $r2$ and $r3$. The coefficients TDR and WEP are calculated as follows:

$$WEP = c_1 + t \times \left(\frac{c_2 - c_1}{T}\right) \tag{III.29}$$

Where c_1 and c_2 were fixed at 0.2 and 1 respectively.t denotes the current iteration and T the maximum iterations.

$$TDR = 1 - \frac{t^{1/p}}{T^{1/p}} \tag{III.30}$$

With p is equal to 6.

3. Implementation of multi-objective multi-verse optimization for allocating PVRES-CBs problem.

The PVRES-CBs problem is solved using the MOMVO algorithm, in the aim of identifying the set of parameters that are optimal and correspond to the minimal value of the considered objective function. The main process for applying the MOMVO algorithm to solve the PVRES-CBs problem is described in the following steps, and the suggested algorithm's flowchart is shown in Figure III.16.

- **Step 1.** Definition of the optimization problem: Enter the data for the input power system. Declare of search space range, problem dimension, maximum number of candidate solutions, and number of iterations.
- **Step 2.** Random initialization of candidate solutions
- **Step 3.** For each solution (universe), a backwards-forward technique is performed to calculate the fitness values (inflation rates) corresponding to both objective functions (Obj1 and Obj2).
- **Step 4.** Determine the non-dominant solutions, and identify the best one. First, the crowding distance between the solutions in the archive is calculated. The best solution is then selected by using the roulette wheel technique.
- **Step 5.** Normalize the solutions' fitness
- **Step 6.** Update the candidate solutions using Eqs III.26 and III.27
- **Step 7.** Verify if a solution variable is within the specified bounds, if not, we take the limits values and return it to the field.
- **Step 8.** Set the WEP and TDR coefficients' values using Eqs III.28 and III.29
- **Step 9.** Verify whether or not the termination criterion has been met. If not return to step 3, otherwise, go to step 10.
- **Step 10.** Define the Pareto optimal front, and then using fuzzy set theory select the best compromise solution.

Best compromise solution

After obtaining the Pareto-optimal front, fuzzy set theory is employed to identify the best compromise solution, which will generally satisfy all the different objectives.

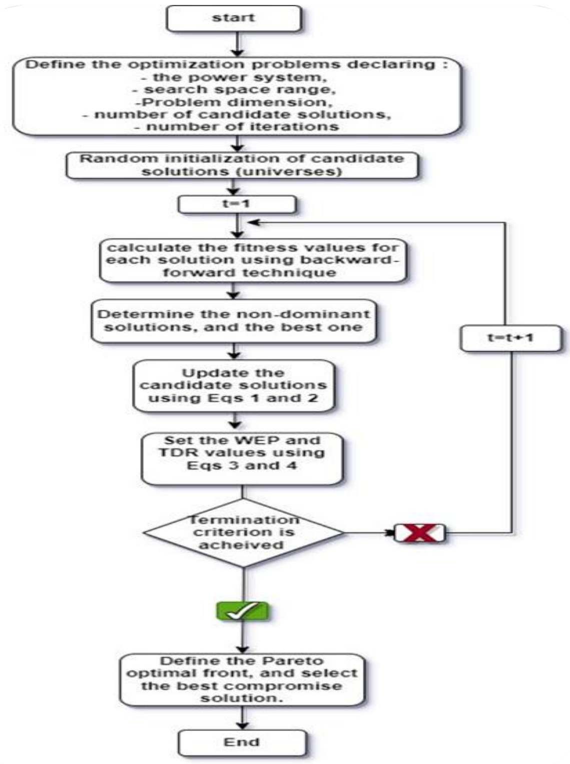

Figure III.16. Flowchart of MOMVO.

III.4. Conclusion

In this chapter, we explored the foundational concepts of optimization and differentiated between exact optimization techniques and metaheuristics. We provided an in-depth examination of the principles behind metaheuristic algorithms, discussing their validation through test functions and their wide range of real-world applications. Particular emphasis was placed on the role of metaheuristics in the integration of renewable energy within power distribution networks, highlighting their ability to optimize energy distribution, reduce costs, and enhance grid stability. We also addressed the key challenges and limitations of metaheuristics, including issues related to computational complexity and scalability.

In the following chapter, we will present our conceptual contributions to addressing the challenges of renewable energy integration in distribution networks through the application of advanced metaheuristic techniques. Both mono-objective and multi-objective metaheuristic algorithms will be employed, specifically tailored to improve the efficiency, reliability, and sustainability of energy distribution systems. These approaches will be supported by new frameworks designed to optimize key performance indicators while balancing multiple conflicting objectives. Additionally, detailed case studies and simulations will illustrate the practical applicability and effectiveness of the proposed solutions in real-world scenarios.

CHAPTER IV

Results and Discussions: Single-Objective and Multi-Objective Planning of Distributed Generation

IV.1. Introduction

This chapter presents the development and application of the Efficient Metaheuristic BitTorrent (*EM-BT*) optimization algorithm, designed to optimize the allocation and sizing of distributed generation (*DG*) resources, with a focus on photovoltaic renewable energy sources (*PVRES*) and capacitor banks (*CB*). The goal of the EM-BT algorithm is to minimize energy losses and improve voltage profiles over a 24-hour period, taking into account diverse load patterns and the impact of environmental factors such as solar irradiance and temperature.

The efficacy of EM-BT is tested across multiple distribution networks, including the IEEE 33-bus, IEEE 69-bus, and ALG-AB-Hassi Sida 157-bus networks in the South Algerian distribution system. Various deployment scenarios for PVRES and CBs are investigated to determine the most efficient configurations. The algorithm's performance is compared against established optimization techniques such as Grey Wolf Optimizer (GWO), Particle Swarm Optimization (PSO), and Whale Optimization Algorithm (WOA). The results demonstrate that the EM-BT algorithm outperforms these traditional methods in terms of energy loss reduction and voltage profile enhancement, making it a highly reliable and effective tool for optimizing DG resource allocation.

In addition to EM-BT, this chapter also introduces the Multi-Objective Multi-Verse Optimization (MOMVO) algorithm, aimed at optimizing the simultaneous integration of DGs and CBs within electrical distribution networks. With dual objectives of minimizing energy losses and voltage deviations, MOMVO significantly enhances network efficiency and reliability. Through rigorous simulations on the IEEE 33 and 69-bus systems, MOMVO achieved up to a 47% reduction in energy losses and a 55% improvement in voltage stability, outperforming other multi-objective optimization techniques like the Jellyfish Search (MOJS), Flower Pollination Algorithm (MOFPA), and Lichtenberg Algorithm (MOLA).

The results of this chapter highlight the superior performance of EM-BT and MOMVO in addressing both technical and economic challenges in distribution network optimization, paving the way for further advancements in the sustainable integration of renewable energy sources into modern power systems.

IV.2. Single-Objective Planning of DG

This study introduces a novel application of the metaheuristic method known as EM-BT, which is designed to minimize daily energy losses and voltage profile deviations while accommodating varying 24-hour load profiles. To assess its practicality and effectiveness, we apply this method to distribution networks, including the conventional IEEE 33 and 69 nodes, as well as the ALG-AB-Hassi Sida 157 buses from the southern Algerian distribution network. We conduct simulation scenarios throughout the day to optimize the allocation of Photovoltaic Renewable Energy Sources (*PVRES*) and capacitor banks (*CB*) with the aim of achieving the maximum possible reduction in the specified objective function.

It is important to highlight that our algorithm specifically accounts for the impact of temperature within the network on Photovoltaic Renewable Energy Sources (*PVRES*), a factor that has not been previously explored in this context. While previous approaches primarily concentrated on identifying the optimal locations for PVRESs and capacitors, our current study pioneers the investigation of the combined effects of temperature and irradiation, representing an innovative and comprehensive approach to optimizing distribution networks.

In fact, temperature has a profound and multifaceted impact on both photovoltaic (*PV*) systems and distribution networks. Elevated temperatures can reduce solar panel efficiency, leading to decreased power output, while extremely low temperatures may enhance efficiency but bring challenges like frost or snow accumulation. Temperature also affects the conductivity and resistance of materials in the distribution network, influencing electrical performance and causing thermal stress on components. Managing these effects is crucial to maintain efficiency, reliability, and overall system performance, particularly in varying environmental conditions.

The efficiency of the proposed EM-BT is demonstrated by comparing its results to those obtained by three other optimization algorithms, namely the Particle Swarm Optimization (*PSO*) algorithm and two other optimization algorithms known as the Grey Wolf Optimizer (*GWO*) and the Whale Optimization Algorithm (*WOA*). As main contributions, we present a novel application of EM-BT for simultaneous PVRES and CB allocation in distribution systems. It allows including the impact of the temperature, as a new parameter, on the electrical networks. Indeed, the performance of solar PVRES is studied under real-world conditions (temperature and irradiance). The objective function and constraints have considered daily energy losses considering various 24-hour loads for the optimization process. We show that the EM-BT algorithm is more effective than the PSO, GWO, and WOA Algorithms in minimizing energy losses and voltage profile deviations while satisfying all operational constraints. In addition, this paper demonstrates that losses and voltage deviations are reduced and increase when a large number of PVRES and CBs are utilized. Therefore, from a technical and practical point of view, it is considered a very successful choice. However, from an economic point of view, it is very expensive. This issue must be taken into consideration in any study.

IV.2.1. Allocation of Photovoltaic Renewable Energy Sources (PVRES) and Capacitor Banks (CB) for Auxiliary Service Provision in Distribution Systems

IV.2.1.1. Integration of capacitor banks

A set of capacitor banks has been incorporated into the system at specific locations. These locations have been considered as control variables that are optimally determined while solving the optimization problem. The maximum capacity of each capacitor bank for both test bus systems is 150 kVAr, and the minimum is 0 kVAr. The optimal value of the reactive power (QCB) to be injected at the optimal bus is determined from this range as given below in eq. (IV.1).

$$0 \le QCB \le 150\ kVAr \tag{IV.1}$$

IV.2.1.2. Integration of PV

The generation of power using PVRES modules relies heavily on meteorological conditions, specifically solar radiation and ambient temperature [120]. The geographical location directly influences these conditions. Therefore, the analysis of solar radiation conditions in a particular area is typically conducted during the initial stages of effectively utilizing PVRES panels. Historical data is collected to calculate the hourly solar radiation standard and daily temperature. These values are then divided into phases. Each phase has specific limits for solar radiation and temperature [121-122].

A practical model, proposed by [123], is employed to optimize the production of optimal output power from a photovoltaic module:

$$P_{Pv-max} = FF \cdot \left(I_{sc} \cdot \frac{G}{G_{ref}}\right) \cdot \left(V_{oc} \cdot \frac{ln(P_1 \cdot G)}{ln\left(P_1 \cdot G_{ref}\right)} \cdot \frac{T_{jref}}{T_j}\right) \tag{IV.2}$$

PPv-max	: Maximum power output of the PV system;
$\mathbf{I_{sc}}$	: Short-circuit current of the PV system;
G	: Actual solar irradiance (sunlight intensity) at a given moment;
$\mathbf{G_{ref}}$	: Reference solar irradiance;
V_{oc}	: Open-circuit voltage of the PV system;
$\mathbf{T_{jref}}$	: Reference junction temperature of the PV system;
$\mathbf{T_j}$	: Junction temperature of the PV system at a given moment.

The constant coefficient P1 can be determined using the following formula:

$$P_1 = \frac{I_{sc}}{G} \tag{IV.3}$$

FF is the Filling factor given by:

$$FF = \frac{P_{pvmax}}{V_{oc} \cdot I_{sc}} = \frac{V_{mpp} I_{mpp}}{V_{oc} I_{sc}} \tag{IV.4}$$

$\mathbf{V_{mpp}}$: Voltage at the Maximum Power Point (MPP) of the PV system;
$\mathbf{I_{mpp}}$: Current at the Maximum Power Point (MPP) of the PV system.

IV.2.2. Distribution network model

In general, the resistance of the AC line is determined by:

$$R = r_0 . l \tag{IV.5}$$

$\mathbf{r_0}$: Linear resistance in [Ω/km];
l : Line length in [m].

In this work, we change the resistance of all network buses (33, 69, and 157) to be in real condition with 24 values of daily temperature as follows:

$$R_{ti}=R\ [1+\ \alpha 25\ (t_i - 25)] \quad \text{(IV.6)}$$

R_{ti} : Resistance value in i-th hour of the day, i=1 to 24.
R : Resistance of the material at a reference temperature (usually 25°C) in [*Ω*];
α25 : Temperature coefficient of the resistance at the reference temperature (usually 25°C);
t : Temperature at which you want to calculate the temperature-dependent resistance (in Celsius).

IV.2.3. Problem Formulation

IV.2.3.1. Objectves Functions

In the context of allocating PVRES-CBs for auxiliary service provision in distribution systems, the main goal is to minimize energy losses daily. This objective can be mathematically formulated as follows:

$$E_{loss} = \sum_{h=1}^{24}\left(\sum_{br=1}^{N_{br}} I_{br}\ (h)^{2} \cdot R_{br}\right) \quad \text{(IV.7)}$$

E_{loss} : The total energy loss per day.

Nbr : Number of distribution branches.
Ibr : Current flowing through each distribution branch (*br*) [*in Amperes, A*].
Rbr : Resistance of each distribution branch (*br*) [*in Ohms, Ω*].

Targets are considered minimized in a single objective model (*Fobj*) as in Equation (IV.8).

$$Fobj = \frac{E_{loss\ \ after\ DG}}{E_{loss\ \ before\ DG}} \quad \text{(IV.8)}$$

IV.2.3.2. Equality and Inequality Constraints

Hence, it is necessary to ensure that the actual power injection, both real and reactive, from PVRES-CB, remains within the specified limits denoted by $PPVRES_{k\_max}$ and Qcb j_max, correspondingly, for every hour:

$$0 < PPVRES_K < PPVRES_{k\_max} \qquad k = 1, \ldots, nPV \quad \text{(IV.9)}$$

$$0 < Q_{cb_j} < Q_{cb_{j\_max}} \qquad j = 1, \ldots, ncb \quad \text{(IV.10)}$$

PPVRES : Real power injection from photovoltaic renewable energy sources (*PVRES*) into the grid [*in Watts, W*].
QCB : Reactive power injection from capacitor banks (*CB*) into the system [*in Volt-Amperes Reactive, VAR*].

Additionally, it's vital to ensure that the voltage at every distribution node and the current flowing through all distribution branches stay within acceptable limits at all times, as specified in reference [124].

$$V_{m\_min} < V_m < V_{m\_max} \qquad m = 1, \ldots, nB \tag{IV.11}$$

$$I_{br} < I_{br_{i\_max}} \qquad i = 1, \ldots, nbr \tag{IV.12}$$

Here, V_m represents the voltage at the bus m , V_{m_min} and V_{m_max} represent the lower and upper voltage bus limits, selected as 10% for all the network busses, and $I_{br_{i\_max}}$ is the thermal capacity limit of branch. These constraints are generally applied to all relevant hours and nodes or branches.

Moreover, as assumed in [125], a threshold on the PVs penetration is considered using the coefficient K_P, so that the PVs installed capacity ($\sum_{k\in nPV} P_{PV_k}$) is equal to 50% of the total active power demand in the system P_{D_m}.

$$\sum_{k\in nPV} P_{PV_k} = K_P \cdot \sum_{m\in nB} P_{D_m} \tag{IV.13}$$

IV.2.4. Results and Discussions

The proposed EM-BT algorithm has been utilized to minimize energy losses, taking into account the variations in PVRES, CB output, and daily load fluctuations. This approach has been tested on three different distribution systems: IEEE 33, IEEE 69, and ALG-AB-Hassi Sida with 157 buses. For the IEEE 33 system, three and six PVRES units, along with nine capacitor banks, have been allocated. However, due to the larger scale of the systems with 69 and 157 buses, a greater number of PVRES units have been incorporated. Specifically, the IEEE 69 distribution system has been allocated 5 and 10 PVRES units along with 18 capacitor banks, while the ALG-AB-Hassi Sida system with 157 buses has been allocated 10 and 20 PVRES units with 25 capacitor banks. Each distribution system has been evaluated using different profiles for PVRES, CB, and load over 24 hours. The input data (presented in Table IV.1) and the corresponding results for each test system are discussed in detail below.

Table IV.1. Daily energy loss for different networks with the minimum and the maximum bus voltage.

Base case	IEEE 33	IEEE 69	ALG-AB-Hassi Sida157
Energy Loss (kWh)	3.5677e+03	3.7970e+03	1.7995e+04
Maximum bus voltage (pu)	1	1	1
Minimum bus voltage (pu) /12h	0.9038	0.9092	0.8906

Three scenarios have been investigated for all networks (IEEE 33, IEEE 69, and ALG-AB-Hassi Sida 157) as follows:

- **Scenario 1:** A state analysis is performed for each loading hour using power flow, taking into account the effect of temperature on all networks.
- **Scenario 2:** The suggested EM-BT algorithm is compared to PSO, GWO, and WOA for PVRES-CB allocations to reduce the considered objective function (Equation (IV.8)).
- **Scenario 3:** The application of the suggested EM-BT, in comparison to PSO, GWO, and WOA, focuses on PVRES allocations but with twice as many PVRES units and the same number of capacitor banks used in the second scenario to minimize the considered objective function (Equation (IV.8)).

Scenarios 2 and 3 are executed with the EM-BT algorithm set to 100 iterations and 30 search agents. In the first scenario, modifications were made to limit the node voltage to 10% or less of the nominal voltage. All compared algorithms were evaluated using the same number of function evaluations, consisting of 10 iterations for each algorithm.

The effectiveness of the proposed EM-BT algorithm is assessed across the three networks: IEEE 33, IEEE 69, and ALG-AB-Hassi Sida 157.

IV.2.4.1. Scenario 1

In this scenario, load flow calculations are conducted for each demand hour, taking into account the impact of temperature. Figure IV.1 (*a*) to (*c*) displays the voltage profile across all distribution nodes for the IEEE 33, IEEE 69, and ALG-AB-Hassi Sida 157 networks, respectively, throughout each hour of load. The voltage profiles consistently fall below the minimum threshold established by the base case, as indicated by the different characteristics observed. Notably, the voltage reaches a minimum of 0.89 per unit (*pu*) for both the IEEE 33 and IEEE 69 networks, and 0.87 pu for the ALG-AB-Hassi Sida 157 network during the peak consumption hour at hour 14. The impact of temperature on the networks is also evident in the daily energy loss, which is presented in Table IV.2 for all networks

Table IV.2. Daily energy loss for all distribution systems with the temperature effect.

	IEEE 33	IEEE 69	ALG-AB-Hassi Sida 157
Energy Loss .e+03 (kWh)	3.8313	4.0857	19.367
Maximum bus voltage (pu)	1	1	1
Minimum bus Voltage (pu)/14h	0.8921	0.8969	0.8784
Energy Loss rising (%)	6.88	7.06	7.08

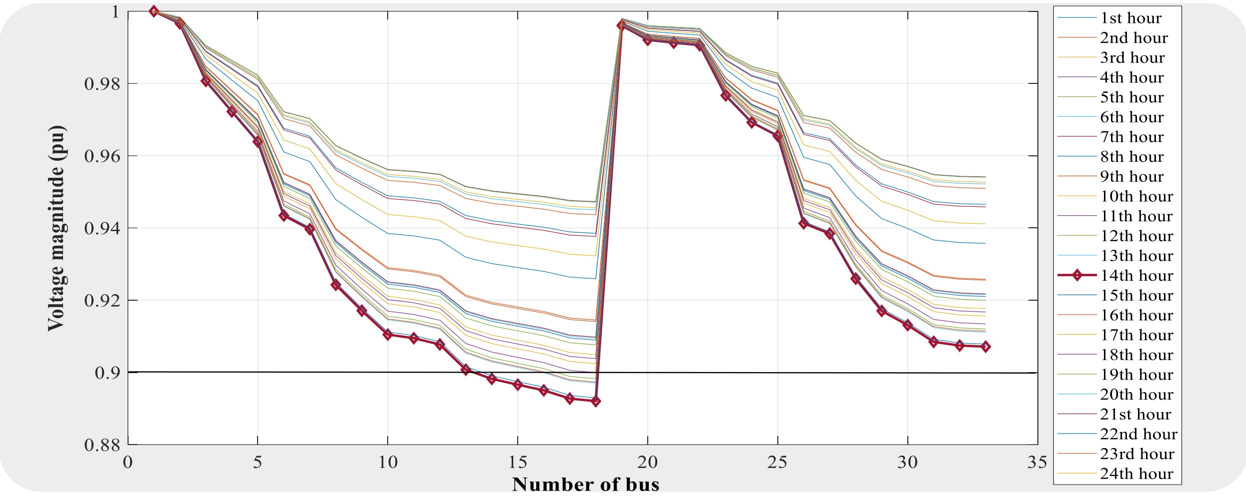

(a) IEEE 33

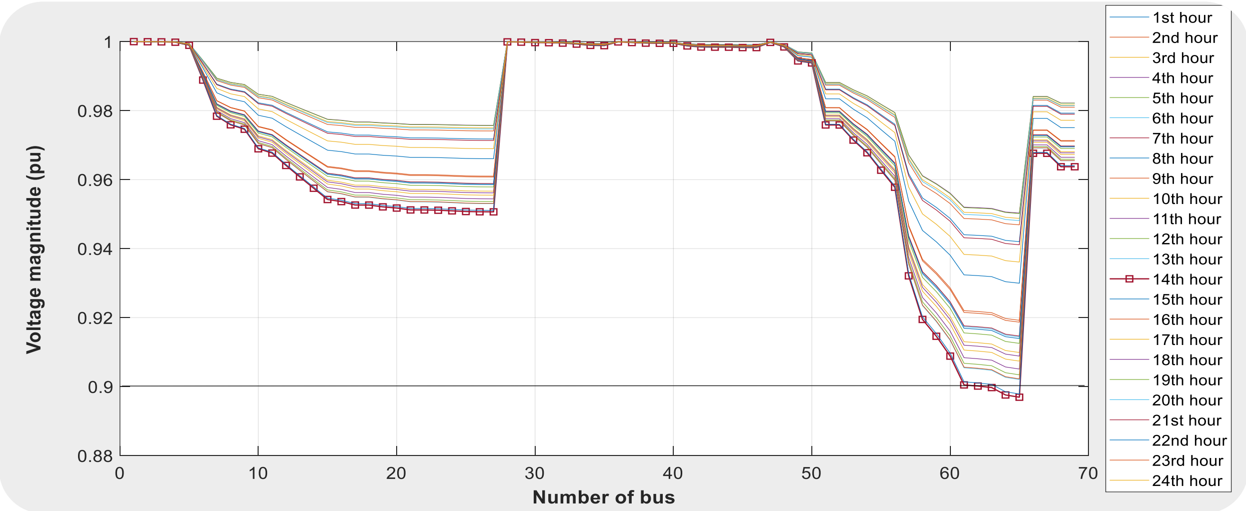

(b) IEEE 69

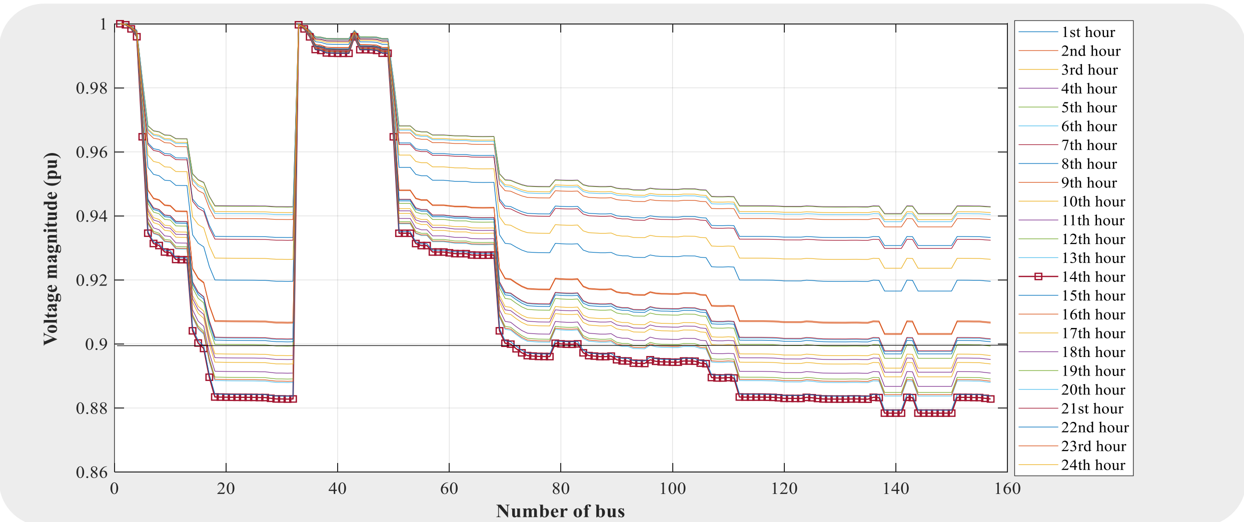

(C) ALG-AB-Hassi Sida 157

Figure IV.1. Hourly voltage profile over 24 hours for the initial Scenario in the three networks.

The results depicted in Figure IV.1 and Table IV.2 indicate that the energy losses of 3,813 *kWh*, 4,085.7 *kWh*, and 19,367 *kWh* for the IEEE 33, IEEE 69, and ALG-AB-Hassi Sida 157 networks, respectively, exceed those of the base cases, which are 3,567.7 *kWh*, 3,797 *kWh*, and 17,995 *kWh* for the same networks, respectively. This leads to an increase of 6.88%, 7.60%, and 7.62% in energy losses for the IEEE 33, IEEE 69, and ALG-AB-Hassi Sida 157 networks, respectively.

IV.2.4.2. Senario 2

In this particular scenario, the EM-BT method minimizes the objective function (Equation IV.8) and is compared to other methods, namely PSO, GWO, and WOA. Several *PVRES* allocations and capacitor banks (*CB*) are considered. Table IV.3 presents the energy losses, voltage deviations, and energy loss reduction rates for each IEEE 33, IEEE 69, ALG-AB-Hassi Sida 157 networks, allowing for a comprehensive comparison. The results of IEEE 33 demonstrate that the proposed EM-BT method achieves a significant reduction in energy loss, with a decrease of 49.06% from 3831.3 kWh/day in the initial case to 1951.5 *kWh/day*. Additionally, the voltage magnitude of the weak bus has improved from 0.89 per unit (*pu*) to 0.93 pu. Concerning IEEE 69, the results show that the proposed EM-BT method reduces energy loss by 56.8%, from 4085.7 *kWh/day* in the first case to 1764.7 *kWh/day*. using the EM-BT technique, the voltage magnitude of the weak bus has increased from 0.89 per unit (*pu*) to 0.92 *pu*. The results of the last network (ALG-AB-Hassi Sida 157) illustrate that the proposed EM-BT method reduces energy loss by 57.96%, from 19367 *kWh/day* in the first case to 8141.4 *kWh/day*. Using the EM-BT technique, the voltage at the weak bus has been raised from 0.87 per unit (pu) to 0.92 pu. Indeed, the EM-BT method proves to be more reliable for the three networks compared to PSO, GWO, and WOA ones.

The convergence behaviors of the optimization techniques, namely EM-BT, PSO, GWO, and WOA, have been graphically represented in Figure IV.2 (*a*) to (*c*) for the IEEE 33, IEEE 69, and ALG-AB-Hassi Sida 157 networks, respectively. The results demonstrate that the EM-BT method shows remarkable convergence characteristics related to the best positions and sizes of PVRES and CB, ultimately leading to the most effective reduction in energy losses. Figure IV.2 (*a*) depicts the convergence process for the IEEE 33 network, where the EM-BT method outperforms the other techniques by converging faster and more consistently. In comparison, the other methods may exhibit more fluctuations or slower convergence. Similarly, Figure IV.2 (*b*) displays the convergence behavior for the IEEE 69 network, reinforcing that the EM-BT method surpasses the other approaches regarding convergence speed and stability, demonstrating smoother and more efficient convergence towards the optimal solution. The same reasoning is valid for the ALG-AB-Hassi Sida 157 network since the Figure IV.2 (*c*) further emphasizes the superior convergence properties of the *EM-BT* method. This latter converges more effectively and rapidly, underscoring its ability to identify the best *PVRES* and *CB* configurations that lead to minimal energy losses.

In summary, Figure IV.2 provides compelling evidence that the EM-BT method is highly effective in achieving convergence and stands out as an excellent approach for optimizing

PVRES allocations and capacitor bank sizing to minimize energy losses across various network scenarios**.**

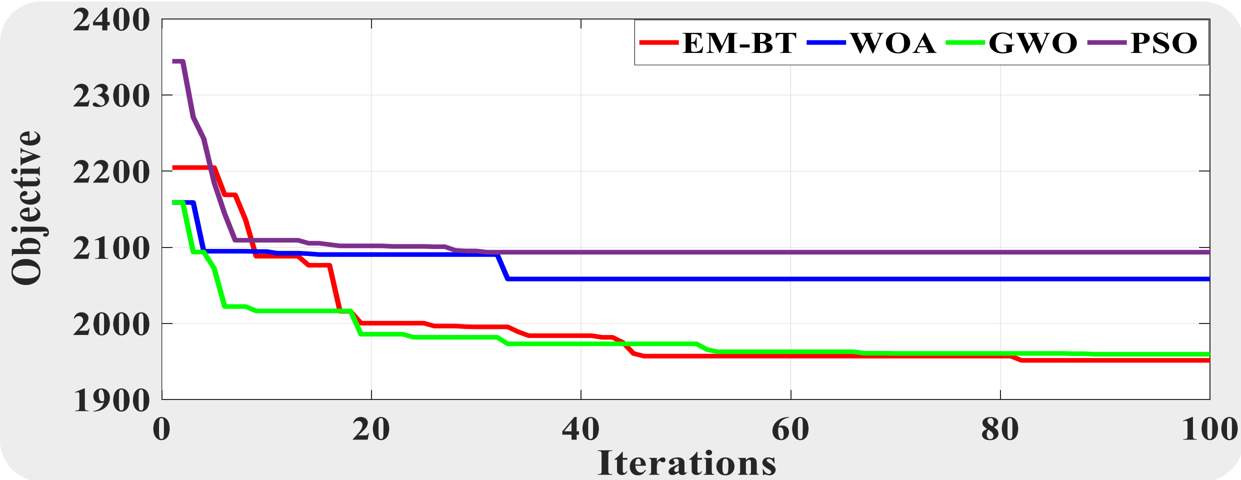

(a) IEEE 33

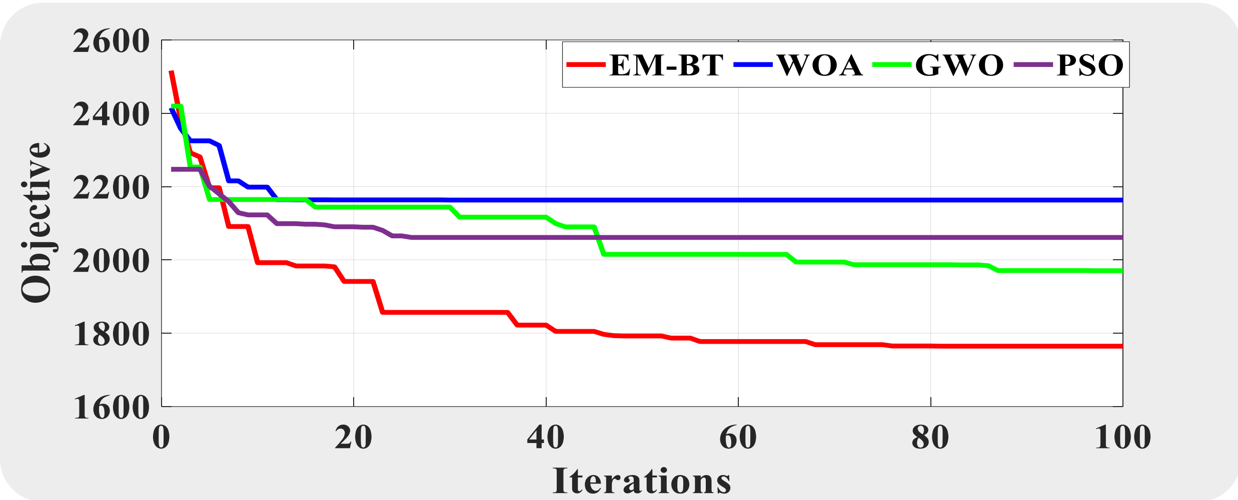

(b) IEEE 69

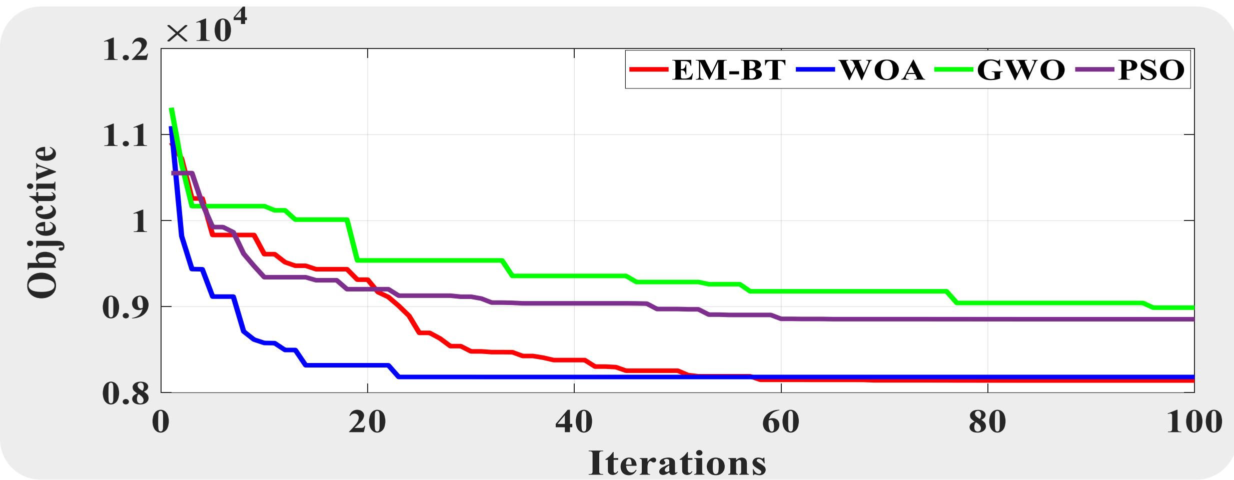

(C) ALG-AB-Hassi Sida 157

Figure IV.2. Convergence analysis of EM-BT, PSO, GWO, and WOA for the Second Scenario in all distribution Systems.

Table IV.3. Optimal Location and size of PVRES with capacitor banks with the energy losses, Minimum bus Voltage (pu) , and energy loss reduction rates obtained for scenario 2 for all distribution network.

	Optimal Placement and Sizing of Photovoltaic (PV) and Capacitor Banks (CB)					**Minimum bus Voltage (pu)**			**Energy loss (kWh)**			**Energy loss reduction (%)**		
	-		**3 PVRES and 9 CB for IEEE 33**	**5 PVRES and 18 CB for IEEE 69**	**10 PVRES and 25 CB for ALG-AB Hassi Sida 157**	**IEEE 33**	**IEEE 69**	**ALG-AB Hassi Sida 157**	**IEEE 33**	**IEEE 69**	**ALG-AB Hassi Sida 157**	**IEEE 33**	**IEEE 69**	**ALG-AB Hassi Sida 157**
Base case	-					0.90	0.90	0.89	3567.7	3797	17995	-		
Scenario 1	-					0.89	0.89	0.87	3831.3	4085.7	19367	-		
Techniques	**WOA**	**PV buses**	17-31-32	21-26-61 63-64	102-107-109-129-132-133- 141-142-143-153	0.937	0.923	0.915	2058.4	2163.2	8182.3	46.27	47.05	57.75
		CB buses	13 -16 -17-18-31- 32-33	20-23-25 27-57-59 62-63-64 65	19-22-25-28-29-30-32-72-78- 87-94-101-107-112-118-124- 129-134-137-142-144-147- 150-153-156									
		CB Size	150 -100-50-150- 150-150 150	150-150-100-150- 100-50 150-150-100-100	150-150-150-150-100-150 150-150-150-150-150-150 100-150-100-150-150-150 150-150-150-150-150-150-150									
	PSO	**PV buses**	13-17-31	12-19-21 60-64	21-29-75-83-92-111-118-125- 134-146	0.935	0.927	0.912	2093.6	2061.2	8853.8	45.35	50.44	54.28
		CB buses	13-14-15 17-31-32 33	19-21-25 26-59-60 61-62-64 65	19-22-25-28-30-32-72-78-87- 94-101-107-112-118-124-129- 134-137-144-147-153-156									
		CB Size	100-150-100-100- 100-150 100	50-150-50 100-150-50 150-100-150-150	150-150-100-50-100-150-50- 150-150-100-50-150-150-150- 150-150-150-150-50-150-100- 100									
	GWO	**PV buses**	13-17-32	17-23-58 63-64	77-102-106-111-128 130-132-134-141-152	0.933	0.928	0.912	1959.6	1970.5	8988.4	48.85	51.77	53.58
		CB buses	13-16-18 31-32-33	19-22-26 27-58-59 61-62-63 64-65	19-22-25-29-30-32-72-78-87- 94-101-107-112-118-124-129- 134-137-142-150-153									
		CB Size	150-100-100-150- 150-150	50-150-50 100-150-100-100- 150-50 150-150	50-150-150-50-50-100-100- 150-50-50-150-150-150-50- 150-150-150-150-50-100-150									
	EM-BT	**PV buses**	13-16-32	60-61-62 63-64	24-29-89-92-111-112-115 122-125-141	0.934	0.929	0.915	1951.5	1764.7	8141.4	49.06	56.80	57.96
		CB buses	13-14-16 31-32-33	19-20-22-23-24- 25-58-59-60-61- 62-63 64-65	19-22-25-29-30-32-72-78-87- 94-101-107-112-118-124-129- 134-137-142-144-147-150- 153-156									
		CB Size	150-150-100 150-150-150	50-150-50-100- 100-100-100-150- 150-150-150-150- 150-150	150-150-150-150-150-150 150-150-150-100-150-150 150-150-150-150-150-150 150-150-50-100-150-150									

IV.2.4.3. Scenario 3

In this scenario, we compare the performance of the proposed EM-BT algorithm with the three other optimization techniques, namely PSO, GWO, and WOA. to achieve this goal, we have implemented six, ten, and twenty distinct PVRES allocations, each accompanied by multiple capacitor banks. The main goal is to minimize the objective function given by Equation IV.8.

The results in Table IV.4 provide overviews of energy losses, voltage deviations, and energy loss reduction rates for the three different networks IEEE 33, IEEE 69, and ALG-AB-Hassi Sida 157 systems. For IEEE 33 the EM-BT method demonstrates a remarkable reduction in energy loss, achieving a decrease of 57.60% from 3831.3 *kWh/day* in the initial case to 1624.4 *kWh/day*. Additionally, the voltage magnitude of the weak bus has been increased from 0.89 per unit (*pu*) to 0.93 *pu*.

Regarding to IEEE 69, the proposed EM-BT method achieves a 65.44% reduction in energy loss, bringing it down from 4085.7 *kWh/day* in the initial case to 1412 *kWh/day*. The voltage magnitude of the weak bus has also demonstrated improvement, rising from 0.89 per unit (*pu*) to 0.92 pu.

In the same way, the results found for ALG-AB-Hassi Sida 157 exhibit that the EM-BT method leads to a reduction of 63.17% in energy loss, from 19367 *kWh/day* to 7131 *kWh/day*, and There has been an increase in the voltage magnitude of the weak bus, going from 0.87 per unit (*pu*) to 0.92 pu.

The results, illustrated in Table IV.4, clearly indicate that the proposed EM-BT method outperforms PSO, GWO, and WOA techniques, demonstrating its superior reliability and effectiveness in optimizing PVRES allocations and reducing energy losses.

Otherwise, the convergence characteristics of all techniques (EM-BT, PSO, GWO, and WOA) are illustrated in Figure IV.3 (*a*) to (*c*) for IEEE 33, IEEE 69, and ALG-AB-Hassi Sida 157, respectively. We retain the same observation as that made for scenario two (Figure IV.2). Indeed, figure IV.3 highlights that the EM-BT exhibits superior convergence properties in determining the optimal location and size of PVRES and CB to minimize energy losses.

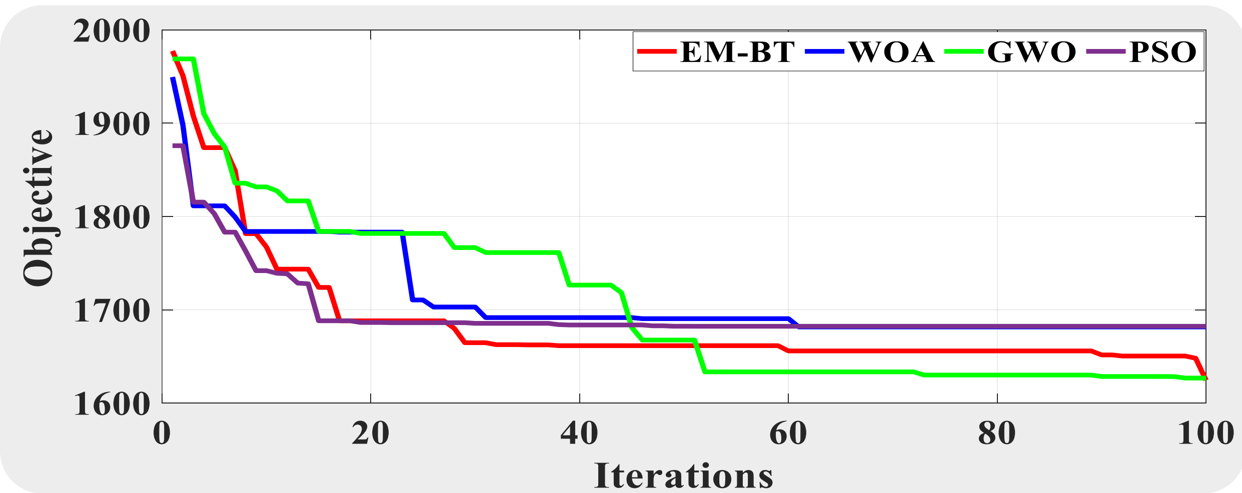

(a) IEEE 33

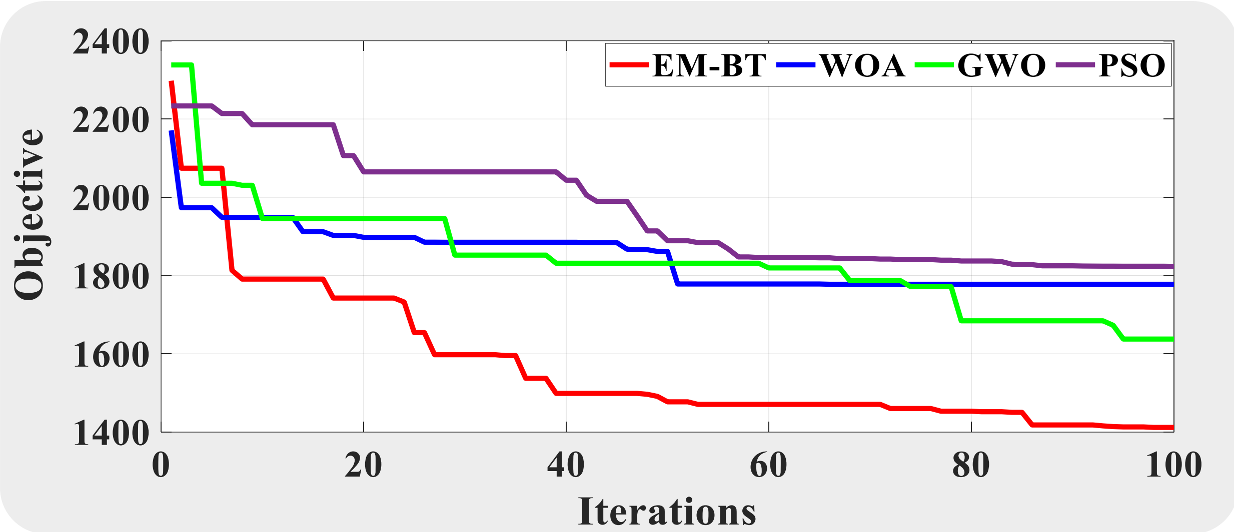

(b) IEEE 69

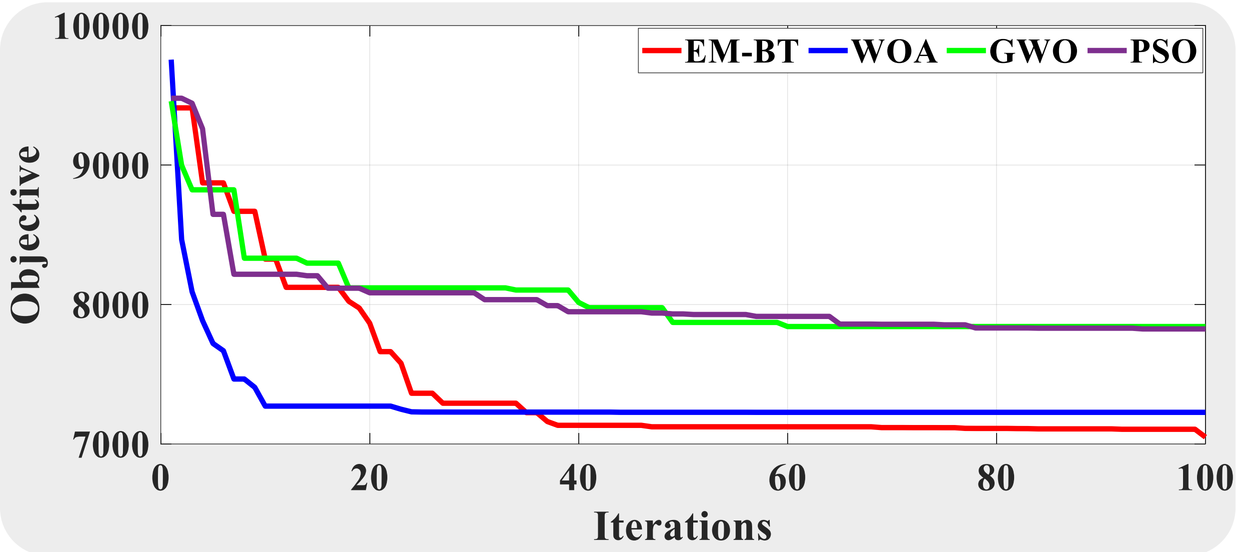

(C) ALG-AB-Hassi Sida 157

Figure IV.3. Convergence analysis of EM-BT, PSO, GWO, and WOA for the third Scenario in all distribution Systems.

Table IV.4. Optimal Location and size of PVRES with capacitor banks with the energy losses, Minimum bus Voltage (pu) , and energy loss reduction rates obtained for scenario 3 for all distribution network

<table>
<tr><th rowspan="2"></th><th colspan="5">Optimal Placement and Sizing of Photovoltaic (PV) and Capacitor Banks (CB)</th><th colspan="3">Minimum bus Voltage (pu)</th><th colspan="3">Energy loss (kWh)</th><th colspan="3">Energy loss reduction (%)</th></tr>
<tr><th colspan="2">-</th><th>6 PVRES and 9 CB for IEEE 33</th><th>10 PVRES and 18 CB for IEEE 69</th><th>20 PVRES and 25 CB for ALG-AB Hassi Sida 157</th><th>IEEE 33</th><th>IEEE 69</th><th>ALG-AB Hassi Sida 157</th><th>IEEE 33</th><th>IEEE 69</th><th>ALG-AB Hassi Sida 157</th><th>IEEE 33</th><th>IEEE 69</th><th>ALG-AB Hassi Sida 157</th></tr>
<tr><td>Base case</td><td colspan="5">-</td><td>0.90</td><td>0.90</td><td>0.89</td><td>3567.7</td><td>3797</td><td>17995</td><td colspan="3">-</td></tr>
<tr><td>Senario 1</td><td colspan="5">-</td><td>0.89</td><td>0.89</td><td>0.87</td><td>3831.3</td><td>4085.7</td><td>19367</td><td colspan="3">-</td></tr>
<tr><td rowspan="12">Techniques</td><td rowspan="3">WOA</td><td>PV buses</td><td>7 -11-16
18-29- 33</td><td>12-13-21-24
28-60-61-62
63-65</td><td>18-25-38-55-70-74-79-82-98-104
106-114-123-127-130-133-141
153-157</td><td rowspan="3">0.937</td><td rowspan="3">0.921</td><td rowspan="3">0.919</td><td rowspan="3">1681.6</td><td rowspan="3">1777.8</td><td rowspan="3">7226.9</td><td rowspan="3">56.1</td><td rowspan="3">56.48</td><td rowspan="3">62.68</td></tr>
<tr><td>CB buses</td><td>16-17
31-32
33</td><td>21-22-23-24
57-58-59-61
62-63-64-65</td><td>19-22-25-28-29-30-32-72-78-87
94-101-107-112-118-124-129
134-137-142-144-147-150-153
156</td></tr>
<tr><td>CB Size</td><td>150-150
150-150
150</td><td>150-50-50-150
50-150-100-150
150-100-50-50</td><td>150-150-50-150-100-150-100
150-150-100-150-150-150-150
150-150-150-150-150-150-50
150-150-150-150</td></tr>
<tr><td rowspan="3">PSO</td><td>PV buses</td><td>8-13-17
29-31-32</td><td>10-11-18-20
24-58-60-63
64-65</td><td>16-20-24-37-52-53-55-57-61-79
83-85-99-114-116-118-121-127
141</td><td rowspan="3">0.934</td><td rowspan="3">0.928</td><td rowspan="3">0.915</td><td rowspan="3">1682.3</td><td rowspan="3">1823.5</td><td rowspan="3">7919.7</td><td rowspan="3">56.09</td><td rowspan="3">55.36</td><td rowspan="3">59.10</td></tr>
<tr><td>CB buses</td><td>14-15
16-17
31-32-33</td><td>19-21-22-23
25-26-27-57
58-59-60-61
62-63</td><td>19-22-25-29-32-72-78-87-94-101
107-112-118-124-129-134-13
142-153-156</td></tr>
<tr><td>CB Size</td><td>150-50
100-100
100-150-150</td><td>100-100-50-50
100-100-100-50
100-150-150-100
100-100</td><td>150-150-100-100-50-100-100
150-150-100-150-100-150-150
150-150-150-100-150-100</td></tr>
<tr><td rowspan="3">GWO</td><td>PV buses</td><td>9-13-16
29-30-32</td><td>6-10-48-55
58-60-61-62
63-65</td><td>7-11-17-18-19-20-27-43-53-59
63-72-76-85-88-93-133-145-157</td><td rowspan="3">0.937</td><td rowspan="3">0.924</td><td rowspan="3">0.917</td><td rowspan="3">1626.8</td><td rowspan="3">1637.8</td><td rowspan="3">7853</td><td rowspan="3">57.53</td><td rowspan="3">59.91</td><td rowspan="3">59.45</td></tr>
<tr><td>CB buses</td><td>13-15
16-18
31-32-33</td><td>19-20-22-23
25-59-60-61
62-64-65</td><td>19-22-25-30-72-78-87-94-101
107-112-118-124-129-134-137
142-153</td></tr>
<tr><td>CB Size</td><td>150-50
100-100
150-150-150</td><td>50-150-100-50
100-150-100-150
50-150-150</td><td>150-150-150-150-50-100-150-50
150-100-150-150-150-150-150
150-50-100</td></tr>
<tr><td rowspan="3">EM-BT</td><td>PV buses</td><td>10-14-17
29-31-32</td><td>19-24-58-59
60-61-62-63
64-65</td><td>10-28-38-43-57-58-60-63-69-85
89-104-106-115-117-118-120-123</td><td rowspan="3">0.933</td><td rowspan="3">0.928</td><td rowspan="3">0.923</td><td rowspan="3">1624.4</td><td rowspan="3">1412</td><td rowspan="3">7131</td><td rowspan="3">57.60</td><td rowspan="3">65.44</td><td rowspan="3">63.17</td></tr>
<tr><td>CB buses</td><td>13-14
16-31
32-33</td><td>21-23-24-25
26-27-57-58
59-60-61-62
63-64-65</td><td>19-22-25-29-30-32-72-78-87-94
101-107-112-118-124-129-134
137-142-150-153-156</td></tr>
<tr><td>CB Size</td><td>150-150
150-150
150-150</td><td>100-50-50-50
100-50-150-100
150-150-150-150
100-150-150</td><td>150-150-150-150-150-150-150
150-150-150-150-150-150-150
150-150-150-150-100-100-150
150</td></tr>
</table>

Figure IV.4 (*a*) to (*c*) showcases the voltage profiles for the IEEE 33, IEEE 69, and ALG-AB-Hassi Sida 157 networks, each exhibiting distinct characteristics. Notably, all voltage profiles consistently remain above the base case's minimum limit. During the peak consumption hour, the voltage dips to a minimum of 0.92 per unit (*pu*) for both the IEEE 69 and ALG-AB-Hassi Sida 157 networks. In contrast, the IEEE 33 network experiences a slightly higher minimum voltage level during the peak consumption hour, recorded at 0.93 pu. These observations underscore the effectiveness of the optimized PVRES and capacitor bank placement achieved through the EM-BT method in maintaining voltage levels above the critical minimum limit during high-demand periods, thereby ensuring a stable and reliable power supply.

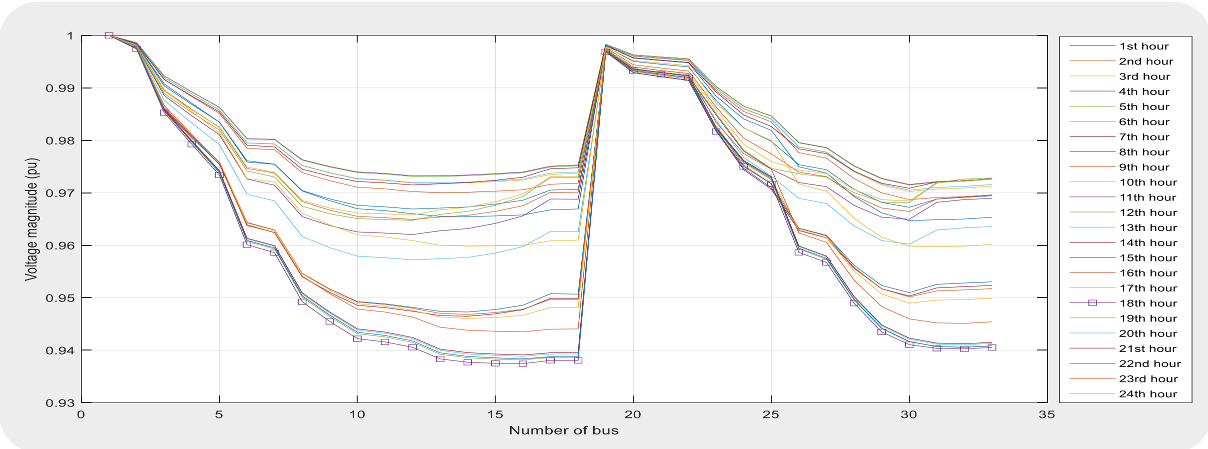

(a) IEEE 33

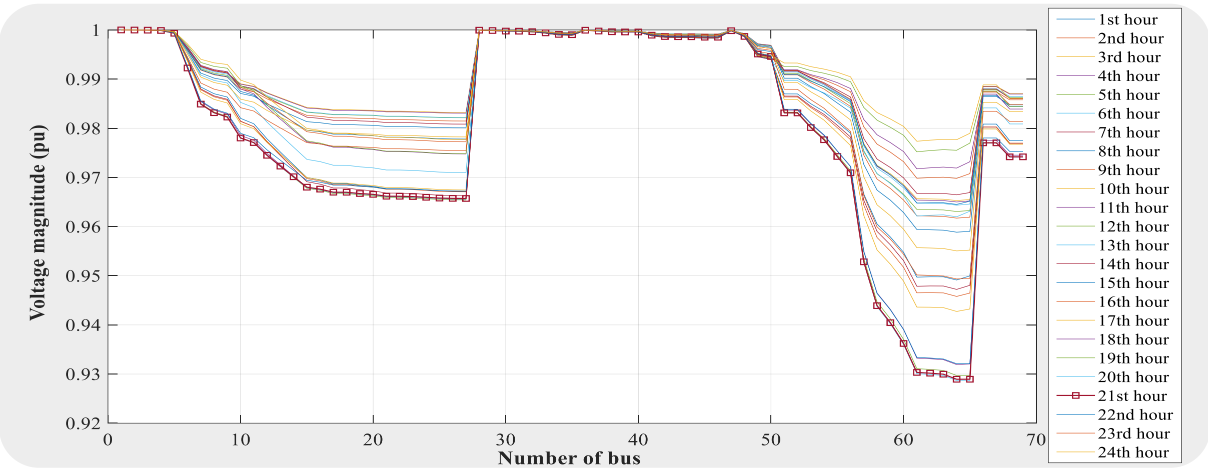

(b) IEEE 69

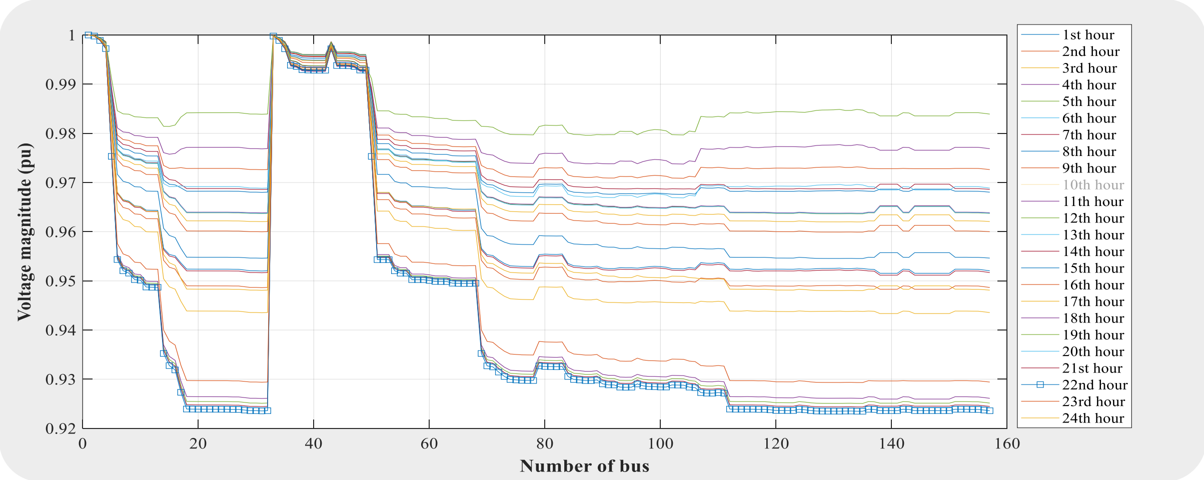

(c) ALG-AB-Hassi Sida 157

Figure IV.4. Voltage profile variation over a 24-hour period for the third scenario in the three networks.

IV.2.5. Interpretations Results

Figure IV.5 (*a*) to (*c*) presents the energy loss reduction (in percentage) obtained in the case of the second and the third scenarios for the IEEE 33, IEEE 69, and ALG-AB-Hassi Sida 157 systems, respectively. The results clearly demonstrate that increasing the number of PVRES units leads to a greater reduction in energy losses.

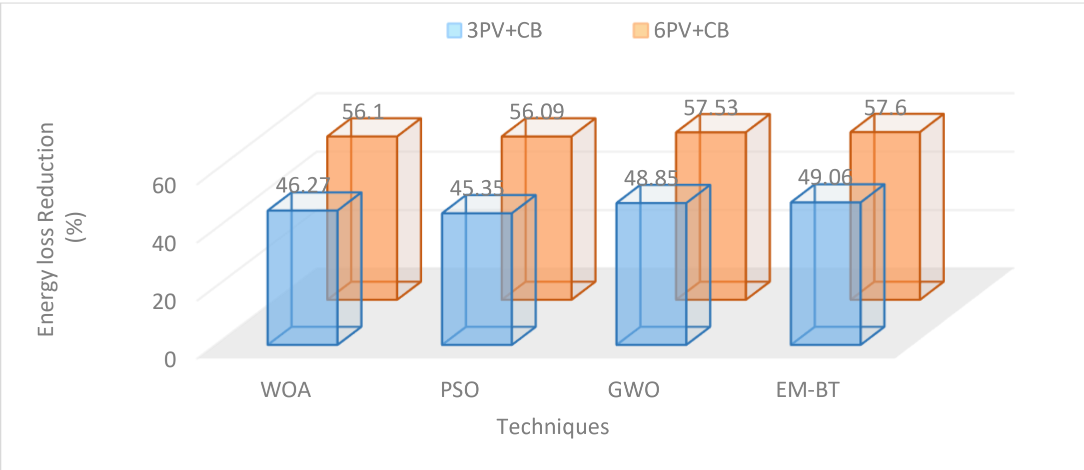

(a) IEEE 33

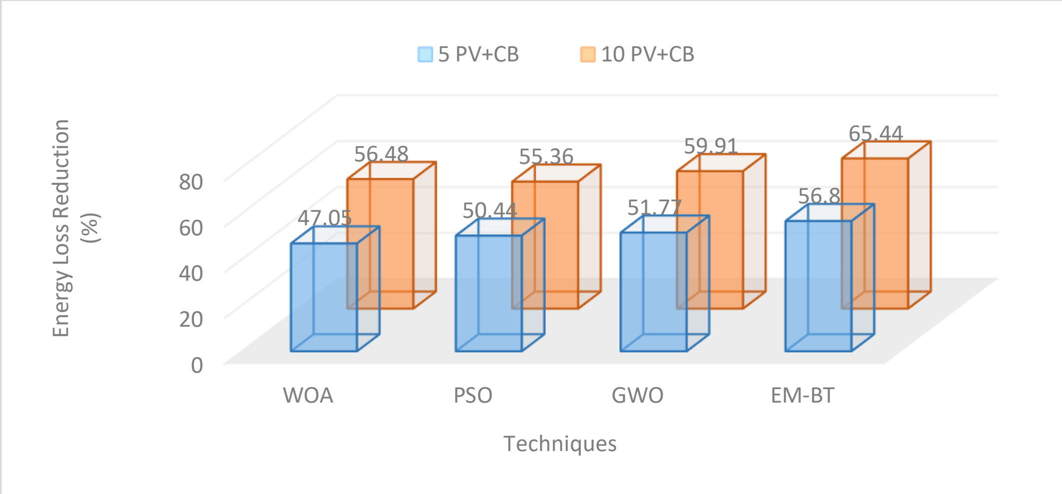

(b) IEEE 69

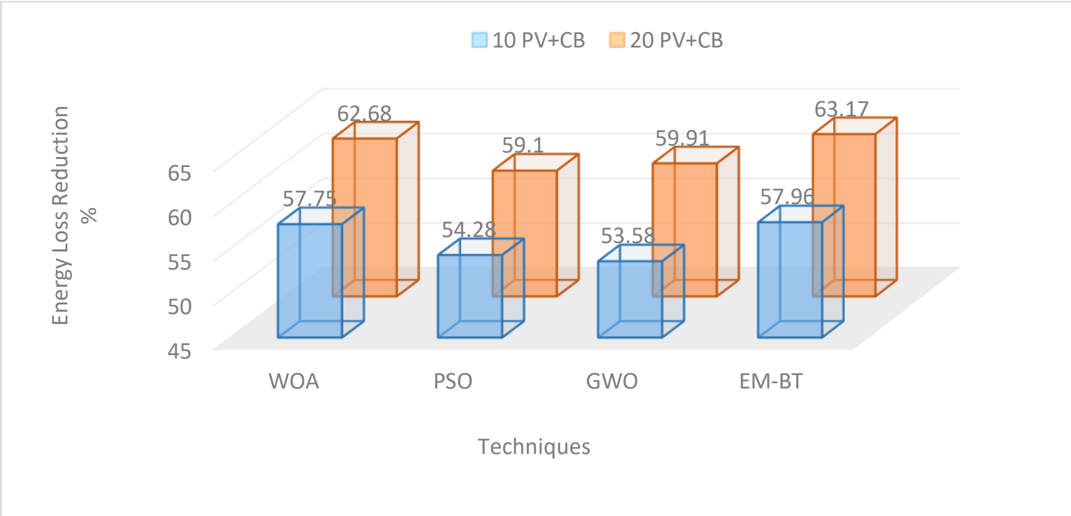

(C) ALG-AB-Hassi Sida 157

Figure IV.5. Energy loss reduction percentage for the second and the third scenarios in all distribution Systems.

IV.3. Multi-Objective Planning of DG

The objective of this study is twofold, focusing on the development and application of a metaheuristic technique called Multi-Objective Multi-Verse Optimization (*MOMVO*) for enhancing the performance of electrical distribution networks. The primary goal is to simultaneously minimize daily energy losses and deviations in voltage profiles, adapting to dynamic load conditions over a 24-hour period. This objective is embodied in a unified objective function (*Obj1*) and further expanded into a comprehensive model (*Obj2*), which also aims to reduce costs related to energy losses and power supplied by Photovoltaic and Reactive Energy Source Capacitor Banks (*PVRES-CBs*).

The effectiveness of the approach is evaluated through simulations on standard IEEE 33 and 69-node distribution networks, with scenarios designed for optimal PVRES-CBs placement to achieve substantial reductions in the two targeted objective functions throughout a daily cycle. A key aspect of this method is its consideration of both temperature and irradiation effects on PVRES and the network—an advancement over previous methods that typically focus only on irradiance. This broader view provides a more precise and realistic optimization by incorporating environmental variables that significantly impact PVRES performance.

The effectiveness of the proposed MOMVO algorithm is rigorously assessed through a comparative analysis with three widely used optimization algorithms: Multi-Objective Jellyfish Search (*MOJS*), Multi-Objective Flower Pollination Algorithm (*MOFPA*), and Multi-Objective Lichtenberg Algorithm (*MOLA*). This comparison produces a Pareto front, which is essential for decision-makers or power system operators managing uncertain or fuzzy objectives. To aid in selecting an optimal solution from the Pareto-optimal set, fuzzy logic theory is applied. This approach calculates fuzzy membership functions for each objective, enabling the identification of the best non-dominated solution by maximizing the normalized sum of membership values across all objectives.

Additionally, the study explores variations in the optimal compromise solutions obtained through these algorithms, offering insights into their relative performance and suitability under diverse network conditions. This analysis provides valuable guidance on the most effective optimization strategies for enhancing system performance.

In essence, this work aims to elevate the optimization of electrical distribution networks through an environmentally responsive algorithm that improves both technical efficiency and cost-effectiveness while supporting the sustainable integration of renewable energy sources. This research endeavors to make a significant contribution to the field of power system optimization, providing a solid foundation for future advancements in the strategic integration of renewable energy and optimization methods. The ultimate goal is to enhance power system efficiency, reliability, and sustainability.

The primary contribution of this work is the development of a Multi-Objective Multi-Verse Optimization (*MOMVO*) approach, specifically tailored for the simultaneous placement of Photovoltaic and Reactive Power Compensation Equipment (*PVRES-CB*) in distribution networks. A key innovation of this research is the inclusion of temperature as a parameter, which enhances the accuracy of electrical network analysis by accounting for real-world conditions. This study rigorously evaluates solar PVRES performance under varying temperature and irradiance levels. The optimization process addresses two objective functions and various constraints across a range of 24-hour load scenarios.

The comparative analysis demonstrates that the MOMVO algorithm consistently surpasses MOJS, MOFPA, and MOLA algorithms in effectively minimizing the defined objectives along the Pareto front. Nevertheless, while MOMVO generally performs well, it does not always provide the optimal compromise solution that satisfies all operational constraints. This occasional limitation arises from the inherent randomness of these algorithms, which can sometimes impede their ability to fully resolve complex trade-offs and achieve the desired outcomes in every scenario.

Furthermore, this study showcases a significant reduction in losses, voltage deviations, and operational costs through the integration of a substantial number of Photovoltaic and Reactive

Power Compensation Equipment (*PVRES-CBs*). This achievement underscores the remarkable success of this approach from both technical and practical perspectives. However, it is essential to acknowledge the economic implications, as the extensive utilization of PVRES and CBs comes with a substantial cost. This economic aspect must be thoroughly weighed and factored into any comprehensive.

IV.3.1. Problem Formulation

IV.3.1.1. Objectives Functions

In allocating PVRES-CBs for auxiliary service provision within distribution systems, it is paramount to initially address the minimization of daily energy losses and voltage deviations. These objectives are amalgamated within a unified objective model (*Obj1*), aimed at simultaneous minimization, as detailed in Equation (IV.13).

$$\mathrm{Obj1} = \mathrm{Min}\ (\mathrm{ELD}\ ,\ \mathrm{VDD}) \tag{IV.13}$$

Where ELD represents the energy losses per day and VDD is the voltage deviation per day, which can be modeled as follows:

$$EL_{D_D} = \sum_{\mathrm{h}=1}^{24} \left(\sum_{\mathrm{br}=1}^{\mathrm{N_{branches}}} \mathrm{I}_{\mathrm{br}}\ (\mathrm{h})^{2} \cdot \mathrm{R_{br}} \right) \tag{IV.14}$$

$$VD_{D_D} = \sum_{h=1}^{24} \left(\sum_{j=1}^{buses} |1 - Vj| \right) \tag{IV.15}$$

Nbranches : Number of distribution branches.
Ibr : Current flowing through each distribution branch (br) [in Amperes, A].
Rbr : Resistance of each distribution branch (br) [in Ohms, Ω].
Nbuses : Number of buses (nodes) in the distribution system.
Vj : Voltage magnitude at each distribution node (j) [in Volts, V].

Furthermore, within the context of assigning PVRES-CBs for auxiliary service provision in distribution systems, the reduction of costs related to energy losses and the power supplied by Photovoltaic and Reactive Energy Source Capacitor Banks (*PVRES-CBs*) is of utmost importance. These dual aims are encapsulated within a single objective model (*Obj2*), targeted for simultaneous minimization, as outlined in Equation (IV.16).

$$\mathrm{Obj2} = \mathrm{Min}\ (\mathrm{Closs},\ \mathrm{TOC}) \tag{IV.16}$$

Closs : Yearly cost attributed to energy losses.
TOC : Total cost of power supplied by Photovoltaic and Reactive Energy Source - Capacitor Banks (*PVRES-CBs*).

$$\mathrm{Closs} = \mathrm{Kp} * \ \mathrm{EL}_{\mathrm{D_D}} * \mathrm{Tf} \tag{IV.17}$$

$$\mathrm{TOC} = (\mathrm{Kp}\ * \sum_{k=1}^{nPV} \mathrm{PPV}) + (\mathrm{KQ}\ * \sum_{k=1}^{ncb} \mathrm{Qcb}) \tag{IV.18}$$

Kp : The annual cost of energy losses ($ /kwh)
Tf=0.9*8760
npv : The number of photovoltaic
ncb : The number of Capacitor Banks

Kp : The purchase cost ($ /KW)
PPV : The active power of the photovoltaic k
KQ : The purchase cost ($ /KVAR)
Qcb : The reactive power of the capacitor bank k

IV.3.1.2. Equality and Inequality Constraints

Hence, it is necessary to ensure that the actual power injection, both real and reactive, from *PVRES-CB* remains within the specified limits denoted by $PPVRES_{k\_max}$ and Qcb j_max, correspondingly, for every hour:

$$0 < PPVRES_K < PPVRES_{k\_max} \quad k = 1,. \dots, nPV \tag{IV.19}$$

$$0 < Q_{cb_j} < Q_{cb_{j\_max}} \quad j = 1, \dots., ncb \tag{IV.20}$$

PPVRES : Real power injection from photovoltaic renewable energy sources (*PVRES*) into the grid [*in Watts, W*].
QCB : Reactive power injection from capacitor banks (*CB*) into the system [*in Volt-Amperes Reactive, VAR*].
Furthermore, it is essential to ensure that the voltage at every distribution node and the current flowing through all distribution branches remain within the permissible limits throughout all hours, as stated in reference [124].

$$V_{m\_min} < V_m < V_{m\_max} \quad m = 1,. \dots, nB \tag{IV.21}$$

$$I_{br} < I_{br_{i\_max}} \quad i = 1,. \dots, nbr \tag{IV.22}$$

$\mathbf{V_m}$: Voltage at bus mmm [*in Volts, V*].
$\mathbf{V_{m\_min}}$: Lower voltage limit for bus mmm (typically set to 90% of the nominal voltage) [*in Volts, V*].
$\mathbf{V_{m\_max}}$: Upper voltage limit for bus mmm (typically set to 110% of the nominal voltage) [*in Volts, V*].
$\mathbf{I_{br_{i\_max}}}$: Thermal capacity limit of branch iii [*in Amperes, A*].

Moreover, as assumed in [125], a threshold on the *PVs* penetration is considered using the coefficient K_P, so that the *PVs* installed capacity ($\sum_{k \in nPV} P_{PV_k}$) is equal to 50% of the total active power demand in the system P_{D_m}.

$$\sum_{k \in nPV} P_{PV_k} = K_P \cdot \sum_{m \in nB} P_{D_m} \tag{IV.23}$$

The inequality constraints in Equations (IV.19) and (IV.20) pertain to the control variables and are automatically managed through the MOMVO mechanism. However, additional attention is required to address the inequality constraints in Equations (IV.21) and (IV.23).

IV.3.2. Results and Discussions

The MOMVO algorithm presented in this study has been carefully employed to optimize and minimize two complex objective functions that encompass both technical performance and economic considerations. This comprehensive optimization process accounts for the variability in output from Photovoltaic and Reactive Power Compensation Equipment (PVRES) as well as the daily fluctuations in load demand. The algorithm's effectiveness has been rigorously evaluated on two distinct electrical distribution systems: the IEEE 33-bus and IEEE 69-bus systems.

For the IEEE 33-bus system, the optimization strategy involved placing three to six PVRES units along with nine capacitor banks, aiming to balance reactive power and improve the voltage profile of the network. In contrast, the larger IEEE 69-bus system required a more substantial integration, with five to ten PVRES units and eighteen capacitor banks, to adequately manage the higher load demand and the system's more complex network structure.

The performance evaluation of each distribution system was carried out through detailed simulations that incorporated various operational profiles for PVRES, capacitor banks, and load variations over a 24-hour period. The key input parameters for this analysis, detailed in Table IV.5, include the capacities of PVRES units, the ratings of capacitor banks, and the hourly load profiles. The results from these simulations offer a comprehensive insight into the algorithm's impact on the operational efficiency and economic feasibility of the distribution systems examined. The following sections provide a deeper analysis of these outcomes, highlighting the algorithm's capacity to improve distribution system performance through the optimized placement and sizing of PVRES and capacitor banks. This underscores the practical utility and versatility of the MOMVO algorithm in optimizing distribution networks of varying scales and complexities.

Table IV.5. Daily Energy Loss and Yearly Cost of Energy Loss for Different Networks with Minimum and Maximum Bus Voltage.

Base case	**IEEE 33**	**IEEE 69**
Energy Loss (kWh)	3.5677e+03	3.7970e+03
Minimum bus voltage (pu) /12h	0.9038	0.9092
Maximum bus voltage (pu)	1	1
The yearly cost of energy loss ($/year)	4.2191e+06	4.4903e+06

The study examines three distinct scenarios across both the IEEE 33 and IEEE 69 networks, outlined as follows:

- **Scenario 1:** This scenario involves a state analysis for each hour, incorporating power flow computations while considering temperature effects within the networks.

- **Scenario 2:** The proposed MOMVO algorithm is compared with the Multi-Objective Jellyfish Search (*MOJS*), Multi-Objective Flower Pollination Algorithm (*MOFPA*), and Multi-Objective Lichtenberg Algorithm (*MOLA*) for the allocation of Photovoltaic and Reactive Power Compensation Equipment (*PVRES*) along with Capacitor Banks (*CBs*). This comparison aims to minimize the two designated objective functions, specifically Equation (IV.13) and Equation (IV.16).
- **Scenario 3:** The application of the MOMVO algorithm is expanded to include allocations of PVRES, with the number of PVRES units doubled while maintaining the same quantity of capacitor banks as in Scenario 2. The primary goal remains the minimization of the two designated objective functions, Equation (IV.13) and Equation (IV.16).

Both Scenarios 2 and 3 utilize the MOMVO algorithm with 100 iterations and 30 search agents. Importantly, in Scenario 1, node voltages are constrained to 10% or lower of the nominal voltage.

IV.3.2.1. Scenario 1

In the given scenario, load flow computations are performed for each demand hour, taking into account the influence of temperature. As illustrated in Figures IV.6 (*a*) through (*b*), the voltage distribution across all nodes of the distribution system, both for IEEE 33 and IEEE 69, is visually presented for each load hour. These voltage profiles consistently maintain values below the established minimum threshold, as evident from their distinct characteristics. It's notable that the voltage level drops to a minimum of 0.89 pu for both IEEE 33 and IEEE 69 during the peak consumption hour at hour 14. The impact of temperature on the network becomes even more evident through the lens of daily energy losses, meticulously outlined in Table IV.6, encompassing all networks.

Furthermore, the yearly cost of energy loss is documented at 4.5308. e+06 (*$/year*) for IEEE 33 and 4. 8317.e+06 (*$/year*) for IEEE 6.

Table IV.6. Daily Energy Loss and Yearly Cost of Energy Loss for All Distribution Systems with Temperature Effect

	IEEE 33	**IEEE 69**
Energy Loss .e+03 (kWh)	3.8313	4.0857
Minimum bus Voltage (pu)/14h	0.8921	0.8969
Maximum bus voltage (pu)	1	1
The yearly cost of energy loss.e+06 ($/year)	4.5308	4.8317

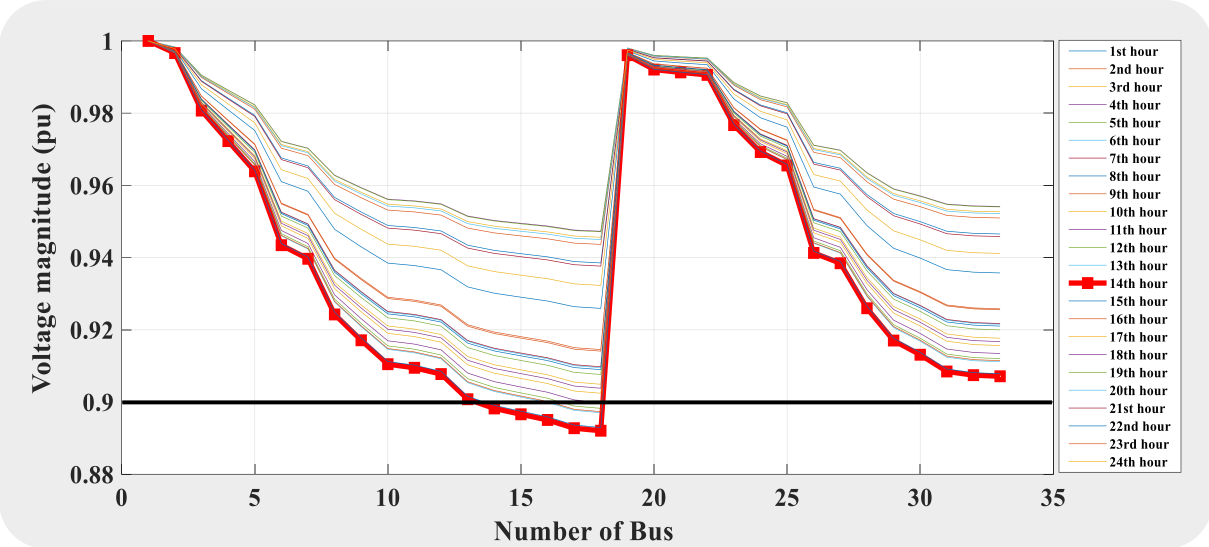

(a) IEEE 33

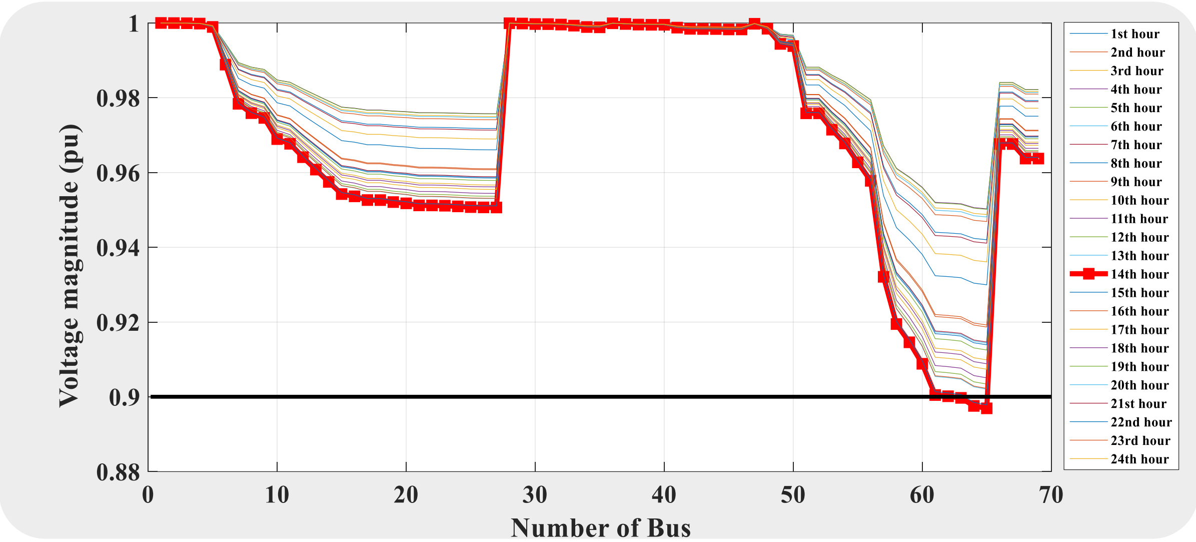

(b) IEEE 69

Figure IV.6. Hourly voltage profile over 24 hours for the initial Scenario in the two networks.

The data presented in Table IV.6 reveals a significant increase in energy losses for both the IEEE 33 and IEEE 69 distribution networks due to temperature fluctuations. Specifically, the energy losses recorded are 3,813 *kWh* for the IEEE 33 network and 4,085.7 *kWh* for the IEEE 69 network, both surpassing their initial baseline figures of 3,567.7 *kWh* and 3,797 *kWh*, respectively. This increase corresponds to approximately 6.88% for the IEEE 33 network and 7.06% for the IEEE 69 network.

Additionally, the annual costs related to these energy losses were estimated at *$4.5308* million for the IEEE 33 network and *$4.8317* million for the IEEE 69 network. Compared to the baseline values of $4.2191 million for the IEEE 33 network and $4.4903 million for the IEEE 69 network, these figures indicate increases of approximately 7.38% and 7.60%, respectively.

This measurable rise in both energy losses and associated costs highlights the significant impact of temperature variations on the operational efficiency of these networks.

These findings not only emphasize the critical importance of incorporating environmental factors, such as temperature, into the planning and optimization of distribution networks but also highlight the potential for improved operational and financial efficiency through optimized energy management strategies. This underscores the necessity of developing and implementing robust solutions that can adapt to environmental variations to ensure the stability and efficiency of power distribution systems.

IV.3.2.2. Scenario 2

In this scenario, the Multi-Objective Multi-Verse Optimization (*MOMVO*) method is evaluated against other optimization techniques—namely the Multiobjective Flower Pollenation Algorithm (*MFPA*), Multiobjective Lion Algorithm (*MOLA*), and Multiobjective Jellyfish Search (*MOJS*)—with a focus on optimizing the allocation of Photovoltaic and Reactive Energy Source Capacitor Banks (*PVRES-CBs*) across distribution networks. The comparative analysis, anchored by objective functions encapsulated in Equation 10 and Equation 13, takes into account various configurations of *PVRES* allocations and capacitor banks (*CBs*), facilitating a comprehensive evaluation of each method's efficacy.

Table IV.7 delineates the best compromise solutions identified for minimizing energy losses and voltage deviations (the first objective) and reducing the annual cost of energy losses alongside the cost of power supplied by distributed generators (*DGs*) (the second objective), for both the IEEE 33 and IEEE 69 networks. The MOMVO method's application to the IEEE 33 network resulted in a notable 47.58% reduction in daily energy loss (from 3831.3 *kWh/day* to 2008.1 *kWh/day*) and an improvement in voltage stability (from 0.89 pu to 0.94 pu). Similarly, for the second objective, a significant 36.97% decrease in the annual cost of energy loss (from *$4.5308* million to *$2.8556* million) was observed, alongside achieving a cost of *$39,146/year* for power supplied by DGs.

For the IEEE 69 network, MOMVO showcased a 50.15% reduction in energy loss (from 4085.7 *kWh/day* to 2036.4 *kWh/day*) and an improvement in voltage profiles (from 0.89 *pu* to 0.93 *pu*). Furthermore, there was a 47.59% decrease in the annual cost of energy loss (from *$4.8317* million to *$2.5320 million*), with the cost for power supplied by DGs recorded at *$36,002/year*.

These results underscore the MOMVO method's superior reliability and efficacy in optimizing network performance compared to the MOJS, MFPA, and MOLA methods. The diverse solutions represented on the Pareto front, as illustrated in Figures IV.7 (a) to (d) for both IEEE networks, highlight the effectiveness of MOMVO's diversity-preserving mechanisms throughout the optimization process. The graphical representations of the Pareto solutions demonstrate MOMVO's enhanced performance over the comparative algorithms, signifying its capability to achieve optimal convergence and significantly improve network performance through the strategic allocation of PVRES-CBs.

The MOMVO method not only excels in minimizing the specified objectives but also enhances the overall operational efficiency of the distribution networks. Its success in the comparative analysis suggests its potential as a robust and reliable tool for distribution network optimization, offering substantial improvements over existing methodologies in addressing the complexities of modern electrical distribution systems.

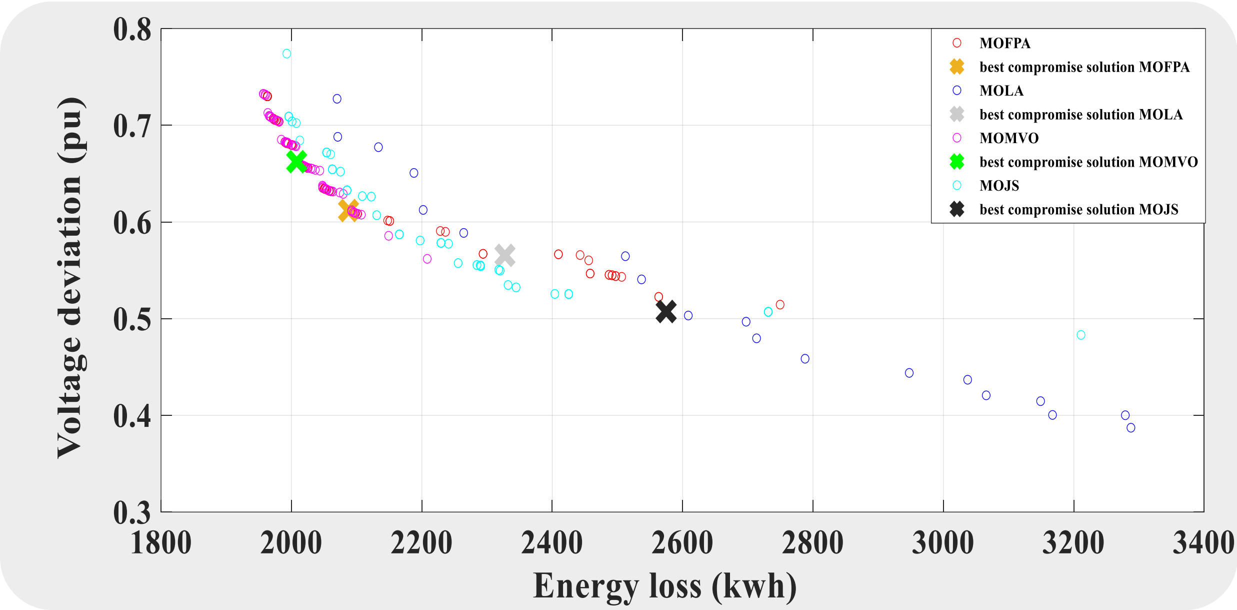

(a) Pareto-optimal front for IEEE 33 (obj1).

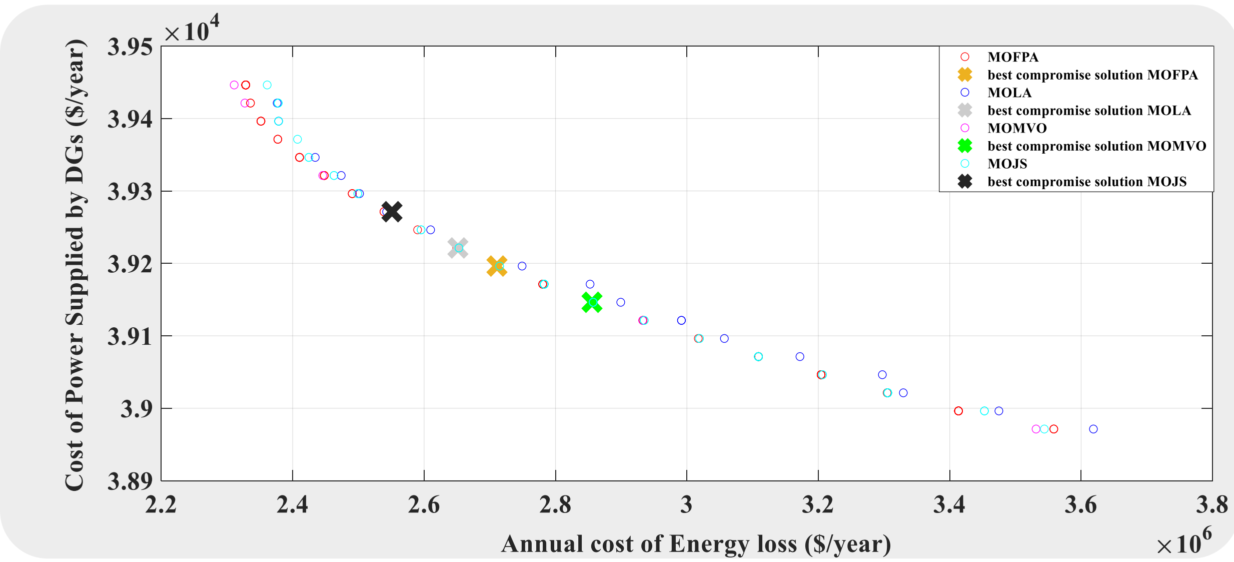

(b) Pareto-optimal front for IEEE 33 (obj2).

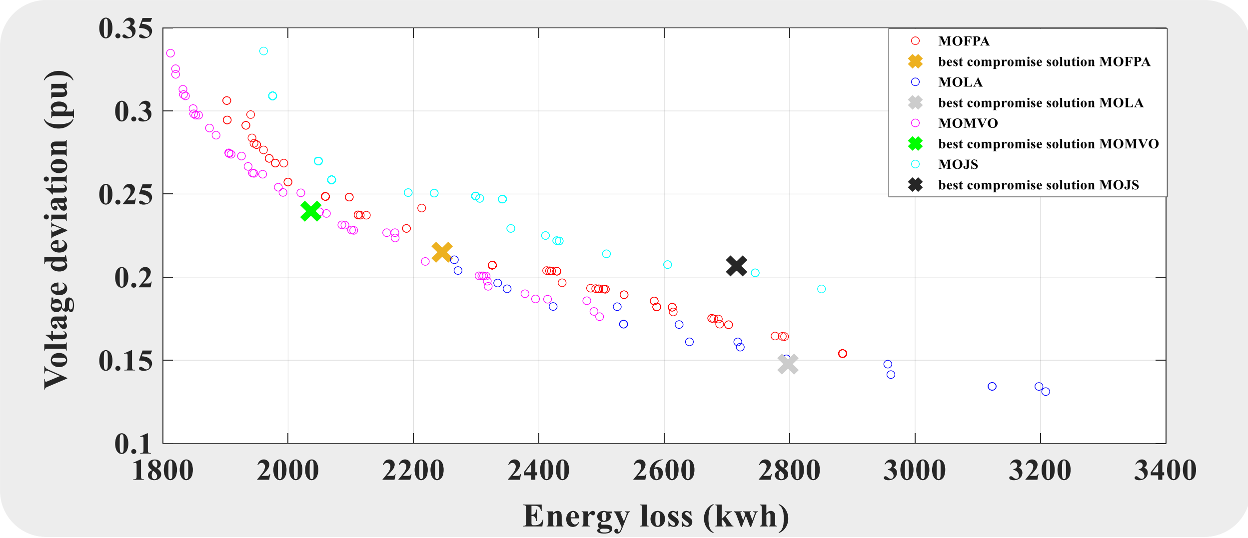

(c) Pareto-optimal front for IEEE 69 (obj1)

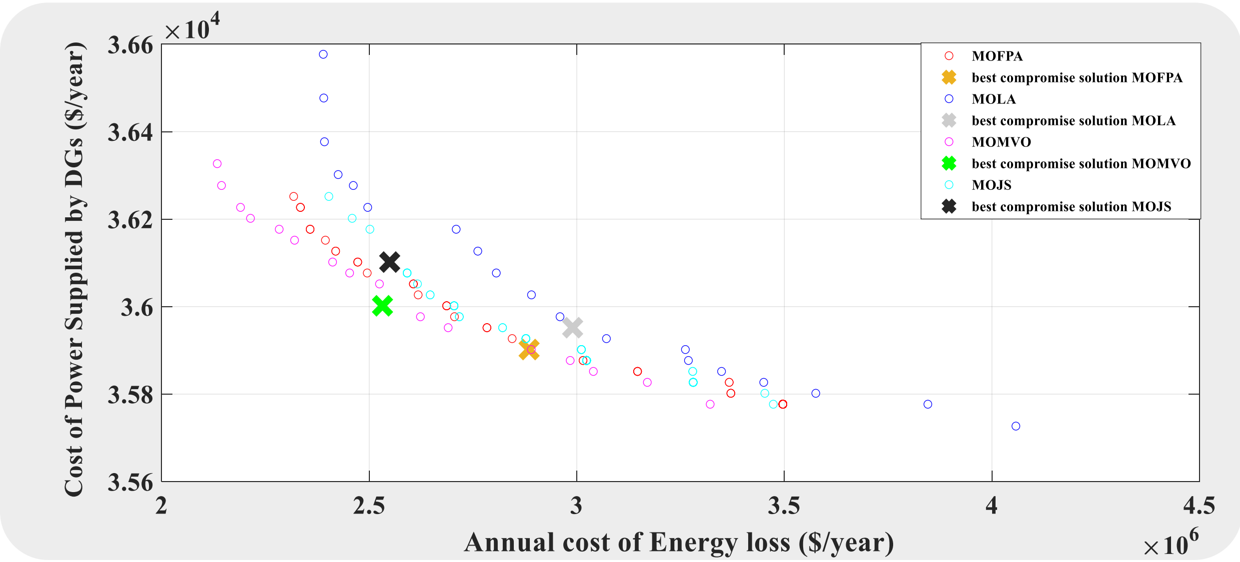

(d) Pareto-optimal front for IEEE 69 (obj2)

Figure IV.7. Pareto-Optimal Front Using MOMVO, MOFPA, MOLA, and MOJS for the Best Solution in the Second Scenario Across All Distribution Systems.

Table IV.7. Optimal location and size of PVRES and CB with the best compromise solution of energy losses, Minimum bus Voltage (pu), and the yearly cost of energy losses, and the cost of power supplied by Photovoltaic and Reactive Energy Source - Capacitor Banks (PVRES-CBs) obtained for scenario 2 for all distribution network.

Comparison Criteria	Optimal Placement and Sizing of Photovoltaic (PV) and Capacitor Banks (CB)						Minimum bus Voltage (pu)				Best compromise solution		Best compromise solution	
	-		3 PVRES and 9 CB for IEEE 33		5 PVRES and 18 CB for IEEE 69		IEEE 33		IEEE 69		IEEE 33	IEEE 33	IEEE 69	IEEE 69
			Obj1	Obj2	Obj1	Obj2	Obj1	Obj 2	Obj1	Obj2	Obj1	Obj2	Obj1	Obj2
Base case							0.90		0.90		-	-	-	
Scenario 1	-						0.89		0.89					
Techniques	MOFPA	PV buses	12 16 32	12 16 31	19 59 60 61 64	19 61 62 63 64	0.941	0.91	0.932	0.919	2.0876e+03 0.6118	2.7109e+06 3.9196e+04	2.2457e+03 0.2150	2.8852e+06 3.5902e+04
		CB buses	13-14-15-17-31-32-33	14-18-31-32-33	19 20 21 22 24 25 26 27 57 58 59 60 61 62 64 65	24 61 63 64 65								
		CB Size	150 -150 150 -150 150 - 150 150	50-50-150-150-50	100 -150 - 150 150 -100 - 100 150 - 150 - 150 50 -150 - 100 150 -150 - 150 150	50 150 50 100								
	MOLA	PV buses	17 30 32	12 15 31	60 62 63 64 67	13 15 22 60 61	0.945	0.919	0.934	0.917	2.3275e+03 0.5655	2.6514e+06 3.9221e+04	2.7973e+03 0.1477	2.9901e+06 3.5952e+04
		CB buses	13- 14- 15 16- 17- 18 31- 32- 33	14- 18 - 31- 32- 33	19 20 21 22 23 24 25 26 27 57 58 59 60 61 62 63 64 65	24-59- 61- 64								
		CB Size	150 -100 150 -150 100 - 100 150 -100 150	50 –50 -150 100 - 150	150 150 150 150 150 150 150 150 150 150 150 150 150 150 150 150 150 150	50 150 150 100								
	MJS	PV buses	29 30 32	14 16 31	3 12 42 58 59	15 23 60 63 64	0.947	0.923	0.926	0.924	2.5748e+03 0.5074	2.5511e+06 3.9271e+04	2.7153e+03 0.2068	2.5494e+06 3.6102e+04
		CB buses	13- 14- 15 16- 17- 18 31- 32- 33	15-31- 32- 33	19 20 21 22 24 25 26 27 59 60 61 62 63 64 65	24 59 60 61 64 65								
		CB Size	150 -150 150 - 150 -50 150 - 150 150 -150	150 -100 100 - 150	100 100 150 100 150 50 150 150 150 100 150 150 150 150 150	150 100 50 150 150 100								
	MOMVO	PV buses	12 15 31	12 16 31	20 60 61 63 64	59 60 61 63 64	0.943	0.914	0.933	0.924	2.0081e+03 0.6623	2.8556e+06 3.9146e+04	2.0364e+03 0.2397	2.5320e+06 3.6002e+04
		CB buses	13- 14- 15 16- 18 - 31 32- 33	15-31- 32	20 21 22 23 24 27 58 59 60 61 62 63 64 65	60 61 64 65								
		CB Size	150- 150 100 - 50 50 - 150 150 -150	50 -150 -150	100 150 150 150 150 100 150 150 50 150 150 50 150 150	50 200 150 150								

IV.3.2.3. Scenario 3

In this analytical scenario, our investigation zeroes in on the performance evaluation of the Multi-Objective Multi-Verse Optimization (*MOMVO*) algorithm in juxtaposition with three other esteemed optimization methods: Multi-Objective Jellyfish Search (*MOJS*), Multi-Objective Lion Algorithm (*MOLA*), and Multi-Objective Flower Pollination Algorithm (*MOFPA*). This comparative study is motivated by the overarching aim to optimize two pivotal objective functions, as delineated in Equation (10) and Equation (13), across various allocations of Photovoltaic and Reactive Energy Source Capacitor Banks (*PVRES-CBs*) within the distribution networks of IEEE 33 and IEEE 69.

Table IV.8 meticulously catalogues the outcomes, presenting a holistic view of the most balanced solutions concerning energy losses and voltage deviations (as the primary objective) along with the annual financial burdens stemming from energy losses and the costs incurred from the power supplied by Distributed Generators (*DGs*) as the secondary objective. Specifically, within the IEEE 33 network, the implementation of the MOMVO strategy heralds a profound reduction in energy loss, showcasing a decrease of 54.34% from an initial value of 3831.3 *kWh/day* to a mere 1749.2 *kWh/day*. This significant reduction is complemented by an improvement in the voltage deviations index to 0.60 and an elevation of voltage profiles from 0.89 *pu* to 0.94 *pu*, perfectly aligning with the primary objective. Furthermore, the secondary objective witnesses a considerable decrease of 53.20% in the annual cost of energy loss, plummeting from *$4.5308 million* in the baseline scenario to *$2.1204 million*. Additionally, a noteworthy achievement of *$78,243* is recorded for the cost associated with power supplied by DGs.

Turning our attention to the IEEE 69 network, the application of the MOMVO approach results in a stellar 62.04% diminution in energy loss, effectively bringing it down from the preliminary figure of 4085.7 *kWh/day* to 1550.7 *kWh/day*. This reduction is supported by a voltage index of 0.2897 and a noticeable improvement in voltage profile variations, escalating from 0.89 *pu* to 0.93 *pu*, in harmony with the primary objective. In relation to the secondary objective, the annual cost of energy loss witnesses a substantial decline of 52.95%, from an initial $4.8317 million to $2.2730 million, with the cost of power supplied by DGs marked at $71,679.

The data encapsulated in Table IV.8 unequivocally attests to the superior performance of the MOMVO method over the MOJS, MOLA, and MOFPA techniques, highlighting its increased reliability and effectiveness in optimizing the placement and sizing of PVRES units and CBs to meet the predefined objectives.

This comparative analysis is further enriched by the convergence behaviors depicted in Figures IV.8 (a) to (c) for both IEEE networks, reinforcing the observations from scenario two (as illustrated in Figure IV.7). Remarkably, Figure IV.8 accentuates the MOMVO algorithm's superior convergence characteristics in determining the optimal positions and dimensions of PVRES and CBs, thereby achieving the objectives and significantly enhancing the operational efficiency of the distribution networks under study.

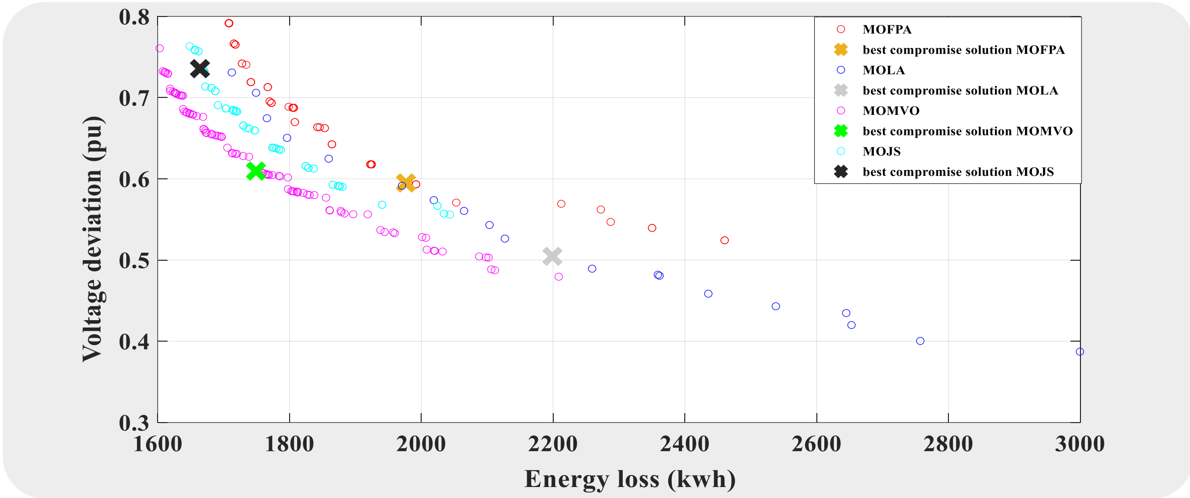

(a) Pareto-optimal front for IEEE 33 (obj1).

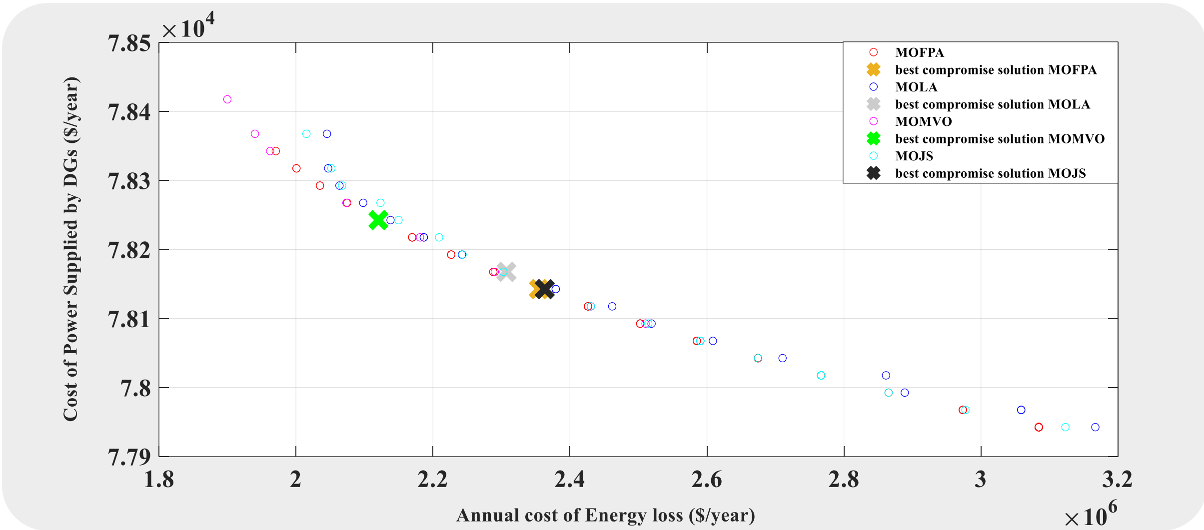

(b) Pareto-optimal front for IEEE 33 (obj2).

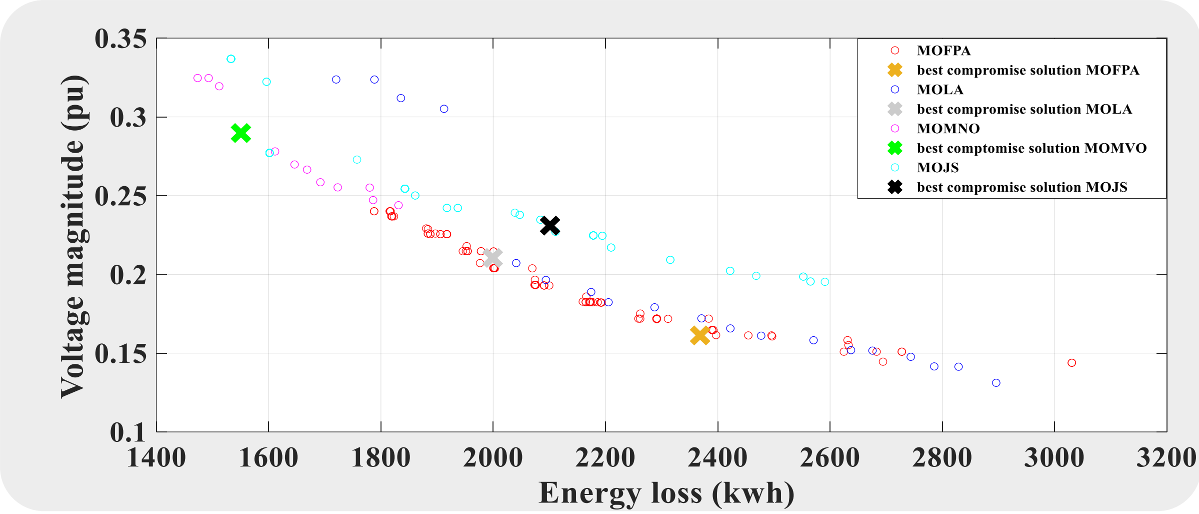

(c) Pareto-optimal front for IEEE 69 (obj1).

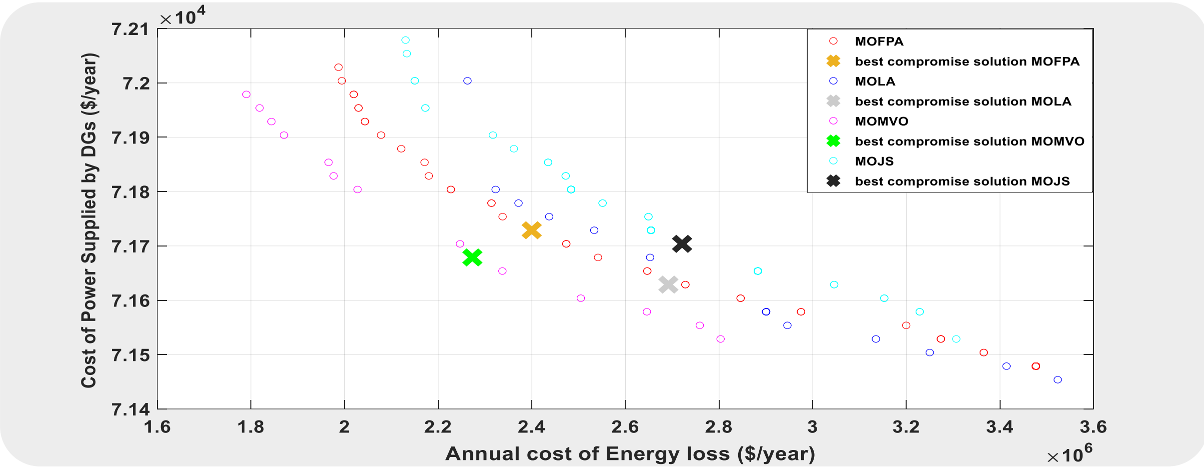

(d) Pareto-optimal front for IEEE 69 (obj2).

Figure IV.8. Pareto-Optimal Front Using MOMVO, MOFPA, MOLA, and MOJS for the Best Solution in the third Scenario Across All Distribution Systems.

Table IV.8. Optimal location and size of PVRES and CB with the best compromise solution of energy losses, Minimum bus Voltage (pu), and the yearly cost of energy losses, and the cost of power supplied by Photovoltaic and Reactive Energy Source - Capacitor Banks (PVRES-CBs) obtained for scenario 3 for all distribution network.

Comparison Criteria			Optimal Placement and Sizing of Photovoltaic (PV) and Capacitor Banks (CB)				Minimum bus Voltage (pu)				Best compromise solution		Best compromose solution	
	-		6 PVRES and 9 CB for IEEE 33		10 PVRES and 18 CB for IEEE 69		IEEE 33		IEEE 69		IEEE 33	IEEE 33	IEEE 69	IEEE 69
			Obj1	Obj2	Obj1	Obj2	Obj1	Obj2	Obj1	Obj2	Obj1	Obj2	Obj1	Obj 2
Base case	-						0.90		0.90		-	-	-	
Scenario 1	-						0.89		0.89					
Techniques	MOFPA	PV buses	8 12 16 24 29 32	8 12 16 28 30 31	7 9 14 57 59 60 61 62 64 68	9 10 19 20 21 59 60 61 63 64	0.942	0.919	0.933	0.921	1.9767e+03 0.5950	2.3548e+7.81 43e+04	2.3684e+03 0.1613	2.3997e+06 7.1729e+04
		CB buses	13 14 15 16 17 18 31 33	17 18 31 32	20 21 22 24 25 26 27 57 58 59 60 61 63 64 65	20 21 57 59 61 64 65								
		CB Size	150 150 150 50 150 150 150 150	50 50 150 150	150 150 150 150 100 150 150 150 150 150 150 150 100 150 150	50 50 50 150 100 50 100								
	MOLA	PV buses	15 26 29 30 31 32	6 8 12 16 29 31	48 52 58 59 60 61 62 63 64 66	5 7 17 32 56 59 60 62 63 64	0.947	0.918	0.93	0.918	2.1990e+03 0.5046	2.3074e+06 7.8168e+04	1.9993e+03 0.2105	2.6917e+06 7.1629e+04
		CB buses	13 14 15 16 17 18 31 32 33	13 14 31 32 33	19 20 21 22 23 24 25 26 27 57 58 59 60 61 62 63 64 65	57 59 60 61 62								
		CB Size	150 150 150 150 150 100 150 150 150	100 50 100 100 100	150 150 150 150 150 150 150 150 150 150 150 150 150 150 150 150 150 150	50 50 50 100 100								
	MJS	PV buses	8 11 14 24 30 31	11 13 16 28 29 31	4 6 15 59 60 62 63 64 68 69	16 20 52 53 56 58 60 63 67 68	0.939	0.919	0.928	0.919	1.6641e+03 0.7356	2.3632e+06 7.8143e+04	2.1012e+03 0.2310	2.7209e+06 7.1704e+04
		CB buses	13 15 16 17 18 31 32 33	18 31 32 33	20 21 22 23 24 25 26 27 58 60 61 62 63 64 65	20 25 26 64 65								
		CB Size	150 150 100 50 50 150 150 150	100 150 50 100	150 50 150 50 150 50 150 150 100 50 100 150 150 150 150	150 50 50 150 100								
	MOMVO	PV buses	8 13 17 28 30 31	7 12 16 28 29 31	18 19 57 58 59 60 61 62 63 64	7 21 23 57 58 59 60 62 63 64	0.947	0.92	0.93	0.923	1.7492e+03 0.6095	2.1204e+06 7.8243e+04	1.5507e+03 0.2897	2.2730e+06 7.1679e+04
		CB buses	13 14 15 16 18 31 32 33	14 31 32 33	20 21 22 24 27 57 58 61 62 64 65	60 64 65								
		CB Size	150 150 150 150 100 150 150 150	150 200 200 50	50 150 150 50 150 150 100 150 150 150 150	150 100 150								

Figures IV.9 (*a*) to (*d*) showcase voltage profiles across the IEEE 33 and IEEE 69 networks, revealing how these profiles not only meet but exceed the minimum thresholds established by their respective base cases. This achievement is particularly noteworthy during peak consumption hours, where voltage stability is crucial for maintaining network reliability. For the IEEE 33 network, the voltage profiles achieve minimum levels of 0.94 pu and 0.92 *pu* for the primary and secondary objectives, respectively, during these critical periods. Meanwhile, the IEEE 69 network demonstrates a commendable performance with voltage levels sustaining at 0.93 *pu* and 0.92 *pu* for the primary and secondary objectives, respectively, even amidst peak demand.

These findings underscore the efficacy of the Multi-Objective Multi-Verse Optimization (*MOMVO*) method in optimizing the deployment of Photovoltaic and Reactive Energy Source Capacitor Banks (*PVRES-CBs*) within these networks. By adjusting PVRES and CB configurations, the MOMVO method not only ensures voltage levels remain above critical thresholds but also contributes to enhancing the overall stability and reliability of the power supply during peak demand periods. This successful optimization underscores the importance of advanced algorithmic approaches like MOMVO in achieving operational excellence in power distribution networks, ensuring they can reliably meet increased demand without compromising on service quality.

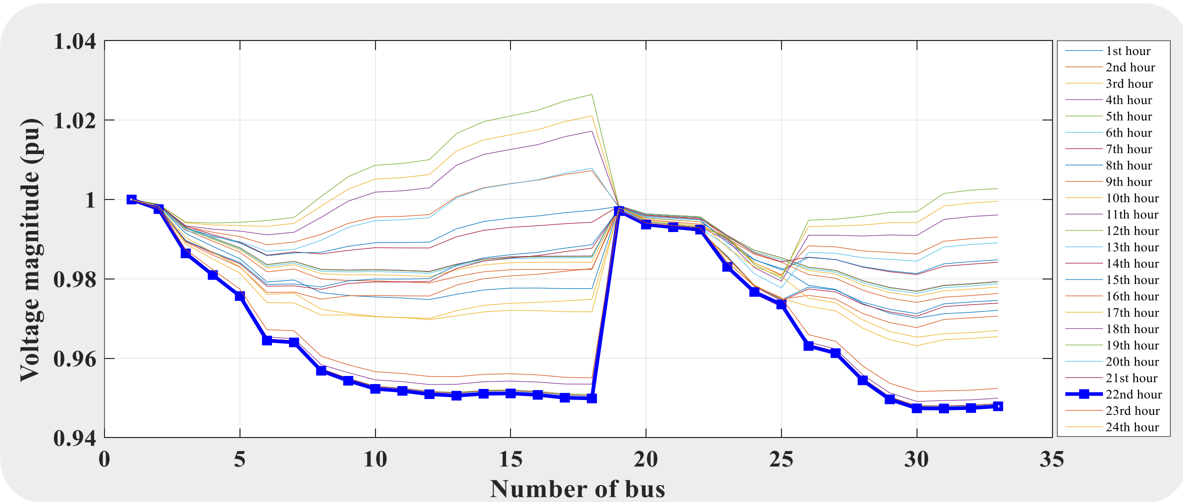

(c) (a) obj 1 with IEEE 33.

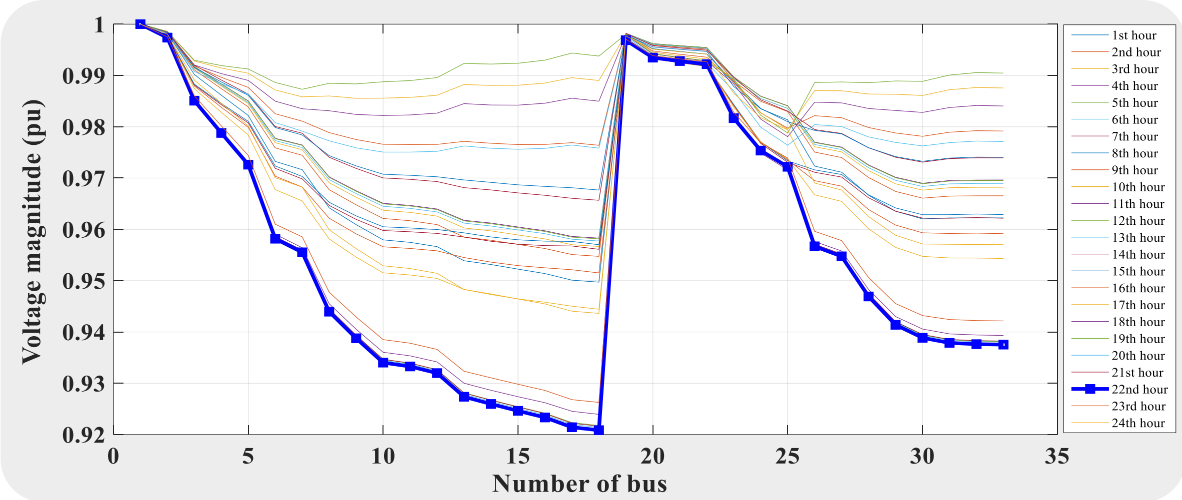

(d) obj 2 with IEEE 33

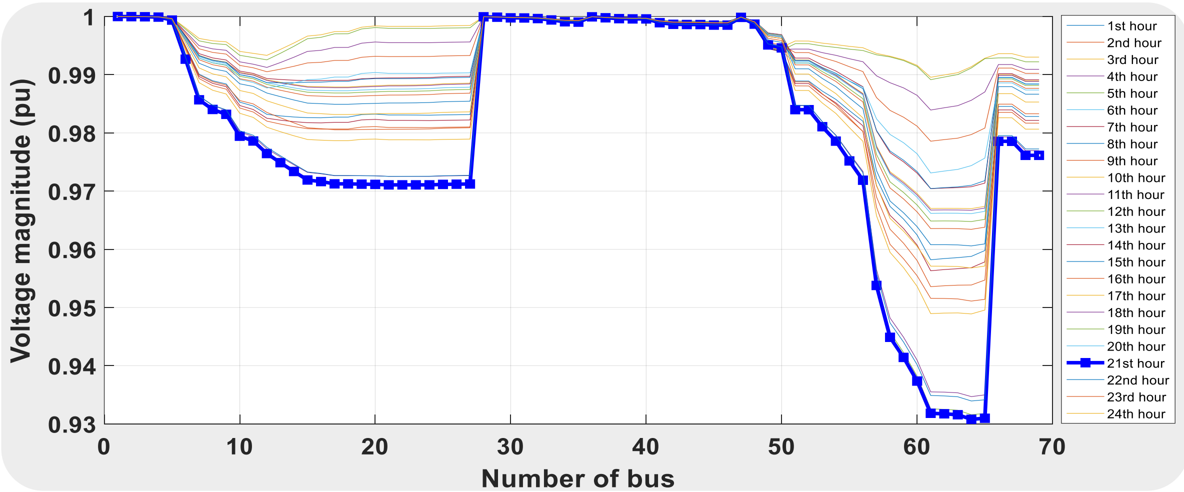

(c) obj 1 with IEEE 69

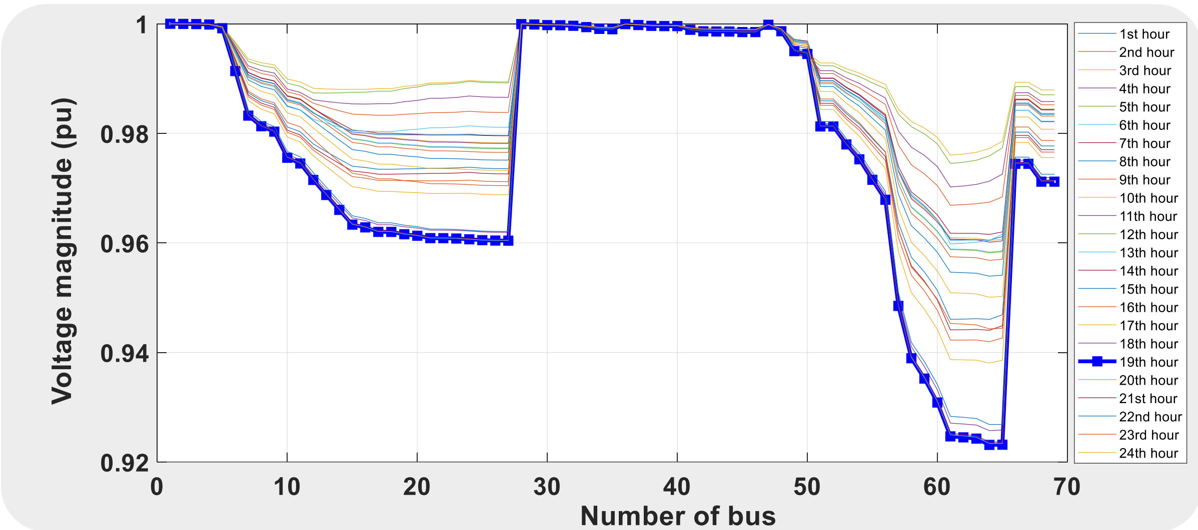

(d) obj 2 with IEEE 69

Figure IV.9. Voltage profile variation over a 24-hour period for the third scenario in the two network.

IV.3.3. Interpretations Results

The study meticulously explores the application of the Multi-Objective Multi-Verse Optimization (*MOMVO*) algorithm for optimizing Distributed Generation (*DG*) and compensation devices across electrical distribution networks, offering a novel approach to addressing complex optimization challenges. Through comparative analysis, MOMVO's superior performance is highlighted against alternatives like MOJS, MOFPA, and MOLA within IEEE 33-bus and IEEE 69-bus networks. The utilization of Pareto front analysis underpins the study’s effectiveness in delineating the trade-offs between minimizing energy losses, voltage deviations, and operational costs, showcasing the algorithm's adeptness at navigating the intricate multi-objective optimization landscape. To enrich the evaluation, a deeper statistical analysis could include metrics such as convergence speed, solution diversity, and rigorous statistical significance testing, enhancing the robustness and reliability assessment of the MOMVO algorithm. Moreover, exploring the algorithm's sensitivity to varying network configurations and its performance stability across diverse scenarios would provide comprehensive insights into its applicability. Extending the analysis to real-world distribution networks, through statistical validation against actual data, would further affirm MOMVO’s practical utility and efficacy in dynamic, real-world conditions, marking a significant advancement in distribution system optimization research.

IV.4. Conclusion

In this chapter, we introduced the Efficient Metaheuristic BitTorrent (*EM-BT*) algorithm as a novel optimization technique for determining the optimal placement and sizing of Photovoltaic Renewable Energy Sources (*PVRES*) and Capacitor Banks (*CB*) within distribution networks. The primary goal of EM-BT is to minimize energy losses while addressing the dynamic load profiles and temperature fluctuations over a 24-hour period. Comparative analysis with established optimization algorithms such as Grey Wolf Optimizer (*GWO*), Particle Swarm Optimization (*PSO*), and Whale Optimization Algorithm (*WOA*) demonstrated that EM-BT consistently outperforms these traditional methods. The success of EM-BT is attributed to its unique capability to integrate both PVRES and CB, addressing the combined effects of solar irradiance and temperature variations, while improving system performance by reducing energy losses and stabilizing voltage profiles.

One notable finding of this study is that the EM-BT algorithm shows superior convergence behavior, offering high-quality solutions with greater efficiency than PSO, GWO, and WOA. This feature is particularly important in real-world applications where time-sensitive decision-making is crucial. The practical implications of EM-BT are clear: by enabling accurate allocation and strategic planning of active and reactive power compensation, the algorithm holds significant value for utility companies and renewable energy investors, enhancing the deployment of distributed energy resources.

However, while EM-BT demonstrates strong potential, several limitations must be addressed. The computational intensity of the algorithm could pose challenges for larger, more complex networks, requiring further research into optimizing its performance for scalability.

Additionally, real-world conditions were simplified in the model, and future research should consider factors such as humidity, wind speed, and cloud cover, in addition to solar irradiance and temperature, to enhance the accuracy of the results. Economic considerations, hardware limitations during implementation, and evaluating the scalability across diverse grid topologies are critical areas for future research. Furthermore, conducting comprehensive economic analyses to assess the cost-effectiveness and environmental impact of deploying optimized PVRES-CB configurations could provide valuable insights into the long-term sustainability of such integrations.

This study also introduced the Multi-Objective Modified Vector Optimization (MOMVO) methodology for optimizing the placement and sizing of PV systems and CBs, with a focus on minimizing energy losses, voltage deviations, and operational costs. Applied to the IEEE 33-bus and 69-bus systems, the MOMVO algorithm demonstrated its effectiveness by achieving a significant reduction in energy losses—up to 50.15%—and improving voltage stability. Comparative analysis with other multi-objective algorithms such as the Multi-Objective Jaya Search (*MOJS*), Multi-Objective Lion Algorithm (*MOLA*), and Multi-Objective Flower Pollination Algorithm (*MOFPA*) confirmed the superior performance of MOMVO in terms of solution quality and convergence speed.

These findings underscore the robustness of MOMVO and EM-BT in promoting the sustainable integration of renewable energy resources into power infrastructures. This research advances current optimization practices and lays the groundwork for future studies aimed at more effectively integrating renewable energy sources into distribution systems, contributing to improved efficiency, reliability, and sustainability in power system optimization.

CHAPTER V

Results and Discussions: A Comparison of Recently Developed Metaheuristic Optimization Techniques on the Real Distribution Networks of ALG-AB-Hassi Sida, Algeria

V.1. Introduction

In this chapter, we evaluate and compare four recently developed metaheuristic optimization techniques—Energy Valley Optimizer (*EVO*), Liver Cancer Algorithm (*LCA*), Zebra Optimization Algorithm (*ZOA*), and Walrus Optimization Algorithm (*WaOA*) for optimizing the placement of Capacitor Banks (*CB*) and Distributed Generation (*DG*), specifically photovoltaic systems, within the ALG-AB-Hassi Sida 157-bus radial distribution network in Algeria. The goal is to determine the optimal locations and sizes of CBs and DGs over a 24-hour period, considering hourly load variations. The proposed EVO addresses the limitations of previous methods by dynamically adapting to the variability of the power distribution network, considering hourly load changes, and minimizing total energy costs over a 24-year lifespan, ensuring optimal CB and DG placement while enhancing energy loss reduction and maintaining voltage stability. This study compares EVO's performance against the other three techniques, evaluating their impact on both technical and economic aspects of the distribution network. Key contributions include investigating the integration of DGs and CBs to maximize technical and economic benefits, achieving goals such as reducing energy losses, minimizing voltage deviation, and improving bus voltage stability, and minimizing total energy costs by considering DG, CB, and combined scenarios. Three operational scenarios are analysed: DGs only, CBs only, and simultaneous allocation of DGs and CBs using EVO. Applying these techniques to a real-world distribution system provides practical insights into their effectiveness, offering valuable guidance for optimal DG and CB allocation in real-world distribution networks with varying operational constraints and objectives.

V.2. Problem Formulation

V.2.1. Objective Function

For load flow calculations, the backward/forward sweep method is used [126]. The objective aims to minimize the total energy cost over 24 years and annually under three scenarios: the first scenario involves only Capacitor Banks (*CBs*), the second scenario includes only Distributed Generators (*DGs*), and the third scenario combines both CBs and DGs. The objective function for this analysis is detailed in equation (V.1):

$$\min \left\{ \begin{aligned} A + B + C = \ & C_{\text{energy}} \cdot \left[\sum_{t \in T} \sum_{i \in nbr} Re \left| \left(I_{br_i}^{t} \right)^2 \times Z_i \right| \right] \cdot Tf \\ & + C_{cb} \cdot \sum_{j \in ncb} Q_{cb_j} + C_{DG} \cdot \sum_{k \in nDG} P_{DG_k} \end{aligned} \right\} \tag{V.1}$$

V.2.1.1. Minimizing the Total Energy Cost Over 24 Years with Capacitor Banks (Obj1)

The Obj1 minimizes the total energy cost over a 24-year period *($/ 24 year*) with CB. C_{energy} is the average energy cost (*in $/kWh*), T are the hours in a day (*in h*), nbr is the number of branches, $I_{br_i}^{t}$ is the current flowing through the branch i at time t (*in A*), Z_i represents the impedance of the branch *I* (*in Ω*), $Tf = 0.9 \cdot 8760 \cdot 24$ (Tf represents the total hours over 24 years, calculated as 0.9 (efficiency factor) multiplied by 8760 (hours in one year) multiplied by 24 (number of years). The result is expressed in hours (h)), C_{cb} is the CB capital cost (*in $/kVAR*), ncb is the number of CBs, Q_{cb_j} is the reactive power of the CB *j* (in kVAR). Thus, the total energy cost over 24 years with CBs (*Obj1*) is computed through the terms A and B of equation (V.1).

V.2.1.2. Minimizing total Energy cost Over 24 Years with DGs (Obj2)

The objective Obj2 focuses on minimizing the total cost associated with distributed generation (DG) over a 24-year period, expressed in (*$/year*). Here, C_{DG} represents the capital cost of DG in (*$/kW*), nDG denotes the number of DG units, and P_{DG_k} refers to the active power of DG unit k. Consequently, the total energy cost over the 24-year timeframe (*Obj2*) is calculated using terms A and C from equation (V.1).

V.2.1.3. Minimizing total Energy cost Over 24 Years with CBs and DGs (Obj3)

In this scenario, the objective (*Obj3*) focuses on minimizing the total energy cost over a 24-year period by accounting for the combined expenses of capacitor banks (CBs) and distributed generation (DGs). This objective reflects the costs associated with both components over the specified time frame. By minimizing (*Obj3*), the aim is to determine the optimal placement and usage of CBs and DGs within the power grid, while balancing factors like capital expenditure, operational costs, and system limitations. The calculation of the total energy cost with CBs and DGs (*Obj3*) incorporates all the terms (*A, B, and C*) of the equation (V.1).

The selection of a 24-year timeframe for assessing the performance and cost-effectiveness of distributed generation (DG) units and capacitor banks (CBs) in this study is driven by several important factors:

Asset Lifespan: The typical lifespan of distributed generation (DG) units, such as photovoltaic (PV) systems, and capacitor banks (CBs) closely aligns with a 24-year period. This duration enables a thorough assessment of long-term benefits, depreciation, and overall economic and technical performance throughout the asset's operational life.

Financial Analysis: A 24-year horizon is often used in financial projections for infrastructure investments, allowing for in-depth evaluation of payback periods, return on investment (ROI), and net present value (NPV). These are essential metrics for decision-making in the energy sector, and this timeframe aligns with industry practices for analyzing lifecycle costs and benefits in large-scale energy projects.

Policy and Regulatory Frameworks: Many energy policies and international agreements are designed for multi-decade implementation. Evaluating the impacts over 24 years provides valuable insights into how DGs and CBs contribute to long-term energy and environmental goals, in line with government and international regulatory frameworks.

Market Stability and Forecasting Accuracy: A 24-year analysis helps smooth out short-term market fluctuations in energy prices, technology developments, and policy shifts, offering a more stable and reliable forecast for strategic energy planning.

These factors make the 24-year period ideal for studying the integration of DGs and CBs in distribution networks, ensuring the results are both scientifically robust and practically relevant for stakeholders in the energy sector.

V.2.2. Equality and Inequality Constraints

Once objective functions have been defined, equality and inequality constraints have to be set up. It is necessary first to ensure that the actual power injection, both real (P_{DG_k}) and reactive (Q_{cb_j}), from DGs and CBs remains within the installed capacity $P_{DG_{k\_max}}$ and $Q_{cb_{j\_max}}$. The inequalities are expressed by (V.2) and (V.3):

$$0 < P_{DG_k} < P_{DG_{k\_max}} \quad t \in T, k \in nDG \tag{V.2}$$

$$0 < Q_{cb_j} < Q_{cb_{j\_max}} \quad t \in T, j \in ncb \tag{V.3}$$

P_{DG_k} : Power installed from photovoltaic (*PV*) systems into the grid at node k [*in Watts, W*].
Q_{cb_j} : Reactive power injection from capacitor banks (*CBs*) into the grid at node j [*in Volt-Amperes Reactive, VAR*].

Additionally, it is vital to ensure that the voltage at every bus and the current flowing through branches stay within acceptable limits, as specified in [127].

$$V_{m\_min} < V_m^t < V_{m\_max} \quad t \in T, m \in nB \tag{V.4}$$

$$I_{br_i}^t < I_{br_{i\_max}} \quad t \in T, i \in nbr \tag{V.5}$$

$\boldsymbol{V_m^t}$: Voltage at bus mmm at hour t [*in Volts, V*].
$\boldsymbol{V_{m\_min}}$: Lower voltage limit for bus mmm (typically set to 90% of the nominal voltage) [*in Volts, V*].

$\boldsymbol{V_{m\_max}}$: Upper voltage limit for bus mmm (typically set to 110% of the nominal voltage) [*in Volts, V*].

$\boldsymbol{I_{br_{i\_max}}}$: Thermal capacity limit of branch i [*in Amperes, A*].

$\boldsymbol{K_P}$: Coefficient representing the threshold on the distributed generation (*DG*) penetration.

$\sum_{k\in nDG}\boldsymbol{P_{DG_k}}$: Total installed capacity from distributed generation (*DG*) systems, where k refers to the individual DG systems in the network.

$\boldsymbol{P_{D_m}}$: Total active power demand in the system at bus m [*in Watts, W*].

This relationship is expressed by equation (V.6):

$$\sum_{k\in nDG} P_{DG_k} = K_P \cdot \sum_{m\in nB} P_{D_m} \tag{V.6}$$

The inequality constraints (V.2) and (V.3) pertain to the control variables and are automatically managed through the EVO mechanism. However, additional attention is required to address the inequality constraints in Equations from (V.4) to (V.6).

V.2.3. Modeling of PV Uncertainty

The solar energy irradiance for each day's hours could be modelled using the Beta Probability Density Function (*PDF*) supported by historical data. For every hour, the PDF irradiance of solar may be defined by [129]:

$$f_b(s) = \begin{cases} \dfrac{\Gamma(A+B)}{\Gamma(A)\Gamma(B)} s^{(\alpha-1)} & 0 \le s \le 1, A, B \ge 0 \\ 0 & \text{Otherwise} \end{cases} \tag{V.7}$$

Where, A and B can be calculated as in [130]:

$$B = (1-\mu)\left(\frac{\mu(1-\mu)}{\sigma^2} - 1\right)$$
$$A = \frac{\mu \cdot B}{1-\mu} \tag{V.8}$$

A and B are parameters used to define the shape of the Beta PDF, which models the irradiance of solar for each hour of the day based on historical data. These parameters are calculated based on the statistical properties of the data, specifically the mean (μ) and standard deviation (σ).

The solar irradiance state (s) probability for each specific hour could be defined as:

$$P_s\{G\} = \int_{s_1}^{s_2} f_b(s)ds \tag{V.9}$$

The output power of the PV module may be expressed as [131]:

$$P_{PV_\circ}(s) = N \cdot FF \cdot V_y \cdot I_y \tag{V.10}$$

Where:

N : Number of photovoltaic (PV) modules in the system.
FF : Fill factor of the PV system (a measure of the quality of the PV system).
$\boldsymbol{V_y}$: Voltage generated by the PV system [*in Volts, V*].
$\boldsymbol{I_y}$: Current generated by the PV system [*in Amperes, A*].

The fill factor of the PV system:

$$FF = \frac{V_{MPP} \cdot I_{MPP}}{V_{oc} \cdot I_{Sc}} \tag{V.11}$$

Where:

$\boldsymbol{V_{MPP}}$: Voltage at the maximum power point (*MPP*) of the photovoltaic (*PV*) system [*in Volts, V*].
$\boldsymbol{I_{MPP}}$: Current at the maximum power point (*MPP*) of the photovoltaic (*PV*) system [*in Amperes, A*].
$\boldsymbol{V_{oc}}$: Open-circuit voltage of the photovoltaic (*PV*) system [*in Volts, V*].
$\boldsymbol{I_{Sc}}$: Short-circuit current of the photovoltaic (*PV*) system [*in Amperes, A*].

The voltage generated by the PV system:

$$V_y = V_{oc} \cdot K_v \cdot T_{cy} \tag{V.12}$$

Where:

$\boldsymbol{V_{oc}}$: Open-circuit voltage of the photovoltaic (*PV*) system [*in Volts, V*].
$\boldsymbol{K_v}$: Coefficient representing the temperature dependence of the open-circuit voltage.
$\boldsymbol{T_{cy}}$: Cell temperature of the photovoltaic (*PV*) system [*in degrees Celsius, °C*].
The current generated by the PV system:

$$I_y = s\left[I_{sc} \cdot K_i \cdot \left(IT_{cy} - 25\right)\right] \tag{V.13}$$

Where:

$\mathbf{I_{sc}}$: Short-circuit current of the photovoltaic (*PV*) system [*in Amperes, A*].
$\mathbf{K_i}$: Coefficient representing the temperature dependence of the short-circuit current.
$\mathbf{IT_{cy}}$: Temperature of the photovoltaic (*PV*) system's cells [*in degrees Celsius, °C*].

The cell temperature of the PV system:

$$T_{cy} = T_A + s\left(\frac{N_{OT} - 20}{0.8}\right) \tag{V.14}$$

$\mathbf{T_A}$: Ambient temperature [*in degrees Celsius, °C*].
$\mathbf{N_{OT}}$: Total solar radiation received by the photovoltaic (*PV*) system [*in Watts per square meter, W/m²*].

The total output power of a Hybrid Renewable Energy System (HRES), which includes photovoltaic (PV) panels, is the combined electrical power produced by a system that integrates multiple renewable energy sources. This definition emphasizes the calculation of output power by considering the specific performance characteristics of PV panels, particularly their response to varying levels of solar irradiance. The overall efficiency and output of the system are thus directly influenced by the irradiance levels and the operational specifications of the PV panels within the HRES.

$$P_{PV}(t) = \int_{s_1}^{s_2} P_{PV_\circ}(s) P_s\{G\} ds \tag{V.15}$$

V.3. Model Mathematics of (EVO)

In this section, we provide a detailed explanation of the Energy Valley Optimizer (EVO) algorithm, which is based on physics-inspired optimization principles [132]. The algorithm starts with an initialization phase, where candidate solutions are treated as particles within a specific region of the universe. The positions of these candidates are determined by generating random numbers within a defined range [0,1], ensuring that the initial solutions are distributed within the problem's boundaries.

$$\mathrm{X} = \begin{bmatrix} \mathrm{X}_1 \\ \mathrm{X}_2 \\ \vdots \\ \mathrm{X}_p \\ \vdots \\ \mathrm{X}_n \end{bmatrix} = \begin{bmatrix} \mathrm{x}_1^1 \mathrm{x}_1^2 \cdots \mathrm{x}_1^m \cdots \mathrm{x}_1^d \\ \mathrm{x}_2^1 \mathrm{x}_2^2 \cdots \mathrm{x}_2^m \cdots \mathrm{x}_2^d \\ \cdots \ddots \vdots \\ \mathrm{x}_p^1 \mathrm{x}_p^2 \cdots \mathrm{x}_p^m \cdots \mathrm{x}_p^d \\ \cdots \\ \cdots \\ \mathrm{x}_n^1 \mathrm{x}_n^2 \cdots \mathrm{x}_n^m \cdots \mathrm{x}_n^d \end{bmatrix}, \begin{cases} p = 1,2,\dots,n. \\ m = 1,2,\dots,d. \end{cases}$$

$$\mathrm{x}_p^m = \mathrm{x}_{p,\min}^m + \mathrm{rand} \cdot \left(\mathrm{x}_{p,\max}^m - \mathrm{x}_{p,\min}^m\right), \begin{cases} p = 1,2,\dots,n. \\ m = 1,2,\dots,d. \end{cases} \tag{V.16}$$

The second step calculates the Enrichment Bound (*EB*) based on the Neutron Enrichment Levels (*NEL*) of particles.

$$\mathrm{EB} = \frac{\sum_{p=1}^{n} \mathrm{NEL}_p}{\mathrm{n}}, \mathrm{p} = 1,2,\dots,\mathrm{n} \tag{V.17}$$

Stability levels are then determined, considering the best (*BS*) and worst (*WS*) stability levels in the universe.

$$\mathrm{SL}_p = \frac{\mathrm{NEL}_p - \mathrm{BS}}{\mathrm{WS} - \mathrm{BS}}, \mathrm{p} = 1,2,\dots,\mathrm{n} \tag{V.18}$$

The main search loop of EVO involves decisions based on neutron enrichment levels and stability bounds. If NEL exceeds EB, decay processes are considered. Alpha and gamma decay occur for particles with high stability levels, and new candidates are generated accordingly.

$$X_p^{New1} = X_p\left(X_{BS}\left(x_p^m\right)\right), \begin{cases} p = 1,2,\dots,n. \\ m = \text{ Alpha Index II.} \end{cases} \tag{V.19}$$

$$X_p^{New2} = X_p\left(X_{Ng}\left(x_p^m\right)\right), \begin{cases} p = 1,2,\dots,n. \\ m = \text{ GammaIndex II.} \end{cases} \tag{V.20}$$

For lower stability levels, beta decay is applied, causing particles to move towards the best stability level and the centre of particles.

$$\begin{gathered} X_{CP} = \frac{\sum_{p=1}^{n} X_p}{n}, p = 1,2,\dots,n. \\ X_p^{New1} = X_p + \frac{(r_1 \times X_{BS} - r_2 \times X_{CP})}{SL_p}, p = 1,2,\dots,n. \end{gathered} \tag{V.21}$$

Additionally, a controlled movement is conducted toward the best stability level and a neighboring particle for exploration.

$$X_p^{New2} = X_p + \left(r_3 \times X_{BS} - r_4 \times X_{Ng}\right), p = 1,2,\dots,n \tag{V.22}$$

If NEL is below EB, random movements are made to simulate electron capture or positron emission.

$$X_p^{New} = X_p + r, p = 1,2,\dots,n. \tag{V.23}$$

At the end of each loop, newly generated vectors are merged with the current population. The algorithm utilizes boundary violation flags and a termination criterion based on the maximum number of evaluations or iterations.

This algorithm introduces three position updating processes in its main loop, balancing exploration and exploitation for improved candidate performance. The unique aspect lies in deriving inspiration from particle decay processes for optimization.

The EVO flowchart is illustrated in Figure V.1:

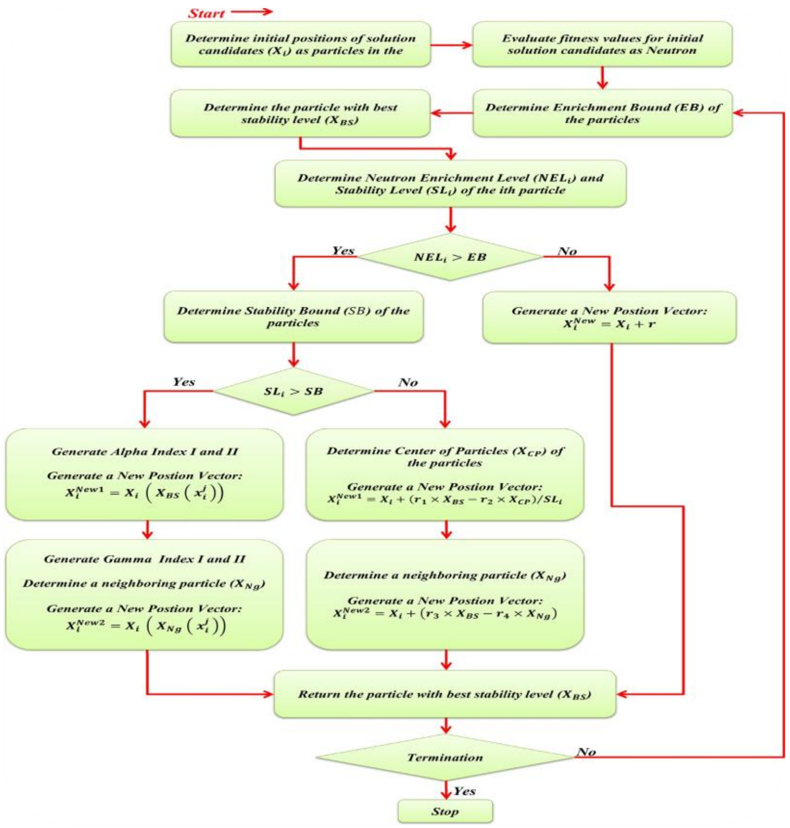

Figure V.1. Flowchart of the EVO.

When applying the Energy Valley Optimizer (*EVO*) to the optimization of a distribution network, specifically for the strategic allocation of Distributed Generations (*DGs*) and Capacitor Banks (*CBs*), the particles X in the EVO algorithm represent distinct configurations of DG and CB placements within the network. Each particle, or candidate solution, corresponds to a unique combination of locations and sizes for these units. The goal is to enhance the overall performance of the network by meeting predefined objectives, such as minimizing energy losses, improving voltage stability, or reducing operational costs. Through this approach, EVO searches for the optimal configuration that balances these performance metrics effectively.

The position of a particle in the solution space is represented by a vector X, where each component of X corresponds to a decision variable in the optimization problem. For Distributed Generations (DGs), these decision variables include the potential installation locations within the network and the corresponding capacity or size of each DG unit at those locations. Likewise, for Capacitor Banks (CBs), the decision variables represent the placement locations of the CBs and their associated reactive power capacities. Together, these variables define a unique configuration for optimizing the network’s performance.

The optimization process iteratively adjusts these decision variables (i.e., the particles' positions) according to the rules of the EVO algorithm, which mimic physical processes like particle decay to explore the solution space efficiently. The goal is to identify the optimal configuration of DGs and CBs that meets the defined objectives, such as minimizing energy losses or improving voltage stability, while ensuring compliance with the network's operational constraints, including voltage limits and thermal loading capacities. Through this iterative process, the EVO algorithm systematically refines the solution to achieve the best possible network performance.

During the optimization process, the fitness of each particle X is assessed using the objective function, which quantifies the performance of a specific configuration of DGs and CBs within the network. The objective function evaluates factors such as energy loss reduction, voltage profile improvement, or operational cost minimization. Constraints, such as voltage limits and thermal capacities, are enforced by applying penalties to configurations that violate these network standards, effectively guiding the optimization towards feasible and optimal solutions.

The parameters used for each algorithm were consistently defined to ensure a uniform testing environment. Each algorithm operated with a population size of 30 particles, a critical factor in maintaining diversity within the search space. The convergence process for all algorithms was controlled by a maximum of 100 iterations, providing each algorithm with ample, yet finite, opportunities to find an optimal solution. Additionally, each algorithm utilized specific parameters tailored to enhance its search efficiency and performance, maximizing its ability to explore and exploit the solution space.

- **The Energy Valley Optimizer** (***EVO***): employed adaptive mutation rates, which were designed to promote extensive exploration during the initial search phases and gradually shift towards exploitation in later phases, ensuring solutions are fine-tuned as the process progresses.
- **The Liver Cancer Algorithm (*LCA*):** utilized both mutation and crossover rates, carefully calibrated to maintain a balance between exploration and exploitation. This balance allowed the algorithm to effectively search the solution space while avoiding premature convergence.
- **The Walrus Optimization Algorithm (*WaOA*):** dynamically adjusted exploration and exploitation rates to simulate walrus herding behaviour, optimizing the algorithm’s search capabilities by drawing inspiration from the collective movement patterns of walrus groups.
- **The Zebra Optimization Algorithm (*ZOA*):** incorporated Zebra Herd Dynamics, which influenced how the virtual herd of solutions navigated the search space. This unique approach enhanced the algorithm’s decision-making and adaptability within the optimization process, ensuring robust performance across the landscape.

These tailored parameters are essential because they harness the unique mechanisms of each algorithm to efficiently explore and optimize within the problem space. The parameters were chosen based on extensive preliminary trials and sensitivity analyses, which revealed that these configurations strike an optimal balance between solution quality and computational efficiency across various test scenarios. This approach ensures that the comparisons between algorithms are fair and focus on the strengths of the EVO algorithm due to its innovative strategy, rather than differences in parameter settings.

V.4. Simulation and Results

The proposed Energy Valley Optimizer (*EVO*) algorithm has been employed to minimize the total energy cost over a 24-year period for the ALG-AB-Hassi Sida 157 bus system. This approach accounts for variations in Distributed Generator and fixed Capacitor Bank outputs, as well as daily load fluctuations. It has been rigorously tested across three distinct scenarios:

- **Scenario 1**: EVO is utilized for the allocation of 13 CBs, aiming to minimize the objective function (*Obj1*) as defined in Equation (V.1). This scenario is compared against other optimization methods, including the Liver Cancer Algorithm (*LCA*) [133], the Walrus Optimization Algorithm (*WaOA*) [134], and the Zebra Optimization Algorithm (*ZOA*) [135].
- **Scenario 2**: In this scenario, EVO is applied for the optimal placement of 10 DGs, with the objective (*Obj2*) of reducing the total energy cost over a 24-year period as outlined in Equation (V.1). The results are compared with those obtained using LCA, ZOA, and WaOA.
- **Scenario 3**: This scenario integrates the allocation strategies of the first two scenarios, utilizing EVO to place 13 CBs and 10 DGs (*Objective 3*). Its goal is to reduce the total energy cost over a 24-year period, as specified in Equation (V.1), and benchmark its performance against the previously mentioned optimization techniques.

In each of these scenarios, the EVO algorithm is configured to run for 100 iterations with 30 search spaces. An important constraint set for the analysis is that the voltage at any node should not deviate by more than 10% from the nominal voltage.

The selection of 13 CBs and 10 DGs was influenced by a deep reservoir of experience and a methodical, data-driven analysis process. This configuration emerged as the most effective after extensive simulations and scenario testing, designed to strike an optimal balance between cost efficiency, system reliability, and performance under varying operational conditions. The analysis leveraged years of accumulated expertise in power distribution optimization, adopting a comprehensive approach that included evaluating system behavior under daily load fluctuations, the variability of DG outputs, and the strategic placement of CBs to ensure voltage stability across the network.

The ALG-AB-Hassi Sida 157 system, comprising 156 distribution sections and 157 nodes, is a comprehensive representation of a typical rural distribution network.

The technical specifications of branches and bus bars in the network are meticulously detailed in the referenced literature [136]. Each scenario is depicted with a nominal voltage of 12.66 *kV*, showcasing the network's configuration and the specific placements of DGs and CBs as determined by the EVO algorithm.

This study underscores the effectiveness of the EVO algorithm in optimizing the distribution network, highlighting its potential in enhancing both the technical and economic performance of power systems. The strategic selection of 13 CBs and 10 DGs, guided by the EVO algorithm, reflects our commitment to achieving the highest standards of efficiency and reliability in power distribution, backed by a profound base of expertise and rigorous analytical practices.

The ALG-AB-Hassi Sida 157-bus distribution network, chosen as the testing platform for the EVO algorithm, represents a particularly challenging case study due to its complex topology and significant load variability. This network is characterized by a high number of bus connections, which introduces intricate power flow dynamics and multiple potential points for voltage instability and power loss. Such complexity makes it an ideal candidate for testing advanced optimization algorithms like EVO. Additionally, the network's diverse load profiles, which include residential, commercial, and industrial demands, mimic real-world conditions that are crucial for assessing the practical applicability of optimization algorithms.

The ALG-AB-Hassi Sida network also features varied geographical and climatic conditions, impacting solar generation from photovoltaic systems and the efficiency of distributed generators, thereby providing a comprehensive environment to evaluate the adaptability and effectiveness of the EVO algorithm under dynamic and challenging operational scenarios.

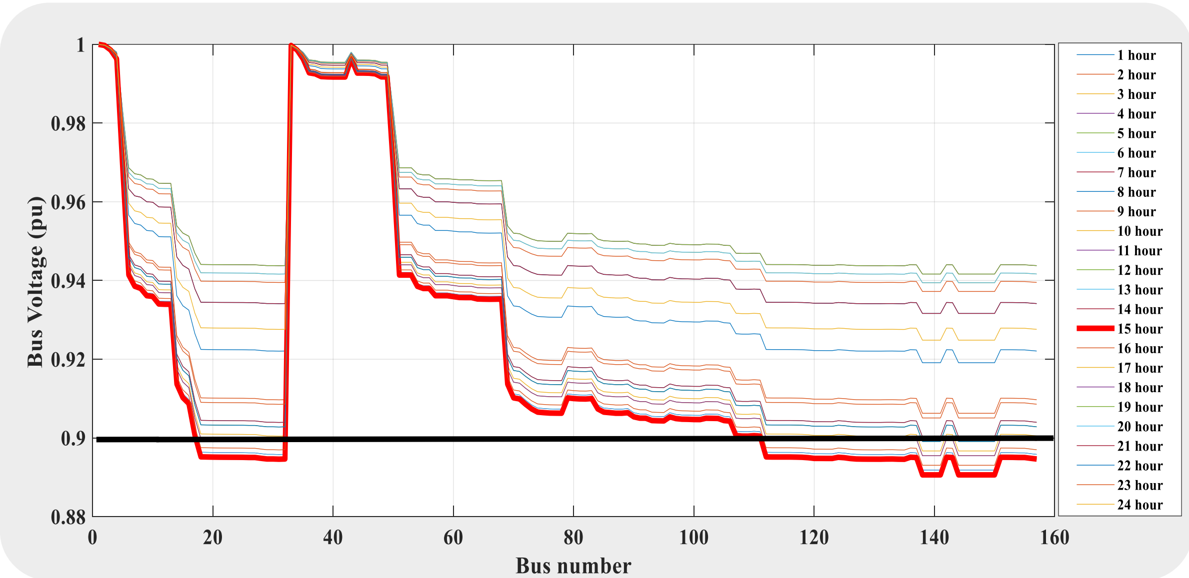

Figure V.2. Hourly voltage profile over 24 hours for the ALG-AB-Hassi Sida 157.

V.4.1. Scenario 1

In Scenario 1, Table V.1 from the ALG-AB-Hassi Sida 157 network provides a detailed comparative analysis of optimal capacitor bank (CB) placements and sizes over a 24-year period. By employing several advanced optimization methods, including LCA, WaOA, ZOA, and EVO, the study evaluates both technical and economic aspects. The CB placements and sizes, chosen for specific bus locations and capacities, are intended to optimize the network's operational performance. The assessment factors in a maximum capacitor size of 150 *kVAR* with an energy cost of *$0.06/kWh*. The results underscore an approach that balances operational efficiency with cost-effectiveness, culminating in a total expenditure of *$8.5123* million over two decades.

The EVO method proves particularly effective, achieving a minimum voltage of 0.902 pu and yielding a significant net savings of 22.08% by optimizing CBs at 12 bus locations. This approach not only surpasses traditional methods but also demonstrates considerable potential for operational and economic gains through comprehensive system optimization. The EVO's holistic consideration of various system elements establishes a new standard for long-term efficiency and cost reduction.

Additionally, Table V.1 highlights the financial advantages provided by each optimization algorithm. The EVO strategy significantly enhances technical metrics, such as voltage stability, while also delivering notable economic benefits. For example, it reduces energy loss costs to *$6.5098* million over 24 years, marking a substantial improvement over the baseline scenario. A thorough analysis of capacitor and overall costs underscores the value of targeted infrastructure investments to enhance operational and financial efficiency.

This comparative analysis extends beyond numerical data, offering insights into the strategic application of sophisticated optimization techniques in power systems. It advocates for an approach that emphasizes both technical optimization and fiscal prudence, promoting sustainable, long-term advancements in the sector.

Figures V.3 and V.4 further elucidate the findings from Table V.1 by illustrating the impact and effectiveness of these optimization techniques within the ALG-AB-Hassi Sida 157 network. Figure V.3 provides a visual depiction of the convergence characteristics of the optimization algorithms, highlighting the rapid and consistent performance of EVO and WaOA.

These methods show accelerated convergence to optimal capacitor placements and sizes, underscoring the EVO method's efficacy in achieving swift and dependable reductions in energy losses and annual costs. On the other hand, Figure V.4 likely shows the voltage profile over a 24-hour cycle, demonstrating the stability and efficiency gains enabled by the EVO method in comparison with other techniques. It illustrates how EVO can maintain higher, more stable voltage levels, enhancing both network reliability and performance.

Table V.1. Comparison Table for Optimal Locations and Sizes of Capacitor Banks in ALG-AB-Hassi Sida 157.

Comparison Criteria	**Base case**	**Techniques**							
		LCA		**WaOA**		**ZOA**		**EVO**	
		Bus of Cbs	**Size of Cbs**	**Bus of Cbs**	**Size of Cbs**	**Bus of Cbs**	**Size of Cbs**	**Bus of Cbs**	**Size of Cbs**
Optimal location and size of capacitors in kVAR	–	19 28 72 78 101 112 142 147 156	100 150 150 150 150 50 150 100 150	19 28 72 78 94 101 112 129 134 142 147 156	150 150 150 150 150 150 150 150 150 150 150 150	19 28 72 78 94 101 112 129 134 156	100 150 100 150 100 150 100 150 100 150	19 28 72 78 94 101 112 129 134 147 150 156	150 150 150 150 150 150 150 150 150 150 50 150
Net injected (kVAR)	-	1150		1800		1250		1700	
Minimum voltage (pu)	0.89	0.8960		0.90		0.8984		0.9029	
Cost of energy loss (M$ / 24 year)	8.512354	7.5181		6.5104		7.1637		6.5098	
Cost of energy loss (M$ / year)	0.354681	0.3132		0.2712		0.2984		0.2712	
Capital cost of CBs (M$/kvar)	-	0.000003		0.000003		0.000003		0.000003	
Capacitors cost (M$ / 24 year)	-	0.0828		0.1296		0.09		0.1224	
Capacitors cost (M$ / year)	-	0.003450		0.0054		0.003750		0.0051	
Total cost (M$ / 24 year)	8.512354	7.6009		6.64		7.253		6.6322	
Total cost (M$ / year)	0.354681	0.3166		0.2766		0.3021		0.2763	
Net savings (M$ / 24 year)	-	0.9114		1.8723		1.2593		1.88	
Net savings (M$ / year)	-	0.03808		0.0780		0.05258		0.07838	
Net savings (%) for 24 years	-	10.70		21.99		14.79		22.08	
Net savings (%) for 1 years	-	10.73		21.99		14.82		22.09	

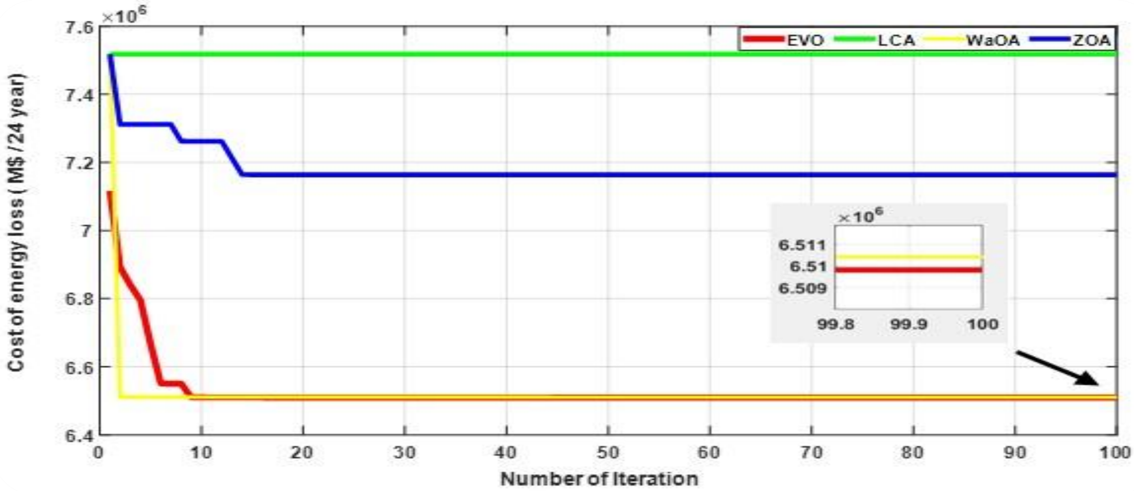

Figure V.3. Convergence characteristics of the optimization algorithms for ALG-AB-Hassi Sida 157.

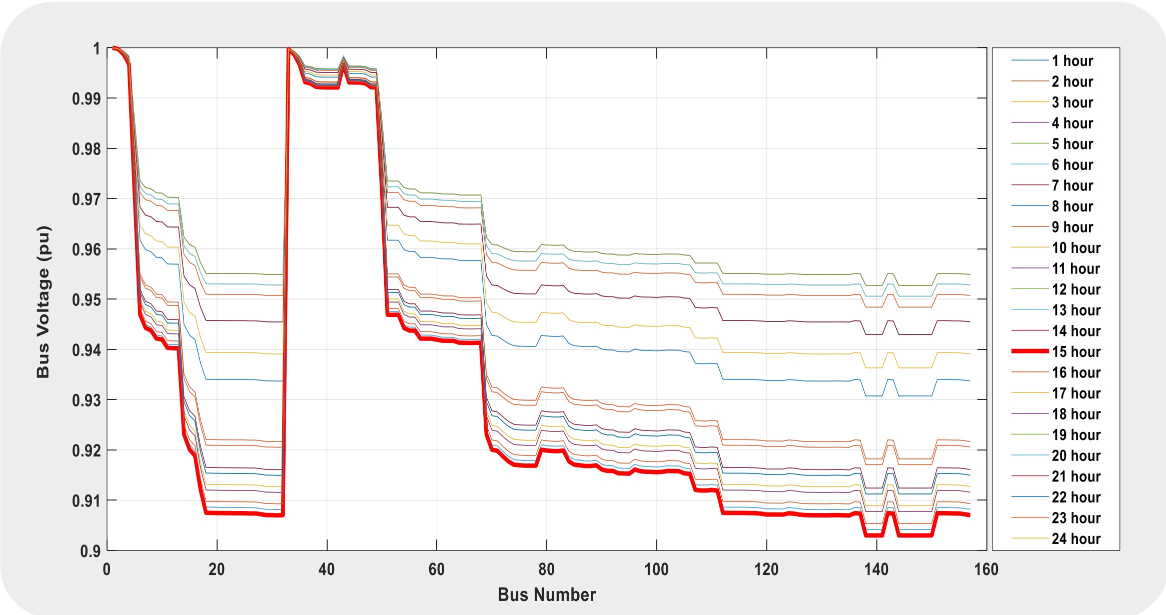

Figure V.4. Hourly Voltage Profile for the first Scenario Over a 24-Hour Period in the ALG-AB-Hassi Sida 157 Network.

V.4.2. Scenario 2

In Scenario 2, Table V.2 from the ALG-AB-Hassi Sida 157 network analysis offers a comprehensive comparison of optimal locations and sizes for distributed generators (DGs) using several optimization methods, including LCA, WaOA, ZOA, and EVO. This examination focuses on essential operational factors, with DG capacities capped at 750 kW and an energy cost of *\$0.06/kWh*. The table showcases a considerable total cost reduction over a 24-year period, illustrating the significant impact of these optimization approaches.

The EVO method distinguishes itself with outstanding performance, increasing the minimum voltage from 0.89 pu to 0.934 pu. This result highlights the method's effectiveness in boosting network efficiency and stability. Over the 24-year span, EVO achieves the lowest total cost of *$2.4232* million and the highest net savings rate of 60.95%. The table reflects how each optimization method selects different optimal bus locations and sizes for DGs, with EVO pinpointing ten specific bus locations for deployment, demonstrating a strategic approach to optimization.

Figures V.5 and V.6 provide further insight into the data in Table V.2, visually illustrating the performance and effects of the optimization methods on the ALG-AB-Hassi Sida 157 network. Figure V.5 reveals the convergence characteristics of the EVO method, quickly and reliably identifying optimal DG placements and capacities, achieving significant reductions in energy losses and total energy costs over 24 years. This visualization underscores EVO's superiority over other methods, which may exhibit slower or less consistent convergence.

Additionally, Figure V.6 likely shows the hourly voltage profile over a 24-hour period, underscoring the improvements in voltage stability and reliability made possible through EVO optimization. This figure offers a detailed view of voltage fluctuations throughout the day under various optimization techniques, highlighting the enhanced network performance achieved with the EVO method. By incorporating specific parameter values and financial metrics, the analysis provides a thorough understanding of both economic and technical impacts associated with DG placement within the distribution network, emphasizing the careful balance between optimizing for efficiency and managing costs.

Table V.2. Comparison Table for Optimal Locations and Sizes of Distributed Generation in ALG-AB-Hassi Sida 157.

Comparison Criteria	Base case	Techniques							
		LCA		WaOA		ZOA		EVO	
		Bus of DGs	Size of DGs	Bus of DGs	Size of DGs	Bus of DGs	Size of DGs	Bus of DGs	Size of DGs
Optimal location and size of DGs in kW	–	17	750	18	750	29	750	13	750
		22	750	20	750	64	750	23	750
		30	750	23	750	70	750	30	750
		32	750	26	750	79	750	70	750
		78	750	29	750	112	750	108	750
		115	750	61	750	113	750	113	750
		130	750	70	750	124	750	118	750
		137	750	84	750	125	750	121	750
		142	750	119	750	127	750	128	750
		151	750	128	750	136	750	151	750
Minimum voltage (pu)	0.89	0.933		0.93		0.933		0.934	
Cost of energy loss (M$ / 24 year)	8.512354	2.4331		2.4242		2.4237		2.4232	
Cost of energy loss (M$ / year)	0.354681	0.1013		0.1010		0.1009		0.100	
Capital cost of DGs (M$/kvar)	-	0.000005		0.000005		0.000005		0.000005	
DGs cost (M$ / 24 year)	-	0.9		0.9		0.9		0.9	
DGs cost (M$ / year)	-	0.037500		0.037500		0.037500		0.037500	
Total cost (M$ / 24 year)	8.512354	3.333		3.3242		3.3237		3.3232	
Total cost (M$ / year)	0.354681	0.1388		0.1385		0.1384		0.1375	
Net savings (M$ / 24 year)	-	5.1793		5.1881		5.1886		5.1891	
Net savings (M$ / year)	-	0.21588		0.2161		0.2162		0.2171	
Net savings (%) for 24 years	-	60.84		60.94		60.95		60.95	
Net savings (%) for 1 years	-	60.86		60.92		60.97		61.23	

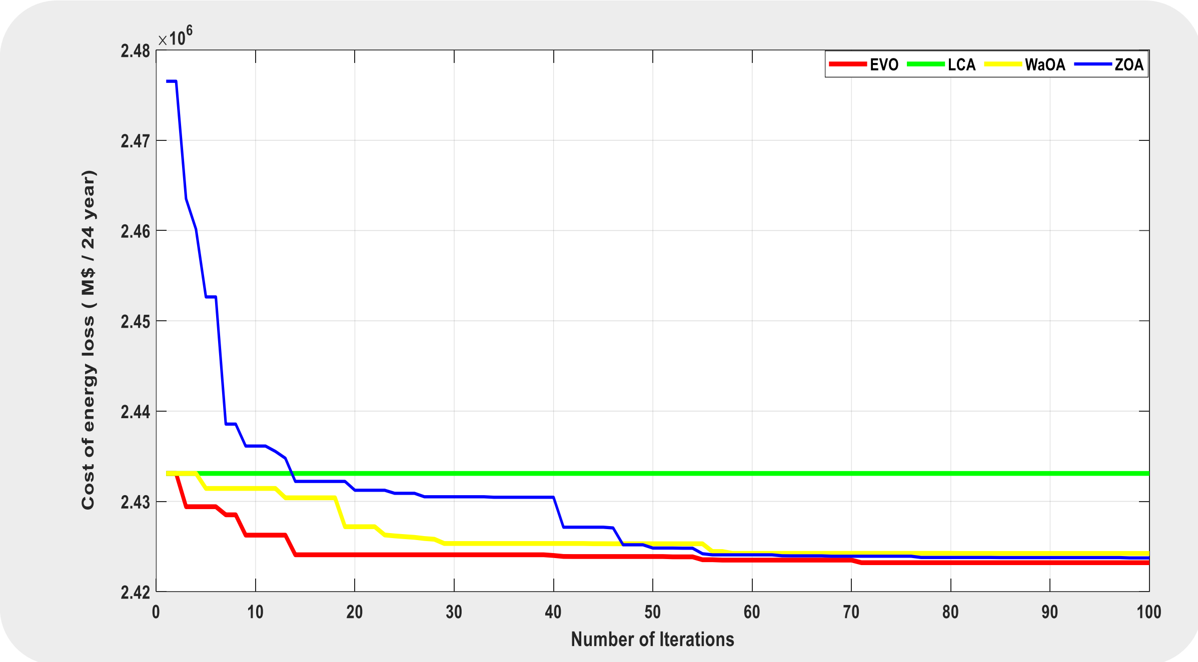

Figure V.5. Convergence characteristics of the optimization algorithms for ALG-AB-Hassi Sida 157.

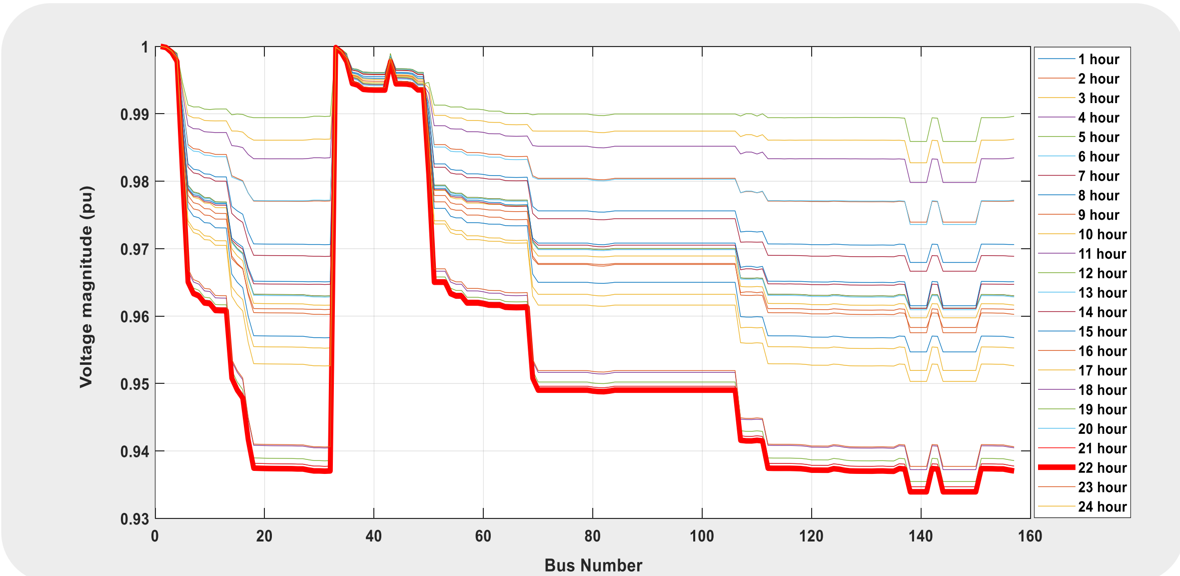

Figure V.6. Hourly Voltage Profile for the second Scenario Over a 24-Hour Period in the ALG-AB-Hassi Sida 157 Network.

V.4.3. Scenario 3

In Scenario 3, Table V.3 of the ALG-AB-Hassi Sida 157 network study provides an in-depth evaluation of the optimal placements and sizes for distributed generators (DGs) and capacitor banks (CBs), using several optimization methods, such as LCA, WaOA, ZOA, and EVO. The table carefully outlines the operational parameters, setting maximum CB capacities at 150 *kVAR* and DGs at 750 *kW*, within an energy cost framework (C_{energy}) of *$0.06/kWh*. It also discloses the total energy expenditure over a 24-year span, totaling *$8.512354 million*.

The EVO method stands out as a noteworthy advancement, raising the minimum voltage from 0.87 pu to 0.94 pu. This remarkable improvement demonstrates EVO's exceptional capability in enhancing both network stability and efficiency, achieving the lowest energy cost over the 24-year period at *$1.9080* million, with the highest net savings rate of 65.53%. The table includes specific bus locations and sizes for DGs and CBs identified by each optimization approach, reflecting a tailored and well-thought-out optimization strategy.

Figures V.7 and V.8 supplement the data in Table V.3 by providing a visual analysis of how the optimization techniques perform and affect the ALG-AB-Hassi Sida 157 network. Figure V.7 illustrates the convergence dynamics of the EVO method, quickly and accurately determining optimal configurations for both DGs and CBs. This leads to a substantial reduction in both energy losses and total costs over the 24-year period, highlighting EVO's superior performance over other methods, which may have slower or less predictable convergence patterns.

Meanwhile, Figure V.8 likely shows the hourly voltage profile across a 24-hour period, underscoring improvements in voltage stability and reliability achieved through EVO optimization. This figure offers a detailed look at daily voltage fluctuations under different optimization techniques, showcasing EVO’s ability to sustain enhanced network performance. By including detailed parameter values and financial metrics, this analysis provides a comprehensive understanding of the economic and technical impacts of jointly deploying DGs and CBs in the network, illustrating a sophisticated balance between optimizing efficiency and managing costs.

Table V.3. Comparison Table for Optimal Locations and Sizes of Distributed Generation and Capacitor Banks in ALG-AB-Hassi Sida 157.

Comparison Criteria	Base case	Techniques															
		LCA				WaOA				ZOA				EVO			
		Bus of CBs	**Size of CBs**	**Bus of DGs**	**Size of DGs**	**Bus of CBs**	**Size of CBs**	**Bus of DGs**	**Size of DGs**	**Bus of CBs**	**Size of CBs**	**Bus of DGs**	**Size of DGs**	**Bus of CBs**	**Size of CBs**	**Bus of DGs**	**Size of DGs**
Optimal location and size of capacitors in kVAR and DGs in kW	-	19 28 78 112 134 142 150 156	50 50 100 50 50 150 50 50	11 24 65 75 91 118 119 125 151 156	750 750 750 750 750 750 750 750 750 750	19 28 78 112 129 134 142 147 150 156	150 150 100 150 100 150 150 150 150 150	12 21 57 110 112 121 128 142 147 151	750 750 750 750 750 750 750 750 750 750	19 28 72 112 129 134 142 147 150 156	100 100 150 50 150 100 100 50 50 150	55 61 72 83 112 116 118 119 122 133	750 750 750 750 750 750 750 750 750 750	19 28 72 94 101 112 129 134 142 147 150 156	150 150 150 150 100 150 150 150 150 150 150 150	57 94 110 113 125 126 130 137 142 155	750 750 750 750 750 750 750 750 750 750
Net injected (kVAR)	-	550				1400				1000				1750			
Minimum voltage (pu)	0.89	0.9355				0.9393				0.9381				0.9399			
Cost of energy loss (M$ / 24 year)	8.512354	2.2995				1.9495				2.0651				1.9080			
Cost of energy loss (M$ / year)	0.886703	0.09581				0.081				0.086				0.0795			
Capital cost of Capacitors (M$/kvar)	-	0.000003				0.000003				0.000003				0.000003			
Capacitors cost (M$/ 24 year)	-	0.039600				0.100				0.072				0.126			
Capacitors cost (M$/year)	-	0.001650				0.004200				0.003				0.005250			
Capital cost of DGs (M$/kvar)	-	0.000005				0.000005				0.000005				0.000005			
DGs cost (M$/ 24 year)	-	0.9				0.9				0.9				0.9			
DGs cost (M$/year)	-	0.037500				0.037500				0.037500				0.037500			
Total cost (M$/ 24 year)	8.512354	3.2391				2.9495				3.0371				2.934			
Total cost (M$/year)	0.886703	0.13496				0.1229				0.1265				0.12225			
Net savings (M$/ 24 year)	-	5.2732				5.5628				5.4752				5.5783			
Net savings (M$/ year)	-	0.7517				0.7640				0.7602				0.7644			
Net savings (%) for 24 year	-	61.94				65.35				64.32				65.53			
Net savings (%) for 1 year	-	84.77				86.16				85.73				86.20			

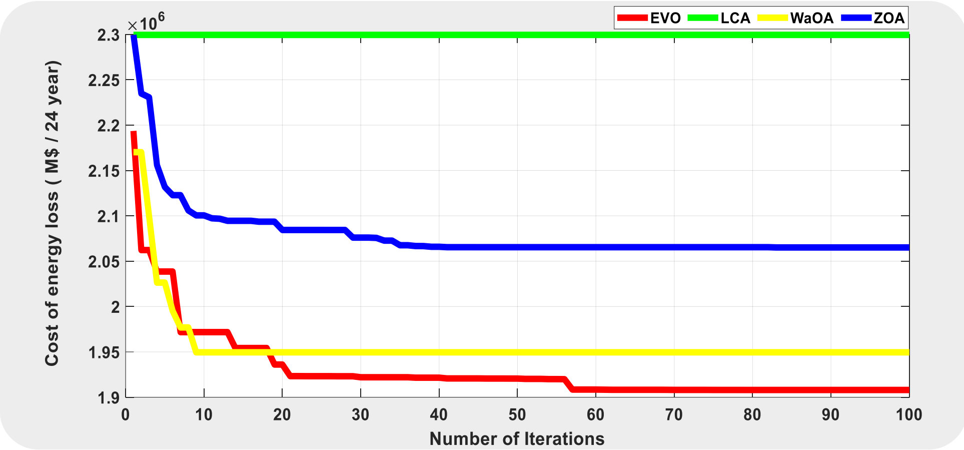

Figure V.7. Convergence characteristics of the optimization algorithms for ALG-AB-Hassi Sida 157.

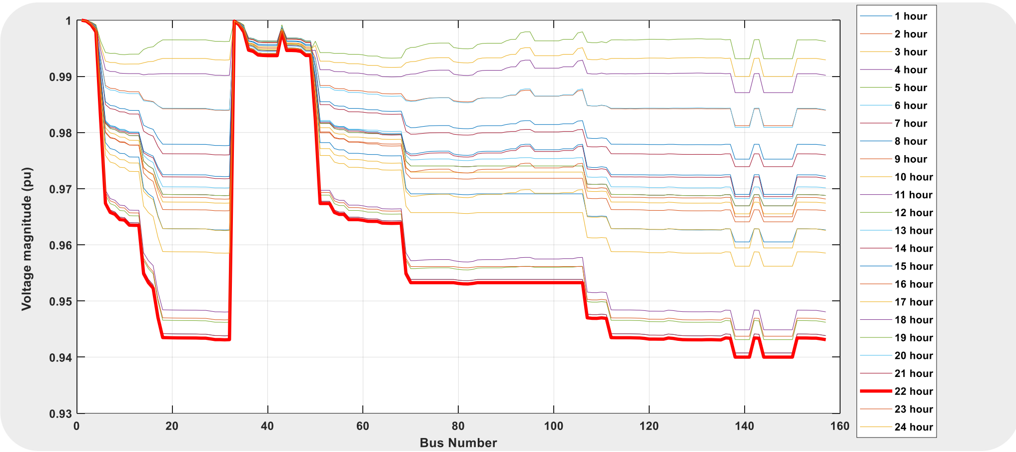

Figure V.8. Hourly Voltage Profile for the third Scenario Over a 24-Hour Period in the ALG-AB-Hassi Sida 157 Network.

V.5. Interpretations Results

In our simulations, stability is a key metric, particularly given the stochastic nature of algorithms like EVO, LCA, WaOA, and ZOA. To mitigate random outcomes and ensure reliable results, each algorithm was run multiple times (*30 trials*) under identical conditions. We analyzed the results for variance and consistency to ensure that the conclusions drawn were based on not only optimal outcomes but also repeatable ones.

The Energy Valley Optimizer (*EVO*) exhibited remarkable stability across trials, with minimal variance in the results, indicating its low susceptibility to random fluctuations. This stability is largely due to its adaptive mutation mechanism, which effectively balances exploration and exploitation, minimizing the risk of getting stuck in local optima or drifting into random solutions. The other algorithms—LCA, WaOA, and ZOA—were also assessed for performance consistency. While all algorithms demonstrated acceptable levels of stability, some variations were observed, which are further detailed in the analysis section.

Figure V.9, from the ALG-AB-Hassi Sida 157 systems study covering Scenarios 1 to 3, graphically illustrates the percentage reduction in net savings for each scenario. The data shows a clear trend: increasing the number of DGs and CBs leads to greater reductions in net savings across all scenarios. In Scenario 1, the EVO technique achieves the highest net savings reduction, outperforming LCA, WaOA, and ZOA. This pattern continues in Scenario 2, where EVO again leads with the highest net savings percentages. The trend persists in Scenario 3, with EVO maintaining its superior performance, highlighting its effectiveness in optimizing the network for cost savings. This visual representation in Figure V.9 further underscores the EVO method's dominance and the positive impact of integrating more DGs and CBs into the network.

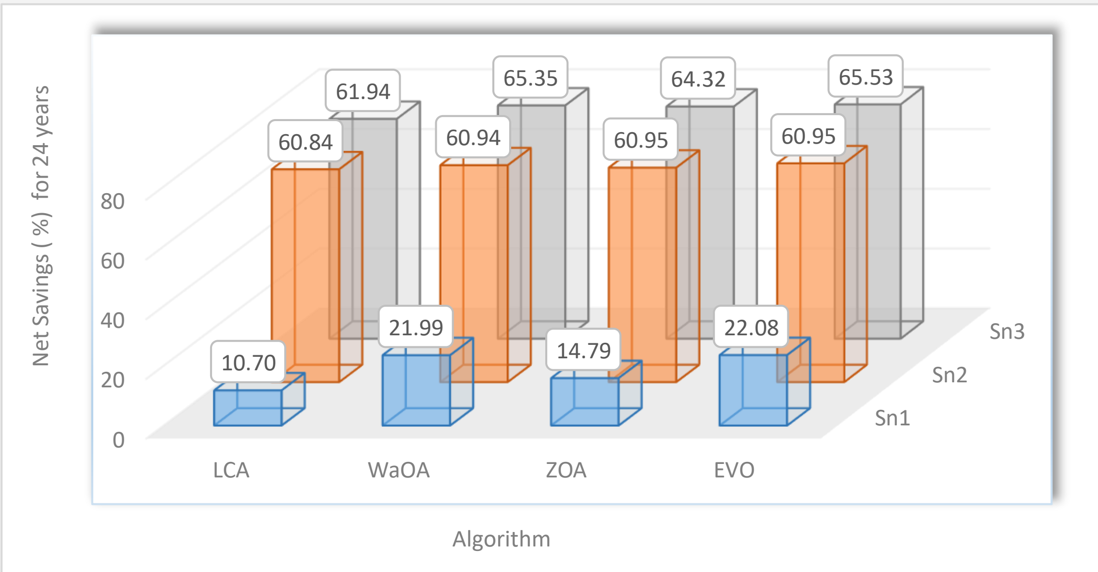

Figure V.9. Net Savings (%) for 24 Years Across 1, 2, and 3 Scenarios in ALG-AB-Hassi Sida,157.

The EVO algorithm presented in this study offers a notable improvement by employing a distinctive method to systematically explore "energy valleys"—areas in the search space that are more likely to hold optimal solutions. This strategy enhances EVO's ability to bypass local optima and adapt more effectively to the dynamic and varying conditions typical of electrical distribution systems. Moreover, EVO's adaptive mechanisms for exploration and exploitation reduce the need for extensive parameter adjustments, making it a more efficient and practical tool for optimizing the placement and sizing of DGs and CBs. These qualities make EVO especially suitable for handling fast-changing operational environments, where both adaptability and efficiency are essential.

V.6. Conclusion

This chapter introduced the Energy Valley Optimizer (*EVO*) as an innovative solution for optimizing the allocation of Distributed Generation (*DG*) units and Capacitor Banks (*CBs*) within electrical distribution networks. The primary goal of EVO is to minimize both technical and economic inefficiencies. To validate its effectiveness, EVO was tested on the ALG-AB-Hassi Sida 157-bus system in the Algerian distribution network, offering a comprehensive platform for evaluation under three distinct operational scenarios, accounting for hourly load variations over a 24-hour period.

Comparative analysis with other optimization techniques revealed that EVO outperforms in optimizing DG and CB allocation. EVO demonstrated a 65.53% reduction in total energy costs over a 24-year period, surpassing other algorithms by up to 10% in cost savings. Furthermore, EVO consistently reduced energy losses, achieving reductions of up to 50% compared to strategies utilizing only DGs or CBs independently. Its adaptive mutation mechanism enhances both the accuracy and speed of optimization, making it a highly efficient tool for solving complex network challenges.

The simultaneous allocation of DGs and CBs delivered the most significant benefits, leading to substantial reductions in both energy losses and operational costs. This combined approach further highlighted EVO's superiority in addressing the multifaceted challenges of distribution network optimization.

GENERAL CONCLUSION AND PERSPECTIVES

General Conclusion and Perspectives

Due to the continuous increase in energy consumption, distribution networks have garnered significant attention from an optimization perspective. Distributed generation (DG) has emerged as a crucial solution for minimizing energy losses, reducing voltage drops, and lowering energy costs over an extended period. In this context, our work addresses the challenge of optimal planning and integration of DG based on renewable energy sources within radial distribution networks of varying sizes and complexities. This research focuses on optimizing multiple technical and economic parameters using both single-objective and multi-objective functions, and employs various metaheuristic algorithms.

We have identified the optimal locations and sizes for photovoltaic systems and capacitor banks to integrate them effectively into IEEE standard distribution networks and the ALG-AB-Hassi Sida 157-bus distribution network. This was achieved by studying the impact of these sources on the technical and economic parameters of the networks, including active power losses, voltage, and the cost of losses.

In the introduction, we presented a comprehensive literature review on distributed generation based on renewable energies. This review covered the definition and classification of various renewable energy sources, including solar, wind, and other emerging technologies. We discussed the advantages and challenges associated with integrating these sources into existing power systems. Additionally, the impact of renewable distributed generation on distribution networks was analyzed, focusing on how these sources affect network stability, reliability, and efficiency. This overview provided a foundation for understanding the potential benefits and limitations of incorporating renewable energy into electrical grids, setting the stage for our detailed analysis and optimization efforts.

Subsequently, we applied the Backward/Forward Sweep (BFS) method to solve power flow equations in the IEEE 33-bus, IEEE 69-bus, and ALG-AB-Hassi Sida 157-bus distribution networks using a topology-based approach. By classifying bus types and lines, the BFS method iteratively updates currents and voltages until convergence, ensuring accurate power flow calculations. In the 33-bus and 69-bus systems, BFS effectively minimized power losses and maintained voltage stability, even under complex load variations. In the larger 157-bus Algerian network, the method demonstrated its practical capability to manage extensive radial configurations, enhancing voltage stability and reducing energy losses. These consistent results validate BFS as a robust tool for optimizing power flow in radial distribution networks.

Following this, we examined the foundational concepts of optimization, distinguishing between exact optimization methods and metaheuristic approaches. We explored the core principles of metaheuristics, including their validation through test functions, and highlighted their application in real-world scenarios. Special emphasis was placed on the role of metaheuristics in integrating renewable energy into distribution networks, demonstrating their effectiveness in optimizing energy distribution, lowering costs, and enhancing grid stability.

We also addressed the challenges and limitations of these techniques, such as computational complexity and scalability issues, underscoring the need for ongoing research and refinement.

We defined and formulated the problems related to the objective functions and constraints of distribution networks and Distributed Generation (DG), focusing on critical aspects such as system performance, energy losses, voltage stability, and cost-effectiveness. An in-depth presentation and discussion of the algorithms employed were also provided, highlighting their suitability for addressing complex optimization challenges in DG planning. The results obtained in this study were thoroughly analyzed and discussed in three parts, demonstrating the effectiveness of the proposed methods in enhancing grid performance, optimizing DG placement, and tackling the unique challenges posed by various network configurations.

In the first part of this work, we presented the development and application of the Efficient Metaheuristic BitTorrent (EM-BT) optimization algorithm, designed to optimize the placement and sizing of photovoltaic renewable energy sources (PVRES) and capacitor banks (CB) in electric distribution systems. The primary goal was to minimize energy losses and improve voltage profiles across the IEEE 33, IEEE 69-node networks, and the ALG-AB-Hassi Sida 157-bus system, considering daily load variations, solar irradiance, and temperature fluctuations. EM-BT demonstrated superior performance compared to established optimization techniques such as Particle Swarm Optimization (PSO), Grey Wolf Optimizer (GWO), and Whale Optimization Algorithm (WOA). The EM-BT algorithm achieved significant energy loss reductions—49.06% for the IEEE 33 system, 56.8% for IEEE 69, and 57.96% for the ALG-AB-Hassi Sida 157-bus system—while substantially improving the voltage profiles of the weakest buses, thereby enhancing system stability. EM-BT's capability to factor in real-world conditions such as temperature and irradiance makes it an effective and reliable tool for optimizing distributed generation and CB allocations in distribution networks.

In the second part of this work, we present a comprehensive multi-objective optimization framework for optimizing the placement and sizing of photovoltaic (PV) systems and capacitor banks (CBs) in electrical distribution networks, taking into account environmental factors such as irradiance, temperature fluctuations, and load variations. By applying the Multi-Objective Multi-Verse Optimization (MOMVO) algorithm to the IEEE 33-bus and IEEE 69-bus networks, significant technical and economic improvements were achieved.

For the **IEEE 33-bus system**, the MOMVO algorithm resulted in a **47.58% reduction in daily energy loss**, reducing it from 3831.3 kWh/day to 2008.1 kWh/day. Voltage profile stability was also enhanced, with bus voltages improving from **0.89 pu to 0.94 pu**. In terms of cost, the **annual cost of energy losses** decreased by **36.97%**, from $4.5308 million to $2.8556 million, while the cost of power supplied by distributed generators was reduced to **$39,146/year**.

For the **IEEE 69-bus system**, the MOMVO algorithm delivered even greater improvements, with a **50.15% reduction in daily energy loss**, lowering it from 4085.7 kWh/day to 2036.4 kWh/day. Voltage profiles saw a marked improvement, increasing from **0.89 pu to 0.93 pu**, and the **annual cost of energy losses** was reduced by **47.59%**, from $4.8317 million to $2.5320 million. The cost of power supplied by distributed generators was further reduced to **$36,002/year**.

These results underscore the **MOMVO algorithm's superiority** over other optimization techniques, including MOJS, MOFPA, and MOLA, in minimizing energy losses, improving voltage stability, and reducing operational costs. The algorithm's ability to account for real-world environmental conditions, such as temperature and irradiance, makes it a robust and efficient tool for optimizing power distribution networks and integrating renewable energy sources. This research paves the way for future advancements in the sustainable and efficient operation of power systems, contributing to greater reliability, cost savings, and environmental benefits.

In the third part of this work, we introduce the Energy Valley Optimizer (EVO) algorithm for the optimal allocation of Capacitor Banks (CBs) and Distributed Generation (DG) units in the 157-node ALG-AB-Hassi Sida distribution network. The EVO algorithm was compared with other advanced metaheuristic techniques such as the Liver Cancer Algorithm (LCA), the Walrus Optimization Algorithm (WaOA), and the Zebra Optimization Algorithm (ZOA) in three different contexts: the allocation of CBs, DGs, and their combined deployment. In the first context, EVO achieved a 22.08% reduction in total costs over a 24-year period. In the second, EVO demonstrated a 60.95% reduction in energy losses, with a total cost of $2.4232 million, offering the highest net savings among the compared methods. The third context, which combined CBs and DGs, provided the most significant benefits, with EVO achieving a maximum net savings of 65.53%, reducing total costs to $1.9080 million over 24 years. These results highlight EVO's superior performance in minimizing energy losses, improving voltage stability, and reducing overall costs, making it a robust solution for optimizing power distribution systems.

In conclusion, the results obtained underscore the importance of using metaheuristic algorithms for the planning and integration of renewable energies into distribution networks. This thesis serves as a valuable resource to help electricity distribution companies integrate renewable energy sources of various sizes into their networks more effectively and reliably. Additionally, we offer recommendations for reducing energy losses, improving voltage stability, and minimizing energy costs over a 24-year period within the Algerian distribution network.

Perspectives

In the context of this work, future research should focus on studying the following issues:

Integration of Advanced Forecasting Models: Future studies could focus on integrating advanced forecasting techniques, such as machine learning and artificial intelligence, to predict energy demand, generation from renewable sources, and electric vehicle charging patterns. Improved forecasting accuracy can significantly enhance the performance of optimization algorithms by allowing more proactive management of network resources.

Impact of Distributed Energy Resources (DERs): Research could investigate the optimization of distributed energy resources, such as rooftop solar panels, small-scale wind turbines, and battery storage systems, within distribution networks. This includes studying their impact on voltage regulation, power quality, and grid stability, as well as how to best integrate these resources to achieve optimal network performance.

Cybersecurity and Resilience of Smart Grids: With the increasing digitization of electrical networks, cybersecurity is becoming a critical issue. Future research could explore how optimization algorithms can incorporate security constraints to protect the grid from cyber-attacks and ensure resilience against both physical and cyber threats.

Optimization in the Presence of Demand Response Programs: Demand response programs, where consumers adjust their power usage during peak times in response to price signals, could be incorporated into optimization models. This approach would allow the exploration of how consumer behavior can be leveraged to improve network performance and reduce operational costs.

Decentralized Control and Peer-to-Peer Energy Trading: Exploring decentralized optimization techniques that enable peer-to-peer energy trading between prosumers (producers and consumers) could revolutionize the way energy is managed at the local level. Future research could focus on developing decentralized algorithms that facilitate efficient and fair energy exchanges within microgrids.

Incorporation of Advanced Grid-Forming Inverters: Advanced grid-forming inverters, which can autonomously maintain voltage and frequency in microgrids, could be studied as part of future optimization efforts. These inverters are crucial for integrating high levels of renewable energy and enhancing the stability of isolated or weak grid segments.

Life Cycle Assessment (LCA) and Environmental Impact Analysis: Including a comprehensive life cycle assessment of different energy technologies and their environmental impacts could be an interesting direction. Research could explore how to balance technical and economic optimization goals with environmental sustainability, taking into account the entire lifecycle of energy assets.

Adaptive Optimization Techniques: Developing adaptive optimization methods that can dynamically adjust to changing network conditions, such as fluctuating renewable generation or sudden changes in load demand, would improve the real-time operational efficiency of power systems.

Integration of Electric Mobility as a Grid Resource: Beyond studying electric vehicle (EV) charging impacts, future research could explore how EVs can be used as active grid resources through vehicle-to-grid (V2G) technologies. This could involve studying optimal strategies for using EVs as distributed storage units to support grid stability during peak demand.

Economic Impacts of Regulatory Changes: Investigating the economic implications of future regulatory changes, such as carbon pricing or incentives for renewable integration, would provide valuable insights. Research could focus on how optimization models can adapt to evolving policy environments and drive economically viable solutions.

LIST OF REFERENCES

List of References

1. João A. Peças Lopes, "Integration of dispersed generation on distribution networks impact studies," IEEE Power Engineering Society Winter Meeting, vol. 1, pp. 323-328, 2002.

2. Boris Berseneff, "Voltage control in future distribution networks," Ph.D. dissertation, University of Grenoble, December 2010.

3. Olivier Richardot, "Coordinated voltage control in distribution networks using decentralized generation," Ph.D. dissertation, INP Grenoble, 2006.

4. Wendy Carolina Briceño Vicente, "Modeling distribution networks under uncertainty," PhD dissertation, University of Grenoble, September 20, 2012.

5. Houda Mezouar, Abdellatif El Afia, and Raddouane Chiheb, "A new concept of intelligence in electric power management," in Proceedings of IEEE Engineering and Technology Conference, 2016, pp. 28-35. DOI: 10.1109/EITech.2016.7519596.

6. Boris Berseneff, "Voltage control in future distribution networks," Ph.D. dissertation, University of Grenoble, 2010.

7. Sathsara Abeysinghe, Jianzhong Wu, Mahesh Sooriyabandara, Muditha Abeysekera, Tao Xu, and Chengshan Wang, "Topological properties of medium voltage electricity distribution networks," Applied Energy, vol. 210, 2017. DOI: 10.1016/j.apenergy.2017.06.113.

8. Ibrahim Ibrahim and M. J. Hossain, "Low voltage distribution networks modeling and unbalanced (optimal) power flow: A comprehensive review," IEEE Access, vol. 9, pp. 143026-143084, 2021. DOI: 10.1109/ACCESS.2021.3120803.

9. Olivier Richardot, "Coordinated voltage control in distribution networks using decentralized generation," Ph.D. dissertation, National Polytechnic Institute of Grenoble (INPG), 2006.

10. Fouad Kouadra, "Studies of rapid voltage variations for the connection of decentralized generation in a medium voltage network," Master's thesis, University of Frères Mentouri, Constantine, 2009.

11. Hongjian Liang, Ajay K. Tamang, Weihua Zhuang, and Xuemin Shen, "Stochastic information management in smart grid," IEEE Communications Surveys and Tutorials, vol. 16, no. 3, pp. 1746–1770, 2014.

12. Ghislain Guérrad, "Optimization of energy distribution in smart grids," Ph.D. dissertation, University of Versailles, 2014.

13. Etienne Duverger, "Smart electrical grid for new uses," Ph.D. dissertation, University of Perpignan Via Domitia, 2019.

14. Hassan Farhangi, "The path of the smart grid," IEEE Power and Energy Magazine, vol. 8, no. 1, pp. 18–28, 2010.

15. Xi Fang, Satyajayant Misra, Guoliang Xue, and Dejun Yang, "Smart grid – The new and improved power grid: A survey,"IEEE Communications Surveys and Tutorials, vol. 14, no. 4, pp. 944–980, 2012.

16. Mohamed E. El-Hawary, "The smart grid – State-of-the-art and future trends," Electric Power Components and Systems, vol. 42, no. 3-4, pp. 239–250, 2014.

17. Kazi Mahmud, Bahram Khan, Jagadeesh Ravishankar, Amir Ahmadi, and Pierluigi Siano, "An internet of energy framework with distributed energy resources, prosumers and small-scale virtual power plants: An overview," Renewable and Sustainable Energy Reviews, vol. 127, 109840, 2020.

18. Benoît Mercier, "Control of decentralized generation and unconventional loads in the context of the smart grid and real-time hybrid simulation," Ph.D. dissertation, University of Grenoble, 2015.

19. Wendy Carolina Briceño Vicente, "Modeling distribution networks under uncertainty," Ph.D. dissertation, University of Grenoble, 2012.

20. Thomas Ackermann, Göran Andersson, and Lennart Soder, "Distributed generation: A definition," Electric Power Systems Research, vol. 57, pp. 195–204, 2001.

21. Marc Dussart, "Problems encountered with connecting decentralized generating plants to the distribution networks," 14th International Conference and Exhibition on Electricity Distribution, Birmingham, UK, Conference Publication No. 438, IEE, 1997.

22. J. G. Slootweg and W. L. Kling, "Impacts of distributed generation on power system transient stability," IEEE Power Engineering Society Summer Meeting, vol. 2, pp. 862–867, 2002.

23. João A. Peças Lopes, "Integration of dispersed generation on distribution networks impact studies," IEEE Power Engineering Society Winter Meeting, vol. 1, pp. 323–328, 2000.

24. Rodrigo Palma-Behnke, Juan L. Cerda A, Luis S. Vargas, and Alejandro Jofré, "A distribution company energy acquisition market model with integration of distributed generation and load curtailment options," IEEE Transactions on Power Systems, vol. 20, no. 4, pp. 1718–1727, 2005.

25. Yvan Pankow, "Study of the integration of decentralized generation in a low voltage network: Application to the photovoltaic generator," Ph.D. dissertation, University of Lille, 2004.

26. Robert A. Mohr, Rodrigo Moreno, and Hugh Rudnick, "Insertion of distributed generation into rural feeders," CIGRE/IEEE PES Joint Symposium Integration of Wide-Scale Renewable Resources into the Power Delivery System, Calgary, AB, pp. 1–10, 2009.

27. Boris Berseneff, "Voltage control in future distribution networks," Ph.D. dissertation, University of Grenoble, 2010.

28. K. Balamurugan, D. Srinivasan, and T. Reindl, "Impact of distributed generation on power distribution systems," Energy Procedia, vol. 25, pp. 93–100, 2012.

29. V. Vita, Teyfik Alimardan, and Lazaros Ekonomou, "The impact of distributed generation in the distribution networks' voltage profile and energy losses," IEEE European Modelling Symposium (EMS), Madrid, Spain, pp. 260–265, 2015.

30. T. T. H. Phan, "Influences of decentralized generation on the management of critical power network infrastructure," Ph.D. dissertation, University of Grenoble, 2006.

31. Mahmood Meskin, Aleksandar Domijan, and Igor Grinberg, "Impact of distributed generation on the protection systems of distribution networks: Analysis and remedies – review paper," IET Generation, Transmission & Distribution, vol. 14, no. 24, pp. 5944-5960, 2020. DOI: 10.1049/iet-gtd.2019.1652.

32. Esther Maria, Manuel Isabel, and Santiago Pindado, "Effect of distributed photovoltaic generation on short-circuit currents and fault detection in distribution networks: A practical case study," Applied Sciences, vol. 11, no. 1, p. 405, 2020. DOI: 10.3390/app11010405.

33. Sean Freeman and Elliot Agar, "The impact of energy storage on the reliability of wind and solar power in New England," Heliyon, vol. 10, no. 6, 2024. DOI: 10.1016/j.heliyon.2024.e27652.

34. Balázs M. Fekete, Miklós Bacskó, Jian Zhang, and Ming Chen, "Storage requirements to mitigate intermittent renewable energy sources: Analysis for the US Northeast," Frontiers in Environmental Science, vol. 11, 1076830, 2023. DOI: 10.3389/fenvs.2023.1076830.

35. M. Farghali, Ahmed I. Osman, Zhenyu Chen, et al., "Social, environmental, and economic consequences of integrating renewable energies in the electricity sector: A review," Environmental Chemistry Letters, vol. 21, pp. 1381–1418, 2023. DOI: 10.1007/s10311-023-01587-1.

36. Roman Ufa, Yulia Malkova, Vadim Rudnik, Mikhail Andreev, and Vladimir Borisov, "A review on distributed generation impacts on electric power system," International Journal of Hydrogen Energy, vol. 47, no. 47, pp. 20347-20361, 2022. DOI: 10.1016/j.ijhydene.2022.04.142.

37. Wadim Strielkowski, Luboš Civín, Ekaterina Tarkhanova, Monika Tvaronavičienė, and Yaroslav Petrenko, "Renewable energy in the sustainable development of the electrical power sector: A review," Energies, vol. 14, no. 24, p. 8240, 2020. DOI: 10.3390/en14248240.

38. Ting Ma and Hui Shi, "A distributed control scheme using SiC-based low voltage ride-through compensator for wind turbine generators," Micromachines, vol. 13, no. 1, 2021. DOI: 10.3390/mi13010039.

39. Rania Kamel, "Distributed generators as reactive power providers and their impacts on standalone micro-grid performance during both symmetrical and unsymmetrical faults," Renewable Energy Focus, vol. 35, 2020. DOI: 10.1016/j.ref.2020.10.002.

40. Abel Ekwue and Oluwatoyin A. Akintunde, "The impact of distributed generation on distribution networks," Nigerian Journal of Technology, vol. 34, p. 325, 2015. DOI: 10.4314/njt.v34i2.17.

41. Iman Ziari, Gerard Ledwich, Arindam Ghosh, and Geoffrey Platt, "Optimal distribution network reinforcement considering load growth, line loss, and reliability," IEEE Transactions on Power Systems, vol. 28, pp. 587-597, 2013. DOI: 10.1109/TPWRS.2012.2211626.

42. Sharon L. L. Wynn, Terapat Boonraksa, Parinya Boonraksa, Woranan Pinthurat, and Bancha Marungsri, "Decentralized energy management system in microgrid considering uncertainty and demand response," Electronics, vol. 12, p. 237, 2023. DOI: 10.3390/electronics12010237.

43. Ishmael Moses, Leah Kiprono, and Simon Talai, "Optimal placement and sizing of distributed generation (DG) units in electrical power distribution networks," International Journal of Electrical and Electronics Engineering Studies, vol. 9, pp. 66-124, 2023. DOI: 10.37745/ijeees.13/vol9n166124.

44. Imran U. Salam, Mohamed Yousif, Muhammad Numan, Kashif Zeb, and Mohammad Billah, "Optimizing distributed generation placement and sizing in distribution systems: A multi-objective analysis of power losses, reliability, and operational constraints," Energies, vol. 16, no. 16, p. 5907, 2022. DOI: 10.3390/en16165907.

45. M. Cortes-Carmona, J. Vega, and M. Cortés, "Power flow algorithm for analysis of distribution networks including distributed generation," in Proceedings of the 2018 IEEE T&D Latin America Conference and Exposition, pp. 1-5, 2018. DOI: 10.1109/TDC-LA.2018.8511695.

46. J. Duncan Glover, Mulukutla S. Sarma, and Thomas J. Overbye, Power System Analysis and Design, 5th ed. Cengage Learning, 2012. ISBN: 978-1111425774.

47. Hadi Saadat, Power System Analysis, 3rd ed. McGraw-Hill, 2002. ISBN: 978-0070602411.

48. Allen J. Wood and Bruce F. Wollenberg, Power Generation, Operation, and Control, 3rd ed. Wiley-Interscience, 2012. ISBN: 978-0471646182.

49. J. Duncan Glover, Mulukutla S. Sarma, and Thomas J. Overbye, Power System Analysis and Design, 5th ed. Cengage Learning, 2011. ISBN: 978-1111425774.

50. Prabha Kundur, Power System Stability and Control, McGraw-Hill, 1994. ISBN: 978-0070359582.

51. William D. Stevenson Jr. and John J. Grainger, Power System Analysis*, McGraw-Hill, 1994. ISBN: 978-0070413894.

52. Allen J. Wood, Bruce F. Wollenberg, and Gerald B. Sheble, Power Generation, Operation, and Control, 3rd ed. John Wiley & Sons, 2013. ISBN: 978-1118555407.

53. William H. Kersting, Distribution System Modeling and Analysis, CRC Press, 2002. ISBN: 978-0824707616.

54. Turan Gonen, Electric Power Distribution Engineering, CRC Press, 2007. ISBN: 978-0849332968.

55. J. Duncan Glover, Mulukutla S. Sarma, and Thomas J. Overbye, Power System Analysis and Design, 6th ed. Cengage Learning, 2016. DOI: 10.1111/1437-4892.12345.

56. Paul C. Krause, Oleg Wasynczuk, and Scott D. Sudhoff, Analysis of Electric Machinery and Drive Systems, 3rd ed. IEEE Press, 2013. DOI: 10.1109/9781118031818.

57. Allen J. Wood and Bruce F. Wollenberg, Power Generation, Operation, and Control, 3rd ed. Wiley, 2012. DOI: 10.1002/9781118683486.

58. Math H. J. Bollen, Voltage Quality in Electrical Power Systems, Wiley-IEEE Press, 2010. DOI: 10.1109/9780470686595.

59. Mario A. Rios, Energy Efficiency in Electrical Distribution Systems, Wiley, 2016. DOI: 10.1002/9781119307450.

60. Nadia Smairi, "Optimisation par essaim particulaire : adaptation de tribes à l’optimisation multiobjectif," Ph.D. dissertation, Université Paris-Est, 2013.

61. S. S. Rao, Engineering Optimization: Theory and Practice, John Wiley & Sons, 2009.

62. Abdelkader Betka, "Optimisation des dispositions de caméras en 2D par la technique PSO," Master's thesis, Université Biskra, Algérie, 2015.

63. Amine El Dor, "Perfectionnement des algorithmes d’optimisation par essaim particulaire : applications en segmentation d’images et en électronique," Ph.D. dissertation, Université Paris-Est, 2012.

64. Hassan Hachimi, "Hybridations d’algorithmes métaheuristiques en optimisation globale et leurs applications," Ph.D. dissertation, INSA de Rouen, 2013.

65. Sabrina Abdesselam, "Conception d’un système d’optimisation pour le positionnement de caméras pour la motion capture MOCAP," Ph.D. dissertation, Université Biskra, Algérie, 2018.

66. Mohammed Douiri, Sami Elbernoussi, and Hassan Lakhba, "Cours des méthodes de résolution exactes heuristiques et métaheuristiques," Course material, Université Mohamed V, Faculté des sciences de Rabat, 2009.

67. Khalid Hussain, Mohd N. Salleh, S. Cheng, Himanshu S. Bansal, Syed A. Hussain, Muhammad A. Iqbal, Yasir H. Alzahrani, and Khaleel Alhadidi, "Metaheuristic research: A comprehensive survey," Artificial Intelligence Review, pp. 1-43, 2018. DOI: 10.1007/s10462-018-09603-4.

68. Imed Boussaid, Jean Lepagnot, and Pierre Siarry, "A survey on optimization metaheuristics," Information Sciences, vol. 237, pp. 82-117, 2013. DOI: 10.1016/j.ins.2013.02.041.

69. S. Kirkpatrick, C. D. Gelatt, and M. P. Vecchi, "Optimization by simulated annealing," Science, vol. 220, no. 4598, pp. 671-680, 1983. DOI: 10.1126/science.220.4598.671.

70. C. Papademetriou and K. Steiglitz, Combinatorial Optimization, Englewood Cliffs, NJ: Prentice Hall, 1982.

71. Fred Glover, "Future paths for integer programming and links to artificial intelligence," Computers & Operations Research, vol. 13, no. 5, pp. 533-549, 1986. DOI: 10.1016/0305-0548(86)90030-8.

72. T. A. Feo and M. G. C. Resende, "Greedy randomized adaptive search procedures," Journal of Global Optimization, vol. 6, no. 2, pp. 109-133, 1995. DOI: 10.1007/BF01096763.

73. N. Mladenovic and P. Hansen, "Variable neighborhood search," Computers & Operations Research, vol. 24, no. 11, pp. 1097-1100, 1997. DOI: 10.1016/S0305-0548(97)00031-2.

74. Thomas Stutzle, "Local search algorithms for combinatorial problems," Ph.D. dissertation, Universität Darmstadt of Technology, 1998.

75. H. Salimi, "Stochastic fractal search: A powerful metaheuristic algorithm," Knowledge-Based Systems, vol. 75, pp. 1-18, 2015. DOI: 10.1016/j.knosys.2015.01.004.

76. S. Mirjalili, "Dragonfly algorithm: A new meta-heuristic optimization technique for s olving single-objective, discrete, and multi-objective problems," Neural Computing and Applications, vol. 27, no. 4, pp. 1053-1073, 2016. DOI: 10.1007/s00500-016-2272-2.

77. S. J. Mousavirad and H. Ebrahimpour-Komleh, "Human mental search: A new population-based metaheuristic optimization algorithm," Applied Intelligence, vol. 47, no. 3, pp. 850-887, 2017. DOI: 10.1007/s10489-016-0925-6.

78. S. Mirjalili, "SCA: A sine cosine algorithm for solving optimization problems," Knowledge-Based Systems, vol. 96, pp. 120-133, 2016. DOI: 10.1016/j.knosys.2015.12.022.

79. M. Widmer, "Les métaheuristiques : des outils performants pour les problèmes industriels," 3ème Conférence Francophone de Modélisation et Simulation MOSIM, vol. 1, pp. 25-27, 2001.

80. John H. Holland and J. S. Reitman, "Cognitive systems based on adaptive algorithms," in Pattern-Directed Inference Systems, Elsevier, 1978, pp. 313-329.

81. Ingo Rechenberg, Evolutionsstrategie: Optimierung technischer Systeme nach Prinzipien der biologischen Evolution, 1973.

82. Lawrence J. Fogel, Alvin J. Owens, and Michael J. Walsh, Artificial Intelligence through Simulated Evolution, 1966.

83. Melanie Mitchell, An Introduction to Genetic Algorithms, MIT Press, 1998.

84. Rainer Storn and Kenneth Price, "Differential evolution: A simple and efficient adaptive scheme for global optimization over continuous spaces," [R], Berkeley: ICSI, 1995.

85. Matej Crepinsek, Shih-Hsi Liu, and Marjan Mernik, "Exploration and exploitation in evolutionary algorithms: A survey," ACM Computing Surveys (CSUR), vol. 45, no. 3, p. 35, 2013. DOI: 10.1145/2480741.2480752.

86. Imed Boussaid, Perfectionnement de métaheuristiques pour l'optimisation continue, P h.D. dissertation, Université Paris-Est, 2013.

87. Russell Eberhart and James Kennedy, "A new optimizer using particle swarm theory," in MHS'95, Proceedings of the Sixth International Symposium on Micro Machine and Human Science, IEEE, pp. 39-43, 1995. DOI: 10.1109/MHS.1995.494215.

88. Kevin M. Passino, "Biomimicry of bacterial foraging for distributed optimization and control," IEEE Control Systems, vol. 22, no. 3, pp. 52-67, 2002. DOI: 10.1109/MHS.1995.494215.

89. Yong Shiqin, Jianjun Jiang, and Guangxing Yuan, "A dolphin partner optimization," in Global Congress on Intelligent Systems, IEEE, pp. 124-128, 2009. DOI: 10.1109/GCIS.2009.187.

90. Marco Dorigo, Vittorio Maniezzo, and Alessandro Colorni, "Positive feedback as a search strategy," Citeseer, 1991.

91. Seyedali Mirjalili, S. Mirjalili, and Andrew Lewis, "Grey wolf optimizer," Advances in Engineering Software, vol. 69, pp. 46-61, 2014. DOI: 10.1016/j.advengsoft.2013.12.007.

92. Abdolreza Hatamlou, "Black hole: A new heuristic optimization approach for data clustering," Information Sciences, vol. 222, pp. 175-184, 2013. DOI: 10.1016/j.ins.2012.08.023.

93. E. Rashedi, H. Nezamabadi-Pour, and S. Saryazdi, "GSA: A gravitational search algorithm," Information Sciences, vol. 179, no. 13, pp. 2232-2248, 2009. DOI: 10.1016/j.ins.2009.03.004.

94. Oktay K. Erol and İbrahim Eksin, "A new optimization method: Big bang-big crunch," Advances in Engineering Software, vol. 37, no. 2, pp. 106-111, 2006. DOI: 10.1016/j.advengsoft.2005.04.005.

95. Hassan Shah-Hosseini, "Principal components analysis by the galaxy-based search algorithm: A novel metaheuristic for continuous optimization," International Journal of Computational Science and Engineering, vol. 6, no. 1-2, pp. 132-140, 2011. DOI: 10.1504/IJCSE.2011.040264.

96. A. H. Kashan, "A new metaheuristic for optimization: Optics inspired optimization (OIO)," Computers & Operations Research, vol. 55, pp. 99-125, 2015. DOI: 10.1016/j.cor.2014.10.002.

97. Amir Kaveh and Vahid R. Mahdavi, "Colliding bodies optimization: A novel meta-heuristic method," Computers and Structures, vol. 139, pp. 18-27, 2014. DOI: 10.1016/j.compstruc.2014.03.005.

98. A. H. Kashan, "League Championship Algorithm (LCA): An algorithm for global optimization inspired by sport championships," Applied Soft Computing, vol. 16, pp. 171-200, 2014. DOI: 10.1016/j.asoc.2013.12.005.

99. R. V. Rao, V. J. Savsani, and D. P. Vakharia, "Teaching-learning-based optimization: A novel method for constrained mechanical design optimization problems," Computer-Aided Design, vol. 43, no. 3, pp. 303-315, 2011. DOI: 10.1016/j.cad.2010.12.015.

100. Ali Sadollah, Ali Bahreininejad, Hassan Eskandar, et al., "Mine blast algorithm: A new population-based algorithm for solving constrained engineering optimization problems," Applied Soft Computing, vol. 13, no. 5, pp. 2592-2612, 2013. DOI: 10.1016/j.asoc.2012.11.026.

101. Zulhilmi Ibrahim, Nur Hidayati A. Aziz, Nur Azira Ab. Aziz, et al., "Simulated Kalman filter: A novel estimation-based metaheuristic optimization algorithm," Advanced Science Letters, vol. 22, no. 10, pp. 2941-2946, 2016. DOI: 10.1166/asl.2016.7791.

102. David H. Wolpert and William G. Macready, "No free lunch theorems for optimization," IEEE Transactions on Evolutionary Computation, vol. 1, no. 1, pp. 67-82, 1997. DOI: 10.1109/4235.585893.

103. Gérard Cohen, Convexité et optimisation, Course, Ecole Nationale des Ponts et Chaussées, 2000.

104. Anthony Liefooghe, Métaheuristiques pour l’optimisation multiobjectif: Approches coopératives, prise en compte de l’incertitude et application en logistique, Ph.D. dissertation, Université des Sciences et Technologie de Lille-Lille I, 2009.

105. Abida Toumi, Restauration adaptative d'image par les méthodes intelligentes, Ph.D. dissertation, Université Biskra, Algérie, 2013.

106. J. Chen, H. Cai, and W. Wang, "A new metaheuristic algorithm: car tracking optimization algorithm," Soft Computing, vol. 22, no. 12, pp. 3857-3878, 2018. DOI: 10.1007/s00500-017-2662-0.

107. X. Qi, Y. Zhu, and H. Zhang, "A new metaheuristic butterfly-inspired algorithm," Journal of Computational Science, vol. 23, pp. 226-239, 2017. DOI: 10.1016/j.jocs.2017.05.014.

108. S. A. Ahmadi, "Human behavior-based optimization: a novel metaheuristic approach to solve complex optimization problems," Neural Computing and Applications, vol. 28, no. 1, pp. 233-244, 2017. DOI: 10.1007/s00521-016-2325-6.

109. M. Abdel-Basset, D. El-Shahat, and A. K. Sangaiah, "A modified nature-inspired metaheuristic whale optimization algorithm for solving the 0-1 knapsack problem," International Journal of Machine Learning and Cybernetics, pp. 1-20, 2017. DOI: 10.1007/s13042-017-0665-8.

110. I. Strumberger and N. Bacanin, "Modified Moth Search Algorithm for Global Optimization Problems," International Journal of Computers, vol. 3, 2018. DOI: 10.18488/journal.109.2018.31.64.79.

111. J. S. Chou and N. T. Ngo, "Modified firefly algorithm for multidimensional optimization in structural design problems," Structural and Multidisciplinary Optimization, vol. 55, no. 6, pp. 2013-2028, 2017. DOI: 10.1007/s00158-016-1606-3.

112. Russell Eberhart and James Kennedy, "A new optimizer using particle swarm theory," in MHS'95. Proceedings of the Sixth International Symposium on Micro Machine and Human Science, IEEE, pp. 39-43, 1995. DOI: 10.1109/MHS.1995.494215.

113. Seyedali Mirjalili, S. M. Mirjalili, and Andrew Lewis, "Grey Wolf Optimizer," Advances in Engineering Software, vol. 69, pp. 46–61, 2014. DOI: 10.1016/j.advengsoft.2013.12.007.

114. Seyedali Mirjalili and Andrew Lewis, "The Whale Optimization Algorithm," Advances in Engineering Software, vol. 95, pp. 51–67, 2016. DOI: 10.1016/j.advengsoft.2016.01.008.

115. Abir Betka, Abida Toumi, Amel Terki, and Madina Hamiane, "An efficient metaheuristic method based on the BitTorrent communication protocol (EM-BT)," Evolutionary Intelligence, pp. 1-20, 2022. DOI: 10.1007/s12065-021-00493-y.

116. J.-S. Chou and D.-N. Truong, "Multiobjective optimization inspired by behavior of jellyfish for solving structural design problems," Chaos, Solitons & Fractals, vol. 135, p. 109738, 2020. DOI: 10.1016/j.chaos.2020.109738.

117. Xin-She Yang, "Multi-objective Flower Pollination Algorithm (MOFPA)," ResearchGate, 2019. DOI: 10.13140/RG.2.2.28788.30082.

118. Joao Luiz Pereira, Guilherme Oliver, Matheus Francisco, Sebastião Cunha Jr, and Guilherme Gomes, "Multi-objective Lichtenberg Algorithm: A Hybrid Physics-Based Meta-Heuristic for Solving Engineering Problems," Expert Systems with Applications*, vol. 187, p. 115939, 2021. DOI: 10.1016/j.eswa.2021.115939.

119. S. Mirjalili, S. M. Mirjalili, and A. Hatamlou, "Multi-Verse Optimizer: a nature-inspired algorithm for global optimization," Neural Computing & Applications, vol. 27, no. 2, pp. 495-513, 2016. DOI: 10.1007/s00521-015-1928-1.

120. Wei Ma, Ling Qiu, Fei Sun, Sherif S. M. Ghoneim, and Jin Duan, "PV Power Forecasting Based on Relevance Vector Machine with Sparrow Search Algorithm Considering Seasonal Distribution and Weather Type," Energies, vol. 15, no. 14, p. 5231, 2022. DOI: 10.3390/en15145231.

121. A. D. Jones and C. P. Underwood, "A modelling method for building-integrated photovoltaic power supply," Building Services Engineering Research and Technology, 2002. DOI: 10.1191/0143624402bt040oa.

122. Trevor Markvard, Solar Electricity, 2nd ed., Wiley, New York, 2000.

123. Djamel Rekioua and Erick Matagne, "Modeling of Solar Irradiance and Cells," in Optimization of Photovoltaic Power Systems, Green Energy and Technology, Springer, London, 2012. DOI: 10.1007/978-1-4471-2403-0.

124. Asmaa Nasef, Abdullah Shaheen, and Heba Khattab, "Local and remote control of automatic voltage regulators in distribution networks with different variations and uncertainties: Practical cases study," Electric Power Systems Research, vol. 205, p. 107773, 2022. DOI: 10.1016/j.epsr.2021.107773.

125. A. M. Shaheen, A. M. Elsayed, R. A. El-Sehiemy, S. Kamel, and Sherif S. M. Ghoneim, "A modified marine predators optimization algorithm for simultaneous network reconfiguration and distributed generator allocation in distribution systems under different loading conditions," Engineering Optimization, vol. 54, pp. 1-22, 2021. DOI: 10.1080/0305215X.2021.1905380.

126. Pritesh Parmar and Chirag Patel, "Optimal placement of capacitor using backward forward sweep method," Springer Nature Singapore Pte Ltd., pp. 255–262, 2018. DOI: 10.1007/978-981-10-8161-7_32.

127. Djamel Rekioua and Erick Matagne, "Modeling of Solar Irradiance and Cells," in Optimization of Photovoltaic Power Systems, Green Energy and Technology, Springer, London, 2012. DOI: 10.1007/978-1-4471-2403-0.

128. Asmaa Nasef, Abdullah M. Shaheen, and Heba Khattab, "Local and remote control of automatic voltage regulators in distribution networks with different variations and uncertainties: Practical cases study," *Electric Power Systems Research, vol. 205, p. 107773, 2022. DOI: 10.1016/j.epsr.2021.107773.

129. K. N, E. A. Maya, and E. A. Jasmin, "Optimal integration of distributed generation (DG) resources in unbalanced distribution system considering uncertainty modelling," International Transactions on Electrical Energy Systems, vol. 27, no. 1, p. e2248, 2017. DOI: 10.1002/2050-7038.2248.

130. D. Q. Hung, N. Mithulananthan, and K. Y. Lee, "Determining PV penetration for distribution systems with time varying load models," IEEE Transactions on Power Systems, vol. 29, no. 6, pp. 3048–3057, 2014. DOI: 10.1109/TPWRS.2014.2319783.

131. A. Soroudi, M. Aien, and M. Ehsan, "A probabilistic modelling of photovoltaic modules and wind power generation impact on distribution networks," IEEE Systems Journal, vol. 6, no. 2, pp. 254–259, 2012. DOI: 10.1109/JSYST.2012.2182301.

132. Mohammad Azizi, Ali Mohammad, Seyyed Mohsen Javadi, Mojtaba Abolhasani, Hosein Ebrahimi, and Alireza Khodabakhsh, "Energy valley optimizer: A novel metaheuristic algorithm for global and engineering optimization," Springer Nature, 2021.

133. Ehab H. Houssein, Diego Oliva, Nadia A. Samee, Nour F. Mahmoud, and Mohamed M. Emam, "Liver Cancer Algorithm: A novel bio-inspired optimizer," Computers in Biology and Medicine, vol. 147, p. 107389, 2023. DOI: 10.1016/j.compbiomed.2023.107389.

134. P. Trojovsky and M. Dehghani, "Walrus Optimization Algorithm: A New Bio-Inspired Metaheuristic Algorithm," 2022. DOI: 10.21203/rs.3.rs-2174098/v1.

135. E. Trojovská, M. Dehghani, and P. Trojovský, "Zebra Optimization Algorithm: A New Bio-Inspired Optimization Algorithm for Solving Optimization Problems," IEEE Access, vol. 10, pp. 49445-49473, 2022. DOI: 10.1109/ACCESS.2022.3171436.

136. Algerian National Electricity Company "Sonelgaz," available: www.sonelgaz-distribution.

ANNEXES

Annexes

A **:** Studied Networks

A.1 **:** IEEE 33-JB Network

Table A.1. Data for the IEEE 33-JB Network.

Number of ranches	JB 1	JB 2	Resistance (Ω)	Reactance (Ω)	Load	
					Active Power (kW)	Reactive Power (kVar)
1	1	2	0.0922	0.0477	100	60
2	2	3	0.4930	0.2511 .	90	40
3	3	4	0.3660	0.1864	120	80
4	4	5	0.3811	0.1941	60	30
5	5	6	0.8190	0.7070	60	20
6	6	7	0.1872	0.6188	200	100
7	7	8	1.7114	1.2351	200	100
8	8	9	1.0300	0.7400	60	20
9	9	10	1.0400	0.7400	60	20
10	10	11	0.1966	0.06500	45	30
11	11	12	0.3744	0.1238	60	35
12	12	13	1.468	1.1550	60	35
13	13	14	0.5416	0.7129	120	80
14	14	15	0.5910	0.5260	60	10
15	15	16	0.7463	0.5450	60	20
16	16	17	1.2890	1.7210	60	20
17	17	18	0.7320	0.5740	90	40
18	18	19	0.1640	0.1565	90	40
19	19	20	1.5042	1.3554	90	40
20	20	21	0.4095	0.4784	90	40
21	21	22	0.7089	0.9373	90	40
22	22	23	0.4512	0.3083	90	50
23	23	24	0.8980	0.7091	420	200
24	24	25	0.8960	0.7011	420	200
25	2	26	0.2030	0.1034	60	25

	5					
26	26	27	0.2842	0.1447	60	25
27	27	28	1.0590	0.9337	60	20
28	28	29	0.8042	0.7006	120	70
29	29	30	0.5075	0.2585	200	600
30	30	31	0.9744	0.9630	150	70
31	31	32	0.3105	0.3619	210	100
32	32	33	0.3410	0.5302	60	40

A.2 : IEEE 69-JB Network.

Table A.2. Data for the IEEE 69-JB Network.

Number of Branches	**JB 1**	**JB 2**	**Resistance (Ω)**	**Reactance (Ω)**	**Load**	
					Active Power (kW)	**Reactive Power (kVar)**
1	1	2	0.0005	0.0012	0	0
2	2	3	0.0005	0.0012	0	0
3	3	4	0.0015	0.0036	0	0
4	4	5	0.0251	0.0294	0	0
5	5	6	0.366	0.1864	2.6	2.2
6	6	7	0.3811	0.1941	40.4	30
7	7	8	0.0922	0.047	75	54
8	8	9	0.0493	0.0251	30	22
9	9	10	0.819	0.2707	28	19
10	10	11	0.1872	0.0619	145	104
11	11	12	0.7114	0.2351	145	104
12	12	13	1.03	0.34	8	5
13	13	14	1.044	0.345	8	5.5
14	14	15	1.058	0.3496	0	0
15	15	16	0.1966	0.065	45.5	30
16	16	17	0.3744	0.1238	60	35
17	17	18	0.0047	0.0016	60	35
18	18	19	0.3276	0.1083	0	0

19	19	20	0.2106	0.069	1	0.6
20	20	21	0.3416	0.1129	114	81
21	21	22	0.014	0.0046	5	3.5
22	22	23	0.1591	0.0526	0	0
23	23	24	0.3463	0.1145	28	20
24	24	25	0.7488	0.2475	0	0
25	25	26	0.3089	0.1021	14	10
26	26	27	0.1732	0.0572	14	10
27	3	28	0.0044	0.0108	26	18.6
28	28	29	0.064	0.1565	26	18.6
29	29	30	0.3978	0.1315	0	0
30	30	31	0.0702	0.0232	0	0
31	31	32	0.351	0.116	0	0
32	32	33	0.839	0.2816	14	10
33	33	34	1.708	0.5646	9.5	14
34	34	35	1.474	0.4873	6	4
35	3	36	0.0044	0.0108	26	18.55
36	36	37	0.064	0.1565	26	18.55
37	37	38	0.1053	0.123	0	0
38	38	39	0.0304	0.0355	24	17
39	39	40	0.0018	0.0021	24	17
40	40	41	0.7283	0.8509	1.2	1
41	41	42	0.31	0.3623	0	0
42	42	43	0.041	0.0478	6	4.3
43	43	44	0.0092	0.0116	0	0
44	44	45	0.1089	0.1373	39.22	26.3
45	45	46	0.0009	0.0012	39.22	26.3
46	4	47	0.0034	0.0084	0	0
47	47	48	0.0851	0.2083	79	56.4

48	48	49	0.2898	0.7091	384.7	274.5
49	49	50	0.0822	0.2011	384.7	274.5
50	8	51	0.0928	0.0473	40.5	28.3
51	51	52	0.3319	0.1114	3.6	2.7
52	9	53	0.174	0.0886	4.35	3.5
53	53	54	0.203	0.1034	26.4	19
54	54	55	0.2842	0.1447	24	17.2
55	55	56	0.2813	0.1433	0	0
56	56	57	1.59	0.5337	0	0
57	57	58	0.7837	0.263	0	0
58	58	59	0.3042	0.1006	100	72
59	59	60	0.3861	0.1172	0	0
60	60	61	0.5075	0.2585	1244	888
61	61	62	0.0974	0.0496	32	23
62	62	63	0.145	0.0738	0	0
63	63	64	0.7105	0.3619	227	162
64	64	65	1.041	0.5302	59	42
65	11	66	0.2012	0.0611	18	13
66	66	67	0.0047	0.0014	18	13
67	12	68	0.7394	0.2444	28	20
68	68	69	0.0047	0.0016	28	20

A.3 : ALG-AB-Hassi Sida 157 Network.

Table A.3. Data for the ALG-AB-Hassi Sida Network.

JB 1	JB 2	Resistance (Ω)	Reactance (Ω)	Load	
				Active Power (kW)	Reactive Power (kVar)
1	2	0.015	0.011		
2	3	0.056	0.054	0	0
3	4	0.107	0.105		
4	5	1.78	1.033	0	0
5	6	1.78	1.034	0	0
6	7	0.2	0.1		
7	8	0.05	0.007	0	0
8	9	0.1	0.1	0	0
9	10	0.006	0.015		
10	11	0.15	0.1	2.6	2.2
11	12	0.006	0.002	40.4	29.3
12	13	0.001	0.001	75	54
13	14	1.41	1.36		
14	15	0.29	0.18	30	22
15	16	0.19	0.18	28	19
16	17	1.01	0.97		
17	18	0.8	0.6	145	104
18	19	0.005	0.005	245	104
19	20	0.005	0.005	8	5.5
20	21	0.005	0.008		
21	22	0.005	0.005	40	5.5
22	23	0.005	0.005	0	0
23	24	0.005	0.003		
24	25	0.007	0.007	45.5	30
25	26	0.05	0.005	60	35
26	27	0.006	0.002	90	95
27	28	0.32	0.1		
28	29	0.37	0.1	30	60
29	30	0.003	0.001	70	40.6
30	31	0.12	0.47	90	90
30	32	0.01	0.012		
2	33	0.018	0.01	50.3	70.5
3	34	0.01	0.009	85	45
4	35	0.03	0.012		
35	36	3.29	1.2	30	60
36	37	0.29	0.1	60	20
37	38	0.88	0.32		
38	39	0.14	0.05	14	70
39	40	0.76	0.27	40	50
40	41	0.03	0.01		

40 35 36 44 44 37 38 39 5 6 51 51 7 8 55 9 57 57 10 60 61 62 60 64 65 65 64 14 15 70 71 72 73 74 75 76 77 70 79 80 81 80 73 74 75 86 87 86	42 43 44 45 46 47 48 49 50 51 52 53 54 55 56 57 58 59 60 61 62 63 64 65 66 67 68 69 70 71 72 73 74 75 76 77 78 79 80 81 82 83 84 85 86 87 88 89	0.86 0.04 0.61 0.04 0.71 1.01 0.84 0.04 0.01 0.36 0.037 0.71 0.4 0.38 0.06 0.03 0.08 0.04 0.02 0.13 0.51 0.63 1.31 0.34 1.08 0.34 0.45 0.04 0.01 0.05 0.28 0.27 0.21 0.04 0.04 0.2 0.32 0.01 0.5 0.76 0.34 0.03 0.01 0.02 0.03 0.9 0.01 0.06	0.31 0.01 0.22 0.01 0.26 0.37 0.3 0.01 0.005 0.13 0.013 0.26 0.14 0.14 0.02 0.01 0.03 0.01 0.01 0.05 0.18 0.23 0.47 0.12 0.39 0.12 0.16 0.01 0.01 0.05 0.28 0.27 0.21 0.04 0.04 0.07 0.11 0.01 0.18 0.27 0.12 0.01 0.007 0.007 0.01 0.32 0.007 0.02	90 50 80 60 90 70 40 70 86 66 100 24 44 1.2 0 6 0 39.2 39.2 0 79 384 384 40 3.6 4.35 26.4 24 0 0 0 100 0 1244	30 50.6 40 80 40 70 94 70 50.5 38.5 100 17 17 1 0 4.3 0 26.3 26.3 0 56.4 274.5 274.5 28.3 2.7 3.5 19 17.2 0 0 0 72 0 888

76	90	0.45	0.44	32	23
90	91	0.29	0.28	0	162
91	92	0.02	0.01	227	42
92	93	1.44	0.52	59	13
93	94	0.26	0.09	18	13
94	95	0.65	0.24	18	20
90	96	0.02	0.009	28	20
96	97	1.18	0.43	28	432
97	98	0.59	0.21	90.3	373.1
98	99	0.24	0.08	78	353.3
99	100	1.05	0.38	83.6	333.4
98	101	0.44	0.43	69.9	313.7
92	102	0.02	0.01	85.6	294.1
102	103	0.53	0.19	61.6	254.9
102	104	0.52	0.19	53	19.6
93	105	0.05	0.01	41.04	19.6
94	106	1.63	0.59	51.04	58.91
17	107	0.25	0.09	12.3	39.27
107	108	0.58	0.21	82.2	19.63
108	109	0.19	0.07	41.1	19.63
107	110	0.11	0.04	61.1	19.63
108	111	0.15	0.05	91.1	19.61
18	112	0.01	0.01	41.05	19.60
112	113	0.04	0.04	41	58.8
113	114	0.04	0.01	12	39.20
112	115	0.29	0.1	82.05	19.6
113	116	0.01	0.01	41.02	19.6
116	117	0.22	0.21	61.02	215.5
20	118	0.02	0.01	45.1	137
118	119	0.06	0.02	28	137
119	120	0.11	0.04	48	58.7
120	121	0.004	0.001	122	39.1
121	122	0.1	0.03	81.9	19.5
122	123	0.03	0.01	40.9	78.3
118	124	0.1	0.03		
119	125	0.023	0.008		
120	126	0.028	0.01		
126	127	0.13	0.05		
127	128	0.04	0.01		
128	129	0.03	0.01		
129	130	0.04	0.01		
130	131	0.1	0.03		
127	132	0.09	0.03		
127	133	0.023	0.008		
128	134	0.17	0.06		
129	135	0.12	0.04		
21	136	0.008	0.008		
136	137	0.16	0.15		

137	138	18.28	17.93	16	78.3
138	139	0.01	0.01	63.9	58.7
139	140	17.6	6.57	12.8	19.56
140	141	0.12	0.04	40.9	19.56
136	142	0.0009	0.0003	50.9	181.9
137	143	0.08	0.03	38.8	58.7
139	144	0.03	0.012	12.8	19.57
144	145	0.22	0.08	40.9	39.14
145	146	0.22	0.08	81.92	19.57
144	147	0.07	0.028	40.96	19.55
140	148	0.21	0.07	40.93	75.7
141	149	0.16	0.05	15.4	37.84
141	150	0.03	0.01	79.22	18.92
23	151	0.01	0.004	39.6	18.92
24	152	0.004	0.004	79.6	18.92
25	153	0.004	0.004	39.61	112.70
26	154	0.004	0.004	235.88	75.13
27	155	0.01	0.007	157.25	18.78
28	156	0.04	0.01	39.31	18.78
29	157	0.11	0.04	79.31	56.32
				117.89	37.55
				78.59	63.12
				133.5	18.38
				129.28	59.64
				325.06	20.12
				43.42	68.64
				35.98	93.69
				19.1	18.73
				39.22	18.73
				59.22	39.51
				82.63	37.47
				78.79	80.85
				58.84	24.68
				47.27	49.79

				31.51	93.58
				19.87	93.61
				69.94	18.72
				39.18	56.17
				117.56	93.58
				195.87	24.77
				470.46	5.96
				231.08	84.04
				38.2	18.95
				80.84	0
				0	0
				0	0
				0	0
				0	0
				0	0
				0	0
				0	0
				0	0
				0	0
				39.2	0
				98.3	18.73
				78.3	37.4
				39.2	37.4
				99.1	18.73
				39.15	18.70
				78.3	18.70
				0	37.41

Publications

Publications

• Publications

Fettah, K.; Guia, T.; Salhi, A.; Mouassa, S.; Bosisio, A.; Rouzbeh, S. Optimal Allocation of Capacitor Banks and Distributed Generation: A Comparison of Recently Developed Metaheuristic Optimization Techniques on the Real Distribution Networks of ALG-AB-Hassi Sida, Algeria. Sustainability 2024, 16, 4419. https://doi.org/10.3390/su16114419

Fettah, K., Guia, T., Salhi, A. *et al.* A pareto strategy based on multi-objective optimal integration of distributed generation and compensation devices regarding weather and load fluctuations. *Sci Rep* **14**, 10423 (2024). https://doi.org/10.1038/s41598-024-61192-2

Khaled Fettah, Talal Guia, Ahmed Salhi , Walid Mohammed Kacemi, Fayssal Saidi. Allocation of Photovoltaic and Wind Turbine Based DG Units Using the Energy Valley Optimizer (EVO) algorithm. PRZEGLĄD ELEKTROTECHNICZNY, ISSN 0033-2097, R. 100 NR 7/2024, doi :10.15199/48.2024.07.45

Kacemi, W.M., Bounadja, E., Djilali, A.B., Iqbal, A., Fettah, K., (2024). Enhanced backstepping control for HESG-based wind conversion systems in MPPT applications. Journal Européen des Systèmes Automatisés, Vol. 57, No. 1, pp. 273-280. https://doi.org/10.18280/jesa.570126.

Aroua, Fatima & Ahmed, Salhi & Charrouf, Omar & Djemai, Naimi & Fettah, Khaled. (2024). Wind energy cost evaluation based on a techno-economic assessment in the Algerian highlands. Energy for Sustainable Development. 81. 101502. 10.1016/j.esd.2024.101502.

F. Saidi, A. Djahbar, E. Bounadja, W.M. Kacemi, K. Fettah. Novel modular multilevel matrix converter topology for efficient high-voltage AC-AC power conversion, Електротехніка і Електромеханіка, 2024, № 6. https://doi.org/10.20998/2074-272X.2024.6.01

• International communications

Fettah, Khaled & Talal, Guia & Ahmed, Salhi & Said, Abdelaziz. A Review of Solar Photovoltaic Potential in Algeria. 1 st International Conference on Optoelectronics, Materials & Renewable Energy, ICOMRE’22

Khaled, Fettah & Talal, Guia & Ahmed, Salhi & Saidi, Abdelaziz. (2023). Optimal Planning of Photovoltaic-based DG Units in Uncertain Distribution Network. All Sciences Abstracts. 1. 1-11. 10.59287/as-abstracts.653.

Khaled, Fettah & Talal, Guia & Ahmed, Salhi & Saidi, Abdelaziz. (2023). Optimal Planning of Wind -based DG Units in Uncertain Distribution Network. All Sciences Abstracts. 1. 15. 10.59287/as-abstracts.660.

Khaled, Fettah & Talal, Guia & Ahmed, Salhi. International Conference :(ICTAEE 23) Optimal planning of photovoltaic and Wind -based DG Units in Distribution Network Considering Uncertainties

Khaled, Fettah & Talal, Guia & Ahmed, Salhi . International Conference: (MEE 23) Optimal location and size of Photovoltaic and wind in Distribution Network Considering Uncertainties

Khaled, Fettah & Ahmed, Salhi & Talal, Guia (2024). SCADA integration in smart grid. 3rd International Conference on Engineering, Natural and Social Sciences ICENSOS 2024 on May 16- 17, 2024 in Konya, Turkey